AlienDive
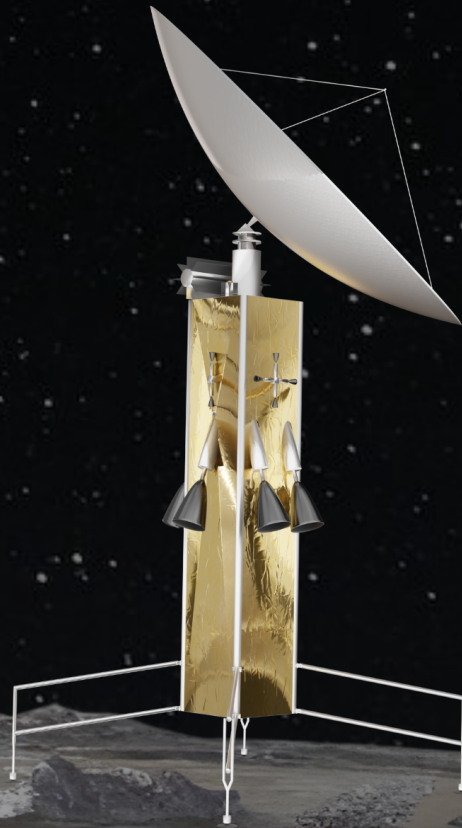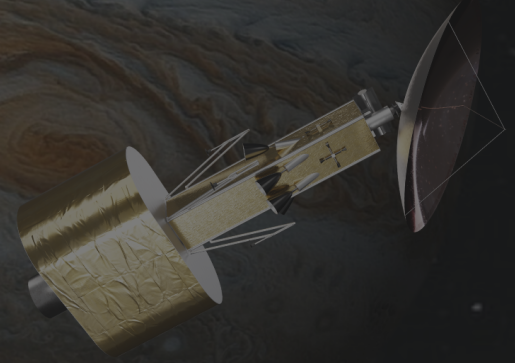
Searching for life in
Europa's subsurface ocean

Final Report DSE 2024
Group 24

TUDelft

This page is intentionally left blank

AlienDive

Searching for life in Europa's subsurface ocean

by

Group 24

Student Name	Student Number
Zayid Almarzooqi	5207290
Dion van der Ark	5548640
Cas Bouter	4969030
Isabelle Joosten	4998480
Laurens Klijn	5548381
Lucas Nebbeling	5574544
Marta Powierza	5444446
Hugo Bessa Rocha	5570875
Lievijn Simons	5312760
Pepijn Wilbrink	5524997
Sunny Zhu	5537908

Nomenclature

Abbreviations

Abbreviation	Definition
ADCS	Attitude Determination and Control System
ASRG	Advanced Stirling Radioisotope Generator
BER	Bit Error Rate
BOL	Beginning Of Life
BPSK	Binary phase-shift keying
CAD	Computer Aided Design
CAGR	Compound Annual Growth rate
CER	Cost Estimate Relation
COSPAR	Committee on Space Research
COTS	Commercial Off The Shelf
DDL	Deorbit, Descent and Landing
DEM	Digital Elevation Map
DSM	Deep Space Manoeuvre
DSN	Deep Space Network
EOI	Europa Orbit Insertion
EOL	End Of Life
EPS	Electrical Power Supply
ESA	European Space Agency
ESTEC	European Space Research and Technology Centre
erfc	Complementary error function
FEA	Finite Element Analysis
FMH	Free Molecular Heating
FOV	Field of View
fps	Frames per second
FY	Fiscal Year
GEO	Geostationary Earth Orbit
GMAT	General Mission Analysis Tool
HDA	Hazard Detection and Avoidance
HGA	High Gain Antenna
HV	High Voltage
IPR	Ice Penetrating Radar
JOI	Jupiter Orbit Insertion

Abbreviation	Definition
L-class	Large Class
LED	Light Emitting Diode
LEIA	LIDAR for Extra terrestrial Imaging Applications
LGA	Low Gain Antenna
LIDAR	Laser Imaging Detection And Ranging
MGA	Medium Gain Antenna
MLI	Multi-layer insulation
MMH	Monomethylhydrazine
NASA	National Aeronautics and Space Administration
O()	Order of
PISCES	Planetary In Situ Capillary Electrophoresis System
PCDU	Power Conditioning and Distribution Unit
PJR	Perjove Raise
PO	Probability
RF	Radio Frequency
RTG	Radioisotope Thermoelectric Generator
SSPA	Solid-State Power Amplifiers
SWOT	Strength, Weakness, Opportunities and Threats
TBD	To Be Determined
TCS	Thermal Control Subsystem
TID	Total Ionising Dose
TRL	Technology Readiness Level
TRN	Terrain Relative Navigation
TWTA	Travelling Wave Tube Amplifiers
UV	Ultraviolet
UHF	Ultra High Frequency
VEEGA	Venus-Earth-Earth Gravity Assist
WCL	Wet Chemistry Lab

Symbols

Symbol	Definition	Unit
A	Area	m^2
A_{eff}	Effective aperture	m^2
A_{ph}	Physical aperture	m^2
AF	Albedo Factor	$-$
a_{par}	Parabola constant	$-$
a	Acceleration	ms^{-2}
B	Magnetic field strength	T
b	Width	m
C	Cost	$\$$
c	Speed of light	ms^{-1}
c_{max}	Maximum distance from neutral axis	m
D	Diameter	m
$\varnothing$	Diameter	m
d	Distance	m
E	Elastic modulus	Pa
E_b	Energy per bit	J
e	Euler's number	$-$
F	Force	N
F_{focal}	Focal length	m
f	Natural frequency	Hz
G	Gain	$-$
g	Gravitational acceleration	$-$
H	Height	m
H_{depth}	Dish depth	m
h	Momentum	$kgms^{-1}$
h_{dive}	Diving depth in water	m
h_{ice}	Ice depth	m
I	Area moment of inertia	m^4
I_{sp}	Specific impulse	s
J	Heat/solar flux	Wm^{-2}
K	Effective length factor	$-$
k	Boltzmann constant	JK^{-1}
L	Length	m
M	Residual dipole moment	Nm
M_0	Starting mass	kg
$M_{s/c}$	Spacecraft dry mass	kg
m	Mass	kg
N	Number of layers	$-$
N_o	Noise spectral density	Ws
P	Power	W
P_{cr}	Critical buckling stress	Pa

Symbol	Definition	Unit
P_{orbit}	Orbital period	s
p	Pressure	Pa
Q	First moment of area	m^3
$\dot{Q}_{out}$	Time derivative of heat flow	W
q	Uniform loading density	Nm^{-1}
R_{data}	Data rate	s^{-1}
R	Planet radius	m
r	Radius	m
T	Temperature	K
T_{thrust}	Thrust	N
T_{torque}	Torque	Nm
t	Thickness	m
t	Time	s
V	Velocity	ms^{-1}
V_{shear}	Shear force	N
V_p	Propellant volume	m^3
V_t	Tank volume	m^3
W	Load	N
y	Distance from the neutral axis	m
Z	Curvature parameter	$-$
α	Thermal expansion coefficient	K^{-1}
α_{surf}	Absorptivity of surface	$-$
β	Phase modulation index	$-$
β	Plate dimension factor	$-$
γ	Correction factor	$-$
Δ	Change	$-$
Δx	Distance between center of mass and center of pressure	m
ϵ_{ap}	Aperture efficiency factor	$-$
ε	Emissivity	$-$
θ	Angle	deg
λ	Wavelength	m
μ	Gravitational parameter	$m^3 s^{-2}$
ν	Poisson ratio	$-$
π	Ratio of circumference to diameter of a circle	$-$
ρ	Reflective coefficient	$-$
ρ	Density	kgm^{-3}
σ	Stefan-Boltzmann constant	$Wm^{-2}K^{-4}$
σ	Stress	Pa
τ	Shear stress	Pa
$\tau_{1/2}$	Half-life	s
ϕ	Incidence angle	$\circ$
Ψ	Maximum thrust over weight	$-$

Executive Overview

For centuries extraterrestrial life has been of interest to many people. Despite numerous missions searching for life, no evidence has been found. Icy moons with subsurface oceans were classified as an appropriate next target for this search, as they are highly likely to contain the three essential ingredients for life [1]. AlienDive is a mission which is designed to explore such an ocean. Consisting of a transfer stage, lander and probe, the mission goal is to find unambiguous signs of life in Europa's subsurface ocean.

Project Description

The mission needs statement is "AlienDive's mission is to search for extraterrestrial life on Jupiter's moon, Europa." The Project Objective Statement is "Design a conceptual mission for the in-situ exploration of Europa's subsurface ocean with life-detection capabilities by a team of 11 students in 10 weeks." To design this mission, user requirements were provided by the stakeholders. One of the main challenges when designing AlienDive is the uncertainty of the ice layer thickness, of which the estimates vary between 1 km and 120 km. The best estimate suggests an ice crust layer of around 24 km [2]. Another major design challenge is the radiation on Europa, located in the middle of the high radiation belt of Jupiter. Lastly, COSPAR, the Committee on Space Research, regulations need to be considered, which may influence several design choices. Furthermore, a stakeholder analysis was performed, which concluded that NASA, ESA, SpaceX, astrobiologists, planetary scientists and COSPAR are the key stakeholders, these shape the design. Additionally, the employees were also defined as key stakeholders due to their impact on the project.

Trade-Off Summary

During the midterm of the design project, four system-level concepts were considered. Concept 1 was a probe and lander, where the lander drills through the ice using a laser, and the probe moves in afterwards. Concept 2 also had a lander and probe, but this time the probe would drill through the ice by itself, whilst the lander merely served as a relay. Concept 3 was an orbiter and probe, where the probe lands itself and then drills through the ice. Concept 4 was similar, but instead of drilling, the probe would move through a natural crack in the ice. Concepts 1 and 4 were discarded early on, as they were deemed infeasible. The remaining concepts were traded off based on four criteria: potential for science with a weight of 30%, technology readiness with a weight of 20%, reliability with a weight of 40%, and mass & cost with a weight of 10%. In the end, concept 2 outperformed concept 3 and was therefore selected. To confirm this choice, a sensitivity analysis was conducted on the results. The analysis revealed that concept 2 was favoured approximately 99.5% of the time.

Science Payload

The scientific payload of the AlienDive mission is divided into a lander and a subsurface probe. The payload of the probe is focused on the primary objective of searching for life in Europa's subsurface ocean and consists of three cameras, three spectrometers, a sonar, and several specialised instruments for detecting organic material. An open channel through the probe allows water to flow through and supplies the instruments with samples. The payload of the lander is meant to characterise Europa on a more global scale. It consists of a magnetometer and a seismometer. In addition to those, the cameras and LIDAR included to facilitate a soft landing may provide valuable scientific data and material for public outreach. Lastly, there is space reserved on the lander to include a surface rover, to be chosen during an open design competition.

Mission Design

AlienDive is planned to be launched in 2034 using a Falcon Heavy launcher. Travelling to Europa will be done using several gravity assists to minimise the Delta-V required. It will arrive at Europa in 2040 and orbit the moon for seven days while transmitting images to Earth, which will be used to select an appropriate landing site. Subsequently, it will autonomously perform a soft landing and deploy a subsurface probe, magnetometer pod, and the winning rover from the competition. The subsurface probe will then descend through the ice crust into the subsurface ocean, deploying RF relays at certain distance intervals to facilitate communication between the probe and the lander.

Transfer Stage Design

The transfer stage is designed to insert the spacecraft into Jupiter's sphere of influence, and subsequently perform the burns needed to put the spacecraft on the correct trajectory to reach Europa. It utilises a hypergolic liquid bipropellant engine for this purpose. Besides the engine and the fuel tanks, the transfer stage includes a guidance, navigation and control subsystem and thermal control subsystem, consisting of radiators and multi-layer insulation. After the spacecraft descends to Europa's surface, the transfer stage is discarded and will perform a crash landing on Europa's surface.

Lander Design

The lander has several tasks: it brings the probe safely to the surface of Europa, acts as a communication relay between the probe and Earth, and collects scientific data. It utilises an RTG as a power source as this was deemed the most feasible option in Europa's harsh radiation environment. The lander has a separate propulsion subsystem for performing the soft landing. The propellant for this subsystem is stored in a torus-shaped tank that wraps around the probe and relays while they are stored in the lander, protecting them from radiation. For attitude determination, the lander makes use of two fine and two coarse sun sensors, a star tracker, and an inertial measurement unit. The attitude is controlled using four reaction wheels, with 12 thrusters that are used for momentum dumping and orienting the spacecraft during landing. During landing, the lander uses a narrow field of view reconnaissance camera, two medium field of view cameras, and a LIDAR. The thermal control subsystem of the lander is similar to that of the transfer stage, but Louvres have been added to have more control over the lander's temperature. The communication subsystem of the lander features space-grade components and an in-house designed high-gain antenna to maximize downlink data rates. This subsystem communicates with NASA's Deep Space Network using X-band frequencies and with the relay transceiver using UHF frequencies to minimize ice attenuation.

Probe design

The probe will be the main scientific vehicle for the AlienDive mission, the lander will deploy it and it will penetrate through the ice layer towards the subsurface ocean. Here it will perform several scientific tasks described earlier in this chapter. The probe contains a drill, two finless RTGs, a PCDU, an IMU, a CDH, a payload bay, a cable and spool system, several RF relays and an anchor. The probe is 4.5 m in length and has a diameter of 0.28 m. Its mass is 553.8 kg. After entering the subsurface ocean, the probe will deploy an anchor to secure its connection to the ice. The probe will drill down until the subsurface ocean is reached, after which it will remain suspended in the ocean gathering data. The probe will communicate with the anchor using acoustic signals, which, in turn, will send and receive UHF signals through the RF relays deployed in the ice. The thermal control contains insulation and a fluid loop, which will distribute the heat to the areas where it is needed. The probe structure is made out of 16 mm thick titanium, which will provide sufficient stiffness to withstand the high pressures in Europa's ocean. Due to the use of RTGs, the end-of-life plan is to let the probe hang onto the anchor for as long as possible to reduce the amount of radioactive fuel that will be spilt after the possible failure.

Table 4 and Table 5 provide the mass and power budgets of the total system.

Table 4: System Mass Budget

Elements	Mass [kg]
Transfer stage dry mass	898.86
Transfer stage wet mass	12222.71
Lander dry mass	813.98
Lander wet mass	1041.36
Total probe mass	553.79
Total system mass	**13817.86**

Table 5: System Power Budget

Elements	Power [W]
Lander	
Required BOL Power	424.57
Total available power	435
Probe	
Required BOL Power	849.24
Total available power	850

Sensitivity Analysis

To investigate the flexibility of the final design, a sensitivity analysis was performed. This was done by changing two types of parameters; technical and scientific. Technical parameters could change by further refining the

design, as values go from estimate to definite. Scientific values can change because of increased insights into Europa's environment, as the scientific community continues its research. Missions like Europa Clipper and JUICE will provide more accurate estimates of critical factors, like the ice-shell thickness. Changes in technical parameters lead to fluctuations in the total system mass ranging from -10.7 to 20.2%, whilst changes in scientific parameters lead to fluctuations in the system mass ranging from -61.3 to 254.3%. This latter value can largely be attributed to the change in orbit inclination, however. A more representative estimate would be system mass fluctuations ranging from -7.0 to 8.2% for scientific parameters. From this, three conclusions can be drawn. Firstly, the design is quite insensitive to changes in our knowledge of the characteristics of Europa. Secondly, reconsidering the decision to explore the polar regions might be prudent, as the significant mass impact of the inclination change could potentially outweigh the mass needed for radiation shielding. Thirdly, the mass of the system would increase in case the performance of the low TRL components was underestimated. It is thus important to monitor the development of these components closely.

Risk Management

Risk management for the AlienDive mission was conducted in the following way: first, risks are identified and analysed in terms of probability and severity. Then, mitigation and contingency plans are set up for each risk. The most severe risks with the highest probability were determined to be the lander tipping over upon landing, failure of the lander feed system, the surface radiation on Europa exceeding the anticipated levels, and failure of the RF relays. The risk of the lander tipping over upon landing is mitigated by designing the legs for a high centre of gravity. In case the risk materialises, the landing legs or excess fuel can be used to elevate the lander to its upright position. Failure of the feed system is mitigated by incorporating strong and reliable feed system components. Should the feed system still fail, the situation should be assessed before taking the next steps. The risk of surface radiation levels exceeding anticipated levels is mitigated by incorporating safety margins of 50 % in the shield design. In case radiation levels still exceed the expected levels, the damage done should be assessed. Lastly, the risk of RF relay failure is mitigated by utilising protective housing able to withstand harsh conditions and implementing redundant relays. Should a relay still fail, attempts must be made to restart it.

Production Plan

The assembly process of the AlienDive spacecraft is split up into two phases. During the first phase, the spacecraft is largely assembled and tested at ESA ESTEC in the Netherlands, apart from any thrusters, RTGs, the fairing adaptor, the probe bus, and the probe heating pipes. During the second phase, the remaining components are added at the Goddard Space Flight Center in the United States of America. To ensure sustainable development, COTS components are used where possible, a partially reusable launcher is used, components are sourced within the EU where possible, international cooperation is utilised, and an open rover design competition will be organised. A plan is also set up to minimise the risk of personnel receiving inappropriate levels of radiation.

Verification & Validation

To ensure that the final design complies with the requirements set and can perform its mission, verification and validation must be conducted at every step in the design process. The effects of all assumptions made during the process are evaluated. Furthermore, any tools used by the team must be verified and validated. For AlienDive, these tools were an Excel design spreadsheet, a Python script developed by the team, and two third-party tools: 3DExperience and GMAT. It was concluded that all these tools were indeed suitable for the task. Whether the obtained design complies with the requirements is evaluated using a compliance matrix. In future stages of the development of AlienDive, the spacecraft will also need to be validated to ensure it is capable of performing the mission.

Future Development

Numerous steps are still necessary to get from AlienDive's current state to a flight-ready spacecraft. First, another design iteration will be conducted to optimise the design. Then, components with a low TRL will be researched and developed, leading to another design iteration to ensure all components are properly integrated into the design. Once the design is finalised, the production phase will begin, during which all components are produced and the spacecraft is assembled. Throughout this phase, verification and validation activities are conducted. Finally, the operations and logistics phase will commence, during which the spacecraft is transported to the launch site, launched, and the mission is carried out.

Contents

1   Introduction

Whoever imagines that extraterrestrial life must dwell in a galaxy far, far away might be astonished to learn that celestial bodies within our own solar system could harbour life, too. Europa, the smallest of the Galilean moons of Jupiter, stands as one of the most intriguing and promising targets in the quest to find extraterrestrial life. Life requires three essential ingredients to emerge: liquid water, an energy source, and specific chemical compounds [1]. Europa is highly likely to possess all three, making it an exceptionally compelling target for in-situ exploration in the search for extraterrestrial life. Firstly, Europa is believed to harbour a salty subsurface ocean that contains approximately twice as much water as all of Earth's oceans combined.[1] Secondly, Europa presents various potential energy sources necessary for life. These include surface chemistry processes, interactions between water and rock beneath the icy crust, tidal forces exerted by Jupiter, and, possibly, hydrothermal vents[1]. Lastly, Europa likely contains the essential chemical components needed for life to thrive [3]. In about five years, NASA's Europa Clipper and ESA's JUICE missions will study Europa up close, but confirming life in its ocean may require direct exploration of its depths. Enter AlienDive: a mission aimed at unambiguously detecting life in Europa's subsurface ocean.

The objective of this report is to present the detailed design phase of the AlienDive mission. The mission comprises three core components: the transfer stage, the lander, and the probe. The transfer stage is responsible for propelling the AlienDive systems into Jupiter's sphere of influence, executing multiple flybys and inclination adjustments to achieve the desired trajectory for a deorbit burn towards Europa. The lander's role is to safely deliver the probe to the surface of Europa through a powered descent and conduct additional scientific tasks. Meanwhile, the probe serves as the primary system to achieve the scientific objectives of the AlienDive mission. Its mission involves navigating through Europa's icy crust to reach its subsurface ocean, where the search for signs of life will commence.

This report will be presented in the following structure. Chapter 2 will provide the project description, laying out the mission objectives and user requirements. A summary of the system concept trade-off will be located in Chapter 3. The scientific payload on board the probe and the lander are discussed in Chapter 4. An overview of the mission design can be found in Chapter 5. Next, the detailed design of the transfer stage is presented in Chapter 6. Chapter 7 details the in-depth design of the lander. The design of the probe is elaborated on in Chapter 8. Subsequently, in Chapter 9, a sensitivity analysis is performed to assess the effect of changing system parameters on the final design. Next, the risk management strategy regarding the technical risks associated with the AlienDive mission is laid out in Chapter 10. Chapter 11 details the production plan and views on sustainable development. Verification and validation of all facets of the AlienDive mission are discussed in Chapter 13. Future development considerations can be found in Chapter 14. Finally, the key conclusions and recommendations can be found in Chapter 15.

---

[1]From `https://europa.nasa.gov/why-europa/ingredients-for-life/`, accessed on 19/05/2024.

2   Project Description

In this chapter, the project is explained. The user requirements are delineated, and the mission is described. In addition, a stakeholder & market analysis is performed.

2.1. Mission & Project Objectives

The goal of this project is to develop a mission to analyse the subsurface ocean of Europa, with the main goal of either finding life or ruling out the possibility of life on Europa. This goal is described in the mission need statement, as can be found below:

Mission Need Statement:
AlienDive's mission is to search for extraterrestrial life on Jupiter's moon, Europa.

The objective of this project is to fulfil this need using a group of students in a set amount of time. The project objective statement is therefore as follows:

Project Objective Statement:
Design a conceptual mission for the in-situ exploration of Europa's subsurface ocean with life-detection capabilities by a team of 11 students in 10 weeks.

2.2. User Requirements

At the start of the project, 16 top-level requirements were defined. The requirements cover the science, performance, schedule, safety, reliability, sustainability, engineering, and mission costs. These criteria form the basis for all other requirements on which the final design is based.

AD-SCI-01: The mission shall be able to unambiguously detect life.

AD-SCI-02: The mission shall provide imagery of Europa's subsurface ocean and the ice-ocean interface.

AD-PERF-01: The mission shall deliver a probe to Europa's subsurface ocean.

AD-PERF-02: The probe shall enable sampling and analysis of both ice shell and ocean material.

AD-PERF-03: The probe shall operate autonomously.

AD-PERF-04: The probe shall operate for a minimum of a year.

AD-SCH-01: The mission shall launch no later than 2035.

AD-SAF-01: The use of hazardous materials for personnel involved shall be minimized.

AD-SAF-02: In case radioactive materials are used, a plan shall be put in place to minimize risk to personnel and population.

AD-REL-01: The probability that a probe is delivered to the subsurface ocean shall be higher than 50%.

AD-SUST-01: The mission shall comply with the COSPAR Policy on Planetary Protection.

AD-SUST-02: A clear end-of-life strategy shall be included in the mission design.

AD-SUST-03: In case radioactive materials are used, a plan shall be put in place to minimize environmental impact.

AD-ENG-01: The landed dry mass of the system shall not exceed 1,500 kg.

AD-ENG-02: The total system shall be launched in a single Falcon Heavy or SLS launch.

AD-COST-01: The total cost of the mission, excluding launch and operations, should be within that of an ESA Large class mission.

Later 5 top-level requirements were added based on mission elements that were added during the design.

AD-SCH-02: The probe shall arrive at Europa within 7 years after launch.

AD-SUST-04: The spacecraft shall contain at least 10 % of reused materials.

AD-SUST-05: A radioactive propulsion system shall not be used.

AD-LAND-01: The mission shall land a lander on Europa's surface.

AD-PERF-05: The system shall be able to communicate with Earth.

2.3. Mission Description

This section aims to outline the main considerations and design problems analysed and presented in this report. The project objective statement: "Design a conceptual mission for the in-situ exploration of Europa's subsurface ocean with life-detection capabilities by a team of 11 students in 10 weeks" introduces a multitude of challenges.

Firstly, as outlined in Section 2.2, a probe shall be delivered to Europa's subsurface ocean. This means that the ice shell of the moon has to be penetrated. The estimates of its thickness vary significantly between 1 km and 120 km depending on the estimation method, but also on the location on the surface of Europa [4]. The most recurring thickness estimate mentions a best estimate thickness of 24.3 km [2]. With a 20% margin added on top of this value, the design thickness used for the AlienDive mission is 30 km.

Another crucial aspect to consider for this mission is the harmful radiation environment around Jupiter. Europa is situated right in the middle of the radiation belt of Jupiter. According to NASA, an orbiter around Europa would only be able to survive for a few months due to the intense radiation.[1] This poses a significant design challenge as the AlienDive mission must not only reach Europa but also land safely and survive on the surface for enough time to enable the completion of in-situ ocean exploration.

Finally, the mission shall comply with the COSPAR planetary protection policy. Within it, five categories of concern are defined with landers to Europa belonging to category IV of quite a high concern. To ensure compliance with COSPAR, aspects such as the mechanisms and timescales of transport to the Europan subsurface ocean environment and the organism survival and proliferation before, during, and after subsurface transfer shall be taken into account and carefully assessed.

2.4. Stakeholder Analysis

This section will discuss the stakeholder analysis. Firstly, the stakeholders will be identified, including all the relevant parties that will either have an interest in the project outcome, an influence on the project outcome, or both. The breakdown of all the identified stakeholders is in Figure 2.1.
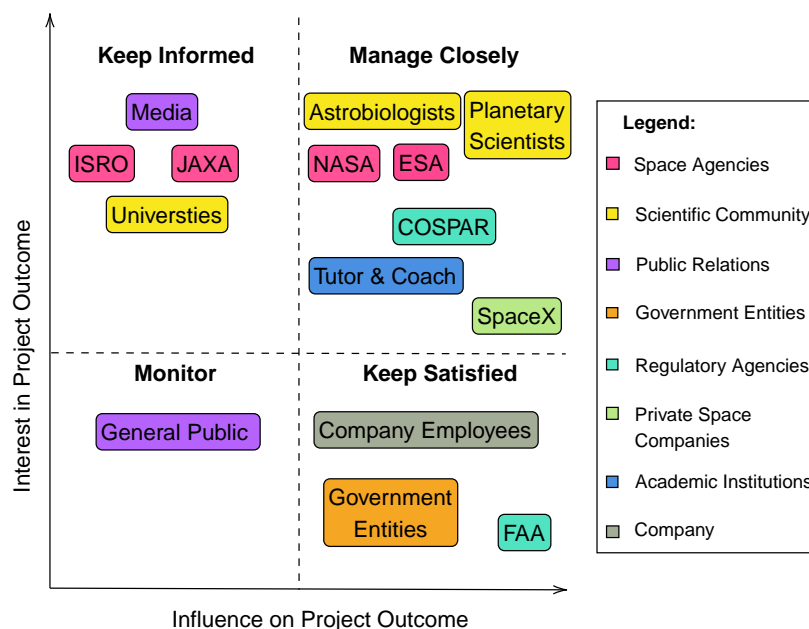

Figure 2.1: Stakeholder analysis of the AlienDive mission

As can be seen in Figure 2.1, the stakeholders with their identifiers are separated into categories. Their

---

[1]From `https://europa.nasa.gov/mission/faq/#:~:text=Initial%20mission%20concept%20studies%2C%20which,have%20a%20multi-year%20lifetime`, accessed on 16/05/2024.

position in the graph dictates whether they need to be managed closely, kept satisfied, kept informed, or monitored. The relative position of a stakeholder in a specific quadrant is not indicative of any additional information. The roles of each stakeholder are elaborated on in the list and if they are a key stakeholder it is indicated with [Key] below:

- **Space Agencies**: Note, other agencies could develop interest later on

  1. NASA [Key] (AD-STK-NASA): They are interested in the project outcome as they also would like to have a better characterisation of Europa to be able to design future missions with more certainty. Moreover, NASA will also develop RTGs and other parts if necessary

  2. ESA [Key] (AD-STK-ESA): ESA provides the funding for the project. They are also interested in the project outcome as they also would like a better characterisation of Europa to be able to design future missions with more certainty.

  3. ISRO (AD-STK-ISRO): ISRO aims to explore different planets in the solar system such as Mars and Venus [2] which means they do have an interest in exploring the solar system. Thus, they would want to be well informed in case they want to plot a mission to the Jovian system.

  4. JAXA (AD-STK-ESA): JAXA is also interested in exploring the solar system and thus they would want to be well informed on the data that is acquired from the Jovian system.

- **Government Entities** (AD-STK-GE): They influence the project outcome as they apply regulatory measures which could change the design. These measures could include the use of a radioisotope thermoelectric generator (RTG) in the mission which would be launched on US soil posing a risk to civilians.

- **Private Space Companies**:

  1. SpaceX [Key] (AD-STK-SX): They have an interest in the project due to the launcher choice, a failure in the launch mission segment could impact the company negatively from a publicity standpoint. They also influence the project outcome because the spacecraft needs to interface correctly with the Falcon Heavy.

- **Scientific Community**:

  1. Astrobiologists [Key] (AD-STK-AB): They have an interest in the project outcome as the mission's main goal is to unambiguously detect life. They would also influence the project outcome as the instruments used to detect life are required to be integrated correctly with the spacecraft.

  2. Planetary Scientists [Key] (AD-STK-PS): They have an interest in the project outcome as it would gather important scientific data. They would also influence the project outcome as the instruments used to provide imagery of the subsurface ocean required to be integrated correctly with the spacecraft.

  3. Universities (AD-STK-UNI): Universities around the world would want to get access to the data that is acquired in order to analyse the data and help the teams at the agencies if there truly is life in Europa.

- **Regulator Agencies**:

  1. COSPAR [Key] (AD-STK-PP): They have both an interest in the project outcome as they want to make sure we won't do any irreversible damage to Europa and they influence it as they apply specific measures which are aimed at protecting the moon which is going to constrict the design.

  2. FAA (AD-STK-FAA): The launch vehicle will be launched from the US which means that there will be regulatory measures on the launch itself which will influence the project outcome.

- **Academic Institutions**:

  1. Tutor & Coach [Key] (AD-STK-TC): They guide the team with their expertise and therefore influence the design choices the team makes which at the end will influence the project outcome. They are also interested in the project outcome because it will advance their knowledge in their fields of research.

- **Public Relations**:

  1. General Public (AD-STK-GP): They will have a small interest in the project outcome as the main goal is detecting life which would be intriguing. It will slightly influence the project outcome as with any mission, the sustainability factor is important which is aimed at protecting the general public

---

[2]From: `https://economictimes.indiatimes.com/news/web-stories/6-upcoming-space-missions-of-isro-in-2024/slideshow/105926819.cms?from=mdr`, accessed on 25/06/2024.

2. Media (AD-STK-MD): They will be interested in the project outcome as giving them updates will be important to maintain good public relations and therefore ensure that the project is viewed in a positive light.

- **Company**:

1. Company Employees [Key] (AD-STK-CE): They are the people working on the project and therefore maintaining a healthy work environment physically and mentally is important and thus will influence the project outcome. Furthermore, they will be interested in the project outcome as many of them would have played some role in ensuring the success of the mission.

2.5. Market Analysis

2.5.1. Market Size

AlienDive research can be considered part of the space exploration industry which now stands at a market value of approximately 656 billion dollars, and is growing with a Compound annual growth rate (CAGR) of 16.21%.[3] Compared to the average inflation of 3-4% and the average CAGR of all industries is approximately 12.04%, both are significantly lower than the Space Exploration Industry.[4] It is expected that the space exploration market will be valued at around 1.8 trillion in 2035.[5] This will be favourable for AlienDive, due to its large budget. The upcoming space exploration phase of ESA, Voyage 2050, which will span from 2035-2050, has three main themes: "New physical probes of the early Universe", "From temperate exoplanets to the Milky Way" and "Moons of the giant planets". This last theme is important for the space market of icy moons. NASA is also already interested in these moons, with Europa being in the top three bodies of interest in the Solar System. Thus the market size of Europa exploration will likely increase in the coming years.

2.5.2. Market Demand for a Europa Lander

Since multiple satellites will have been sent to Europa by the time AlienDive launches, means that the next step should entail a lander mission. The first successful satellite sent to Mars was the Mariner 4 in 1964. The first successful lander, the Viking 1, was launched in 1975. Eleven years after the first satellite, The first satellite that will be analysing Europa was sent in 2023, the JUICE mission, and an additional satellite, Europa Clipper, that will be sent in 2024. Eleven years later in 2034, it would make sense to have a lander mission. Additionally, the difference between the first moon orbiter and the lander is even shorter. This, however, was likely caused by the space race.

With Europa lander concepts dating back to 2005, it has been considered for a while. It was also reconsidered multiple times during the 2005-2021 period. The motivation for a lander is also emphasised in a NASA review, despite that, it was discarded due to current infeasibility and in favour of Enceladus Orbilander and the Uranus Orbiter and Probe [5].

2.5.3. Other Proposed Missions

Other L-class missions that will be sent between 2030-2035 are Athena and LISA. These are part of the Cosmic Vision theme of ESA. Both are being launched between 2030-2035. Since ESA only has one L-class mission per decade, this makes them competitors for the AlienDive mission. [6] In the future there would likely be more L-class missions however due to the launch date constraint this will not be possible for the AlienDive mission.

2.5.4. Market Position

Europa takes an interesting position in the market of planetary exploration. Due to its difficulty and high science potential, it has several strengths, weaknesses, opportunities and threats. These can be seen in the SWOT diagram in Figure 2.2.

---

[3]From `https://www.sphericalinsights.com/reports/space-exploration-market`, accessed on 14/06/2024

[4]From `https://pages.stern.nyu.edu/~adamodar/New_Home_Page/datafile/histgr.html`, accessed on 14/06/2024

[5]From `https://www.thenationalnews.com/future/space/2024/04/08/global-space-economy-projected-to-be-worth-18-trillion-by-203` accessed on 14/06/2024

[6]From   `https://sci.esa.int/web/cosmic-vision/-/59977-missions-ofopportunity#:~:text=Large%20(L%2Dclass)%20missions,carried%20out%20with%20international%20partners.`, accessed on 14/06/2024
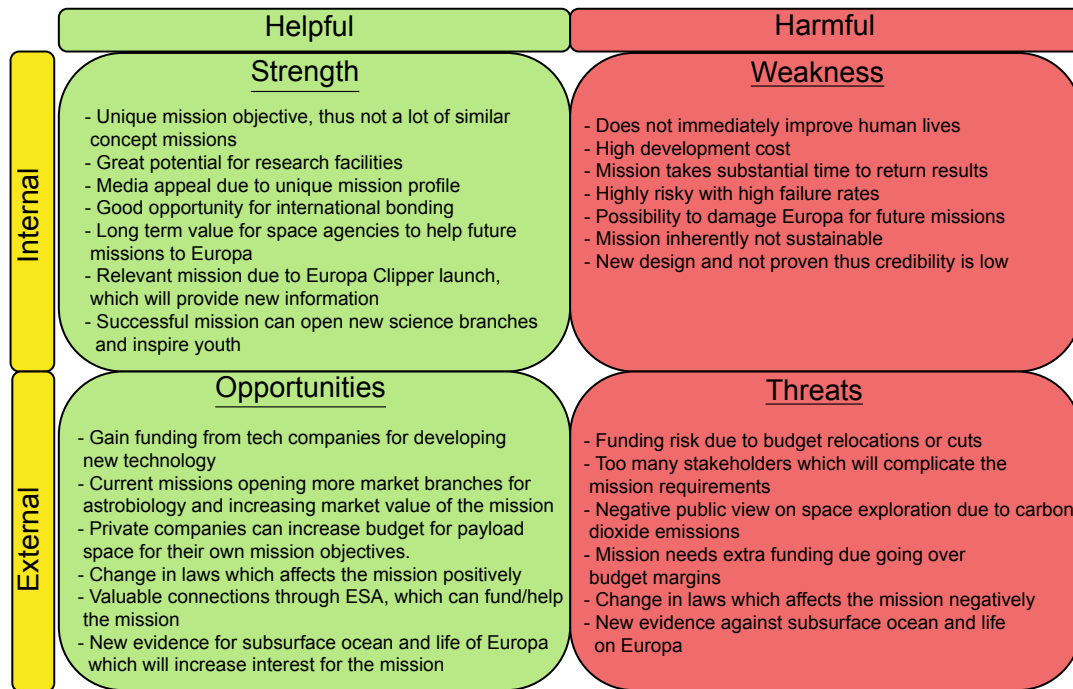
Helpful	Harmful
Strength - Unique mission objective, thus not a lot of similar concept missions - Great potential for research facilities - Media appeal due to unique mission profile - Good opportunity for international bonding - Long term value for space agencies to help future missions to Europa - Relevant mission due to Europa Clipper launch, which will provide new information - Successful mission can open new science branches and inspire youth	**Weakness** - Does not immediately improve human lives - High development cost - Mission takes substantial time to return results - Highly risky with high failure rates - Possibility to damage Europa for future missions - Mission inherently not sustainable - New design and not proven thus credibility is low
Opportunities - Gain funding from tech companies for developing new technology - Current missions opening more market branches for astrobiology and increasing market value of the mission - Private companies can increase budget for payload space for their own mission objectives. - Change in laws which affects the mission positively - Valuable connections through ESA, which can fund/help the mission - New evidence for subsurface ocean and life of Europa which will increase interest for the mission	**Threats** - Funding risk due to budget relocations or cuts - Too many stakeholders which will complicate the mission requirements - Negative public view on space exploration due to carbon dioxide emissions - Mission needs extra funding due going over budget margins - Change in laws which affects the mission negatively - New evidence against subsurface ocean and life on Europa

(Internal / External axis labels on the left)

Figure 2.2: Market SWOT analysis of the AlienDive mission.

The strengths of the AlienDive mission primarily lay in the unique science potential. It has invaluable data about possible extraterrestrial life and Europa. This will be very useful for follow-up missions. Due to the recent JUICE and Europa Clipper, which will provide data until around 2035 [6], the motivation to explore Europa will be increased. If useful data about extraterrestrial life is found, this has a chance to open up new branches of science and possibly excite a new space race to Europa. The main weakness of the AlienDive mission is the high risk and high cost. Due to the dangerous and unknown environment of Europa, there are a multitude of factors that could negatively impact the mission. It also takes a long time for it to provide useful data. The opportunities are based on external factors like private companies buying payload space or developing new technology. Current missions can also better the market position of AlienDive by providing more motivation to go to Europa or open new research branches. The biggest threat to the mission is budget cuts or relocations, due to the competition of other missions, this could prove to be difficult to get the funding from ESA. This would become an even bigger problem if extra funding is needed due to unforeseen issues. Also, the public view on space exploration could be negatively impacted due to carbon emission concerns. It comes as no surprise that data disproving an ocean on Europa could cancel the mission as a whole.

2.5.5. Increasing Market Position

Several measures can be taken to improve the market position of the AlienDive mission. The first and most important one is to enhance the scientific potential of the mission. Maximising the amount of useful data that can be generated, can increase the encouragement of the academic community to launch the mission. Additionally, science objectives, like monitoring Jupiter's moons during the journey to Europa can be included. Another way to boost the incentive to launch the mission is to include experimental technology which still needs to be flight tested. For example, a new way to generate energy or a new RTG concept can be integrated into the design. To make sure the money invested in AlienDive helps the local economy, most of the components will be produced and tested in Europe. This will also help with publicity for a more positive look at the mission. To focus on the publicity of the mission a design challenge can be set up. In this concept, volume, mass, and power will be allocated to a small rover designed and built by students. This will likely entice the public to look closer at the mission and support it. It will also help students get more real-life experience and educate the next generation of space mission designers. Lastly, it is vital to communicate well with multiple branches of the scientific community to see what is crucial for their field to have on the mission. This would engage the academic community even more in the mission.

2.5.6. Possible Follow-up Missions to AlienDive

If the AlienDive mission is deemed feasible and yields positive results, massive stimulus will be generated for sending another mission. This would likely be to see if terrestrial life on Europa would be feasible. It could also include sample retrieval missions. It could also have a massive impact on icy moon exploration

3   Trade-Off Summary

During the midterm of this design project, a trade-off was performed to determine the most promising system-level concept. In this section, the concepts discussed are shortly explained and a summary is given of the trade-off and its outcome.

Four different concepts were considered during the system-level concept trade-off. The first concept consists of a lander that uses a laser to drill through the ice, which lowers a scientific probe into the ocean (Concept 1). This concept was however discarded early on due to the large amount of power required for such a laser, in addition to other problems such as attenuation due to vapours that would be created during melting. Another concept that was discarded early on was a concept that dropped a self-sufficient probe onto the surface that could locate and enter the ocean through pre-existing plumes on the surface of Europa, using an orbiter to communicate to Earth (Concept 4). The reason for this discarding was the large uncertainty on the existence of these plumes, lowering the flexibility of the mission significantly. Additionally, communication through the plume would turn out challenging due to the high level of RF attenuation and lack of possibility of dropping relays.

The two feasible options considered were to use a lander for communication with Earth, and a probe that moves through the icy crust using a heated drill (Concept 2), or a self-sufficient probe moving through the ice using a heated drill, but now using an orbiter to communicate with Earth rather than a lander (Concept 3). A more detailed overview of these two concepts is shown in Table 3.1.

Table 3.1: Overview of the two system-level concepts considered for the trade-off in the midterm of the project [7].

Element	Concept 2: Lander+Ice-Breaking Probe	Concept 3: Self-Sufficient Probe
Ice-breaking Method	Heated drill	Heated drill
Power System	*Probe*: RTG or micro-nuclear reactor *Lander*: RTG	*Probe*: RTG or micro-nuclear reactor
Orbiter Presence	No	Yes
Communications System	Fibre-optic tether or RF relay transceivers	Fibre-optic tether or RF relay transceivers
Mass	8446.7 kg	10 014.2 kg
Cost (FY2024)	M$560.7	M$630.0

The concepts were scored on four different criteria: The potential for science, given a weight of 30%, since science increases the value of the mission; The technology readiness of the concept, given a weight of 20%, as a high Technology Readiness Level (TRL) will reduce the risk of the mission and reduce development time; The reliability of the concept, given a weight of 40%, since an unreliable concept is unlikely to reach the science goals; And lastly the mass and cost of the concept, given a weight of 10%, since a low-cost mission is desired over a more expensive one, it is not necessarily a deal-breaker criteria.

The trade-off summary table is found in Table 3.2. The conclusion of this trade-off is that the lander + ice-breaking probe concept equalled or outperformed the self-sufficient probe in all categories. It allows for more science to be done, as the lander is used for surface measurements, it has to survive a much smaller dose of radiation and is less heavy. In addition, planetary landers are not a new concept, so the technology readiness level of the concept is not much of a drawback.

Table 3.2: Summary Table of Mission Concept Level Trade-Off [7].

Criteria	Potential for Science	Technology Readiness	Reliability	Mass and Cost	Total Score
Weights	30	20	40	10	100
Concept 1: Ice-Breaking Lander + Probe	N/A	No available ice-breaking mechanisms that could be used (0)	N/A	N/A	N/A
Concept 2: Lander + Ice-Breaking Probe	Lander can be used for seismic measurements, gives information about Europa's interior (3)	Landers successfully deployed in the past, low technology readiness to enter the ocean (2)	In case of probe failure surface sampling is still possible which can partially fulfil mission objectives, lander radiation is 5.481×10^9 rad per year (2)	Mass: 8.5 tons Cost: M\$561 (2)	230
Concept 3: Self-Sufficient Probe	Orbiter's possible scientific experiments overlap with existing missions (2)	Orbiters successfully done in the past, low technology readiness to enter the ocean (2)	In case of probe failure only imaging is possible, limited science that can be done, orbiter radiation is 10×10^{10} rad per year (1)	Mass: 10 tons Cost: M\$630 (1)	150
Concept 4: Self-Sufficient Plume Probe	N/A	No previously done concepts of communications with the probe in the plume (0)	Large uncertainty in terms of characteristics of the plumes environment and probe survival possibilities (0)	N/A	N/A

Legend	Excellent (3)	Good (2)	Acceptable (1)	Unacceptable (0)

To confirm that this concept is actually the desired choice, a sensitivity analysis was performed on the results. In this analysis, a Monte-Carlo simulation was performed on the weights and scores of the trade-off. Even when varying these scores randomly, the lander + ice-breaking probe concept won approximately 99.9% of the tested events. Even in the cases where both scores fell within the overlap between the highest possible scores for Concept 3 and the lowest possible scores for Concept 2, Concept 2 won around 99.5% of the time, solidifying its position as the winner of the trade-off.

4 Scientific Payload

This chapter describes the scientific payload included in the mission. Firstly the science traceability matrix is included in Section 4.1, then the probe and lander payload is outlined in Section 4.2 and Section 4.3.

4.1. Science Traceability Matrix

The Science Traceability Matrix is an essential component of any scientific space mission design. For Alien-Dive, the Science Traceability Matrix was established during the baseline phase [8]. An updated version of the matrix is given in Table 4.1. The last column denotes the instrument that was selected to fulfil each requirement; a more detailed description of each instrument and the selection process is given in Section 4.2.

Table 4.1: Science Traceability Matrix

Physical Parameter	Observable	Requirements	Instruments
Science goal 1: directly detect active microbial life in Europa's subsurface ocean			
Active movement	Particle movements unrelated to the flow of the surrounding water [9]	The payload shall determine flow direction to within an accuracy of TBD.	Ultrasonic sonar, microscope
		The payload shall determine flow velocity to within an accuracy of TBD.	
		The payload shall determine particle movement direction to within an accuracy of TBD.	
		The payload shall determine particle velocity to within an accuracy of TBD.	
Cell replication	Feature growth in a sample [9]	The payload shall determine the size of a sample to within an accuracy of TBD.	Microscope
		The payload shall determine the size of a sample once every 30 minutes.	
Science goal 2: directly detect active multicellular life in Europa's subsurface ocean			
Active movement	Particle movements unrelated to the flow of the surrounding water [9]	The payload shall determine flow direction to within an accuracy of TBD.	Ultrasonic sonar, context camera
		The payload shall determine flow velocity to within an accuracy of TBD.	
		The payload shall determine particle movement direction to within an accuracy of TBD.	
		The payload shall determine particle velocity to within an accuracy of TBD.	
Controlled growth	Feature symmetry in a sample [9]	The payload shall capture images of a sample with a resolution of TBD.	Context camera, detail camera, microscope
Science goal 3: detect chemical signatures of life in Europa's subsurface ocean			
Possible protein formation	Presence of amino acids [10]	The payload shall be able to detect amino acids at concentrations higher than TBD.	
		The payload shall determine the concentration of amino acids in a sample to within an accuracy of [TBD].	

Amino acids of biological origin	Chirality excess of amino acids [10]	The payload shall determine the chirality ratio of a sample of amino acids to within an accuracy of TBD.	
Presence of cell membranes	Presence of phospholipids [10]	The payload shall be capable of detecting phospholipids at concentrations higher than TBD.	
		The payload shall determine the concentration of phospholipids in a sample to within an accuracy of TBD.	
Presence of genetic material	Presence of nucleotides [10]	The payload shall be capable of detecting nucleotides at concentrations higher than TBD.	
		The payload shall determine the concentration of nucleotides in a sample to within an accuracy of TBD.	
Presence of spore-producing bacteria	Presence of dipicolinic acid [10]	The payload shall be capable of detecting dipicolonic acid at concentrations higher than TBD.	
		The payload shall determine the concentration of dipicolonic acid in a sample to within an accuracy of TBD.	
Presence of biological carbon-based compounds	Carbon isotope ratio skewed towards lower mass [9]	The probe shall determine the carbon isotope ratio in a sample to within an accuracy of TBD.	
Science goal 4: characterise the habitability of Europa's subsurface ocean environment			
Temperature		The payload shall determine water temperature to within an accuracy of TBD.	Thermocouple
Acidity		The payload shall determine water pH to within an accuracy of TBD.	Wet Chemistry Lab
Salinity	Water conductivity	The payload shall determine the concentration of salts in the water to within an accuracy of TBD.	
Abundance of CHNOPS [10]	Concentration of carbon	The payload shall determine the concentration of carbon in the water to within an accuracy of TBD.	
	Concentration of hydrogen	The payload shall determine the concentration of hydrogen in the water to within an accuracy of TBD.	
	Concentration of nitrogen	The payload shall determine the concentration of nitrogen in the water to within an accuracy of TBD.	
	Concentration of oxygen	The payload shall determine the concentration of oxygen in the water to within an accuracy of TBD.	
	Concentration of phosphorus	The payload shall determine the concentration of phosphorus in the water to within an accuracy of TBD.	
	Concentration of sulphur	The payload shall determine the concentration of sulphur in the water to within an accuracy of TBD.	

4.2. Probe Payload

Based on the science traceability matrix, a number of scientific instruments was chosen for the subsurface probe. Most instruments were chosen to fulfil more than one requirement in order to save mass, volume, and power. A summary of the probe scientific payload is given in Table 4.2, and the function of each instrument as well as the reasoning for its selection are outlined in the following subsections.

Table 4.2: An overview of the scientific instruments selected for the payload of the AlienDive subsurface probe.

Instrument	Mass [kg]	Volume [L]	Peak Power [W]
Context Camera (incl. lens)	0.35	0.88	2.5
Detail Camera (incl. lens)	0.36	1.1	2.5
Microscope (camera + lens + light)	0.33	0.41	3.0
Thermocouples (2x)	0.050	Negligible	Negligible
PISCES	3.0	8.7	2.0
Life Marker Chips	4.6	Unknown	35
Raman Spectrometer	0.01	0.072	Unknown
Fluorescence Spectrometer	0.69	0.66	Unknown
UV Spectrometer	0.0050	0.0025	Unknown
Ultrasonic Sonar	0.51	1.6	5.0
Wet Chemistry Lab	0.50	Negligible	30
Flashlight	2.0	Negligible	50
Total	**17.5**	**32.4**	**145**

4.2.1. Sampling Channel

Although the Sampling Channel is, strictly speaking, a structural element of the probe and not a scientific instrument, it is included here for clarity as it is integral to the functioning of several instruments. The Sampling Channel is an open channel that runs through the probe's payload section, allowing water to continuously flow through it. It has hatches on both ends to close off the channel for certain measurements, for example, for capturing microscope images that would become blurry due to the water's constant movement. There are several tubes branching off from the channel, supplying the Life Marker Chips and the spectrometers with water samples. Each of these tubes can also be closed off with a hatch to control the amount of water fed to the instruments. Figure 4.1 shows how the Sampling Channel is oriented within the scientific payload. Once the water has passed through the instruments, it is channelled into a sample disposal tank to avoid contamination of the ocean.
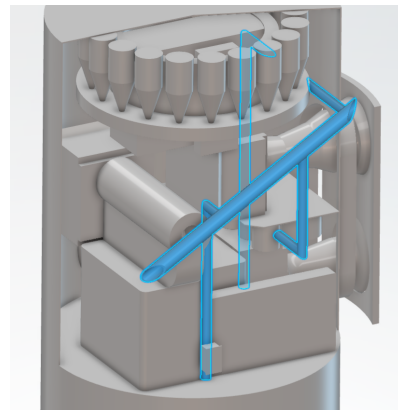
Figure 4.1: The Sampling Channel and attached tube system within the probe payload section.

4.2.2. Cameras

The AlienDive subsurface probe will carry three different cameras, each with its own function. The basis for each camera design is the Malin Space Science Systems (MSSS) ECAM-C50[1], chosen for its low mass and power consumption, as well as its versatility. The ECAM-C50 is designed to work seamlessly with three different off-the-shelf lenses, and MSSS offers customised lenses for this camera as well. By using the same body for every camera in the probe (as well as the lander, as discussed in Section 4.3), the complexity of the payload is kept to a minimum. In addition, the ECAM-C50 is already flight-proven.

The first of the three cameras is the so-called Context Camera. This camera looks to the outside of the

---

[1]From: `https://satsearch.co/products/msss-ecam-c50`, accessed on 19/06/2024.

probe and will be programmed to capture one image of the environment every 30 minutes at a resolution of 640x480 pixels. The lens used on this camera is the MSSS ECAM-WFOV[1], which provides a field of view measuring 77° horizontally and 55° vertically. The images taken are compressed in JPEG format with a ratio of 30:1 before being sent to the lander. In addition, the images are analysed by the probe's onboard computer. If significant differences between the most recent image and the previous image are detected, the Detail Camera is triggered. The Detail Camera is pointed in the same direction as the Context Camera, but captures images at a resolution of 2048x1080 pixels and is equipped with an ECAM-NFOV lens. This lens has a field of view of 25° horizontally and 19 ° vertically. Together, these cameras largely cover science goal 2 as described in Table 4.1.

The subsurface ocean environment is expected to be extremely dark due to the thick layer of ice covering it. To ensure that the images taken have sufficient scientific value, the payload is designed to include an LED flashlight mounted on the outside of the probe skin, surrounding the Detail and Context Cameras.

The final camera onboard the probe is mounted to a microscope pointed towards the Sampling Channel inside the probe. For the initial sizing of this microscope, a miniaturised, portable field microscope produced by Carson[2] was used as a reference. In later design stages, a custom microscope must be developed to ensure compatibility with the camera body and other onboard systems. The reference microscope has a magnification factor that can be set to anywhere between 100x and 250x and includes a light. This light must also be included in the payload to illuminate the Sampling channel and allow for images to be captured with the microscope. The microscope covers a large part of science goal 1, as detailed in Table 4.1.

4.2.3. Thermocouples

Two thermocouples are included in the probe, of which one is active and the other is included for redundancy. The thermocouple sizing is roughly based on the RS PRO IEC Exposed Junction Type K Thermocouple[3], which can measure temperatures between −75 °C and 250 °C. The thermocouples are included to contribute to science goal 4 as outlined in Table 4.1.

4.2.4. Wet Chemistry Lab

The AlienDive Wet Chemistry Lab (WCL) concept is heavily based on the WCLs aboard the 2007 Mars Phoenix Lander developed for chemical analysis of Martian regolith [11]. The 2007 Phoenix Mars Lander contained four WCLs that were part of a larger experiment called the Microscopy, Electrochemistry, and Conductivity Analyser (MECA). Each Phoenix WCL consisted of a beaker containing several sensors and electrodes, and an actuator assembly used for mixing soil, water, and reagents [11].

The implementation of a WCL on the AlienDive subsurface probe differs significantly from the Phoenix Lander. The WCLs on the Phoenix Lander were designed for analysis of solid materials, which had to be actively sampled and dissolved in water before obtaining data - this is where the aforementioned actuator assembly comes in. The AlienDive WCL does not require such an actuator assembly as the materials it will analyse are already dissolved in water. This eliminates most of the moving parts that were necessary in the Phoenix Lander. The electrodes are directly integrated into the Sampling Channel, requiring no additional sample handling. This approach also allows for measurements at regular intervals as water is continuously flowing through the Sampling Channel, providing context for other measurements. Together with the thermocouples, the Wet Chemistry Lab covers science goal 4 as outlined in Table 4.1.

4.2.5. PISCES

The Planetary In Situ Capillary Electrophoresis System, abbreviated to PISCES, is a lab-on-a-chip capillary electrophoresis instrument proposed by Willis et al. in 2012 [12]. Although in 2012 the instrument was still in development, the proposal did state that the instrument was possible to build using readily available components. Although it was not specifically developed for use on Europa, PISCES seems particularly suitable for AlienDive's scientific payload. It has been demonstrated to function at temperatures below −20 °C, has a sensitivity in the parts-per-trillion range, and can analyse samples whether they are in liquid, gaseous, or solid form [12]. It can detect the presence of amines, amino acids, short peptides, aldehydes, ketones, carboxylic acids, thiols, and polycyclic aromatic hydrocarbons in a sample, all of which are chemical compounds linked to the formation of life [12]. PISCES contributes to science goal 3 as stated in Table 4.1.

---

[2]From: https://microscopeinternational.com/carson-mp-250-microflip-100x-250x-led-and-uv-lighted-pocket-microscope-with-flip accessed on 19/06/2024.

[3]From: https://nl.rs-online.com/web/c/automation-control-gear/sensors/thermocouples/?pn=1&applied-dimensions= 4294569320,4294560724,4294556296,4294563863,4294571614,4294566973,4294564610&sortBy=P_brand&sortType=ASC, accessed on 19/06/2024.

4.2.6. Life Marker Chips

Life Marker Chips are a type of instrument developed for the European Space Agency's ExoMars mission [13]. They detect specific molecules using antibody-based detectors. This works according to a sort of "lock and key" principle: for each molecule of interest, an antibody is developed that only reacts with that specific molecule; any other molecule is simply ignored by the instrument [14]. Although this comes with a disadvantage, namely that since the antibodies cannot be regenerated each individual Life Marker Chip can only be used once, there is a great advantage to this approach as well. Since the antibodies only react to their target molecule, the signal associated with the target molecule will not be obscured by the presence of other compounds [14]. That means that Life Marker Chips can detect traces of a molecule of interest that would get lost in the more complex signals generated by, for example, a spectrometer. Because of that, combined with their narrow use case and limited capacity, Sephton et al. recommend using Life Marker Chips in combination with more broad detection methods [14]. In that way, samples that have been deemed particularly promising based on data collected by said broad detection methods can be analysed further by the Life Marker Chips. Using that method, the Life Marker Chips included in the AlienDive probe payload are expected to contribute to science goal 3 as stated in Table 4.1.

4.2.7. Spectrometers

Spectroscopy is considered an essential tool in the search for extraterrestrial life [15][16]. There are many types of spectrometers available, three of which have been selected to be included in the probe payload: a Raman spectrometer, fluorescence spectrometer, and ultraviolet spectrometer. Each of these spectrometer types is mentioned in [16] as promising methods to detect biosignatures. Together, the three spectrometers cover science goal 3, and may also contribute to science goal 4, as outlined in Table 4.1.

Raman spectrometers are frequently mentioned in literature regarding the search for life as they are sensitive to compounds containing carbon [16]. The Raman spectrometer selected for the AlienDive probe is the Hamamatsu C14214MA TF series mini-spectrometer[4], selected for its small size and mass. It operates at wavelengths between 790 and 1050 nanometres with a spectral resolution of at least 0.6 nanometres. The selected fluorescence spectrometer is the Hamamatsu C10082CA TM series mini-spectrometer[4], also chosen for its compactness. It operates at wavelengths between 200 and 800 nanometres with a spectral resolution of at least 6 nanometres. Finally, the selected UV spectrometer is the Hamamatsu C16767MA Micro series mini-spectrometer[4], a highly miniaturised spectrometer operating at wavelengths between 190 and 440 nanometres with a spectral resolution of at least 5.5 nanometres.

4.2.8. Ultrasonic Sonar

To cover science goals 1 and 2 in Table 4.1, an ultrasonic sonar is included in the payload. This instrument is meant to detect objects in the water and gather information about their movement. Although it cannot directly measure the flows surrounding the probe, a high-performance sonar instrument can detect objects underwater smaller than 10 mm [17]. The flow direction and velocity of the water can then be derived from the movement of objects. If a particle is found to move in a way that is contradictory to the flow it is in, that could be an indication that the particle is a life form capable of actively propelling itself [9]. For sizing purposes, the Ping360 Scanning Imaging Sonar produced by Blue Robotics[5] is used as a reference.

4.2.9. Data budget

Assuming a probe lifetime of 1 year, from the moment it enters the ocean, a data budget was determined and divided over the instruments. The limiting factor here is the amount of data that can be transmitted over the relays before they run out of power. This is further elaborated upon in Section 8.7. The data budget allocation is shown in Table 4.3.

---

[4]From: `https://www.hamamatsu.com/us/en/product/optical-sensors/spectrometers/mini-spectrometer.html`, accessed on 19/06/2024.

[5]From `https://bluerobotics.com/store/sonars/imaging-sonars/ping360-sonar-r1-rp/`, accessed on 18/06/2024.

Table 4.3: The data budget allocation for the scientific payload of the probe

Instrument	Total data generated [Gbit]	Fraction of total [%]	Amount of measurements:
Thermocouple	0,00035	0,0041	17546
Context camera	1,4	17	17546
Ultrasonic sonar	0,088	1,0	17546
Wet Chemistry Lab	0,0088	0,10	17546
Microscope	4,8	56	8000
Raman Spectrometer	0,084	0,98	2400
PISCES	0,0024	0,028	2400
Life Marker Chips	0,000040	0,00047	80
Fluorescence Spectrometer	0,084	0,19	2400
UV Spectrometer	0,012	0,14	2400
Detail Camera	2,0	24	3387

4.3. Lander Payload

Although the top-level science requirements listed in Section 2.2 do not specify any activities to be conducted on the surface of Europa, it was determined during the design process that it is possible to include a limited number of scientific instruments in the lander itself. In addition to this, some of the onboard systems used for landing site selection can be used after landing to gather additional data. Each instrument is explained in more detail in the subsections that follow.

4.3.1. Seismometers

Since the lander will stay in one place on the surface for the remainder of the mission after deploying the ice-breaking probe, it may be interesting to use it to collect seismic data. Such data can be used to more accurately predict what the inner structure of Europa looks like [18]. A recent advancement in seismometer technology is the concept of miniaturised seismometers. Such a seismometer, the SEIS-SP, has been deployed before on the InSight lander on Mars, in 2018 [19]. The SEIS-SP experiment consists of three Micro-Electrical-Mechanical System (MEMS) sensors, allowing the instrument to be made very small: each sensor measures a mere 25 mm by 25 mm, with a thickness of approximately 5 mm.[6] The experiment is also lightweight, with the full package, including electronics, weighing only 0 635kg. It is resistant to shocks and vibrations and has a wide operational temperature range, from $-80\,°C$ to $60\,°C$. In addition to that, it does not require any levelling and consumes only 0.36 W while active [19]. Despite these advantages, the sensitivity of this instrument is comparable to that of the (much larger) seismometers used on the Apollo missions [19]. It would be valuable to include a similar instrument on the AlienDive lander, as it would not take up much space, mass, or power, but could contribute significantly to humanity's knowledge of Europa's inner structure.

4.3.2. Magnetometer

Another way to deduce information about Europa's inner structure is by measuring the magnetic field surrounding the moon. In fact, a large part of the evidence supporting the existence of Europa's subsurface ocean was discovered using a magnetometer aboard the Galileo probe: the magnitude of the magnetic field the probe measured during a close flyby could only be explained by a current flowing near Europa's surface, leading to the conclusion that there must be a global salty ocean beneath Europa's ice crust [20]. To better understand the characteristics of this ocean on a global scale, it is beneficial to include a magnetometer in the AlienDive lander as well.

The issue with magnetometers is that, since any electric current generates a magnetic field, a magnetometer mounted inside a spacecraft will measure the magnetic field generated by the spacecraft's own systems, making it difficult to accurately characterise Europa's magnetic field. This problem can be mitigated by placing the magnetometer far away from any other systems. In the design of the Europa Clipper, this is done by mounting the magnetometers on an 8.5 m long boom [21]. For AlienDive, however, this would take up too much volume

---

[6]The thickness of the sensors is not explicitly mentioned in [19]. However, this source does provide an image of one of the sensors and the thickness has been estimated based on the known dimensions and this image.

within the spacecraft. A mission concept from 2018 [22] suggests placing a magnetometer inside a separate probe that is deployed from the lander once it has reached the ground. This probe would be connected to the lander by cables for power and communication, but be otherwise physically separated from the lander. For AlienDive, this method would be much more suitable in terms of mass and volume requirements, although it does add complexity to the mission.

For initial sizing purposes, it is assumed that a magnetometer onboard the AlienDive lander would be deployed on a separate probe that is shot out of the lander using a loaded spring system. For the mass, volume, and power requirements of the magnetometer, the Europa Clipper magnetometer [21] was used as a reference.

4.3.3. Cameras

The AlienDive lander has three cameras on board, all using the MSSS ECAM-C50 camera body as a basis - the same as used in the probe. One of these cameras is called the Reconnaissance Camera. The Reconnaissance Camera is mounted to a narrow field of view custom lens. During the reconnaissance orbit, this camera is used to map the surface of Europa to aid in landing site selection, as outlined in Section 5.3. These images, however, will also have significant scientific value and may be combined with images gathered during the Europa Clipper mission to create a comprehensive map of the Europan surface [23], as well as analysed by planetary geologists for more clues regarding geological processes on the moon.

In addition to the Reconnaissance Camera, the lander includes two so-called Landing Cameras. These cameras are both mounted to MSSS ECAM-MFOV lenses, which have a horizontal field of view of 44° and a vertical field of view of 33°. They are used to capture images of the surface as the spacecraft is descending and landing, a process further outlined in Figure 5.8. As with the images captured by the Reconnaissance Camera, those captured by the Landing Cameras may also be used to create a surface map of Europa and for geological research.

4.3.4. LIDAR

The LIDAR onboard the lander, the LIDAR for Extraterrestrial Imaging Applications (LEIA) produced by MDA[7], is used to create Digital Elevation Maps (DEMs) of the surface of Europa during the landing phase of the mission. The use of these DEMs in the landing process is outlined in Figure 5.8. In addition to being useful for landing, the DEMs also provide valuable scientific data that can be used for more accurate mapping of Europa. After landing, it may be possible to use the LIDAR to construct a three-dimensional model of the lander's surroundings, which besides science may also be interesting for public outreach.

4.3.5. Competition Rover

There is some space reserved in the lander for a small surface rover as part of a public outreach programme. An open competition will be organised to select a rover, and as such, it is as of yet unknown which science instruments will be on board this rover.

---

[7]From: `https://satsearch.co/products/mda-leia-lidar-for-extra-terrestrial-imaging-applications`, accessed on 19/06/2024.

5 Mission Design

This chapter details the mission design of the AlienDive mission. Section 5.1 details the operations and logistics related to the mission. The launch and trajectory to Europa are discussed in Section 5.2. Information on the reconnaissance orbit can be found in Section 5.3. Next, the deorbit, descent and landing sequence is laid out in Section 5.4. Subsequently, the total system overview is presented in Section 5.5. Finally, a functional analysis is provided in Section 5.6.

5.1. Operations and Logistics
An overview of the mission operations can be found in Figure 5.2. The operations are divided into categories, which are described in more detail in the following subsections.

O: Travel to Europa
The AlienDive Spacecraft is planned to launch on the 14th of May, 2034, from Kennedy Space Center in Florida. The spacecraft is injected into a transfer orbit to Jupiter and will arrive there in February 2038. Subsequently, the spacecraft is placed in a transfer orbit to Europa, where it is expected to arrive in June 2040. Once it has been inserted into orbit around Europa, the spacecraft will orbit the moon for seven days while a suitable landing site is selected based on images taken by the lander and sent back to Earth for analysis. Finally, the lander will separate from the transfer stage, descend to the surface, and autonomously perform a soft landing on Europa's ice crust. More details about the launch and travel to Europa are given in Section 5.2.

I: Break through Ice
Once the spacecraft has landed, the probe is powered up and released from the lander onto the surface. Next, the thermal system and drill of the probe are activated, allowing it to descend through the ice crust. Along the way, RF relay transceivers are deployed at different places within the ice. Once the probe reaches the subsurface ocean, it will deploy an anchor to attach itself to the bottom of the ice crust.

S: Conduct Scientific Operations
Scientific operations already begin when the spacecraft is in orbit around Europa. The spacecraft captures images of the surface which are sent back to Earth to select a landing site, and it continues doing this until landing. Once landed, the lander releases a magnetometer instrument along with the probe and collects seismic data using a built-in seismometer. Throughout the ice-breaking phase of the mission, the probe collects data on the ice temperature and composition as it descends through the crust. Once it has reached the ocean, it collects scientific data. While collecting data, the probe will also slowly unspool the cable used to anchor it to the ice, to allow it to descend further into the ocean and collect data at different depths.

C: Communicate with Earth
Operations related to communication are conducted throughout the entire mission, from launch to retirement. While travelling to Europa, the spacecraft maintains status communication with Earth. Once in orbit, it will send images of Europa's surface to Earth to aid in the selection of a landing site. Once the probe has started traversing the ice crust, it communicates its status and the scientific data collected with the lander using the RF relays it deploys in the ice along the way. The lander then relays the information it receives to Earth using NASA's Deep Space Network. Status communication is maintained with both the lander and the probe up until the end of their lifetimes. Figure 5.1 shows the downlink communication flow diagram. The amount of data gathered by the probe over a year is limited by the battery life and maximum data rate (discussed in section Section 8.7) of the RF relay transceiver modules to approximately 9.6 Gb. The probe needs to be operational in the subsurface ocean for one year, meaning 0.184 Gb of data, of which the majority is scientific data, is stored every week on the probe. Every week this data is transmitted to the lander over 5 hours and 20 minutes. Here, the data is stored with the addition of scientific and housekeeping data from the lander. To reduce the cost of communicating with the Deep Space Network, a total of 0.368 Gb per week is communicated to the DSN over 5 hours en 15 minutes once a week.
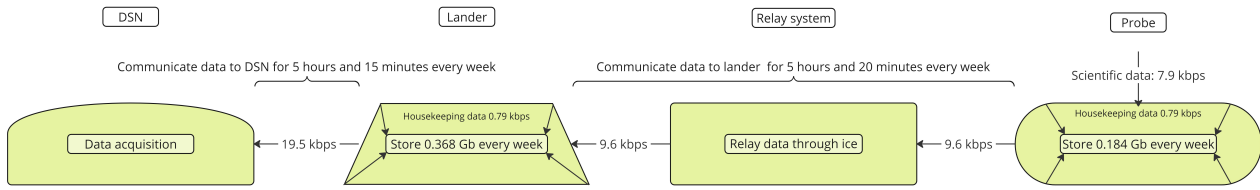
Figure 5.1: Downlink communication flow diagram

E: Commence End-of-Life Procedures

This phase includes implementing strategies to avoid contamination and space debris, and safely deactivating the mission's instruments and systems. Scientific instruments are deactivated first, followed by all other onboard systems. The communication systems are the last ones to be deactivated, so that status communication can be maintained for as long as possible. This is necessary to ensure that end-of-life procedures are implemented correctly. Once the ground station receives confirmation that this is indeed the case, the communication systems are shut off and the probe and lander are retired.
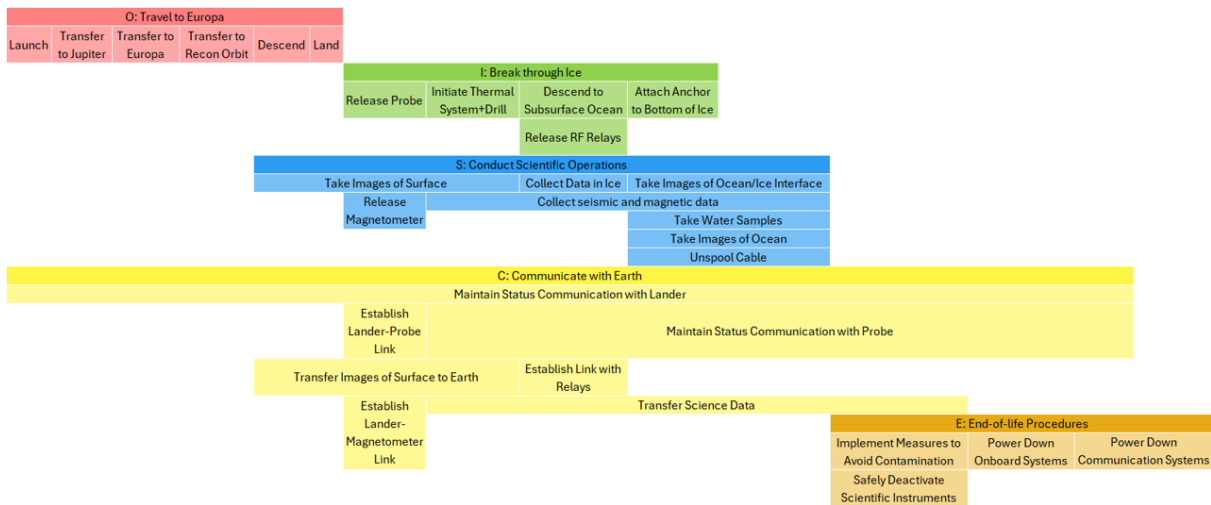
Figure 5.2: An overview of the timeline of the AlienDive mission from the moment of launch to the moment of decommissioning.

5.2. Launch & Trajectory

According to the top-level user requirement AD-SCH-01, the mission shall launch no later than 2035. To ensure compliance with this requirement while allowing for allocating as much time for the design phase as possible, the launch dates analysed were between 2033 and 2035. Firstly, a desired trajectory to arrive at Jupiter's orbit was chosen, which allowed for establishing the launch window. Figure 5.3 presents the final trajectory from Earth to Jupiter.

In order to minimise the Delta-V for the mission, multiple gravity assists shall be used to arrive at Jupiter. The most effective in terms of Delta-V savings is the Venus-Earth-Earth Gravity Assist (VEEGA) [24]. The gravity assist around Venus and the first gravity assist around Earth are used to increase the apocentre of the orbit to enable the spacecraft to obtain a sufficient amount of energy to go to Jupiter. Subsequently, the second assist via Earth serves the purpose of decreasing the velocity increment necessary for Jupiter's orbit insertion

Figure 5.3: Trajectory from Earth to Jupiter.

[24]. This trajectory allows for the launch of the largest dry mass. It is thus chosen for the AlienDive mission, as its primary objective is to gather scientific data on Europa which requires large amounts of payload.

For utilising VEEGA, it is determined using an interplanetary trajectory simulation software[1] that launching in midyear 2034 is desired. This takes into account the positioning of the planets in the Solar System throughout

---

[1]From `https://krafpy.github.io/KSP-MGA-Planner/`, accessed on 06/06/2024.

the whole trajectory. For the launch, the most favourable date is established to be on the 14th of May 2034 from Kennedy Space Center, but the launch window shall be a week long. The flybys around Venus, Earth, and Earth will be performed according to the timeline indicated in Figure 5.3. The launch vehicle used would be Falcon Heavy, and it would provide all the required Delta-V for achieving the trajectory to Jupiter, excluding the insertion into an orbit around the planet. The JOI burn of 839 m/s will be performed about 12 hours after a flyby around Ganymede, which will save approximately 400 m/s of Delta-V [25]. During the optimal launch window, no additional deep-space manoeuvre (DSM) Delta-V is needed. Moreover, in the next phases of the design, the trajectory will be analysed more extensively and possibly improved. Additional flybys might be added to the sequence to further reduce the Delta-V budget. For example, similarly to Galileo, the AlienDive spacecraft could perform flybys around the asteroids 951-Gaspra and 243-Ida which are located in the asteroid belt between Mars and Jupiter [26].

Following JOI, the spacecraft propelled by the transfer stage will begin its 1 year and 4 month journey to Europa. The trajectory taken will consist of 9 Ganymede flybys and 2 Callisto flybys, as detailed in Table 5.1. This strategy was chosen considering the Delta-V budget and the Total Ionising Dose (TID) the spacecraft would receive during the tour. With an increasing tour time, the required Delta-V for the manoeuvres decreases while the TID increases [25]. Both of these parameters can drive the mass of the spacecraft up, as a high Delta-V would increase the necessary propellant mass and a high TID would require more radiation shielding. The 1 year and 4 month-long tour minimises both of these parameters, as well as allows for imaging the surface of Ganymede and Callisto during flybys to increase the scientific value of the mission.

Table 5.1: Journey from Jupiter to Europa

Event		Date (GMT)	Delta-V [m/s]	v_∞ [m/s]	Altitude [km]
JOI		2039 FEB 01	839		
PJR		2039 APR 22	162		
Ganymede flyby	1	2039 AUG 17		5698	294
Ganymede flyby	2	2039 OCT 06		5629	185
Ganymede flyby	3	2039 NOV 18		5595	109
Callisto flyby	4	2039 DEC 28		6314	200
Ganymede flyby	5	2040 MAR 04		3806	205
Ganymede flyby	6	2040 MAR 30		3814	559
Ganymede flyby	7	2040 APR 15		3715	2170
Callisto flyby	8	2040 APR 30		1816	2879
Ganymede flyby	9	2040 MAY 03		1489	15818
DSM		2040 MAY 10	17		
Ganymede flyby	10	2040 MAY 26		1347	581
Ganymede flyby	11	2040 JUN 02		1396	3970
Europa Arrival		2040 JUN 04		1485	312

The tour begins with the raising of the perijove (PJR) of the orbit around Jupiter to achieve the first flyby around Ganymede. Then, the Ganymede flybys decrease the orbital period, and the two Callisto flybys further increase the pericentre. This allows for decreasing the needed Delta-V for Europa Orbit Insertion (EOI). Moreover, as shown in Figure 5.4, Ganymede and Callisto are outside the main radiation belts for Jupiter, as their orbits' semi-major axes are 15.31 and 26.89 times the radius of Jupiter, respectively. This means that the TID for the mission is minimised by choosing this trajectory. Moreover, it introduces the possibility of imaging these moons, which broadens the science that can be performed during the mission. The altitude of the Ganymede flybys is as low as 109 km, thus using the on-board camera described in Section 5.3, a
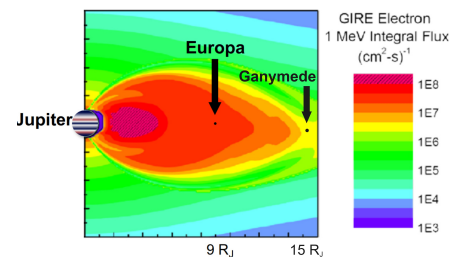

Figure 5.4: Radiation distribution around Jupiter[2]

---

[2]From `https://nepp.nasa.gov/docs/etw/2021/14-JUN-21_Mon/1130_McClure-Keynote-Europa-CL21-2225.pdf`, accessed on 13/06/2024.

resolution of 3.7 m/pixel can be achieved. For Callisto, the flyby altitude is 200 km yielding a resolution of 6.7 m/pixel.

After the tour around Ganymede and Callisto, the spacecraft will arrive at Europa on the 4th of June 2040. The transfer stage will perform the EOI burn, inclination change and circularisation to reach the desired near-polar reconnaissance orbit. There, it will begin the imaging of Europa's surface to find a safe landing site, as elaborated on in Section 5.3. The Delta-V that the spacecraft shall provide from JOI until circularisation in the target orbit is shown in Table 5.2. The table presents the required Delta-V for each manoeuvre and the design Delta-V to which margins have been applied. According to ESA standards, a margin of 5 % was applied to calculated manoeuvres such as JOI, PJR, DSM, EOI, inclination change, and circularisation [27]. In the case of gravity assists of planetary moons like Ganymede and Callisto, a Delta-V margin of 10 m/s shall be included to account for preparation and correction of each of these manoeuvres [27].

Table 5.2: Delta-V for JOI until circularisation in the Europa reconnaissance orbit

Event	Delta-V [m/s]	Incl. Margin [m/s]
JOI	839	880.95
PJR	162	170.1
Ganymede flybys	0	90
Callisto flybys	0	20
DSM	17	17.85
EOI	239.7	251.7
Inclination change	2033.8	2135.5
Circularisation	416.7	437.6

The EOI burn is designed to bring the spacecraft into a highly eccentric orbit (e = 0.74) with the pericentre at 312.16 km altitude. Taking into account the velocity acquired at the last Ganymede flyby, the Delta-V necessary for this manoeuvre is 839 m/s. Due to the DSM that will be performed amidst Jovian moon flybys, the inclination change that has to be done to reach the target of 85° is estimated to be only 10° according to 2012 Report of the Europa Lander [25]. The manoeuvre will be performed at the apocentre to minimise the needed Delta-V. Then, the orbit will be circularised to reach the target reconnaissance orbit.

5.3. Reconnaissance Orbit

The reconnaissance orbit is near circular with an inclination of 85 degrees, the mean altitude of 312.16 km, and other specifications as depicted in Table 5.3. This is a frozen orbit [28]. It means that it is positioned in low-drift regions which do not require high Delta-V for orbit maintenance making it desirable for the mission. This specific orbit requires as little as 0.02 m/s per day of Delta-V.

Table 5.3: Reconnaissance orbit parameters

Parameter	Value	Unit
Semi-major axis	1872.96	km
Eccentricity	0.0001	-
Inclination	85	deg
Argument of pericentre	-130	deg
Period	2.50	h
Mean altitude	312.16	km

This orbit will be used for reconnaissance of the surface of Europa to find a safe landing site. NASA's General Mission Analysis Tool (GMAT) software[3] was used to simulate such orbit while accounting for the moon's properties. This was used to visualise the orbit in the mission timeline as shown in Figure 5.5 and Figure 5.6.

---

[3]From `https://software.nasa.gov/software/GSC-17177-1`, accessed on 17/06/2024.

The GMAT simulation uses an inertial coordinate system MJ2000Eq. The x-axis points on the line formed by the intersection of Europa's equatorial plane and the ecliptic plane, in the direction of Aries. The z-axis is normal to the moon's equator at the J2000 epoch and the y-axis completes the right-handed system.
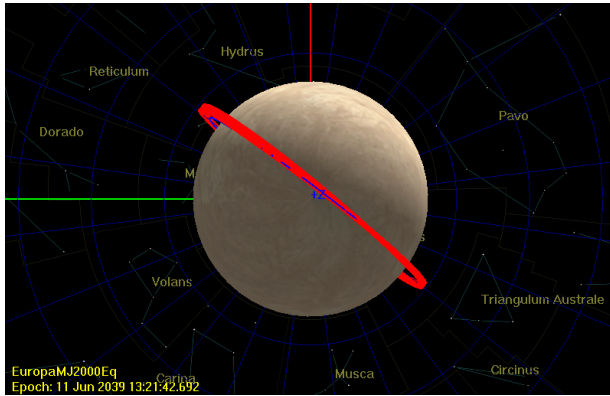
Figure 5.5: Orbit top view
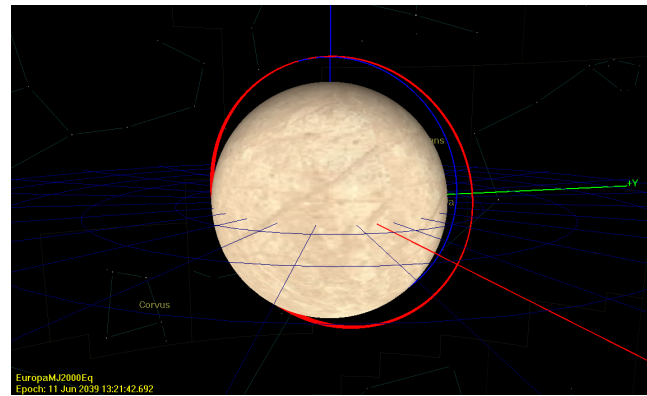
Figure 5.6: Orbit side view

The aim of the reconnaissance phase is to minimise the time of orbiting the moon to limit the TID received by the spacecraft, while still gathering a sufficient number of high-resolution images. For this purpose, the landing area has been narrowed down according to radiation distribution on the surface. The part imaged will be the leading edge half of the moon, above 80° latitude and below −80° latitude. The polar regions are preferred since they receive a much lower flux of lower energy electrons than equatorial regions due to the pitch angle of the charged particles [29]. Thus, the 85° of inclination is chosen for the orbit as it will enable landing on corresponding latitudes. Moreover, the landing site shall be limited to the leading edge of the moon. This is due to the fact that the leading side receives only 5.481×10^9 rad per year while the trailing side of Europa receives about 8.614×10^9 rad per year [30].

Constraining the area of interest enables the use of a narrow field of view (FOV) camera lens for ECAM-C50 from Malin Space Science Systems.[4] It would provide high-resolution images of approximately 10.5 m/pixel and other specifications shown in Table 5.4.

Table 5.4: Performance specifications of the reconnaissance camera ECAM-C50[4]

Parameter	Value	Unit
FOV horizontal	5	deg
FOV vertical	3.75	deg
Frame size horizontal	2592	px
Frame size vertical	1944	px
Horizontal ground coverage per image	27.26	km
Vertical ground coverage per image	20.44	km
Resolution	10.52	m/pixel
Frame rate	0.06	fps

Using this instrument allows for fully imaging the entire region of interest within one orbit of Europa around Jupiter. Europa's orbital period is over 85 hours (3.55 Earth days) while the reconnaissance orbit is only 2.5 hours, which means that 34 full orbits of the spacecraft will be completed in one revolution of Europa around Jupiter. Using trigonometry it can be calculated that the position of the spacecraft at 85 degrees latitude shifts approximately 25 km with each orbit. As shown in Table 5.4, the ground covered horizontally by each image is 27.26 km resulting in over 2 km overlap between each consecutive orbit. Furthermore, it was checked that the frame rate of 0.06 fps is sufficient as it will result in an image taken every 18.16 km on the ground leading to over 2 km overlap from 20.44 km vertical ground coverage per image.

---

[4]From `https://www.msss.com/files/ECAM-C50_M50.pdf`, accessed on 10/06/2024.

According to the mission timeline, the orbiting phase shall take no longer than 7 days until the landing procedures commence, in order to limit the TID. The complete imaging of the leading edge of the polar regions (above 80° and below −80° latitude) shall take 3.55 Earth days. This data will be continuously transmitted to Earth where a team of planetary scientists and engineers will uninterruptedly analyse and determine the best landing site. Within 3.55 days, the landing area shall be chosen and communicated to the spacecraft. The spacecraft will then have the same amount of time until it performs the first burn to lower the pericentre and begins the landing sequence. This will allow it to potentially cover the same ground for the second time until it reaches the desired location for the burn. Using GMAT, the maximum orbiting time was simulated yielding the ground track of the spacecraft as shown in Figure 5.7. The red lines indicate regions above which the spacecraft orbits, and it can be seen that at latitudes 85° and −85° their density is the highest. The blue line indicates the trajectory of the spacecraft after it performs the deorbit burn to land. This aligns with the orbital inclination of 85° and the calculations to ensure sufficient surface imaging ground coverage.

The high-resolution images from each orbit shall be almost fully transmitted to Earth during said orbit. This is necessary to allow the scientists on Earth to analyse the data as quickly as possible. For this purpose, a compression factor of 7 was applied to limit the data rate. This decreases the data rate from 2418.65 kbit/s to 345.52 kbit/s. The time of transmission then depends on the position of Europa in its orbit around Jupiter, as it affects its distance from Earth. In the scenario of the shortest distance between Europa and Earth, the transmission
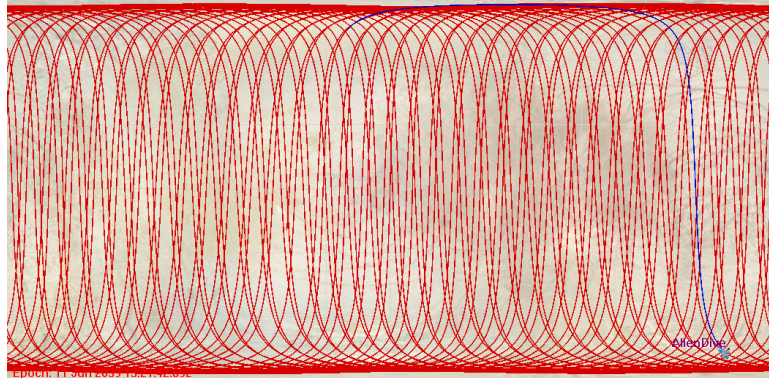
Figure 5.7: Ground track of the reconnaissance orbit

time of one image after compression is 1.81 minutes. Transmitting all the images gathered within one orbit would take approximately 36,22% of that orbit. Conversely, in the case of the largest distance, the time of one image transmission is 4.91 minutes resulting in 98.29% of the orbit needed for transmission.

For the data transmission, the fraction of the orbit visible to Earth was also calculated. Firstly, it is considered that Europa will be hidden behind Jupiter during a part of its orbit which would restrict data transmission opportunities. To calculate this, a conservative assumption is made that Earth, Jupiter, and Europa are in approximately the same plane relative to the Sun's equator. This is justified as Earth and Jupiter have an inclination with respect to the Sun's equator of 7.25° and 6.09°, respectively.[5] Then, Europa's orbit is negligibly inclined 0.47° relative to Jupiter's equatorial plane. With this assumption, it was calculated using trigonometry that data transmission is possible in 96.67% of Europa's orbit around Jupiter. This can possibly be improved by gimballing the antenna. However, if improvements cannot be achieved, the data gathered during orbiting the furthest from Earth will have to be partially transmitted during the following orbits.

The visibility of the orbit from Earth's surface when it comes to the position of spacecraft with respect to Europa itself was also analysed. Due to the geometry of the reconnaissance orbit and its high inclination of 85°, there is a possibility of achieving a 100% communication time depending on the location of the ascending node. It was calculated that approximately 37% of orbits of this geometry would have constant spacecraft visibility from Earth. In the future during the further design phases, as the trajectory is revised and the simulations are improved, this shall be accounted for more in-depth. At this point of the design, it is assumed that to achieve this, the trajectory from JOI to EOI can be adjusted slightly using the remaining Delta-V to perform additional DSM to ensure this best-case scenario orbit is achieved. If this cannot be done due to an insufficient Delta-V budget, a higher compression factor can be applied to the data transmitted back to Earth to ensure a suitable landing site can still be chosen on time.

5.4. Deorbit, Descent & Landing

After selecting the approximate landing area, the Deorbit, Descent & Landing (DDL) sequence will commence. Part of this sequence is inspired by the 2012 Report of the Europa Lander [25]; however, the calculations have been tailored to the specific parameters of this mission. Initially, the transfer stage will execute a small burn of approximately 59 m/s to transition from the nearly circular orbit into an elliptical orbit with a pericentre altitude of

---

[5]From `https://nssdc.gsfc.nasa.gov/planetary/factsheet/jupiterfact.html`, accessed on 10/06/2024.

5 km. This manoeuvre will be executed such that at the pericentre, the transfer stage will immediately perform the deorbit burn of 1443 m/s to initiate the spacecraft's descent. This burn will reduce the translational velocity of the spacecraft to approximately 50 m/s. After this burn, the transfer stage will separate from the lander and crash into the surface of Europa. The lander will free fall for 1 km. During this phase, the lander will adjust its orientation to capture images for Terrain Relative Navigation (TRN). It will do this by comparing real-time images taken by the lander with those captured during the reconnaissance phase of the mission. By analysing terrain features, the lander will determine its relative velocity and position with respect to the surface and adjust its trajectory, such that it will reach the selected landing area. The TRN imaging will be conducted using the same camera model as the reconnaissance camera, but with a different lens that offers a wider field of view[4]. At the deorbit altitude of 5 km, these cameras can cover combined horizontal and vertical distances of 8 and 5 km, respectively.

At an altitude of approximately 4 km, the lander will begin its powered descent, maintaining a constant deceleration of 1.65 m/s^2 to achieve the desired vertical velocity of 0.5 m/s at 50 m. Throughout this phase, the lander will continue imaging for TRN. At approximately 1 kilometre altitude, the lander will transition from TRN to Hazard Detection and Avoidance (HDA). It will use Laser Imaging Detection And Ranging (LIDAR) to map the ground below in 3D. This process will generate Digital Elevation Maps (DEMs), which the lander will analyse in real-time to identify potential hazards in the landing area. Subsequently, the onboard computer will select the optimal landing site and adjust the trajectory if necessary. The LIDAR for Extra-terrestrial Imaging Applications (LEIA) from MDA[6] will be used for this.

Finally, as previously mentioned, the lander will achieve a vertical velocity of 0.5 m/s at an altitude of 50 m. It will then begin its final descent, maintaining this speed until touchdown. The entire DDL sequence described above is also illustrated in Figure 5.8. Additionally, the actual Delta-V values for this sequence are provided in Table 5.5. For the first two burns, a 5 % margin is applied according to ESA standards as mentioned before. For the last burn, the 5 % margin is added along with an additional 100 m/s to account for the remaining horizontal velocity after deorbit and any potential trajectory adjustments during the TRN and HDA phases.
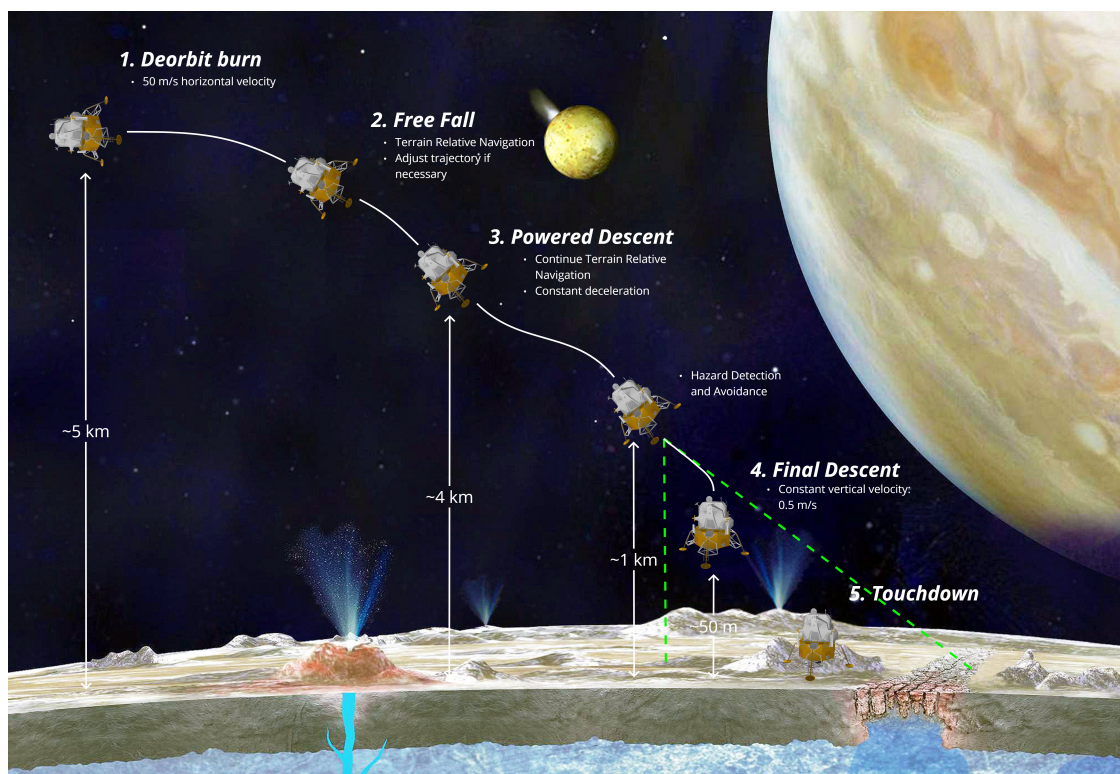
Figure 5.8: Descent & landing sequence of the lander; background from NASA/JPL-Caltech[7]

---

[6]From `https://satsearch.co/products/mda-leia-lidar-for-extra-terrestrial-imaging-applications`, accessed on 05/06/2024.

[7]From `https://www.jpl.nasa.gov/images/pia16826-taste-of-the-ocean-on-europas-surface-artists-concept`, accessed on 14/06/2024.

Table 5.5: Delta-V for descent and landing

Event	Delta-V [m/s]	Incl. Margin [m/s]
Lower pericentre	59.9	62.9
Deorbit burn	1142.9	1515
Descent burn	114.2	219.9

5.5. Total System Overview

In this section, the final design of the entire mission system is shown. It is composed of three main components: the transfer stage, the lander, and the probe. The full assembly is shown in Figure 5.9.
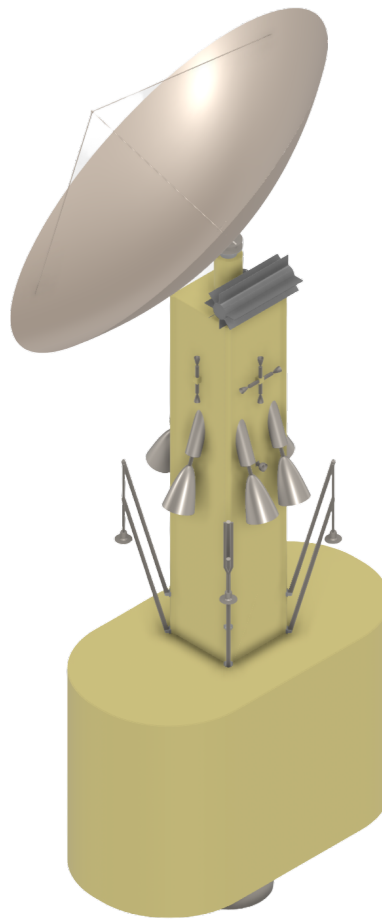
Figure 5.9: Isometric view of the entire spacecraft assembly.

The stadium-shaped part is the transfer stage. Its main function is to provide Delta-V to the entire assembly, from JOI to its final burn putting the spacecraft on a Europa descent trajectory, after which it separates from the lander. The lander's main task is to safely land on Europa's surface and release the probe. In Figure 5.9, the lander is the rectangular part, with six thrusters attached around it. After landing, it will gather data about the surface environment on Europa using its separate scientific payload, and transmit data gathered by itself and the probe to Earth. The probe is the main component of the mission, as its task is to identify whether there is life in Europa's subsurface ocean. It first has to dig itself through approximately 30 km of ice using its integrated drill. Once it reaches the ocean, it anchors itself to the ice and explores up to 1 km ocean depth. The transfer stage, lander and probe are explained in much more detail in Chapter 6, Chapter 7 and Chapter 8 respectively. The total power and mass budget are shown in Table 5.7 and Table 5.6 respectively. The power budget only includes power for the lander and the probe, as the transfer stage does not generate its own power and draws power from the power sources of the other two elements.

Table 5.6: System Mass Budget

Elements	Mass [kg]
Transfer Stage	
Transfer stage dry mass	898.86
Propellant Mass	11323.85
Transfer stage wet mass	12222.71
Lander	
Lander dry mass	813.98
Propellant mass	227.38
Lander wet mass	1041.36
Probe	
Probe mass w/o relays	511.71
Relays mass	42.08
Total probe mass	553.79
Total system mass	**13817.86**

Table 5.7: System Power Budget

Elements	Power [W]
Lander	
Required BOL Power	424.57
Total available power	435
Margin	10.43
Probe	
Required BOL Power	849.24
Total available power	850
Margin	0.76

5.6. Functional Analysis

A functional flow diagram (FFD) in Figure 5.10 and Figure 5.11 shows the flow of functions required to satisfy the stakeholder requirements. It identifies the desired capabilities and functions of the mission in a way that enables translating them into functional requirements, for both the system and individual subsystems. In the diagram, the functions are identified for the entire life cycle of the product. The high-level mission phases are defined as follows: design mission, assemble spacecraft, perform testing & qualification, operate spacecraft, and retire spacecraft.

The functional breakdown structure (FBS) presented in Figure 5.12 and Figure 5.13 is a graphical tool to help visualise all functions a mission requires to fulfil the stakeholder requirements. This includes functions of the system that need to be designed as well as the people designing them. The FBS contains the same functions as the FFD.

AlienDive Mission
Functional Flow Diagram

High-level Functional Flow Diagram

F0 Design Mission — **F1** Produce Spacecraft — **F2** Perform Testing & Qualification — **F3** Operate Spacecraft — **F4** Retire Spacecraft

F0 — Design Mission

- F0.1 Form Functions & Requirements — Design Team
  - F0.1.1 Form Functions — Design Team
    - F0.1.1.1 Generate Function Flow — Design Team
    - F0.1.1.4 Refine Function Flow — Design Team
    - F0.1.1.5 Generate Function Breakdown — Design Team
  - F0.1.2 Form Requirements — Design Team
    - F0.1.2.1 Form Requirements from Functions — Design Team
    - F0.1.2.2 Quantify Requirements — Design Team

- F0.2 Design Preliminary Systems — Design Team
  - F0.2.1 Generate Design Options — Design Team
    - F0.2.1.1 Brainstorm Design Concepts — Design Team
    - F0.2.1.2 Make Design Discovery Tree — Design Team
    - F0.2.1.3 Prune Unfeasible Designs — Design Team
  - F0.2.2 Analyse Options — Design Team
    - F0.2.2.1 Determine Design Aspects — Design Team
    - F0.2.2.2 Quantify Performance — Design Team
  - F0.2.3 Choose Option — Design Team
    - F0.2.3.1 Establish Weights for Design Aspects — Design Team
    - F0.2.3.2 Perform Trade-off — Design Team
  - F0.2.4 Finalise Preliminary Design — Design Team
    - F0.2.4.1 Verify Requirement Completion — Design Team

- F0.3 Optimise Design — Design Team
  - F0.3.1 Optimise Individual Elements — Design Team
    - F0.3.1.1 Find Governing Equations — Design Team
    - F0.3.1.2 Parameterise Design — Design Team
    - F0.3.1.3 Establish Cost Function — Design Team
    - F0.3.1.4 Write Governing Equations in terms of Parameters
    - F0.3.1.5 Write Cost Function in terms of Parameters — Design Team
    - F0.3.1.6 Optimise — Design Team
  - F0.3.1 Analyse Total Performace — Design Team
    - F0.3.1.1 Establish Total Cost Function — Design Team
    - F0.3.1.2 Perform Analysis — Design Team
  - F0.3.2 Change Design — Design Team
    - F0.3.2.1 Establish Complete Design — Design Team
    - F0.3.2.2 Find Possible Improvements — Design Team
  - F0.3.3 Analyse Total Performace — Design Team
    - F0.3.3.1 Establish Total Cost Function — Design Team
    - F0.3.3.2 Perform Analysis — Design Team
  - F0.3.4 Finalise Spacecraft Design — Design Team
    - F0.3.4.1 Perform Final Spacecraft — Design Team
    - F0.3.4.2 Verify Fulfilment of Requirement — Design Team
    - F0.3.4.3 Document design performance — Design Team
  - F0.3.5 Set up Ground Systems — Design Team
    - F0.3.5.1 Calculate final link budget — Design Team
    - F0.3.5.2 Design Ground Systems — Design Team

- F0.4 Perform V&V — Design Team
  - F0.4.1 Plan V&V — Design Team
    - F0.4.1.1 Establish Verification Items — Design Team
    - F0.4.1.3 Plan Verification Techniques — Design Team
    - F0.4.1.2 Establish Validation Items — Design Team
    - F0.4.1.4 Plan Validation Techniques — Design Team
  - F0.4.2 Execute V&V Plan — Design Team
    - F0.4.2.1 Execute Verification Plan — Design Team
    - F0.4.2.2 Execute Validation Plan — Design Team
    - F0.4.2.3 Verify Completion of V&V — Design Team
  - F0.4.3 Determine Results — Design Team
    - F0.4.3.1 Confirm Fulfilment of Requirement — Design Team
  - OR → Return To F0.2 Design / Continue to F1 Manufacturing

F1 — Spacecraft Assembly

- F1.1 Develop Software — Software Eng. Team
  - F1.1.1 Develop Flight Software — Software Eng. Team
    - F1.1.1.1 Develop Subsystem Software — Software Eng. Team
    - F1.1.1.2 Develop Autonomous Control Software — Software Eng. Team
  - F1.1.2 Develop Ground Software — Software Eng. Team
    - F1.1.2.1 Develop Communication software — Software Eng. Team
    - F1.1.2.2 Develop Data Handling Software — Software Eng. Team

- F1.2 Develop Communication software — Manuf. Engineer
  - F1.2.1 Produce Structural Parts — Manuf. Engineer
    - F1.2.1.1 Produce Fasteners — Manuf. Engineer
    - F1.2.1.2 Produce Formed Parts — Manuf. Engineer
    - F1.2.1.2 Produce Machined Parts — Manuf. Engineer
  - F1.2.2 Produce Electronics — Manuf. Engineer
    - F1.2.2.1 Produce Circuitboards — Manuf. Engineer
    - F1.2.2.2 Produce Wiring Elements — Manuf. Engineer
    - F1.2.2.3 Produce Chips — Manuf. Engineer

- F1.3 Assemble Spacecraft — Manuf. Engineer
  - F1.3.1 Assemble Sub-Assemblies — Manuf. Engineer
    - F1.3.1.1 Align Parts — Manuf. Engineer
    - F1.3.1.2 Join Joints — Manuf. Engineer
    - F1.3.1.3 Fasten Fasteners — Manuf. Engineer
  - F1.3.2 Assemble Spacecraft — Manuf. Engineer
    - F1.3.2.1 Align Sub-Assemblies — Manuf. Engineer
    - F1.3.2.2 Join Joints — Manuf. Engineer
    - F1.3.2.3 Fasten Fasteners — Manuf. Engineer
  - F1.3.3 Integrate — Manuf. Engineer
    - F1.3.3.1 Integrate Payload — Manuf. Engineer
    - F1.3.3.2 Integrate Electronics — Manuf. Engineer
    - F1.3.3.3 Integrate Software — Software Eng. Team

F2 — Perform Testing & Qualification → FFD2

- F2.1 Perform Testing — V&V Team
  - F2.1.1 Perform Structural Tests — V&V Team
    - F2.1.1.1 Perform Quasi-Static Tests — V&V Team
    - F2.1.1.2 Perform Dynamic Tests — V&V Team
    - F2.1.1.3 Perform Vibration Tests — V&V Team
  - F2.1.2 Perform Subsystem Tests — V&V Team
    - (EXAMPLE) F2.1.2.1 Test Communications Pointing System — V&V Team
  - F2.1.3 Perform Environmental Tests — V&V Team
    - F2.1.3.1 Perform Thermal Test — V&V Team
    - F2.1.3.2 Perform Vacuum Test — V&V Team
    - F2.1.3.3 Perform Radiation Test — V&V Team
  - F2.1.4 Perform System Tests — V&V Team
    - F2.1.4.1 Perform End-to-End Information Flow — V&V Team
    - F2.1.4.2 Perform Stress Test — V&V Team

- F2.2 Acquire Qualifications — V&V Team
  - F2.2.1 Quantify Requirements — V&V Team
    - F2.2.1.1 Send Email — V&V Team
    - F2.2.1.2 Send Reports — V&V Team
  - F2.2.2 Test to Acquire Preliminary Qualifications — V&V Team
    - F2.2.2.1 Verify High-level Requirements — V&V Team
  - F2.2.3 Test to Acquire Final Qualifications — V&V Team
    - F2.2.3.1 Provide Proof of Subsystem Success — V&V Team
    - F2.2.3.2 Provide Proof of System Success — V&V Team

Key:
- Function — Identifier / Responsible System
- OR operator
- AND operator
- Phase
- Top Level Function
- Level 2 Function
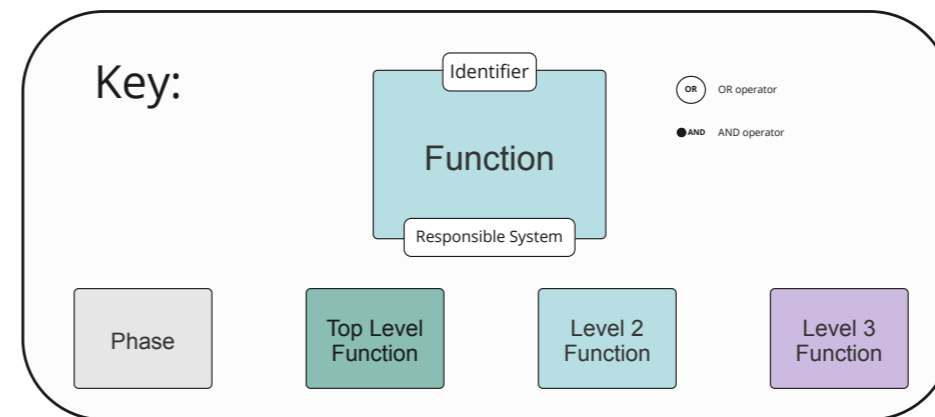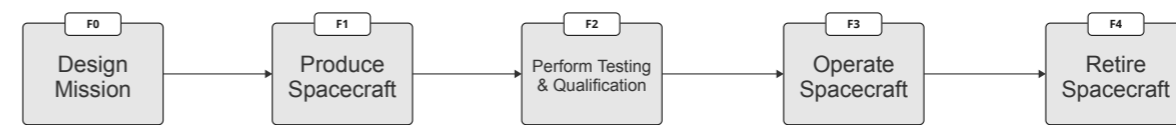- Level 3 Function

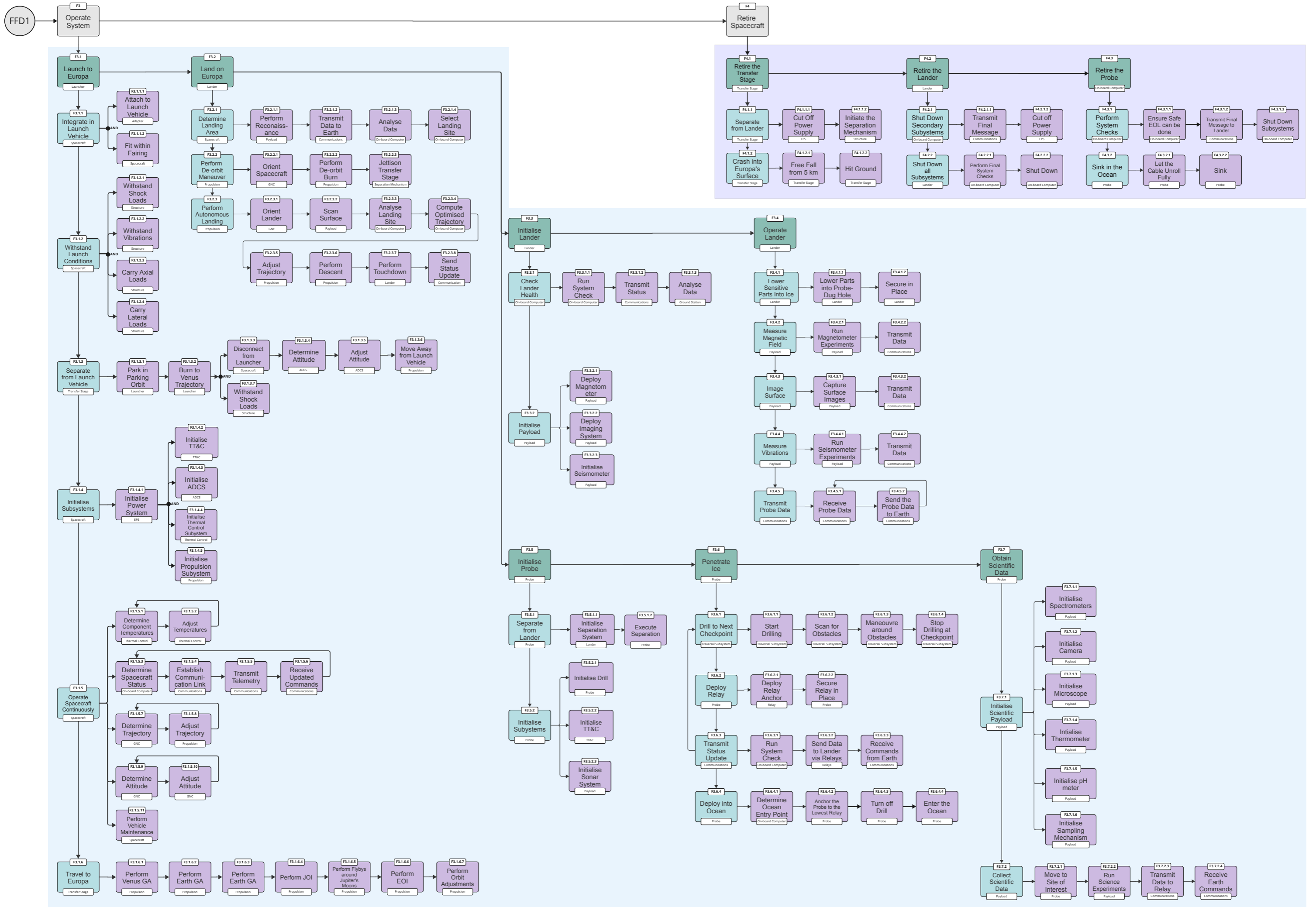**Figure 5.11:** Second part of the Functional Flow Diagram

Figure 5.12: First part of the Functional Breakdown Structure

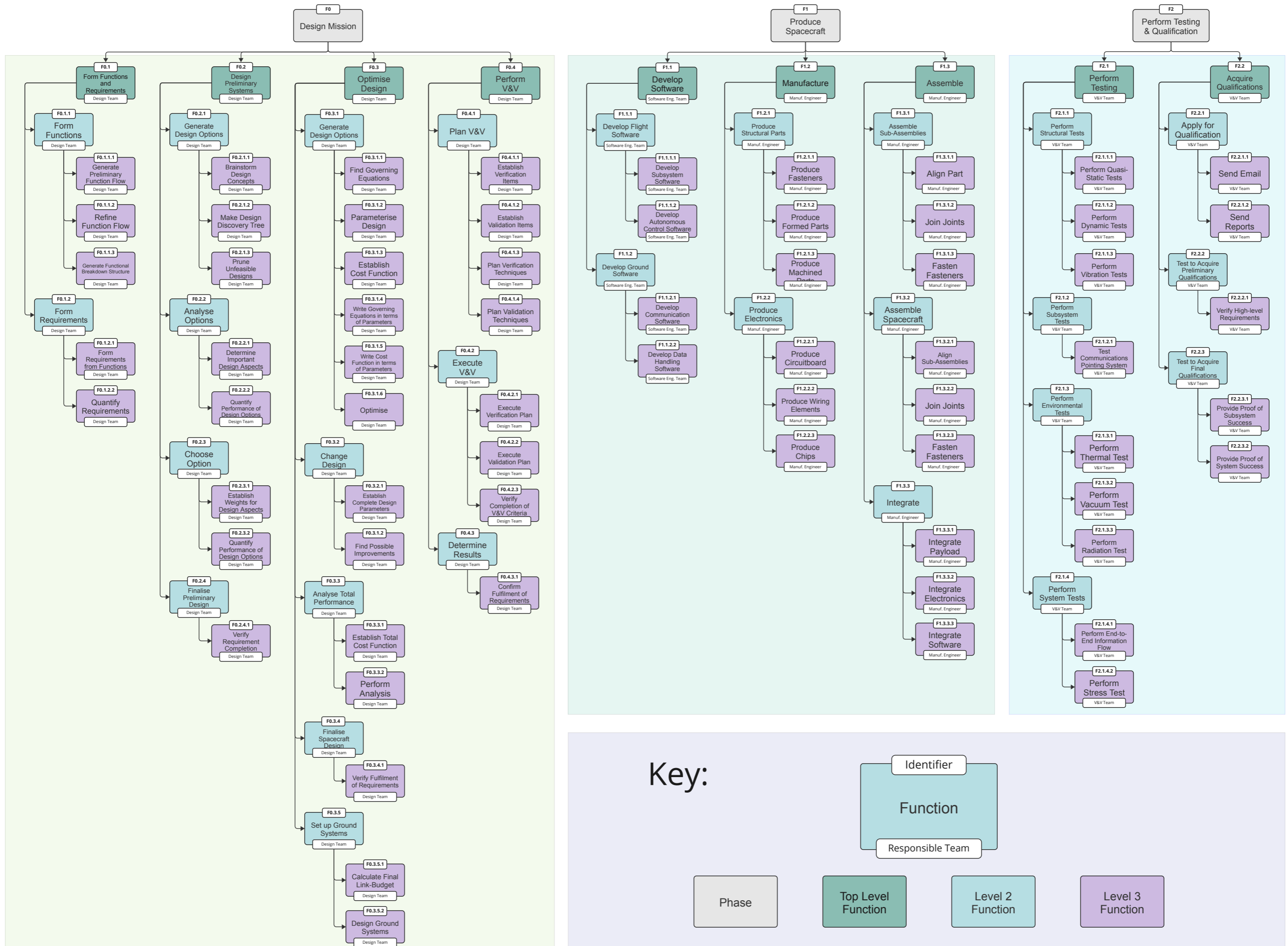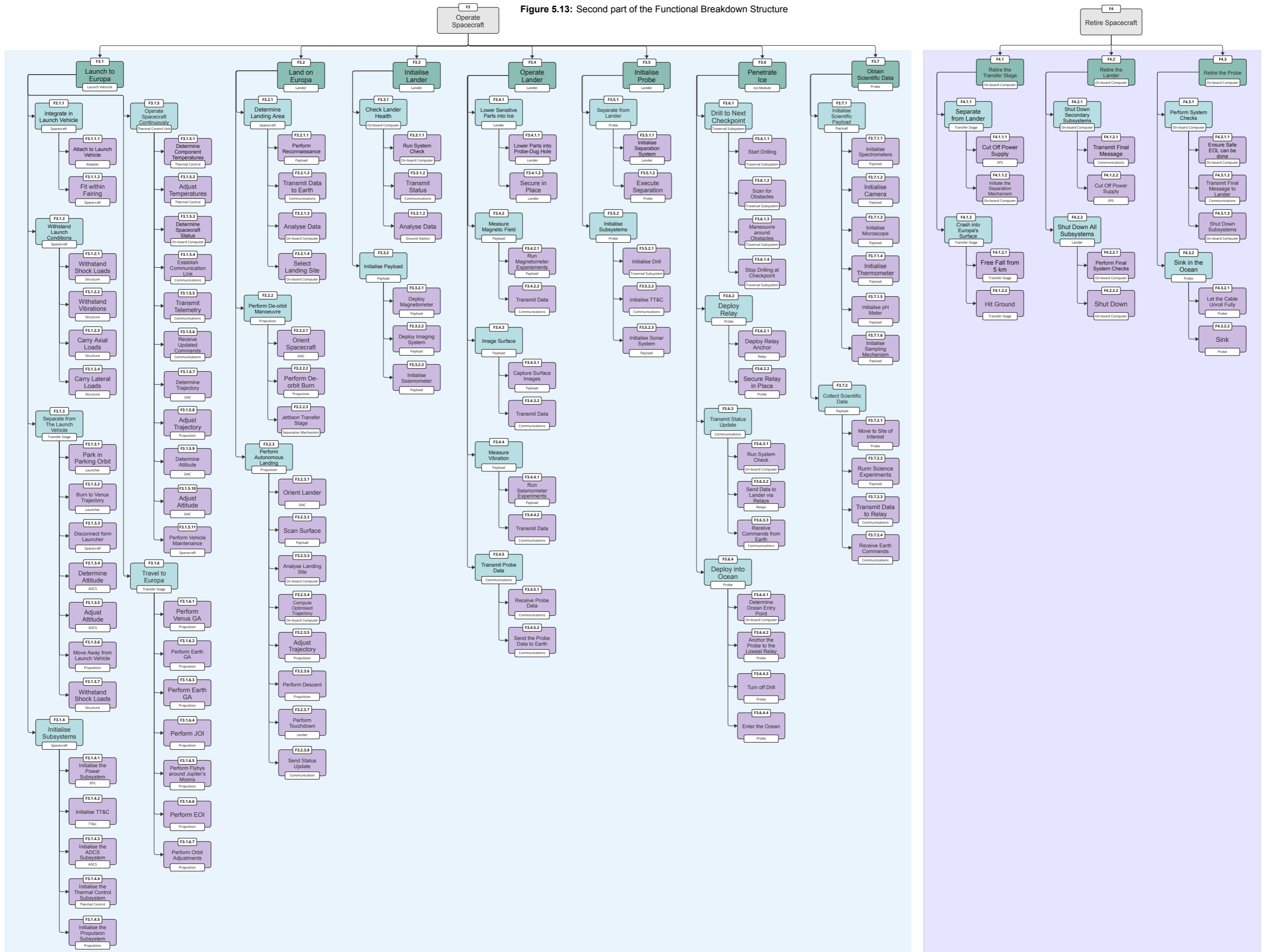**Figure 5.13:** Second part of the Functional Breakdown Structure

F3 — Operate Spacecraft

F3.1 — Launch to Europa (Launch Vehicle)
- F3.1.1 Integrate in Launch Vehicle (Spacecraft)
  - F3.1.1.1 Attach to Launch Vehicle (Adapter)
  - F3.1.1.2 Fit within Fairing (Spacecraft)
- F3.1.2 Withstand Launch Conditions (Spacecraft)
  - F3.1.2.1 Withstand Shock Loads (Structure)
  - F3.1.2.2 Withstand Vibrations (Structure)
  - F3.1.2.3 Carry Axial Loads (Structure)
  - F3.1.2.4 Carry Lateral Loads (Structure)
- F3.1.3 Separate from The Launch Vehicle (Transfer Stage)
  - F3.1.3.1 Park in Parking Orbit (Launcher)
  - F3.1.3.2 Burn to Venus Trajectory (Launcher)
  - F3.1.3.3 Disconnect form Launcher (Spacecraft)
  - F3.1.3.4 Determine Attitude (ADCS)
  - F3.1.3.5 Adjust Attitude (ADCS)
  - F3.1.3.6 Move Away from Launch Vehicle (Propulsion)
  - F3.1.3.7 Withstand Shock Loads (Structure)
- F3.1.4 Initialise Subsystems (Spacecraft)
  - F3.1.4.1 Initialise the Power Subsystem (EPS)
  - F3.1.4.2 Initialise TT&C (TT&C)
  - F3.1.4.3 Initialise the ADCS Subsystem (ADCS)
  - F3.1.4.4 Initialise the Thermal Control Subsystem (Thermal Control)
  - F3.1.4.5 Initialise the Propulsion Subsystem (Propulsion)
- F3.1.5 Operate Spacecraft Continuously (Thermal Control Unit)
  - F3.1.5.1 Determine Component Temperatures (Thermal Control)
  - F3.1.5.2 Adjust Temperatures (Thermal Control)
  - F3.1.5.3 Determine Spacecraft Status (On-board Computer)
  - F3.1.5.4 Establish Communication Link (Communications)
  - F3.1.5.5 Transmit Telemetry (Communications)
  - F3.1.5.6 Receive Updated Commands (Communications)
  - F3.1.5.7 Determine Trajectory (GNC)
  - F3.1.5.8 Adjust Trajectory (Propulsion)
  - F3.1.5.9 Determine Attitude (GNC)
  - F3.1.5.10 Adjust Attitude (GNC)
  - F3.1.5.11 Perform Vehicle Maintenance (Spacecraft)
- F3.1.6 Travel to Europa (Transfer Stage)
  - F3.1.6.1 Perform Venus GA (Propulsion)
  - F3.1.6.2 Perform Earth GA (Propulsion)
  - F3.1.6.3 Perform Earth GA (Propulsion)
  - F3.1.6.4 Perform JOI (Propulsion)
  - F3.1.6.5 Perform Flybys around Jupiter's Moons (Propulsion)
  - F3.1.6.6 Perform EOI (Propulsion)
  - F3.1.6.7 Perform Orbit Adjustments (Propulsion)

F3.2 — Land on Europa (Lander)
- F3.2.1 Determine Landing Area (Spacecraft)
  - F3.2.1.1 Perform Reconnaissance (Payload)
  - F3.2.1.2 Transmit Data to Earth (Communications)
  - F3.2.1.3 Analyse Data (On-board Computer)
  - F3.2.1.4 Select Landing Site (On-board Computer)
- F3.2.2 Perform De-orbit Manoeuvre (Propulsion)
  - F3.2.2.1 Orient Spacecraft (GNC)
  - F3.2.2.2 Perform De-orbit Burn (Propulsion)
  - F3.2.2.3 Jettison Transfer Stage (Separation Mechanism)
- F3.2.3 Perform Autonomous Landing (Propulsion)
  - F3.2.3.1 Orient Lander (GNC)
  - F3.2.3.2 Scan Surface (Payload)
  - F3.2.3.3 Analyse Landing Site (On-board Computer)
  - F3.2.3.4 Compute Optimised Trajectory (On-board Computer)
  - F3.2.3.5 Adjust Trajectory (Propulsion)
  - F3.2.3.6 Perform Descent (Propulsion)
  - F3.2.3.7 Perform Touchdown (Lander)
  - F3.2.3.8 Send Status Update (Communication)

F3.3 — Initialise Lander (Lander)
- F3.3.1 Check Lander Health (On-board Computer)
  - F3.3.1.1 Run System Check (On-board Computer)
  - F3.3.1.2 Transmit Status (Communications)
  - F3.3.1.3 Analyse Data (Ground Station)
- F3.3.2 Initialise Payload (Payload)
  - F3.3.2.1 Deploy Magnetometer (Payload)
  - F3.3.2.2 Deploy Imaging System (Payload)
  - F3.3.2.3 Initialise Seismometer (Payload)

F3.4 — Operate Lander (Lander)
- F3.4.1 Lower Sensitive Parts into Ice (Lander)
  - F3.4.1.1 Lower Parts into Probe-Dug Hole (Lander)
  - F3.4.1.2 Secure in Place (Lander)
- F3.4.2 Measure Magnetic Field (Payload)
  - F3.4.2.1 Run Magnetometer Experiments (Payload)
  - F3.4.2.2 Transmit Data (Communications)
- F3.4.3 Image Surface (Payload)
  - F3.4.3.1 Capture Surface Images (Payload)
  - F3.4.3.2 Transmit Data (Communications)
- F3.4.4 Measure Vibration (Payload)
  - F3.4.4.1 Run Seismometer Experiments (Payload)
  - F3.4.4.2 Transmit Data (Communications)
- F3.4.5 Transmit Probe Data (Communications)
  - F3.4.5.1 Receive Probe Data (Communications)
  - F3.4.5.2 Send the Probe Data to Earth (Communications)

F3.5 — Initialise Probe (Lander)
- F3.5.1 Separate from Lander (Probe)
  - F3.5.1.1 Initialise Separation System (Lander)
  - F3.5.1.2 Execute Separation (Probe)
- F3.5.2 Initialise Subsystems (Probe)
  - F3.5.2.1 Initialise Drill (Payload)
  - F3.5.2.2 Initialise TT&C (Communications)
  - F3.5.2.3 Initialise Sonar System (Payload)

F3.6 — Penetrate Ice (Ice Module)
- F3.6.1 Drill to Next Checkpoint (Traversal Subsystem)
  - F3.6.1.1 Start Drilling (Traversal Subsystem)
  - F3.6.1.2 Scan for Obstacles (Traversal Subsystem)
  - F3.6.1.3 Manoeuvre around Obstacles (Traversal Subsystem)
  - F3.6.1.4 Stop Drilling at Checkpoint (Traversal Subsystem)
- F3.6.2 Deploy Relay (Probe)
  - F3.6.2.1 Deploy Relay Anchor (Relay)
  - F3.6.2.2 Secure Relay in Place (Probe)
- F3.6.3 Transmit Status Update (Communications)
  - F3.6.3.1 Run System Check (On-board Computer)
  - F3.6.3.2 Send Data to Lander via Relays (Relays)
  - F3.6.3.3 Receive Commands from Earth (Communications)
- F3.6.4 Deploy into Ocean (Probe)
  - F3.6.4.1 Determine Ocean Entry Point (On-board Computer)
  - F3.6.4.2 Anchor the Probe to the Lowest Relay (Probe)
  - F3.6.4.3 Turn off Drill (Probe)
  - F3.6.4.4 Enter the Ocean (Probe)

F3.7 — Obtain Scientific Data (Probe)
- F3.7.1 Initialise Scientific Payload (Payload)
  - F3.7.1.1 Initialise Spectrometers (Payload)
  - F3.7.1.2 Initialise Camera (Payload)
  - F3.7.1.3 Initialise Microscope (Payload)
  - F3.7.1.4 Initialise Thermometer (Payload)
  - F3.7.1.5 Initialise pH Meter (Payload)
  - F3.7.1.6 Initialise Sampling Mechanism (Payload)
- F3.7.2 Collect Scientific Data (Payload)
  - F3.7.2.1 Move to Site of Interest (Probe)
  - F3.7.2.2 Runn Science Experiments (Payload)
  - F3.7.2.3 Transmit Data to Relay (Communications)
  - F3.7.2.4 Receive Earth Commands (Communications)

F4 — Retire Spacecraft

F4.1 — Retire the Transfer Stage (On-board Computer)
- F4.1.1 Separate from Lander (Transfer Stage)
  - F4.1.1.1 Cut Off Power Supply (EPS)
  - F4.1.1.2 Initiate the Separation Mechanism (On-board Computer)
- F4.1.2 Crash into Europa's Surface (Transfer Stage)
  - F4.1.2.1 Free Fall from 5 km (Transfer Stage)
  - F4.1.2.2 Hit Ground (Transfer Stage)

F4.2 — Retire the Lander (On-board Computer)
- F4.2.1 Shut Down Secondary Subsystems (On-board Computer)
  - F4.2.1.1 Transmit Final Message (Communications)
  - F4.2.1.2 Cut Off Power Supply (EPS)
- F4.2.2 Shut Down All Subsystems (Lander)
  - F4.2.2.1 Perform Final System Checks (On-board Computer)
  - F4.2.2.2 Shut Down (On-board Computer)

F4.3 — Retire the Probe (On-board Computer)
- F4.3.1 Perform System Checks (On-board Computer)
  - F4.3.1.1 Ensure Safe EOL can be done (On-board Computer)
  - F4.3.1.2 Transmit Final Message to Lander (Communications)
  - F4.3.1.3 Shut Down Subsystems (On-board Computer)
- F4.3.2 Sink in the Ocean (Probe)
  - F4.3.2.1 Let the Cable Unroll Fully (Probe)
  - F4.3.2.2 Sink (Probe)

6 Transfer Stage Design

In this chapter, the transfer stage responsible for delivering the manoeuvre burns in the trajectory from Earth to Europa. An overview is given in Section 6.1. The subsystems will be discussed in Section 6.2, Section 6.4,Section 6.5.

6.1. Transfer Stage Overview

After the final stage of the Falcon Heavy brings the assembly to Jupiter's sphere of influence, the transfer stage starts its tasks. Its role is to insert the entire spacecraft into Jupiter's sphere of influence and then perform multiple burns, putting the spacecraft on the required trajectory to reach Europa, as described in Chapter 5. As it reaches Europa's orbit, the transfer stage will also perform a burn to achieve an inclination change. Its final task is to perform a deorbit burn, after which it separates from the lander and its work is completed.

The transfer stage is stadium-shaped and its dimensions are optimised to fit both propellant tanks for the liquid bipropellant engine, attached to the bottom of this stage. The transfer stage is less complex than the lander and the probe, as its only task is to provide Delta-V. Hence, it only houses four subsystems: thermal control, which also helps to keep the lander temperatures during transit within the allowed range; the propulsion subsystem, which is responsible for achieving this vehicle's main task; the GNC system, which allows for correct attitude determination; and finally, the structures subsystem, including the separation mechanism and radiation shielding. The links between the subsystems and the lander are shown in Figure 7.1.

6.1.1. Transfer Stage System Requirements

The system requirements for the transfer stage are listed below:

- **AD-ENG-02-TS-01**: The transfer stage shall withstand the static loads of the Falcon Heavy.
- **AD-ENG-02-TS-02**: The transfer stage shall withstand the dynamic loads of the Falcon Heavy.
- **AD-ENG-02-TS-03**: The transfer stage shall fit inside the payload fairing of the Falcon Heavy.
- **AD-PERF-01-TS-01**: The transfer stage shall maintain a temperature between 263.15 K and 313.15 K.
- **AD-PERF-01-TS-02**: The transfer stage shall be able to withstand the radiation environment.
- **AD-PERF-01-TS-03**: The transfer stage shall deliver the lander and probe into Europa's orbit.
- **AD-PERF-01-TS-04**: The transfer stage shall deliver a deorbit burn to the lander.
- **AD-PERF-01-TS-05**: The transfer stage shall perform the inertial measurements for the spacecraft during its transit to Europa.
- **AD-SUST-01-TS-04**: The transfer stage shall crash into the surface of Europa after providing the deorbit burn.

6.2. Propulsion Subsystem

As mentioned in Section 5.2, the transfer stage is responsible for getting the entire assembly into Europa's orbit. To perform all of the necessary manoeuvres, a total Delta-V of 5581.89 m/s is required. The initial step in designing a propulsion system capable of this is to choose a type of propulsion. Thereafter, a corresponding engine is chosen. During this step, it is important to keep in mind that due to radiation considerations, the assembly should not be in Europa's orbit for longer than required. This means that it should be able to descend onto Europa's surface after seven days. Once the engine is chosen, the propellant storage method is designed, and a feed system is developed to deliver the propellant to the engine.

6.2.1. Propulsion Subsystem Requirements

The subsystem requirements of the transfer stage propulsion subsystem are listed below:

- **AD-PERF-01-TS-03-PROP-01**: The propulsion subsystem shall deliver a total Delta-V of 5581.89 m/s.
- **AD-PERF-01-TS-04-PROP-01**: The propulsion system shall be able to provide a Delta-V of 4350.2 m/s within a period of 7 days.
- **AD-ENG-01-TS-02-PROP-01**: The full assembly shall not experience a net acceleration higher than 6 g.

- **AD-ENG-01-TS-03-PROP-01**: The engine shall fit in the Falcon Heavy adapter.

- **AD-SUST-01-TS-04-PROP-01**: The propulsion subsystem shall not contaminate the surface after crashing into Europa's surface.

6.2.2. Type of Propulsion

Many considerations must be into account when choosing a suitable method of propulsion for a mission. In general, there are two main types of propulsion: thermal and electrical. Both of these have many subcategories, shown in Figure 6.1. There exist alternative propulsion methods as well, such as solar sails, which do not require any propellant. However, solar sails were determined to not be a feasible option for this mission as they get less effective further from the sun, and it is not possible to use them to propel a spacecraft towards the sun, limiting the possibilities for gravity assist manoeuvres. The main advantage of electric propulsion is the fact that it is more mass-efficient than thermal propulsion due to its higher specific impulse.[1] The drawback is that it provides lower thrust[2], meaning that it takes a longer time to reach the desired Delta-V. Furthermore, power requirements for electric propulsion systems rise significantly with increasing thrust. As mentioned in the previous section, the spacecraft shall be able to provide a Delta-V of 4350.2 m/s in seven days. Even an electric engine with a relatively high thrust of 1.08 N, and an I_{sp} of 2750 s has a burn time of 526.3 days [31]. This value was determined by rewriting the rocket equation in terms of burn time:

$$t_b = \frac{M_0 \cdot \left(1 - \frac{1}{e^{\frac{\Delta V}{I_{sp} g_0}}}\right)}{T_{thrust}} \cdot I_{sp} \cdot g_0 \tag{6.1}$$

Here, t_b is the burn time and M_0 is the initial mass of the transfer stage including fuel.

For this reason, electric propulsion is discarded. Another option that was analysed in detail is nuclear propulsion. This option was also discarded. Firstly, such an engine has very high development costs, which is not the case for chemical propulsion.[3] Nuclear Thermal Propulsion (NTP) is regarded as a high-priority technology for the future. It provides double the I_{sp} of chemical propulsion and around the same thrust, meaning that it can reach locations much faster with lower mass, but is currently not fully developed [32]. Combining this with the fact that both the lander and the probe use RTGs as a power supply, as explained in Section 7.2 and Section 8.2 respectively, and the requirement to not contaminate Europa's surface, it is more convenient to not add another radioactive part to the assembly.

Thus, chemical propulsion is chosen. Generally, monopropellant is not used for orbit insertion, which is one of the tasks of the transfer stage [31]. Adding the fact that monopropellant has a lower I_{sp} than bipropellant, leading to a higher mass, this option is discarded. Another possibility is the use of solid propellant, but these engines also have a lower I_{sp} than bipropellant engines, which would lead to a larger total propellant mass [31]. Furthermore, once ignited, a solid engine does not stop burning until the propellant is depleted [33]. This means that at least eight tanks are needed, as a minimum of eight burns are performed by the transfer stage, as described in Chapter 5. This would significantly increase the structural mass of the propulsion subsystem. Accordingly, solid rocket propulsion is discarded and liquid bipropellant engines are selected for the transfer stage.

6.2.3. Engine

Now that a propulsion type has been selected, a corresponding engine that can deliver the right amount of thrust needs to be chosen. For this choice, several aspects must be taken into consideration. Firstly, the maximum acceleration that the spacecraft components are designed to withstand is 6g. Therefore, the engine should not provide an acceleration higher than 6g. For most engines, it is not possible to regulate the thrust.[4] For this reason, the limiting case is at the end of the spacecraft's final burn, when it has the lowest mass and thus produces the highest acceleration. This mass is the dry mass of the transfer stage plus the wet mass of the lander and is equal to 2067.72 kg. Using Newton's second law, this leads to a total maximum thrust of:

$$T_{thrust} = m \cdot a = 2067.72 \cdot 6 \cdot 9.81 = 121706 N$$

Multiple engines were selected for a trade-off. Some were taken from the SMAD [31], whilst others were taken from known engine manufacturers, such as Aerojet Rocketdyne [2] and Sierra Space.[5] Table 6.1 shows

---

[1]From `https://www.esa.int/Enabling_Support/Space_Engineering_Technology/What_is_Electric_propulsion`, accessed on 15/06/2024.

[2]From `https://sci.esa.int/web/smart-1/-/34201-electric-spacecraft-propulsion`, accessed on 15/06/2024.

[3]From `https://iq.direct/blog/416-10-advantages-and-10-disadvantages-of-nuclear-rocket-engines.html`, accessed on 18/06/2024.

[4]From `https://satcatalog.s3.amazonaws.com/components/1015/SatCatalog_-_Aerojet_Rocketdyne_-_R-4D-11_490N_300-to-1_-_Datasheet.pdf?lastmod=20210710070936`, accessed on 19/06/2024.

[5]From `https://satsearch.co/products/sierra-space-vrm1500-h-hypergolic-mmh-mon-1500-lbf-engine`, accessed on 19/06/2024.
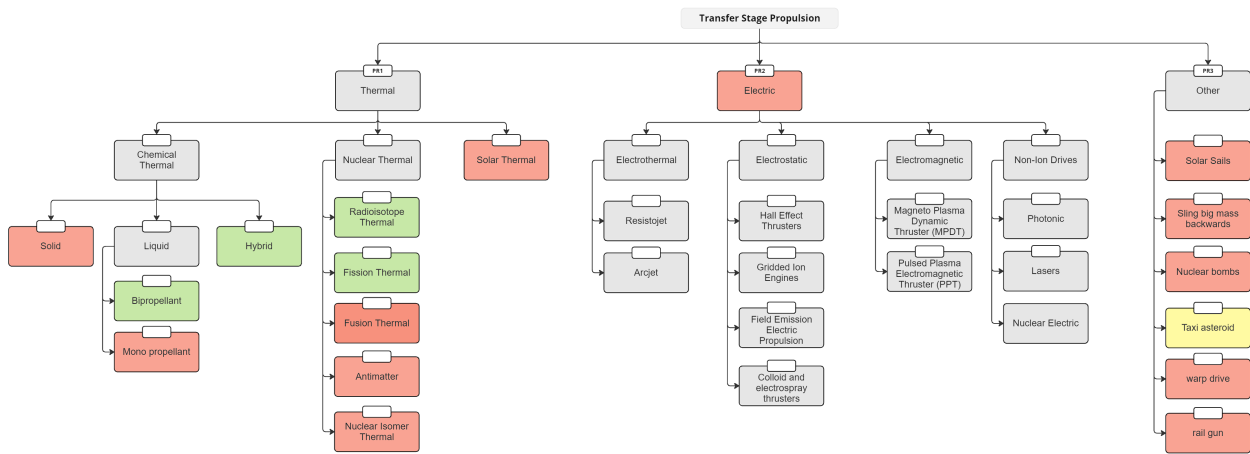
Figure 6.1: Propulsion System Design Option Tree: Red means that the option is discarded early on, yellow means that the option is considered more in depth but later discarded and green means that it is a possible option

seven of the best-considered options. The engine is chosen by ensuring that it provides at least the minimum thrust and not more than the maximum thrust and then selecting the engine that requires the least propellant. The higher the specific impulse of an engine, the lower the required propellant mass, thus the engine with the highest specific impulse is chosen. The minimum thrust threshold was not analysed in detail, as bipropellant engines with low thrust generally have a lower specific impulse and thus would not be selected. As seen in Table 6.1, the winner is the VRM1500-H Hypergolic MMH/MON 1500-lbf Engine, developed by Sierra Space[5]. This is not the engine with the highest I_{sp}, but the VR650-D GOX/CH4 650-lbf Thruster was discarded because of the propellant type: gaseous methane and gaseous oxygen. Under normal pressure conditions, the density of this fuel is 0.72 kg/m^3.[6] To obtain a reasonable density, the tanks would have to be strongly pressurised, leading to significant increases in structural weight. XLR-132 was also discarded as it exceeds the maximum acceleration of 6g.

Table 6.1: Considered Engines for the Transfer Stage

Engine	Propellant	Isp	Thrust [N]	g
LE-5B	LOX/LH2	447	137300	6.16
VRM1500-H Hypergolic MMH/MON 1500-lbf Engine	**MMH/MON-3**	**323**	**6672**	**0.3**
R-4D-11 490 N (110 lbf) Bipropellant Rocket Engine	MMH/NTO (MON-3)	315.5	511	0.02
XLR-132	NTO/N2H4	340	16700	0.75
RL10B-2	LOX/LH2	465.5	110100	4.94
5lb- Cb	NTO/MMH	293	22	0.001
R-1E	NTO(MON-3)/MMH	280	111	0.005

6.2.4. Propellant Storage

A liquid bipropellant engine requires two propellant tanks: one for the fuel and one for the oxidiser. The chosen engine uses Monomethylhydrazine (MMH) as fuel and MON-3 as oxidiser. Hydrazine is harmful to the environment, but considering that it is only used in space for the transfer stage, environmental concerns are not an issue.[7] However, another concern is the effect it has on workers exposed to it. Breathing it in can cause liver and kidney failure and infertility.[8] To minimise the effects on the workers exposed to hydrazine, some measures can be taken in the workplace. This includes providing the workers with hazard information and training, as well as equipping the workplace with special amenities, such as eye wash fountains and emergency showers.[9] There was, however, no better propellant option for this mission. The closest competitor

---

[6]From `https://www.aqua-calc.com/page/density-table/substance/methane-coma-and-blank-gas`, accessed on 18/06/2024.
[7]From `https://www.canada.ca/content/dam/eccc/migration/ese-ees/d66353c2-717c-4db5-95c1-931b0eaeaa14/feqg_hydrazine_en.pdf`, accessed on 17/06/2024.
[8]From `https://wwwn.cdc.gov/TSP/PHS/PHS.aspx?phsid=499&toxid=89`, accessed on 17/06/2024.
[9]From `https://nj.gov/health/eoh/rtkweb/documents/fs/1006.pdf`, accessed on 17/06/2024.

was LOX/LH2, but engines using this propellant were discarded because they usually generate too much thrust. Moreover, these propellants are not suitable for long-term missions, because they have to be stored at extremely low temperatures. Current methods to keep them at low temperatures, by e.g. using specialised MLI, can only reduce boil-off to around 3% per month, which is still too much for long-term missions [34].

The tanks are not pressurised, as a pump-fed system is used to transport the propellant from the tanks to the engine. The tank must be designed such that it can withstand all expected loads, the limit case for which is during launch. Two stresses need to be taken into account: the stresses caused by the fluids inside the tank (σ_f) and the stresses caused by the weight of the fuel tank itself (σ_w). Since the fuel tank is not part of the primary structure and thus does not carry any loads from the rest of the spacecraft structure, these are the only considered stresses. (σ_f) is caused by the vapour and hydrostatic pressures of the propellant [33]. The vapour pressure is dependent on the type of propellant and the temperature. Assuming that the tanks stay at room temperature during launch, it is 4511 Pa for MMH and 50 000 Pa for MON-3 [33]. Hydrostatic pressure during launch is calculated with the following equation [33]:

$$p_{hyd} = \rho \cdot \Psi \cdot g \cdot H \tag{6.2}$$

Ψ is the maximum T/W ratio, which in this case is 7, as the maximum acceleration of the launcher is 6g. H is the total height of the tank. For clarity, the tank size parameters are shown in Figure 6.2.

The optimal shape for a fuel tank in terms of structural efficiency is a sphere [33]. Nonetheless, this is not the shape chosen for the propellant tanks, because to facilitate the mounting of the tanks, both of them should have the same height. To make this possible, the tanks are chosen to be cylinders with spherical end caps, which is the next best option: cylindrical tanks with spherical end caps only need to be half as thick as simple cylindrical tanks experiencing the same pressure [33]. The equation for the thickness of the latter case is:

$$t = \frac{p_b \cdot r}{\sigma_y} \tag{6.3}$$

Figure 6.2: Dimensions of the cylindrical tank with spherical caps

where p_b is the burst pressure, r is the inner diameter of the cylinder, and σ_y is the yield strength of the material. Burst pressure is simply the design pressure multiplied with a safety factor of 1.5 [33]. In this case, the design pressure is simply the vapour pressure summed with the hydrostatic pressure. For a cylindrical tank with spherical caps, the required thickness is:

$$t = \frac{p_b \cdot r}{2\sigma} \tag{6.4}$$

After comparing different materials, grade 5 titanium was chosen as the material to be used for the tanks, as it leads to the lowest amount of mass when performing preliminary analysis with the above equations. Rewriting Equation 6.4 to calculate the stress experienced due to the fluids inside the tank leads to:

$$\sigma_f = \frac{p_b \cdot r}{2 \cdot t} \tag{6.5}$$

σ_w is determined by calculating the force caused by the mass of the tank during launch, which is

$$F = m \cdot g \cdot \Psi \tag{6.6}$$

This force is then divided by the cross-sectional area of the cylinder wall, which is

$$A = \pi \cdot \left(\left(\frac{D}{2} + t \right)^2 - \left(\frac{D}{2} \right)^2 \right) \tag{6.7}$$

D is the inner diameter of the tank and t is the tank thickness. σ_w can then be calculate by dividing Equation 6.7 by Equation 6.6.

The total stress experienced by the tank is σ_f plus σ_w. Two failure modes need to be taken into account, namely failure by yielding and failure due to buckling. The tank should not yield, because as the tank reaches the plastic regime, it deforms much quicker with increasing load. This deformation can lead to stress concentrations, which can lead to failure at certain locations. The safety factor for yielding is 1.5, which means that

the tank should not experience stress higher than $\frac{\sigma_y}{1.5}$. Buckling is taken into account by determining the critical buckling stress. According to literature, the critical buckling stress for a cylindrical fuel tank with spherical caps is [35]:

$$\sigma_{cr} = 1.28 \cdot \left(\frac{H}{D}\right)^{-0.0256} \cdot \frac{t}{D} \cdot E \tag{6.8}$$

H is the total height of the tank, which is $D + h$. h is the height of the cylindrical part of the tank, in between the two spherical caps and D is the diameter of the spherical caps, as well as the width of the tank. E is the elastic modulus.

Determining the optimal dimensions for height, diameter and thickness of both tanks, to minimise the combined mass, is done with an algorithm, that calculates the minimum required thickness for a certain diameter of a tank. This is done by means of many automatic iterations. The program sets a certain tank diameter D for the fuel tank, which automatically calculates the height h of that tank, as the required inner volume is predetermined by the required propellant volume. The inner volume of the tank is higher than the needed volume. This extra volume is called ullage volume and is added due to thermal expansion of the propellant, which is caused by temperature differences and ejection of dissolved gasses. The extra volume is usually 5 % of the total tank volume [33]. When height and diameter are determined, the algorithm calculates the minimum thickness required for that tank to reach either the critical buckling stress or the yield stress. For both of these stresses safety margins are taken into account. For both buckling as well as yield, this safety factor is 1.5 for propellant tanks [33].

After setting the variables for the fuel tank, it does the same procedure for the oxidiser tank, keeping in mind that there are limits on the combined diameter and height. If the tanks are stacked on top of each other there is a limit on the combined height. This seemed to be the better option in terms of volume efficiency, but it turns out that this is not the case. If the tanks are stacked on top of each other, they have quite large diameters, which leads to the spherical caps taking up a lot of volume. After some iterations, it turns out that it is not possible to fit the tanks on top of each other, without exceeding the maximum transfer stage height. Therefore they are arranged next to each other. In this case, the parameter that influences each other is the tank diameter. The combined diameter can only be 4.5 m, as explained in Section 6.5. The maximum height of each tank is then equal to the height of the transfer stage, which is 4 m. With these constraints, the algorithm runs many iterations, with four variables, namely the diameter of each tank and the thickness of each tank. It then finds the combination of the four variables that leads to the lowest mass, still satisfies all constraints and makes sure that it does not fail by buckling or yield. The tank also includes add-ons like mounting provisions and propellant management devices. For a titanium tank, the estimated mass is multiplied by a factor of 1.41 to get a more realistic mass estimate [33]. The final values of the tank dimensions are shown in Table 6.2 and Table 6.3. As can be seen, for both the fuel tank and the oxidiser tank, buckling is the critical failure mode. The difference of actual experienced stress and critical buckling stress is zero, taking into account a safety margin of 1.5. The final tank design with its dimensions is shown in Figure 6.7.

Table 6.2: Parameters of the fuel tank of the transfer stage

Parameter	Value	Unit
Fuel mass	4281.23	kg
Fuel Volume (Liquid)	4.87	m³
Ullage Volume	0.26	m³
Tank Volume	5.12	m
Tank Cylinder Height	0.77	m
Tank Diameter	1.82	m
Tank Thickness	1.40	mm
Difference Actual and Buckling Stress	0	MPa
Difference Actual and Yield Stress	852.26	MPa
Tank Mass	93.26	kg

Table 6.3: Parameters of the oxidiser tank of the transfer stage

Parameter	Value	Unit
Oxidizer mass	7042.62	kg
Oxidizer Volume (Liquid)	5.14	m³
Ullage Volume	0.27	m³
Tank Volume	5.14	m
Tank Cylinder Height	0.71	m
Tank Diameter	1.88	m
Tank Thickness	1.80	mm
Difference Actual and Buckling Stress	0	MPa
Difference Actual and Yield Stress	823.75	MPa
Tank Mass	123.56	kg

Table 6.4: Masses of the full propellant storage system

Parameter	Mass [kg]
Total Tank Mass incl. add-ons	305.77
Feed System Mass	42.88
Total Mass	**348.65**

6.2.5. Propellant Feed System

For the transfer stage, a pump-fed system is chosen. This is mainly due to the mass that it saves, compared to a pressure-fed system. Pump-fed systems generally have to withstand only pressures in the range of 0.07 MPa to 0.6 MPa, which is much lower than pressure-fed systems, which need to withstand pressures of 2 MPa to 5 MPa [33]. Substituting the lower value of 2 MPa into the equation for burst pressure already leads to a tank mass of at least 1 ton. The feed system was not designed in detail, but a mass estimate was determined, using the fact that usually, a pump feeding system weighs about 12.3 % of the total propulsion system dry mass. This number is also shown in Table 6.4.

6.2.6. Using Thermal Energy From the RTG

Both the RTG on the probe and the RTG on the lander emit a lot of useless thermal energy. On Europa, this heat is turned into useful energy by partially using it to aid in the penetration of the ice shell. During transit, however, the thermal energy is simply lost to the environment. Therefore, it is analysed whether this heat can somehow be used to make the propulsion system more efficient. An interesting option is diverting the heat from the RTG to the propellant. By pre-heating the propellant, the flow from the tanks to the engine can be optimised to minimise energy losses. This is especially true for MMH, as its viscosity drastically increases as soon as the temperature drops below 0 ° C [36]. According to a study on the flow of MMH at different temperatures, the propulsion subsystem loses its efficiency, as the exhaust velocity decreases by 7.7% when the temperature of MMH drops from 20 ° C to −40 ° C [37]. Instead of keeping the propellant at suitable temperatures by means of an expensive thermal control system, it could be possible to utilise the excess heat from the RTG to complete this task. This has not been analysed in this design but would be an interesting approach to consider in the further development of the AlienDive mission.

6.3. Guidance, Navigation & Control Subsystem

The transfer stage includes an Inertial Measurement Unit (IMU) that will handle all inertial measurements during the journey to Europa of the whole spacecraft. IMUs will actually be installed on both the transfer stage and the lander. Having IMUs on both vehicles is crucial because if only the lander were equipped with an IMU, the separation from the transfer stage could introduce accuracy issues. This is particularly problematic because there is no opportunity to recalibrate the IMU during the immediate descent that follows separation. The selected IMU for the transfer stage is the ASTRIX 1090 from Airbus[10], chosen for its high radiation resistance of 100 krad and commercial availability. Like the IMU on the lander, this IMU is shielded with an aluminium box, as explained in Section 7.4. The specifications of the IMU are shown in Table 7.12.

Table 6.5: Product specifications of the ASTRIX 1090[9]

Parameter	Value	Unit
Mass	4.5	kg
Dimensions	⌀263 x 192	mm
Power	13.5	W
Radiation Resistance	100 (TID)	krad
Rotational Measurement Range	140	deg/s
Linear Measurement Range	1.1 or 20	g
Operating Temperature	-25 to +60	°C

---

[10]From `https://www.airbus.com/en/space/equipment/avionics/astrix-inertial-measurement-iru-series.`, accessed on 04/06/2024

The subsystem requirement of the transfer stage Guidance, Navigation & Control (GNC) subsystem is listed below:

- **AD-PERF-01-TS-05-GNC-01**: The GNC subsystem shall perform the inertial measurements of the whole spacecraft during its transit to Europa.

6.4. Thermal Control Subsystem

In this section, the sizing of the thermal control subsystem (TCS) of the transfer stage will be done. Before starting with the design, a background on the equations will be given. Then the assumptions will be stated. Afterwards, the design process will be laid out and finally, the results will be explained. It is good to note at this point that the lander's TCS was sized before the transfer stage's TCS, but for the sake of consistency with the report, the transfer stage's TCS will be discussed first.

6.4.1. TCS Requirements

The subsystem requirements of the transfer stage thermal control subsystem are listed below:

- **AD-PERF-01-TS-01-TCS-01:** The TCS shall be able to maintain the temperature of the transfer stage temperature range of 263.15 K to 313.15 K.

- **AD-PERF-01-TS-01-TCS-02:** The TCS shall be able to transport the heat throughout the transfer stage.

6.4.2. Thermal Balance

The TCS onboard the transfer stage was sized using the thermal balance equation Equation 6.9:

$$\dot{Q}_{in} = \dot{Q}_{out} \qquad (6.9) \qquad\qquad \dot{Q}_{out} = A_{emitting}\varepsilon\sigma T^4 \qquad (6.10)$$

Where $\dot{Q}_{in}$ is the heat flow absorbed by the transfer stage and $\dot{Q}_{out}$ is the heat flow emitted from the spacecraft. This relation comes from the first law of thermodynamics which states that energy cannot be created or destroyed. In the context of space, the only form of heat transfer is radiation as it is a vacuum. $\dot{Q}_{in}$ comes from the electronics onboard the spacecraft and all the celestial bodies in space such as the sun, earth, and sun rays reflected from celestial bodies commonly known as albedo. $\dot{Q}_{out}$ comes from the heat emittance of the spacecraft which can be calculated using Stefan Boltzmann's Law shown by the relation in Equation 6.10:

Where $A_{emitting}$ is the area emitting the heat which for the spacecraft is taken as the exposed surface area, ε is the emissivity of the surface, σ is the Stefan–Boltzmann constant which is 5.67×10^{-8} Wm^{-2}K^{-1} and T is the temperature of the spacecraft. Using Equation 6.9 and Equation 6.10 taking into account all sources that cause heat flow into the spacecraft results in Equation 6.11:

$$\dot{Q}_{electronics} + \sum_{1}^{m}\left(J_{source}\left(\frac{R}{R+h}\right)^2 \cdot AF \cdot \alpha_{(surf)m}A_{(abs)m}\right) = \sum_{1}^{n}\left(A_{(emitting)n}\varepsilon_n\right)\sigma T^4 \qquad (6.11)$$

Where $\dot{Q}_{electronics}$ is heat dissipated from the electronics and RTG, J is the heat flux with the subscripts showing from which source the heat flux is coming, A_{abs} is the surface area that is receiving the heat flux, $\left(\frac{R}{R+h}\right)$ is a scaling factor applied to the flux based on how far the spacecraft from the surface of the planet or sun, h is the altitude of orbit and R is the planet's radius, α_{surf} is the absorptivity of the surface, AF is the albedo factor if the heat flux is coming from the reflection of the solar rays from a planet. A summation operator has been added to take into account the fact that different areas will absorb and emit differently based on the surface.

Assumptions

The temperature calculated Equation 6.11 is assumed to be the temperature of the entire spacecraft. This also means that the heat generated from electronics is assumed to be spread across the spacecraft uniformly and is not concentrated in a specific part of the spacecraft. This assumption implies that some parts of the spacecraft might be overestimated or underestimated. This can be taken into account by putting keep a margin for the cold and hot temperature to take into account any local temperature changes. Moreover, only two surfaces are assumed to absorb the incoming heat; the high-gain antenna surface and the area that contains the thruster of the transfer stage (the two opposite surfaces). View factors will not be taken into account. This means the temperatures calculated will be higher than what it is in reality because the surface area is absorbing 100% of the heat. This is a conservative assumption to make as it will be seen later on the limiting case is the upper range of the temperature and not the lower range.

6.4.3. Thermal Design Process

1. Identify the maximum and minimum operating temperature of the components of the spacecraft. Because the spacecraft will be assumed to be homogeneous, the component with the strictest temperature requirements will be looked at and the TCS will be designed to satisfy that requirement.

2. The spacecraft will go through different thermal cases throughout the journey and thus every case will be thermally analysed. From there the hot and cold states of the spacecraft will be identified and the extreme cases will be used to design the TCS.

3. From the cases identified it will be already known whether the transfer stage would have a very high or very low temperature therefore, TCS solutions will be already selected to cool or heat the spacecraft.

4. The solutions selected will be sized using Equation 6.11 in such a way that all the cases are satisfied.

The operating temperature is what will be used as design points to size the TCS. The components that will limit this is the fuel onboard the transfer stage which has an operating temperature range of 273.15 K to 313.15 K.

6.4.4. Thermal Case Analysis

For the thermal case analysis, the journey of the spacecraft will be partitioned into different cases. These cases will all have a hot state and a cold state which will be the result of the spacecraft either facing the sun or eclipsed by the celestial body it is currently near to. This goes for all the cases except the first two cases where the spacecraft has just separated from the fairing and therefore will be absorbing free molecular heating (FMH). An overview of all the thermal cases is shown in Table 6.6.

Table 6.6: Overview of all the thermal cases the spacecraft will encounter in its trajectory.

Thermal Cases	Cold State	Hot State
1. Separation while Eclipsed	150 km altitude with no FMH	Separation altitude with maximum FMH
2. Separation while Facing the Sun	250 km altitude with no FMH	Separation altitude with maximum FMH
3. Orbit/flyby around Earth	Eclipsed by Earth while being at an altitude of 11 764 km	Facing the Sun while being at an altitude of 3336 km
4. Journey to Venus from Earth	Spacecraft position: Earth	Spacecraft position: Venus
5. Venus Flyby	Eclipsed by Venus while being at an altitude of 3184 km	Facing the Sun while being at an altitude of 3184 km
6. Earth to Jupiter	Spacecraft position: Jupiter	Spacecraft position: Earth
7. Jupiter Flyby	Eclipsed by Jupiter while being at an altitude of 894 861 km	Facing the Sun while being at an altitude of 894 861 km
8. Ganymede Flyby	Eclipsed by Ganymede or Jupiter while being at an altitude of 15 818 km	Facing the Sun while being at an altitude of 109 km
9. Europa Orbit	Eclipsed by Europa or Jupiter while being at an altitude of 312 km	Facing the Sun while being at an altitude of 312 km

A few things to note about Table 6.6 is that firstly the case of the journey from Venus to Earth will not be considered because it will be the same as the journey to Venus from Earth. Moreover, there will be many flybys of Ganymede but only the extreme thermal cases will be analysed. In theory, it is better to look at every instant of the spacecraft and check its current thermal state in the trajectory but in practice, to preliminary size the spacecraft, it is better to start analysing the extreme cases first.

Without doing any calculations, it is already possible to identify the extreme hot and cold states of the spacecraft. The limiting hot state of the spacecraft will be at the point where the spacecraft is performing a flyby of Venus and facing the sun. This is because it will be at the closest point to the sun and therefore experience the highest heat flux from the sun. The limiting cold state is harder to identify in between the thermal cases but generally speaking, it will be at its cold state when it has entered the Jovian system and is eclipsed by either Jupiter, Ganymede, or Europa.

6.4.5. Component Selection

As mentioned earlier, it is already known that the spacecraft will experience a limiting hot case and cold case therefore, it is required to select components which will cool down the spacecraft to a temperature of 313.15 K and heat up the spacecraft to a temperature of 273.15 K. The TCS that is on the lander was specifically chosen to be passive and not active to avoid increasing the power requirement of the spacecraft. Furthermore, adding an active TCS will lower the reliability as it would require some mechanism which if it fails could be catastrophic if the spacecraft has no other way of regulating its temperature. This choice of course will be justified after showing the final result of the analysis. To heat up the spacecraft a very common choice used is multi-layer insulation (MLI) [25]. This lowers the emissivity of the spacecraft which in turn means that all the heat will be kept in the spacecraft increasing the temperature of the spacecraft. The layers of MLI can be broken down into three significant layers; The outer cover, the spacer layers, the reflector layers, and finally the inner cover. All the other components on the MLI Figure 6.3 are not looked into with much detail because it does not influence the design as much compared to the aforementioned layers which influence the mass and the emissivity. As it can be seen from Figure 6.3, the MLI comprises one inner cover and outer cover and N layers of Spacer and reflector layers. The variable N determines the overall effective emissivity of the MLI $\varepsilon_{MLI_{eff}}$ using Equation 6.12.
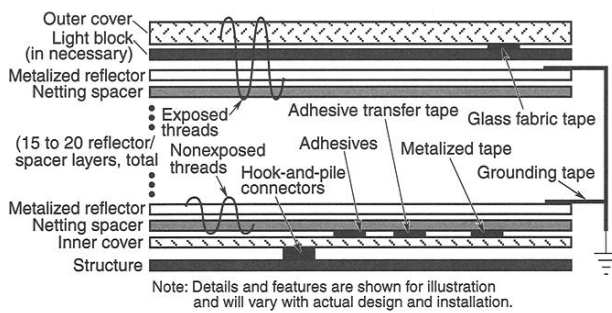
$$\varepsilon_{MLI_{eff}} = \cfrac{1}{\frac{1}{\varepsilon_{outer}} + \frac{1}{\varepsilon_{inner}} - 1} \left(\frac{1}{N+1} \right) \quad (6.12)$$

Figure 6.3: Typical structure of MLI [38]

Where ε_{outer} is the emissivity of the outer cover and ε_{inner} is the emissivity of the inner cover. Theoretically speaking, if N is increased to a high number the $\varepsilon_{MLI_{eff}}$ should approach zero. However, in practice, using more than 25 layers has a diminishing effect and will only cause an increase in mass [38], therefore the range for the variable N that will be used is between 1 and 25 layers.

To cool down the spacecraft, paints and coating could be used which have a specific emissivity and absorptivity. Looking back at Equation 6.11, it can be shown that if the emissivity is increased and the absorptivity is decreased the temperature of the spacecraft will be lower. This makes sense because if the spacecraft is allowed to emit more and absorb less heat its overall equilibrium temperature will be lower. Therefore, a design parameter for the paint or coating to select the most optimal solution will be the ratio $\frac{\varepsilon}{\alpha}$ of which the maximum value of this ratio is needed. These will act as passive radiators for the transfer stage. These radiators will use the same outer cover as the MLI to cover the truss structure such that it is possible to paint over the cover. Both of these components will be sized in Section 7.5 as the sizing needs to be done concurrently to balance the heat flow of the spacecraft such that it can be within the allowable operating temperature range of all components in all the thermal cases.

6.4.6. TCS sizing

For the TCS sizing, Equation 6.11 will be used to calculate the temperature at each of the thermal cases. The variables that will change are the areas of the spacecraft that will be covered using either the MLI or radiators. It will be assumed that the area that is allowed to be used for either the radiators or the MLI is entire that is exposed to the vacuum of space except for the area that is covered by the attachment point between the lander and the transfer stage and the thruster that is on the transfer stage. It is also assumed that the lander's TCS is already sized but the discussion of how it's sized will be in Section 7.5. For the TCS sizing, these steps were followed:

1. Make an initial guess of the type of MLI and Radiator to be used and the Area it occupies. The combined area will be restricted to the outer surface area of the transfer stage excluding the bottom area of the transfer stage which will be used as the absorption surface and the attachment area of the lander and transfer stage.

2. Use Equation 6.11 to calculate the temperature of each thermal case in its hot and cold state.

3. Check if all the thermal cases satisfy the temperature requirement. If yes, freeze the design. If not,

Change the type of MLI and Radiator used and the area it occupies.

4. repeat steps 2 and 3 until an optimal solution is reached.

These steps were done using the Excel sheet solver which allows the user to set a goal, select the variable cells and put constraints on certain values such as area for this case such that it does not vary the area of the radiators and MLI above the allowable area. Running the iterations results in the optimal configuration shown in Table 6.7:

Table 6.7: Radiator and MLI area for the Transfer stage

Component	Value	Unit
Radiator Area	0.14	m^2
MLI Area	30.89	m^2

The MLI and Radiator in Table 6.7 have properties listed in Table 6.8

Table 6.8: Radiator and MLI properties [38]

Parameter	Value	Unit
Radiator		
Emissivity	0.92	-
Absorptivity	0.17	-
MLI		
Emissivity of Outer Cover (Kapton)	0.81	-
Emissivity of Inner Cover (Aluminized Kapton)	0.05	-
Effective Emissivity	0.0019	-
Outer Cover Areal Density	0.271	kg/m^2
Reflector Layer Areal Density	0.011	kg/m^2
Spacer Layer Areal Density	0.00715	kg/m^2
Inner Cover Areal Density	0.05	kg/m^2
Mass of MLI	23.94	kg
Mass of Radiator	2.35	kg
Total TCS mass of the Transfer Stage	26.29	kg

The resultant temperatures of the limiting thermal cases at their cold and hot state are given in Table 6.9:

Table 6.9: Equilibrium Temperature of the limiting thermal cases of the Transfer Stage

Thermal Case	Cold State Temperature [K]	Hot State Temperature [K]
5. Venus Flyby	285.18	306.06
9. Europa Orbit	285.37	292.10

6.5. Structures

In this section, the structure of the transfer stage is discussed. First, however, the launch loads of the Falcon Heavy launcher are specified, as these loads are the leading factors in the design of the structure. Afterwards, the detailed design of the transfer stage structure is explained.

6.5.1. Launch loads

The launch subjects the spacecraft to a large magnitude of axial and lateral acceleration, vibration and shock loads. Since surviving the launch is critical for mission success, these loads are thus considered in the structural design of all three mission elements. The Falcon Heavy is used for the launch of the AlienDive mission. From its user manual [39], an overview of the launch loads is found in Table 6.10. The load diagram is found in

Figure 6.4. In addition to these launch loads, the axial and lateral natural frequencies of the primary structure shall be above 25 Hz and 10 Hz respectively, and above 35 Hz for the secondary structures.
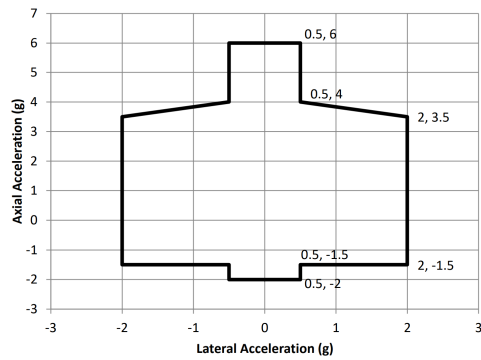
Figure 6.4: Falcon Heavy launch load diagram [39, p. 17]

Table 6.10: Overview of the Falcon Heavy Launch Loads

Parameter	Value	Unit
Max. axial compression	6	g
Min. axial acceleration	-2	g
Max. lateral acceleration	2	g
Min. axial frequency	25	Hz
Min. lateral frequency	10	Hz
Min. secondary frequencies	35	Hz

6.5.2. Structures Requirements

The requirements for the structure of the transfer stage are listed below:

AD-ENG-02-TS-01-STRUC-01: The structure shall carry lateral loads of ±2 g.

AD-ENG-02-TS-01-STRUC-02: The structure shall carry axial loads between −2 g and 6 g.

AD-ENG-02-TS-02-STRUC-03: The structure shall have a natural frequency higher than 25 Hz in the axial direction.

AD-ENG-02-TS-02-STRUC-04: The structure shall have a natural frequency higher than 10 Hz in the lateral direction.

AD-PERF-01-TS-01-STRUC-05: The structure shall withstand a temperature difference of 30 K.

6.5.3. Structure design

The critical load case for the structure of the transfer stage is the launch since the maximum acceleration due to the thrust of the transfer stage itself is only 2.7 g. The transfer stage is thus designed for axial accelerations of 6 g, lateral accelerations of 2 g, and to keep the axial and lateral frequency above 25 and 10 Hz respectively. A yield safety factor of 1.1 is applied to the axial and lateral load, in addition to a design load safety factor of 1.25. The structure is designed to carry the mass of the entire spacecraft, thus the transfer stage, lander and probe. For additional safety, the frequencies are multiplied by a factor of 1.2 to ensure the spacecraft resists the launch vibrations.

The structure of the transfer stage is built as a truss structure consisting of 6 axial beams and 3 horizontal "rings" around the two propellant tanks. Since the structure fits tightly around the two side-by-side propellant tanks, the horizontal rings are not circular but have a straight part between two circular arcs.

The structure is designed for strength, stability (buckling) and vibration (natural frequencies). Both the vertical and horizontal elements of the transfer stage structure are sized using a similar method, with only the internal loads differing between the two.

Since the spacecraft experiences a lot of different environments during the length of the mission, it will experience a range of equilibrium temperatures. Using the values from the thermal subsystem, the maximum temperature increase is taken to be 30 K. The expansion/contraction caused by this temperature difference results in an additional compressive/tensile load depending on the shape of the beam element and mechanical properties of the material, as seen in Equation 6.13. Here, E is the elasticity modulus, A is the area of a beam cross-section, α is the thermal expansion coefficient, and ΔT.

$$F_{thermal} = E \cdot A \cdot \alpha \cdot \Delta T \tag{6.13}$$

It is thus important to take this thermal load into account when sizing for strength and buckling, as the extra thermal load could cause the structure to fail. In practice, the axial thermal load was calculated based on the required structural area after designing for all of the failure modes. This load was added to the total axial load, and the structural design was iterated until convergence.

In designing for strength, axial, bending, shear and torsional stresses are to be kept below the yield stress of the structural material. While small torsional loads could be induced during attitude control manoeuvres, torsional loads in the beam elements are assumed to be negligible. Since axial and bending stresses work in the same plane, the total stress is a combination of both. The governing equation for this stress (including

the additional thermal stress) is found in Equation 6.14. The required size of beam elements is then found by rewriting the equation and substituting the material tensile strength for the axial stress σ. For shear stresses, a similar process is performed using the shear stress equation (Equation 6.15), but instead of the tensile yield strength of the material, the shear strength of the material is substituted for the shear stress τ.

$$\sigma = \frac{F_{axial}}{A} + \frac{F_{lat} \cdot c_{max}}{I} + E\alpha\Delta T \qquad (6.14) \qquad\qquad \tau = \frac{VQ}{It} \qquad (6.15)$$

Where c_{max} is the maximum distance from the neutral axis, I the area moment of inertia, A the area, V the internal shear force, Q the first moment of area, and t the thickness of the beam element.

The method used for designing for buckling depends more on the shape of the structure. Since the transfer stage structure consists of beam elements, only Euler buckling is considered. Since the structure is only connected to the launcher on one side, the boundary conditions for Euler buckling are taken as fixed-free, which is the worst-case situation for buckling and is thus a conservative design choice. The equation for the critical buckling load F_{crit} is found in Equation 6.16, which is equalled to the maximum axial load in the beam element. Here, L is the length, A is the area, and I is the area moment of inertia of the beam element.

Finally, the axial and lateral natural frequencies of the beam elements need to be larger than those specified by the launch provider. For these frequencies, it is assumed that all of the mass is concentrated on top of the beam element, as this is the most conservative method to design for vibration resistance [40]. The governing equations for the axial and lateral natural frequencies of beam elements are found in respectively Equation 6.17 and Equation 6.18. The frequencies are then equalled to the launcher frequencies, and after rewriting, the required size of the beam elements is again calculated. Here, L is the length, A is the area, I is the area moment of inertia of the beam element, and m is the mass of the spacecraft. Note that for horizontal beam elements, the lateral frequency of the beam element has to be larger than the axial frequency of the launcher, instead of the lateral frequency, as the direction of the frequencies has to match.

$$F_{crit} = \frac{\pi^2 EI}{4L^2} \qquad (6.16) \qquad f_{ax} = 0.16\sqrt{\frac{AE}{mL}} \qquad (6.17) \qquad f_{lat} = 0.276\sqrt{\frac{EI}{mL^3}} \qquad (6.18)$$

The shape of the cross-section of the beam chosen for the beam elements is a thin-walled cylinder, as this shape is very weight-efficient and strong against buckling, which in addition to the vibration loads was identified as the most critical failure mode. For the material of the structure, titanium was chosen due to its high strength and stiffness for a relatively low density. The material properties of titanium are shown in Table 6.11. All subsequent calculations involving titanium will utilise these values.

Table 6.11: Material properties of Titanium Ti-6Al-4V (Grade 5), Annealed

Parameter	Value	Unit
Density	4430	kg/m^3
Yield Stress	880	MPa
Elastic Modulus	113.8	GPa
Poisson's Ratio	0.342	-

The size of both the vertical and horizontal beam elements are found in Table 6.12.

Table 6.12: Sizing of beam elements of the transfer stage structure.

Element	Failure mode	Total length [m]	Radius [mm]	Thickness [mm]
Vertical beam	Axial vibration	2.8	95.1	5
Horizontal ring	Buckling	11.4	44.6	5

In addition to the main structure, secondary and tertiary structures are present that support or provide attachment points for the internal components of the spacecraft. As a result of the preliminary nature of the design, it is difficult to make an accurate estimate of the mass of these elements. To account for these structures in the mass budget, the mass of the secondary and tertiary structures of the transfer stage are taken as respectively 10 and 5% of the primary structure mass. The mass breakdown of the transfer stage structure is found in Table 7.28. A better visualisation of the layout of the structure is found in Figure 7.15.

---

[5]From `https://asm.matweb.com/search/SpecificMaterial.asp?bassnum=mtp641`, accessed on 03/06/2024.

Table 6.13: Mass breakdown of the transfer stage structure.

Element	Mass [kg]
Primary structure	404.4
Secondary structures	40.4
Tertiary structures	20.2
Total mass	**465**
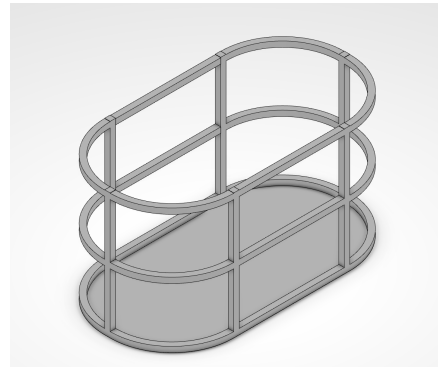
Figure 6.5: Visualisation of the layout of the transfer stage (Square cross sections seen in the figure are cylindrical in the design)

6.6. End-of-Life Procedures

The end-of-life of the transfer stage is after the spacecraft descends to the Europa surface. After the de-orbit burn, the transfer stage will no longer be needed and should be handled appropriately. According to the COSPAR regulations, the mission should have a low probability (1×10^{-4}) of infecting the subsurface ocean[41].

After the deorbit burn, the transfer stage will crash into Europa. This should not damage the moon and further exploration as the transfer stage will not penetrate through the ice layer. This can be substantiated by the discovery of craters with a diameter larger than 20 km on the Europa surface [42]. The impact craters are often 10-20 times larger than the object that hit the surface.[11] It is a valid assumption to say that these asteroids were magnitudes bigger than the transfer stage, and even they could not penetrate through the thick ice layer. The transfer stage also has no radioactive material which could damage the environment. The transfer stage can thus safely be crashed into Europa without bringing the moon into endangerment.

6.7. Visualisation of Layout

To prove the components can fit together as intended, a CAD assembly was made. An isometric view of this assembly can be seen in Figure 6.6, whilst Figure 6.7 shows the layout. Early estimates indicated that the length of the Falcon Heavy fairing would be more constraining than its diameter. Therefore, it was chosen to put the propellant tanks side-by-side, rather than on top of each other. The transfer stage also contains an inertial measurement unit, thruster, and coupling to both the lander and the Falcon Heavy fairing adapter. These were all placed in the middle. Cables, pipes and the propellant feed system (including the pumps) would all go in the empty area around the tanks.
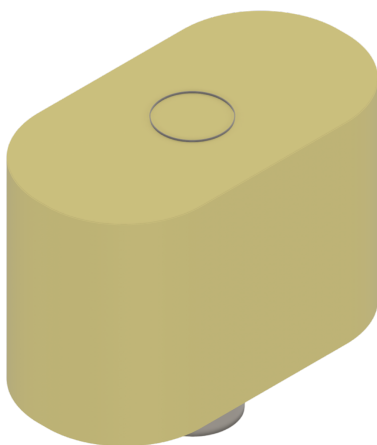
Figure 6.6: An isometric view of the transfer stage
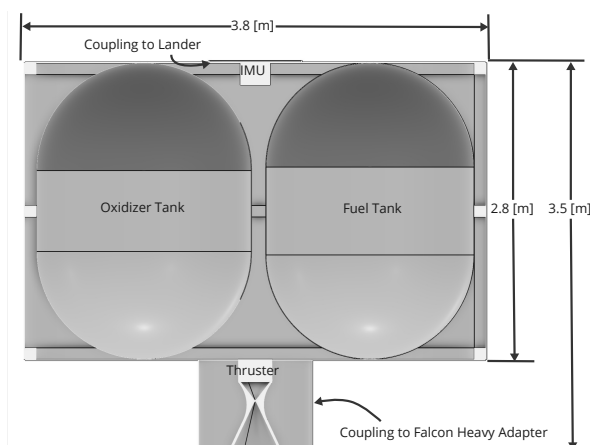
Figure 6.7: A cross-section of the transfer stage

---

[11]From https://www.lpi.usra.edu/science/kiefer/Education/SSRG2-Craters/craterstructure.html:~:text=Impact%20Crater%20Structure,crater%20depends%20on%20its%20size., accessed on 18/06/2024.

7   Lander Design

This chapter discusses the design of the lander. Section 7.1 provides an overview of the purpose and requirements of the lander, then, Section 7.2, Section 7.3, Section 7.4, Section 7.5, Section 7.6, Section 7.7, Section 7.8, Section 7.9 discuss the power, propulsion, GNC, thermal, radiation, communication, CDH and structures systems respectively. Finally, Section 7.10 details the end-of-life procedures, and Section 7.11 provides a summary of how all the components fit together in the lander.

7.1. Lander Overview

In this section, a summary of the design of the lander is given. The main function of the lander is to safely land the probe on Europa's surface and serve as a relay to Earth. Next to this, the lander also has secondary science goals, which mainly deal with characterising the surface environment of Europa. Because of this, the lander also contains a scientific payload. Many subsystems are present in the lander to ensure its correct functioning. As is described in Section 5.1, the lander begins its tasks as soon as the entire assembly is inserted into Europa's orbit. For seven days, it will take images of the surface to discover a suitable landing site. Subsequently, the transfer stage performs a de-orbit burn, after which the lander separates from the transfer stage and performs a powered descent to make a soft landing on the surface. After this, the probe is released onto the ice shell, where it starts to drill through the ice. The electronics that are prone to radiation damage, including the science payload of the lander are then lowered into the initial hole created by the probe, as a means of using the water ice as a barrier against radiation. After that, the science payload conducts its measurements. The body of the lander serves merely as a relay station to send the data acquired by both probe and lander payload back to Earth, through the antenna that is located on top of the vehicle. The lander is designed as a large truss structure, that is fully covered with thermal protection measures. It is powered by an RTG, as solar arrays or fuel cells are not viable options. To ensure a very specific landing trajectory, the lander is equipped with variable thrust liquid bipropellant engines and a complex GNC subsystem. The CDH subsystem keeps all subsystems linked and enables the autonomous functioning of the vehicle and the communications subsystem is responsible for sending data back to Earth. A detailed hardware diagram, containing every link between the subsystems of the lander and how these are interconnected with the transfer stage is shown in Figure 7.1.

7.1.1. Lander System Requirements

The system-level requirements of the lander are listed below:

AD-ENG-02-LD-01: The lander shall withstand the static loads of the Falcon 9 Heavy.

AD-ENG-02-LD-02: The lander shall withstand the dynamic loads of the Falcon 9 Heavy.

AD-ENG-02-LD-03: The lander shall be able to fit inside the payload fairing of the Falcon 9 Heavy.

AD-PERF-01-LD-01: The lander shall withstand the radiation environments throughout the mission.

AD-PERF-01-LD-02: The lander shall maintain a temperature range of 233.15 K to 313.15 K.

AD-PERF-01-LD-03: The lander shall provide attitude determination & control for the whole spacecraft.

AD-PERF-01-LD-04: The lander shall perform reconnaissance before descent.

AD-PERF-01-LD-05: The lander shall perform the powered descent during descent.

AD-PERF-01-LD-06: The lander shall be able to perform inertial measurements during its descent.

AD-PERF-01-LD-07: The lander shall have a lifetime of at least 14 years.

AD-PERF-01-LD-08: The lander shall be powered appropriately during its lifetime.

AD-LAND-01-LD-01: The lander shall be able to select a safe landing spot during descent.

AD-LAND-01-LD-02: The lander shall provide soft landing on the surface of Europa.

AD-LAND-01-LD-03: The lander shall be stable upright after touchdown on the surface.

AD-SCH-01-LD-01: The lander shall be produced and tested before 2035.

AD-PERF-05-LD-01: The lander shall be able to communicate with Earth.

AD-PERF-05-LD-02: The lander shall be able to communicate with the probe.

Figure 7.1: Hardware and software diagram for the lander and transfer stage
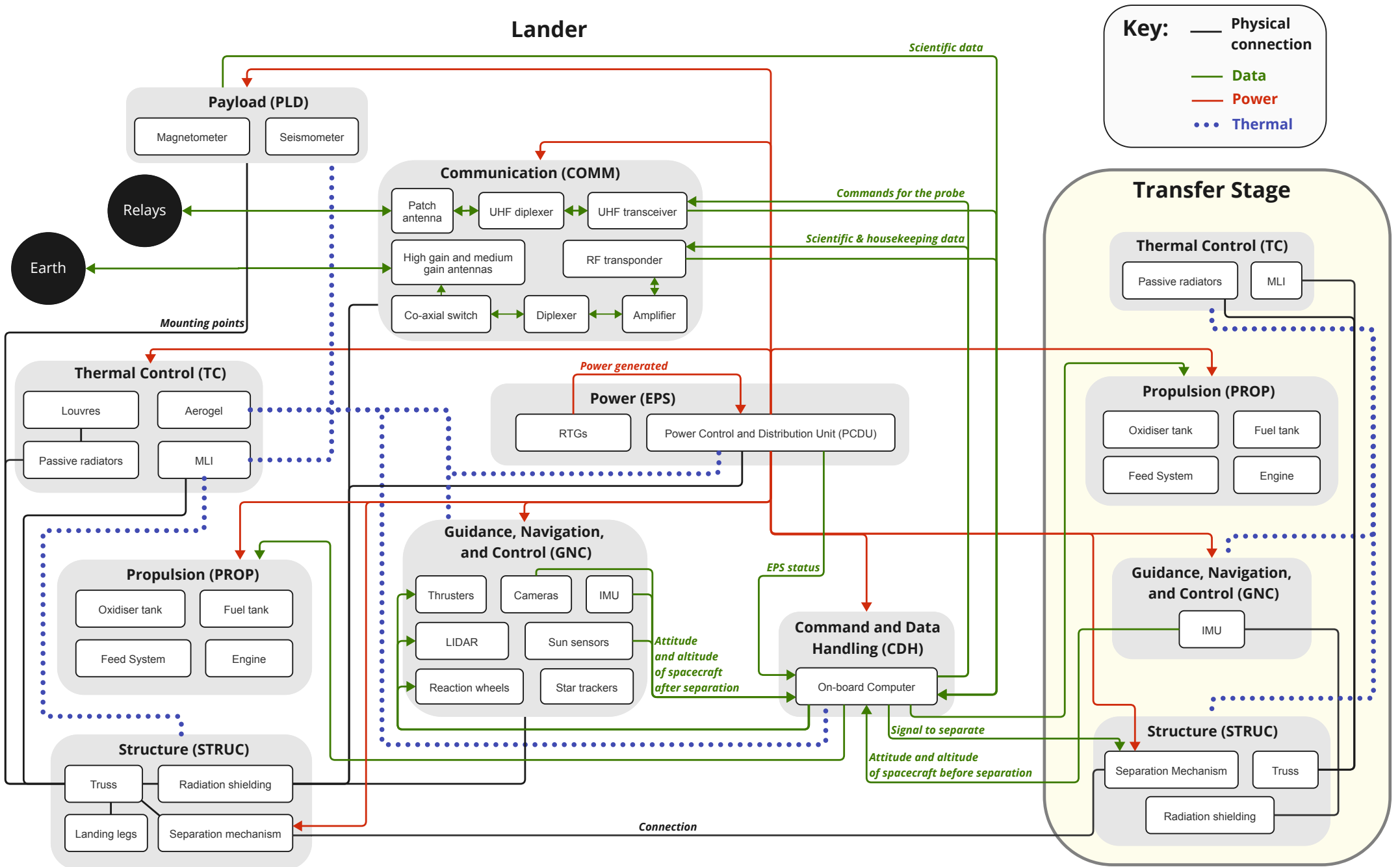
7.2. Power Subsystem

The lander plays a vital part in the mission, it is important for gathering data and communicating with the earth and the probe. It needs enough energy to fulfil these objectives. This will be done by the electrical power supply subsystem (EPS). It is important to make sure that all the subsystems get enough energy, without increasing the mass to an infeasible necessity.

7.2.1. Choice of Power Source

Due to the infeasibility of many commonly used power sources, only RTGs were deemed to be a usable power source for the lander. Solar panels are unfeasible due to the harsh radiation on the Europa surface, and batteries and fuel cells were discarded due to their low energy supply. An overview of this can be seen in Figure 7.2.
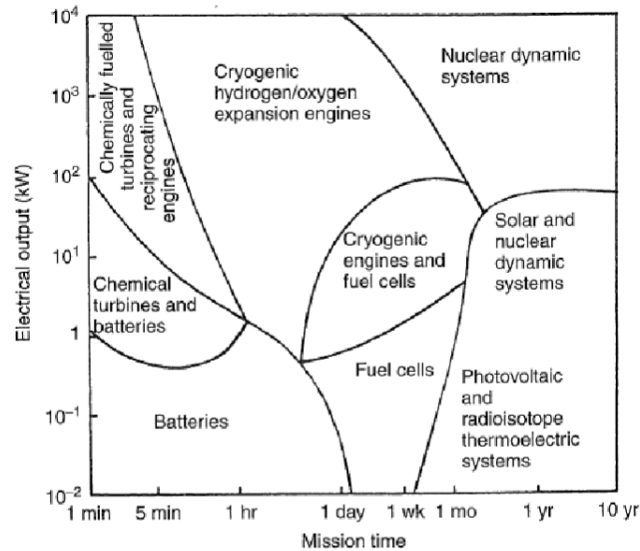
Figure 7.2: Viable choices for the EPS subsystem based on lifetime and power requirements [40]

When designing and choosing an RTG, a margin should be included to account for degradation. For RTGs, this is mainly due to the half-life of the radioactive substance in the power source. Plutonium was chosen for the AlienDive mission due to its half-life of 87.7 years [43] and its common use in RTGs. Equation 7.1 is used [40] to include this degradation.

$$P = P_0 \cdot e^{\frac{-0.693}{\tau_{1/2}} \cdot t} \tag{7.1}$$

Here P represents the power needed at BOL, P_0 the power required at EOL, the lifetime of the mission and $\tau_{1/2}$ the half-life of the radioactive substance. When assuming a lifetime of 20 years, which is a conservative assumption, this will result in a factor of 1.17.

7.2.2. Power budget

To choose an appropriate power source, the power budget should be looked at. For this, the power requirements of all of the subsystems were comprised in one table which can be seen in Table 7.1. For the EPS subsystem, this value was set to be 10% of the maximum power required[31], this will be discussed later in the section. For the propulsion, the power input was determined to be as large as possible without increasing the mass of the RTG. This is possible since the probe EPS subsystem will produce most of the required propulsion power. Any excess power can be used to optimise the thruster performance and thus save propellant mass.

Table 7.1: Power budget for the AlienDive Lander

ID	Subsystem	Power Input [W]
1	Scientific payload	12.6
2	Propulsion	60
3	Thermal control	0
4	Guidance, Navigation and Control	118.68
5	Electronic Power Supply	30.2
6	Earth Communication	97.5
7	Probe Communication	5.1
8	Command and Data Handling	5
9	Recon payload	1.6
10	Landing payload	88.2

This will not all work together at the same time but will be phased instead. These modes have been defined as follows, Earth Communication mode, Probe Communication mode, Science mode, Manoeuvre mode power, Recon mode, Journey mode and Landing mode. In Table 7.2, the modes and their respective required power have been given.

Table 7.2: Power modes of the AlienDive Lander

Mode	Power Required [W]	Active Subsystems
Earth Communication Mode	263.9	3,4,5,6,8
Probe Communication Mode	132.8	3,4,5,6,7
Science Mode	145.3	1,3,5,8
Maneuver Mode	215.5	2,3,4,5,8,9
Recon Mode	253.0	3,4,5,6,8,9
Journey Mode	153.9	3,4,5,8
Landing Mode	302.1	2,3,4,8,10

The highest required power is in the landing mode. This consumes 302.1 W. Due to the criticality of the EPS in this mission, the subsystem should be able to supply this at EOL, even though this would be halfway through the mission. Additionally, according to ESA guidelines, there should be a 20% power margin for newly developed power supplies [27]. This will result in a design power of 424.6 W at BOL.

7.2.3. EPS Subsystem Requirements
- **AD-PERF-01-LD-08-EPS-01:** The EPS subsystem shall provide the probe with an average and peak power of 425 W at BOL.
- **AD-PERF-01-LD-08-EPS-02:** The EPS subsystem shall safely distribute and condition all of the EPS power.
- **AD-PERF-01-LD-08-EPS-03:** The EPS subsystem shall provide health and safety information containing the produced power and power usage.
- **AD-PERF-01-LD-08-EPS-04:** The EPS subsystem shall protect itself and others from electromagnetic interference, transients, bus faults, and load faults, such as filtering, overvoltage, and short circuit protection.
- **AD-PERF-01-LD-08-EPS-05:** The EPS subsystem shall provide appropriate voltage levels for all the subsystems
- **AD-PERF-01-LD-01-EPS-06:** The EPS subsystems shall have a lifetime of at least 14 years.
- **AD-PERF-01-LD-01-EPS-07:** The critical EPS subsystem components shall withstand 100 krad of radiation during its lifetime.

  • **AD-ENG-02-LD-01-EPS-08:** The EPS subsystem shall withstand the launch loads.
  • **AD-ENG-02-LD-02-EPS-09:** The EPS subsystem shall not resonate with the launcher.
  • **AD-SCH-01-LD-07-EPS-10:** The EPS subsystem shall be developed before 2035.

7.2.4. RTG selection

For this, the developed RTGs were looked at. These were not up to par with the requirements and were thus quickly discarded. Conceptual RTGs looked like a decent option due to the high specific power and efficiency. The 16-GPHS STEM-RTG was determined to fit the design the best, due to its high power generation, 425 W [44], which is near perfect for the design, thus this will be used for the lander EPS subsystem. However, the choice of the lander RTG was mostly based on the probe RTG to minimise the development costs. This will be discussed in the power generation of the probe.

The dimensions of this RTG are 0.47 m in diameter and 1.07 m in length [44]. The TRL of this RTG was 2 in 2015, but it should be ready for planetary exploration in 2029 [44], which gives a margin before the launch of the AlienDive mission.

A supplementary Advanced Stirling radioisotope generator (ASRG) is included to improve the mission's market position. This is purely for testing and it will be assumed that it will be supplied by an external institution, for example, NASA. This will also help please NASA as a stakeholder. The power of this ASRG will again be used to optimize the thrusters and is not relied on for critical subsystems and thus not taken into account for the power budget. This scaled-down ASRG will be around 2.31 kg and produces 10 W of power [44].

7.2.5. Power Conditioning and Distribution Unit selection

The Power Conditioning and Distribution Unit (PCDU) is a vital system for satellites. It is in charge of controlling and distributing the power. Due to the requirements of the lander EPS subsystems, it should be able to handle 435 W and it should last 20 years while minimising the volume and mass. Due to the need for different voltages, it would make the most sense to design it in-house, however, a weight estimation can be given by taking 11.7%[31] of the RTG weight. This will result in a PCDU mass of 6.5 kg. An estimation can also be given on the power density of a PCDU. This is assumed to be 145 W/kg [40]. This would be around 3 kg. For safety, the 6.5 kg is taken as the weight of the PCDU.

The volume is also important since it needs to fit in the electronics box. For this, Commercial off-the-shelf (COTS) PCDUs can be examined. Volumes of <1000 cm^3 were not uncommon and can thus be given as a good estimate [45].

7.2.6. Harness selection

The electrical harness, the cables that deliver the power to each subsystem, is vital for the functioning of the spacecraft. An entire harness design is out scope of this report, nevertheless, some first estimates can be given. To account for the cabling, a 38% mass margin has been added [31]. This will come down to a wire mass of 21.2 kg. Due to the flexibility of the wiring, it will be easier to keep a margin in the 3D model of the lander. A volume estimate will be quite hard to give and will not provide lots of clarity.

The harness has been split into three different cables: 5V, 28V, and high voltage (HV) wires. This combination can provide appropriate voltage levels for each component while keeping the harness as simple as possible. The HV wires are situated between the PCDU and the RTG to minimise power loss.

7.2.7. Lander EPS overview

Now that all the components have been sized, a quick overview will be given. The produced power is 435 W including the ASRG. An overview of the mass can be seen in Table 7.3.

Table 7.3: Mass overview of the EPS subsystem on the lander

Component	Mass [kg]
16-GPHS-STEM-RTG	52.8
ASRG	2.31
PCDU	6.5
Harness	21.1
Total	**82.71**

7.3. Propulsion Subsystem

For the lander, the propulsion system has different characteristics compared to the transfer stage. This is mainly attributed to the fact that gravity losses have to be taken into account as well. Furthermore, as explained in Section 5.4, there is a very specific landing trajectory, which needs to be taken into account in the design of the lander propulsion system, in particular for the choice of engine. In general terms, the thrust needs to be at least that high enough to provide an upwards acceleration. The maximum mass of the spacecraft at the start of the descent burn is 1592.99 kg. Since the gravitational acceleration on Europa is 1.315 m/s^2, the minimum thrust at the beginning of the burn is 2094.78 N. Furthermore, the required thrust range is 1855.7 N to 3671.1 N. The reason for this is that a constant deceleration is needed for the descent, as explained in Section 5.4, and since the mass during descent decreases because of the expelled propellant, the thrust has to decrease as well.

7.3.1. Propulsion Subsystem Requirements

- **AD-PERF-01-LD-05-PROP-01**: The propulsion subsystem shall deliver a total Delta-V of 219.89 m/s

- **AD-PERF-01-LD-05-PROP-02**: The lander shall have a minimum thrust of 2094.78 N at the start of the burn.

- **AD-PERF-01-LD-05-PROP-03**: The propulsion subsystem shall provide variable thrust in a range of 1855.7 N to 3671.1 N.

- **AD-PERF-01-LD-06-PROP-01**: The propulsion subsystem shall ensure that the vertical speed at landing does not exceed 0.5 m/s.

- **AD-ENG-01-LD-01-PROP-01**: The lander shall not experience a net acceleration higher than 6 g.

- **AD-PERF-01-LD-05-PROP-04**: The lander shall have at least two engines to counteract the torque that having only one engine would cause.

7.3.2. Type of Propulsion

For the landing, there are fewer propulsion options than for the transfer stage, due to the requirement for high thrust. Since the minimum thrust at the start of the burn is 2094.78 N, electric propulsion is out of the question. Nuclear propulsion is discarded, because the required Delta-V is only 219.88 m/s, which means that using a chemical propulsion system is much more cost and weight-efficient, due to the higher development costs of a nuclear propulsion system and the mass that a reactor would have.[1] Looking at chemical propulsion, monopropellant is generally not used for landing [31], which is why it is discarded. Solid rocket engines provide high thrust, but are also not suitable for this landing approach, because the lander should have very specific speeds at certain altitudes, to survey the area for a good landing site, as explained in Section 5.4. For this to be possible, very specific thrust levels are needed, which is not possible with solid rocket propulsion. Naturally, it is possible to make variable thrust on a solid rocket engine, by designing the interior of the fuel tank, such that its burning surface changes at just the right rate and at just the right time [33]. This however would introduce a lot of complexity and thus cost into the design. For the reasons stated above, the only viable option for the lander is therefore liquid bi-propellant.

7.3.3. Engine

For the engine selection, it is necessary to choose one that can provide variable thrust, which is necessary for the exact landing trajectory. Most bi-propellant rocket engines do not provide variable thrust, which limits the choice of engines.[2] The total thrust range needed is 1855.7 N to 3671.1 N. Since the centre of the bottom side of the lander cannot house an engine, because that is the location where the probe exits the vehicle, the engines have to be mounted on the side and at least two are needed to counteract the resulting torque that only one engine would cause. No engines that can provide the required thrust range could be found. This problem can be solved by simply increasing the number of engines used. For example, two engines that have a thrust range of 400 N to 500 N have a combined range of 800 N to 1000 N, whereas using four engines, each with a range of 150 N to 250 N, meaning that they individually also only provide a range of 100 N, leads to a combined thrust range of 600 N to 1000 N. Thus, by doubling the number of engines, the range is increased by twice the amount. After looking at available engines, the only way to provide thrust in the required range turns out to be by using 6 engines for the maximum thrust and then turning 2 off two of them to use 4 for the lowest required thrust. This means that the minimum thrust per engine has to be at most 463.9 N and the maximum thrust has to be at least 611.9 N. The only feasible engine that can provide the required thrust range

---

[1]From `https://iq.direct/blog/416-10-advantages-and-10-disadvantages-of-nuclear-rocket-engines.html`, accessed on 18/06/2024.

[2]From `https://satcatalog.s3.amazonaws.com/components/1015/SatCatalog_-_Aerojet_Rocketdyne_-_R-4D-11_490N_300-to-1_-_Datasheet.pdf?lastmod=20210710070936`, accessed on 19/06/2024.

needed from a single engine is the"AMBR 556 N (125 lbf) Dual Mode High-Performance Rocket Engine" [2]. Its characteristics are shown in Table 7.4. By using 6 initally and 4 at the end of these engines, the total required thrust range can be achieved.

Table 7.4: Considered engines for the lander

Engine	Propellant	Specific Impulse [s]	Minimum Thrust [N]	Maximum Thrust [N]	Nominal Thrust [N]	g [m/s^2]
R-4D-15 HiPAT™ 445 N (100 lbf) Dual Mode High Performance Rocket Engine	Hydrazine/ NTO (MON-3)	329	329	556	445	0.33
AMBR 556 N (125 lbf) Dual Mode High Performance Rocket Engine	**Hydrazine/ NTO(MON-3)**	**329**	**325**	**645**	**522.5**	**0.38**
AJ10-220 62.3 N (14.0 lbf) Reaction Control Thruster	MMH/ NTO (MON-3)	285	59.2	65.4	62.3	0.046
R-4D-11 490 N (110 lbf) Bipropellant Rocket Engine	MMH/ NTO (MON-3)	311	378	511	490	0.36
R-4D-15 HiPAT™ 445 N (100 lbf) High Performance Rocket Engine	MMH/ NTO (MON-3)	320.6	378	511	445	0.33

7.3.4. Propellant Storage

Initially, the lander propellant storage was supposed to be similar to the transfer stage system. However, after realising that critical components of the probe and the relays have to be substantially shielded against radiation, it turned out that the required aluminium thickness to shield the components would lead to a significant increase in overall lander mass. An alternative solution is to use the propellant to shield against radiation. As it turns out, like water in power plants [3], the propellant is also great at attenuating radiation [46]. For this reason, it is decided to place the propellant tanks in such a way, that they wrap around the probe and the relays. The architecture of such a tank is shown in Figure 7.3. The propellant tank is situated between two cylindrical shells, which are connected by two semi-torus caps at the ends. A cross-sectional view from the side of this shape with dimensions is shown in Figure 7.4 and from the top in Figure 7.5 .
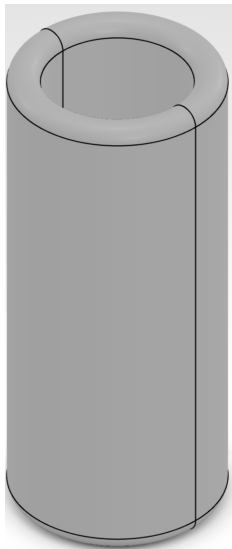
Figure 7.3: Isometric view of lander propellant tank
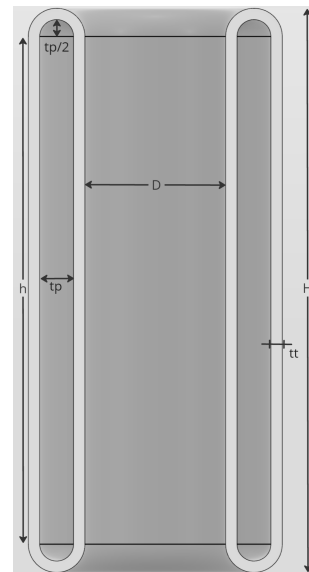
Figure 7.4: Lander propellant tank viewed from the side

---

[3]From https://www.nrc.gov/waste/spent-fuel-storage/pools.html, accessed on 18/06/2024.
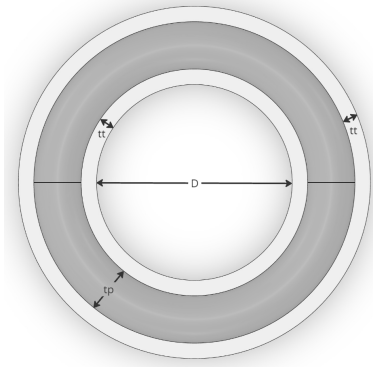
Figure 7.5: Lander propellant tank viewed from the top

Two sections of the probe need to be covered, namely the one containing all of the payload and another, which houses the relays. The fuel tank covers one, whereas the oxidiser tank covers the other. Conveniently, to cover both regions, both tanks need to have a height H of 1 m. The diameter D is determined by the probe width and is set to be 0.3 m. Since the height and the diameter are already fixed, the only variables left are the tank thickness t_t and the propellant thickness t_p. The latter value is determined by the required volume of the tank, which as for the transfer stage is the required volume of the propellant plus a 5 % margin to take into account the potential growth of the fluids inside the tank. The volume of the propellant region in the tank is given as follows:

$$V_p = \pi \cdot \frac{H - t_p}{4} \cdot ((D + 2 \cdot t_p)^2 - D^2) + 2 \cdot \pi^2 \cdot \frac{D + t_p}{2} \cdot (\frac{t_p}{2})^2 \tag{7.2}$$

Because this equation is a polynomial equation in terms of t_p it has several roots and was thus solved numerically, the only meaningful solution having been chosen. When t_p is determined, the only remaining variable is t_t, which can be solved by calculating the minimum thickness, such that the tank does not fail due to yield or buckling. For buckling, the tank is approximated as a thin cylindrical shell, which has a critical buckling stress of [35]:

$$\sigma_{cr} = 1.19 \cdot (\frac{H}{D})^{-0.0256} \cdot \frac{t_t}{D} \cdot E \tag{7.3}$$

Grade 5 titanium is again used for this tank, due to weight-saving benefits. σ_w is calculated as follows:

$$\sigma_w = \frac{W}{A_t} = \frac{m \cdot g \cdot \Psi}{\pi \cdot ((\frac{D}{2} + t_t)^2 - \frac{D}{2}^2 + (\frac{D}{2} + 2 \cdot t_t + t_p)^2 - (\frac{D}{2} + t_t + t_p)^2)} \tag{7.4}$$

W is the weight of the tank during launch and A_t is the cross-sectional area of the tank seen from above. m also depends on the t_t, as the equation for the mass is as follows:

$$m = V_t \cdot \rho \tag{7.5}$$

In this case, ρ is the density of titanium and V_t is the volume of the tank walls, which is calculated in the following way:

$$V_t = \frac{\pi \cdot (H - t_p) \cdot ((D + 2 * t_t)^2 - D^2)}{4} + \frac{\pi \cdot (H - t_p) \cdot ((D + 4 \cdot t_t + 2 \cdot t_p)^2 - (D + 2 \cdot t_t + 2 \cdot t_p)^2)}{4}$$
$$+ (2 \cdot \pi^2 \cdot ((\frac{t^p}{2} + t_t)^2 - (\frac{t_p}{2})^2) \cdot (\frac{D}{2} + t_t + \frac{t_p}{2})) \tag{7.6}$$

The same algorithm as for the transfer stage is used to determine the minimum required value for t_t, as this leads to the lowest tank mass. In this case, both tanks are independent of each other and the only constraints are that the tank should not fail due to yield or buckling. Because the loads on this structure are so low, the minimum thickness calculated by the algorithm for either of the tanks is below 0.2 mm. However, the minimum manufacturable thickness of titanium is 0.8 mm [4], which is why this value is chosen as the tank thickness for both tanks. Similar to the transfer stage, a pump-fed system is chosen due to weight-saving reasons. The mass of the feed system is also estimated by taking the estimate that about 12.3 % of the total propulsion system dry mass is part of the feed system. The final dimensions of the lander propellant tanks are shown in the Table 7.5, Table 7.6 and Table 7.7. With the propellant thickness of 0.108 m, the probe receives 20 times less radiation than without the shielding from the tanks [46].

---

[4]From https://www.sbi.at/en/applications/aeronautics/space-fuel-tanks, accessed on 18/06/2024.

Table 7.5: Parameters of the fuel tank of the lander

Parameter	Value	Unit
Fuel Mass	129.58	kg
Fuel Volume (Liquid)	0.13	m^3
Ullage Volume	0.0068	m^3
Tank Volume	0.14	m^3
Tank Height	1	m
Tank Diameter	0.3	m
Tank Propellant Thickness	0.108	m
Tank Wall Thickness	0.0008	m
Tank Mass	7.19	kg

Table 7.6: Parameters of the oxidiser tank of the lander

Parameter	Value	Unit
Oxidiser Mass	129.58	kg
Oxidiser Volume (Liquid)	0.095	m^3
Ullage Volume	0.0047	m^3
Tank Volume	0.095	m^3
Tank Height	1	m
Tank Diameter	0.3	m
Tank Propellant Thickness	0.081	m
Tank Wall Thickness	0.0008	m
Tank Mass	9.05	kg

Table 7.7: Masses of the full propellant storage system of the lander

Parameter	Mass [kg]
Total Tank Mass incl. add-ons	22.92
Feed System Mass	3.21
Total Mass	**26.13**

7.4. Guidance, Navigation & Control Subsystem

While en route to Europa, the spacecraft (lander + transfer stage) will encounter various disturbance forces and torques. These disturbances can cause the spacecraft to deviate from its intended course and alter its attitude or orbit, potentially jeopardising the mission. Therefore, ensuring that the spacecraft can correct these disturbances effectively is crucial. Since it is assumed that the launcher can take us to Jupiter, only disturbances after JOI will be investigated.

7.4.1. Requirements

The subsystem requirements for the lander GNC subsystem are listed below

- **AD-PERF-01-LD-01-GNC-01**: The GNC subsystem shall be able to determine the spacecraft's attitude.
- **AD-PERF-01-LD-01-GNC-02**: The GNC subsystem shall provide 3-axis control of the spacecraft.
- **AD-PERF-01-LD-01-GNC-03**: The GNC subsystem shall use the same propellants as the lander engines.
- **AD-PERF-01-LD-01-GNC-04**: The GNC subsystem shall be able to provide a torque of at least 0.028 26 Nm
- **AD-PERF-01-LD-01-GNC-05**: The GNC subsystem shall be able to store at least a momentum of 22.76 Nms.
- **AD-PERF-01-LD-01-GNC-06**: The GNC subsystem shall be able to dump a momentum of 45.52 Nms within two orbits.
- **AD-PERF-01-LD-01-GNC-07**: The GNC subsystem shall have a pointing accuracy of at least 0.002°.
- **AD-PERF-01-LD-02-GNC-08**: The GNC subsystem shall provide imaging of Europa's surface in the reconnaissance orbit.
- **AD-LAND-01-LD-01-GNC-09**: The GNC subsystem shall be able to image Europa's surface during descent.
- **AD-LAND-01-LD-01-GNC-10**: The GNC subsystem shall be able to scan Europa's surface in 3D during descent.
- **AD-LAND-01-LD-01-GNC-11**: The GNC subsystem shall be able to change the lander's trajectory during descent.

7.4.2. Disturbance Forces & Torques

The five main types of disturbances that the spacecraft will experience are: gravity gradient, solar radiation, residual dipole, RF forces and thermal radiation.

This list is not exhaustive, as it does not account for internal disturbances caused by leaks, moving parts, propellant slosh, and other factors. However, it will still provide a sufficient understanding of the forces and torques needed to size the control instruments appropriately. The worst-case torque must be identified to determine the sizing. Each disturbance will be analysed in more detail below. Certain assumptions are made for some calculations, which will be checked later in Chapter 13. Additionally, the calculations will only use the final design values. Consequently, the process of iterating calculations and (re)selecting components will not be discussed to maintain clarity and ease of understanding.

Gravity Gradient

If the vertical axis (rotational symmetry axis) of the spacecraft is not aligned with the gravitational field of a celestial body, it will experience a gravity gradient over its body. This will result in a net torque on the spacecraft. The resulting torque can be quantified using Equation 7.7 [31][47].

$$T_{torque,g} = \frac{3\mu}{2R} \begin{bmatrix} I_{zz} - I_{yy} & I_{xy} \\ I_{xy} & I_{zz} - I_{xx} \\ I_{xz} & I_{yz} \end{bmatrix} \begin{bmatrix} \theta_x \\ \theta_y \end{bmatrix} + \begin{bmatrix} I_{yz} \\ -I_{xz} \\ 0 \end{bmatrix} \tag{7.7}$$

Here, T represents the torque due to the gravity gradient, μ is the standard gravitational parameter, R is the distance from the body in question to the spacecraft, I is the mass moment of inertia around the specified axis, and θ is the angle by which the vertical deviates from the magnetic field.

To find the worst-case torque, both the gravity fields of Jupiter and Europa must be considered. Furthermore, since the worst-case is being analysed, the angles θ_x and θ_y can be assumed to equal 45°. The moments of inertia are obtained by modelling the spacecraft in 3DEXPERIENCE. The transfer stage and the lower part of the lander are modelled as a rectangular box, while the upper part is modelled as a cylinder. This makes the vertical/axial axis a symmetry axis. Both the transfer stage and the lander (incl. probe) are assigned a mass of 12 222.7 kg and 1595.1 kg respectively, with the assumption that the mass is uniformly distributed. Additionally, the contribution of the antenna is neglected in the moment of inertia estimation. Table 7.8 shows the parameters that will be used to calculate the torques caused by Jupiter's and Europa's gravity fields.

Table 7.8: Parameters for gravity gradient torque calculations

Parameter	μ	R	I_{xx}	I_{yy}	I_{zz}	I_{xy}	I_{xz}	I_{yz}	θ_x	θ_y
Jupiter	1.27×10^{17}	7.42×10^{8}	2.26×10^{4}	2.26×10^{4}	1.89×10^{4}	0	0	0	45	45
Europa	3.20×10^{12}	1.87×10^{6}								
Unit	m^3s^{-2}	m	kgm^2	kgm^2	kgm^2	kgm^2	kgm^2	kgm^2	deg	deg

By plugging these values into Equation 7.7, A torque of 3.78×10^{-3} and 2.39×10^{-6} for Jupiter and Europa are obtained respectively. From these results, it is clear that the gravity gradient effect of Europa will be more limiting than that of Jupiter.

Solar Radiation

The radiation pressure from the Sun can cause the spacecraft to experience a torque. This occurs when the solar radiation force is applied at a point that is not the centre of mass, meaning the centre of pressure does not coincide with the centre of mass. The solar radiation force can be calculated using Equation 7.8 [31].

$$F_{solar} = \frac{J_s}{c} A \tag{7.8}$$

Here, J_s is the solar flux, c is the speed of light, and A is the surface area that is irradiated. The solar radiation torque can then be calculated using Equation 7.9 [31].

$$T_{torque,s} = F_{solar} \Delta x (1 + \rho) \cos(\phi) \tag{7.9}$$

Here, Δx is the distance between the centre of mass and the centre of pressure, ρ is the reflectance coefficient, and ϕ is the incidence angle. For the worst-case scenario, the maximum distance between the centre of mass and the centre of pressure is around 6.5 m, the reflectance coefficient is equal to 1, and the incidence angle

will be 0. With a solar flux of approximately 50.26 W/m^2 at Jupiter and Europa[5] and a surface area of 21.8 m^2, the solar radiation torque can be calculated to be equal to 7.30 × 10^{-7} Nm. This value is significantly lower than the torque due to the gravity gradient and will, therefore, not be limiting the design.

Residual Dipole
The spacecraft's current loops can generate torque due to interactions with the magnetic fields of Jupiter and Europa. This can be calculated using Equation 7.10 [31].

$$T_{torque,d} = MB \tag{7.10}$$

Here, M represents the residual dipole moment of the spacecraft, and B is the magnetic field strength of the disturbing body. Typical values for the residual dipole moment range from 0.1 Am^2 to 20 Am^2 [48]. Additionally, Jupiter and Europa have maximum magnetic field strengths of 1.431 × 10^{-3} T and 2.20 × 10^{-7} T, respectively [49, 20]. For the worst-case scenario, a residual dipole of 20 Am^2 and Jupiter's magnetic field strength will be used. Substituting these values into the equation yields a torque of 0.028 26 Nm. This torque exceeds the gravity gradient torque and thus will be the more limiting factor for the design.

Radio Frequency Forces
A transmitting antenna can also produce a torque. This torque can be calculated using Equation 7.11[31]

$$T_{torque,RF} = \frac{P}{c}\Delta x \tag{7.11}$$

Here, P is the transmitted power, c is the speed of light, and Δx is the distance of the antenna boresight from the spacecraft centre of mass. However the antenna's boresight will always be on the vertical axis of the spacecraft, where the centre of mass will be close to, thus it can be assumed that there will be no torque produced by the transmitting antenna but only a force. This force will be equal to $\frac{P}{c}$. The transmitting power of the antenna is 11.5 W, which results in a force of 3.84 × 10^{-8} N.

Thermal Radiation
Lastly, radiation emitted from a radiator will exert a force, and if this force acts at a distance from the centre of mass, it will generate torque. The thermal force can be computed using Equation 7.12 [47].

$$F_{thermal} = \frac{2}{3}\frac{\sigma\epsilon AT^4}{c} \tag{7.12}$$

Here, σ represents the Stefan-Boltzmann constant, which equals 5.67 × 10^{-12} W/cm^{2}K^4, ϵ is the emissivity of the radiator, A denotes the area of the radiator, and T stands for the temperature of the radiator. The emissivity, area and temperature of the radiator are equal to 0.92, 8.69 m^2 and 313 K, respectively. Additionally, the radiator is assumed to be at a distance of 6.5 m from the centre of mass of the spacecraft for a worst-case estimate. Calculating the force and multiplying it by the moment arm results in a thermal torque of 6.29 × 10^{-5} Nm. This value is lower than the torque generated by the residual dipole, and therefore, it is limiting for the design.

7.4.3. Sensors
To determine the attitude of the spacecraft sensors are needed. For this mission, the sensors will be selected mainly based on the radiation requirement since it is the most limiting requirement. These will be elaborated upon more in Section 7.6.

Sun Sensors
A configuration of two fine sun sensors and two coarse sun sensors will be used for attitude determination. Two sensors are necessary because each can only measure along two orthogonal axes, and at least three axes are required for complete attitude determination. To achieve this, the two fine sun sensors will be placed on different planes. Additionally, two coarse sun sensors were included for redundancy in case the fine sun sensors fail. Coarse sun sensors normally have low mass and power consumption so it is a good redundancy measure. For the fine sun sensor, the Leonardo Smart Sun Sensor (S3)[6] will be used and for the coarse suns sensor the Solar MEMS ACSS[7] will be used. the specifications of the sensors can be found in Table 7.9.

The table shows that the Leonardo S3 sensor has a minimum reliability rating of 350 FITS, meaning 350 sensors are expected to fail per billion operating hours. The journey from Earth to Europa will take approximately

---

[5]From `https://nssdc.gsfc.nasa.gov/planetary/factsheet/jupiterfact.html`, accessed on 03/06/2024.
[6]From `https://www.satcatalog.com/component/s3-smart-sun-sensor/.`, accessed on 04/06/2024
[7]From `https://solar-mems.com/space-equipment/acss/`, accessed on 04/06/2024.

2221 days, equivalent to 53 304 hours. Therefore, during the journey, an expected 0.0187 sensors might fail. Consequently, it is reasonable to conclude that additional redundant fine sun sensors are unnecessary.

Table 7.9: Product specifications of the Leonardo S3[6] and Solar MEMS ACSS[7]

Parameter	Leonardo S3	Solar MEMS ACSS	Unit
Mass	0.33	0.04	kg
Dimensions	112 x 12 x 43	65 x 47 x 13	mm
Power	1	0.09	W
Radiation Resistance	100 (300 optional)	200	krad
FOV	128 x 128	60	deg
Accuracy	<0.02	<1.0	deg
Resolution	<0.005	<0.05	deg
Operating Temperature	-25 to +60	-55 to +105	°C
Reliability	270-350	-	FITS

Star Trackers

In addition to sun sensors, star trackers will be included in the attitude determination system. This is necessary because sun sensors cannot always be illuminated by the sun. Conversely, star trackers can be blinded by the sun and become inoperative. Therefore, each system serves as a backup for the other. The Leonardo SPACESTAR[8] will be used for the star tracker. Its specifications are shown in Table 7.10.

Table 7.10: Product specifications of the Leonardo SPACESTAR[8]

Parameter	Value	Unit
Mass	1.6	kg
Dimensions	164 x 164 x 284	mm
Power	6	W
Radiation Resistance	>18 years GEO	-
FOV	20 x 20	deg
Bias	7.7 (pitch & yaw) 10.6 (roll)	arcsec
Low Frequency Error	<12 (pitch & yaw)	arcsec
Random Error	7.5	arcsec
Operating Temperature	-30 to +60	°C
Reliability	120-170	FITS

The table indicates that this model lacks a specific radiation resistance number, a common trait among commercially available star trackers listed on SatSearch and SatCatalog. However, given that the S3 model, also manufactured by Leonardo, boasts a similar lifespan in GEO (>15 years)[6], it is inferred that the star tracker should similarly possess robust radiation resistance capabilities. Moreover, with a minimum reliability of 170 FITS, equating to an expected failure rate of 0.00906 components for this mission, incorporating an additional sensor should suffice for redundancy. Therefore, a total of two star trackers will be employed.

Inertial Measurement Unit

Another method to determine the spacecraft's attitude is by measuring rotational accelerations to calculate its orientation. Additionally, understanding the spacecraft's linear accelerations is crucial for navigation. As mentioned in Section 6.3, the IMU on the transfer stage will provide these measurements until just before separation. Subsequently, the lander will rely on its IMU for continued measurements. The ASTRIX 1090[9]

---

[8]From https://satcatalog.s3.amazonaws.com/components/288/SatCatalog_-_Leonardo_-_SPACESTAR_-_Datasheet.pdf?lastmod=20210708041624, accessed on 06/06/2024.

[9]From https://www.airbus.com/en/space/equipment/avionics/astrix-inertial-measurement-iru-series, accessed on 04/06/2024.

from Airbus will be used for this. Its specifications can be found in Table 7.12

7.4.4. Actuators

In addition to determining its attitude, the spacecraft must also have the capability to control its attitude. Control around three axes will be essential to ensure the spacecraft can orient itself correctly for communication, specific burns, and other manoeuvres.

Reaction Wheels

To control its attitude, the spacecraft will use four reaction wheels. While only three are theoretically needed for full three-axis control, an additional wheel ensures functionality even if one wheel fails [47]. Before selecting the reaction wheels, the required torque and momentum storage must be calculated. Previous analysis identified the torque due to the residual dipole as the most critical factor, necessitating that each reaction wheel provides at least 0.028 26 Nm of torque. For momentum storage, the in-orbit cyclic nature of the worst-case torque must be considered. Assuming, for simplicity, that the worst-case torque acts for a quarter of the orbit and is sinusoidal, the momentum can be calculated using Equation 7.13 [47]:

$$h_{req} = 0.707 T_{worst} \frac{T_{orbit}}{4} \tag{7.13}$$

Here T_{worst} represents the worst-case torque, and T_{orbit} is the period of the orbit around Europa, equal to 8998 s. Furthermore, 0.707 is the root mean squared average of the sinusoidal function. Plugging in the values gives a momentum of 22.76 Nms. Ideally, the reaction wheel should be capable of storing more momentum to minimize the need for momentum dumping using thrusters. Based on these values and the radiation environment, the HR12-50[10] from Honeywell was selected as the best option. Its specifications are shown in Table 7.11.

Table 7.11: Product specifications of the HR12-50[10]

Parameter	Value	Unit
Mass	9.5	kg
Dimensions	⌀316 x 159	mm
Power	22	W
Radiation Resistance	300	krad
Momentum	50	Nms
Reaction Torque (max. speed)	0.1 to 0.2	Nm
Operating Temperature	-30 to +70	°C

Table 7.12: Product specifications of the ASTRIX 1090[9]

Parameter	Value	Unit
Mass	4.5	kg
Dimensions	⌀263 x 192	mm
Power	13.5	W
Radiation Resistance	100 (TID)	krad
Rotational Measurement Range	140	deg/s
Linear Measurement Range	1.1 or 20	g
Operating Temperature	-25 to +60	°C

This reaction wheel can store up to 50 Nms of momentum. Consequently, momentum dumping will need to be performed approximately every two orbits, as the accumulated momentum will reach 45.52 Nms by that time. Although it is ideal to minimise momentum dumping, the lander's size significantly restricts the size of the reaction wheels, which in turn limits the maximum momentum storage.

Reaction Control Thrusters

Reaction control thrusters are required to dump the stored momentum of a reaction wheel. To do this the thrusters must be capable of rotating the spacecraft around its three axes. Additionally, during landing, the spacecraft needs to be able to translate in any direction as well. To minimise complexity and mass, it is most efficient to place all the thrusters on the lander rather than on the transfer stage or a combination of both. Therefore, to enable rotational motion during transit to Europa and translational motion during landing, a 12-thruster configuration will be used. The thruster arrangement on the lander is shown in Figure 7.6 and Figure 7.7.

---

[10] From https://satcatalog.s3.amazonaws.com/components/219/SatCatalog_-_Honeywell_-_HR12-50_-_Datasheet.pdf?lastmod=20210708033734, accessed on 16/06/2024.
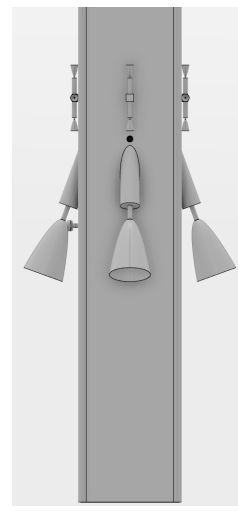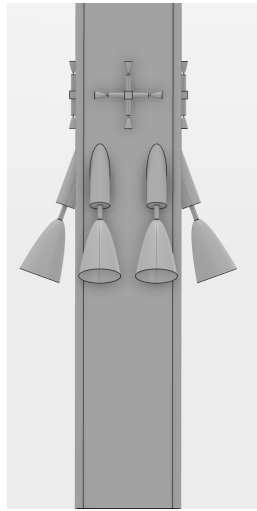
Figure 7.6: Side view 1 of reaction control thrusters

Figure 7.7: Side view 2 of reaction control thrusters

To determine the required thrust of the thrusters, the process of momentum dumping must be analyzed. The required thrust can be calculated using Equation 7.14 [47].

$$T_{req} = \frac{h}{Lt} \tag{7.14}$$

Here h is the momentum to be dumped, L is the moment arm of the thruster(s), and t is the burn time. This shows that momentum dumping is highly reliant on the burn time, which is not a significant limitation compared to other requirements. However, the burn time should be shorter than the period of two orbits around Europa. A more critical requirement is the type of propellant that can be used. To avoid the need for different propellant tanks, it is ideal for the thrusters to use the same propellant as the lander main engine, NTO/Hydrazine. Considering these constraints, the DST-11H[11] bipropellant thruster was found to be the most suitable. Its specifications can be seen in Table 7.13.

Table 7.13: Product specifications of the DST-11H[11]

Parameter	Value	Unit
Mass	0.77	kg
Length	262	mm
Power	41	W
Nominal Thrust	22	N
Specific Impulse	310	s
Propellant	Hydrazine/MON	-

To dump the momentum at nominal thrust, two thrusters can be fired. With a moment arm equal to 0.8 m (the distance between the two thrusters), a total burn time of 2.6 s would be required. Firing the two thrusters would generate a couple moment of 17.6 Nm, which is more than sufficient to overcome the worst-case disturbance torque in necessary.

7.4.5. Landing Instruments
As described in Section 5.3 and Section 5.4, one reconnaissance camera, two landing cameras, and LIDAR are required to facilitate landing site selection, TRN, and HDA. The specifications of the cameras (excluding previously described performance specifications) and the LIDAR are provided below.

---

[11] From `https://www.moog.com/content/dam/moog/literature/sdg/space/propulsion/moog-bipropellant-thrusters-datasheet.pdf`, accessed on 11/06/2024

Table 7.14: Product specifications of the ECAM-C50[12]

Parameter	Value	Unit
Mass	0.59	kg
Length	97 x 78 x 198	mm
Power	1.6	W
Operating Temperature	-30 to +40	°C
Mean Time To Failure	7.9	Hours

Table 7.15: Product specifications of the LEIA[13]

Parameter	Value	Unit
Mass	<7	kg
Dimensions	260 x 220 x 170	mm
Power	40-85	W
Radiation Resistance	100 (TID)	krad
Range/Resolution	1500/1.5	m
Range/Resolution	150/0.15	mm
Operating Temperature	-10 to +35	°C

7.5. Thermal Control Subsystem

In this section, The lander's Thermal Control Subsystem will be sized. This is sized the same way as the transfer stage with the addition of an extra component which are the louvres.

7.5.1. TCS Requirements

- **AD-PERF-01-LD-02-TCS-01:** The TCS shall be able to maintain a temperature of 273.15 K to 313.15 K while the lander is orbiting Europa
- **AD-PERF-01-LD-02-TCS-02:** The TCS shall be able to maintain a temperature of 273.15 K to 313.15 K once the lander has landed on Europa's surface
- **AD-PERF-01-LD-02-TCS-03:** The TCS shall be able to maintain a temperature of 233.15 K to 313.15 K once the lander has released the probe and electronic box
- **AD-PERF-01-LD-02-TCS-04:** The TCS shall be able to transport the heat throughout the Lander.

Assumptions

The Assumptions will be the same as Section 6.4 with one additional assumption that the lander legs will be perfectly insulated from the environment and thus conduction to the legs will not be considered in the calculations. The dominating heat source in the Lander is the RTG and the rest of the heat sources/sinks could be considered as negligible.

7.5.2. Thermal Design Process

The thermal design process will be the same as the transfer stage. The operating temperature range for the lander changes depending on the thermal case there will be 3 extra cases that will be added which will be when the lander has separated from the Transfer stage, the lander has reached Europa's surface and finally the lander has released the probe and the electronic box. These cases mainly have a temperature range coinciding with the subsystem requirement **AD-PERF-01-LD-TBD-TCS-01**, **AD-PERF-01-LD-TBD-TCS-01**, **AD-PERF-01-LD-TBD-TCS-01**. For the first case, the main limiting factor of the temperature range is the propellant used to land the lander, the second case is limited by the payload onboard the lander, and the third case is limited by the telecommunications subsystem.

7.5.3. Thermal Case Analysis

Table 7.16 gives an overview of the thermal cases that will be experienced by the lander.

---

[11]From `https://www.msss.com/files/ECAM-C50_M50.pdf`, accessed on 10/06/2024.

[12]From `https://satsearch.co/products/mda-leia-lidar-for-extra-terrestrial-imaging-applications`, accessed on 05/06/2024.

Table 7.16: Thermal cases of the Lander

Thermal Case	Cold State	Hot State
10. Europa Orbit without the CS	Eclipsed by Europa or Jupiter at an altitude of 312 km	Facing the sun at an altitude of 312 km
11. Europa's surface with probe and electronic box	Eclipsed by Jupiter	Facing the sun
12. Europa's surface without probe and electronic box	Eclipsed by Jupiter	Facing the sun

From Table 7.16, the limiting hot state and cold state for the lander will be the moment the transfer stage separates from the lander which will cause it to have less area to emit the same amount of heat coming from the RTGs, therefore drastically increasing the temperature of the lander. The limiting cold state occurs when the lander is on the surface of Europa and has released the probe and electronics, thus not being able to utilise the heat from the RTG and the electronic box making the temperature drop to a lower equilibrium temperature.

7.5.4. Component Selection

The components used on the transfer stage which are the MLI and the radiators will also be used on the lander. The only difference will be that louvres are going to be used which will go over the radiators. These louvres will change the effective emissivity depending on whether the louvre is open or closed. An active form of thermal control will be used because the lander needs to be able to change its emissivity to allow less heat to escape once the probe and electronics are released. The specifications of the louvres will be given after sizing.

7.5.5. TCS Sizing

For the TCS sizing of the lander, the same steps are taken but with the louvres taken into consideration in the calculations

1. Make an initial guess of the type of MLI, Radiator, and louvres to be used and the Area it occupies. The combined area will be restricted to the outer surface area of the lander excluding the bottom area of the lander which will be used as the absorption surface. Furthermore, the available area of the louvres will be restricted to the area of the radiators on the rectangular prism part of the lander due to manufacturing restrictions.

2. Use Equation 6.11 to calculate the temperature of each thermal case in its hot and cold state.

3. Check if all the thermal cases satisfy the temperature requirement. If yes, freeze the design. If not, change the type of MLI, Radiator, and Louvre used and the area it occupies.

4. Repeat steps 2 and 3 until an optimal solution is reached.

Running the iterations results in the optimal configuration shown in Table 7.17:

Table 7.17: Radiator, MLI, and Louvre area for the Lander

Component	Value	Unit
Radiator Area	8.68	m^2
MLI Area	9.12	m^2
Louvre Area	2.86	m^2

The MLI and Radiator in Table 7.17 have the same properties as in Table 6.8. The properties of the louvres are given in Table 7.18.

Table 7.18: Louvre properties and Total Mass of the TCS on the Lander [38]

Parameter	Value	Unit
Louvres		
Emissivity (Open)	0.67	-
Emissivity (Closed)	0.08	-
Areal Density	3.2	kg/m^2
Mass		
MLI	7.03	kg
Radiation	0.04	kg
Louvres	9.15	kg
Total TCS mass of the Lander	**16.18**	**kg**

In Table 7.18 it can be seen that the emissivity of the louvres is a lower value when they are closed. This is useful specifically when the lander releases the probe which reduces the amount of heat generated by the lander which ends up cooling it down. This is why it is necessary to close the louvres to ensure that the emissivity decreases thus heat flows at a slower rate making the equilibrium temperature of the spacecraft higher. The resultant Temperatures of all three thermal cases at their cold and hot state are given in Table 7.19:

Table 7.19: Equilibrium Temperature of the thermal cases of the lander

Thermal Case	Cold State Temperature [K]	Hot State Temperature [K]
10. Europa Orbit without the CS	302.76	309.86
11. Europa's surface with probe and electronic box	302.84	310.65
12. Europa's surface without probe and electronic box	233.15	250.33

7.6. Radiation

In the design, the extreme radiation environment around Jupiter was also taken into account. As the lander structure is a truss with only MLI around it, it needs additional radiation shielding to ensure the survival of the components. Firstly, the components that require radiation protection were established. These include most elements of the communication subsystem except for the high gain and medium gain antennas. They will be placed in a separate electronics box together with the on-board computer for the command and data handling subsystem. Next to this, the GNC components such as LIDAR, sun sensors, star trackers, reaction wheels, IMUs, cameras, and the competition rover need to be shielded separately. An overview of the design TID requirements for each of these components is presented in Subsection 7.6.1. This is followed by a description of the radiation protection strategy for the AlienDive mission in Subsection 7.6.2.

7.6.1. Radiation Requirements

AD-PERF-01-LD-04-RAD-01: The electronics box shall receive no more than 100 krad TID during the mission.

AD-PERF-01-LD-04-RAD-02: The LIDAR shall receive no more than 100 krad TID during the mission.

AD-PERF-01-LD-04-RAD-03: The star trackers shall receive no more than 100 krad TID during the mission.

AD-PERF-01-LD-04-RAD-04: The IMU shall receive no more than 100 krad TID during the mission.

AD-PERF-01-LD-04-RAD-05: The cameras shall receive no more than 100 krad TID during the mission.

AD-PERF-01-LD-04-RAD-06: The sun sensors shall receive no more than 200 krad TID during the mission.

AD-PERF-01-LD-04-RAD-07: The reaction wheels shall receive no more than 200 krad TID during the mission.

AD-PERF-01-LD-04-RAD-08: The shielding on the lander shall limit the TID received by the competition rover to 2 Mrad.

7.6.2. Radiation Protection Strategy

After establishing the TID requirements for components, a strategy for radiation protection is developed. Aluminium was chosen as the material for additional radiation shielding due to its electromagnetic, neutron, and X-ray/gamma shielding properties as well as low density[50]. It is widely used in the space industry for example in the planned mission of Europa Clipper.[14]

The radiation shielding strategy is divided into phases. Phase 1 is the trajectory between JOI and EOI, while phase 2 will be the reconnaissance orbit around the moon. Subsequently, phase 3 represents the operations on Europa's surface after landing. Phase 3 will only be relevant for the components inside the electronics box as they have to be operational after landing, while the other components of the GNC subsystem are only needed for the trajectory and landing. The radiation shielding strategy for the surface is to lower the electronics box using a cable into the hole left behind the drilling probe. The effectiveness of the water ice in radiation shielding on Europa can be seen in Figure 7.8 from the Nature Astronomy journal [51].
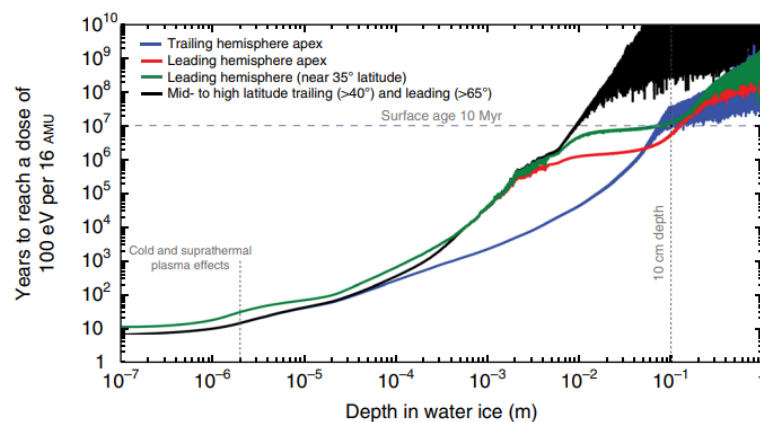
Figure 7.8: Radiation dosage received at a certain depth in water ice on Europa [51]

The radiation dosage of 100 eV per 16 AMU is equivalent to 6.03×10^{10} rad. As seen in the figure above, the TID reduces as much as 1000 times with just 1 mm depth into the water ice. For the AlienDive mission, the electronics box shall be lowered into the ice for as deep as 1 to 2 metres. Thus we would expect an over 10^7 times reduction in the received radiation at the leading hemisphere of Europa. From this information, it is approximated that the maximum radiation dosage per year the electronics box may receive is less than 6 krad per year. This is considered negligible for the design as the spacecraft on the journey from Jupiter to Europa and in Europa's orbit would receive a radiation dose in the order of over 10^9 rad per year without shielding. Thus, for the radiation-resistant design, phase 1 of JOI to EOI and phase 2 of reconnaissance will be the main considerations.

For phase 1, which takes 1 year and 4 months, the radiation doses received by the spacecraft are estimated based on previous missions such as Galileo and Juno [52]. They correspond to the radiation calculations done for the Europa Clipper mission[2]. These estimates were used to make the graph in Figure 7.9 showing the relation between aluminium shield thickness and the time to receive a certain TID in phase 1. Similarly, based on estimates by the Europa Clipper team, the same relationship is depicted for the 7-day-long phase 2 in Figure 7.10. This graph for simplicity assumes that no radiation has been gathered before Europa's orbit insertion.

---

[14]From `https://europa.nasa.gov/mission/about/`, accessed on 17/06/2024.
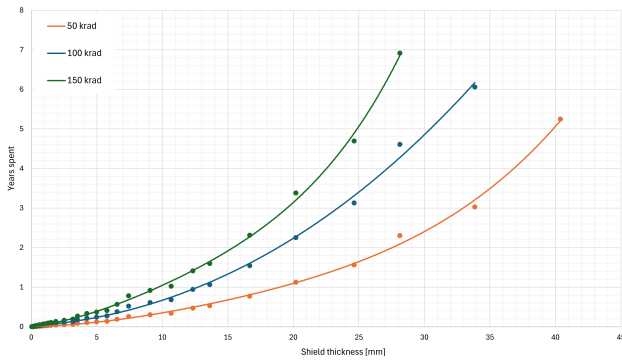
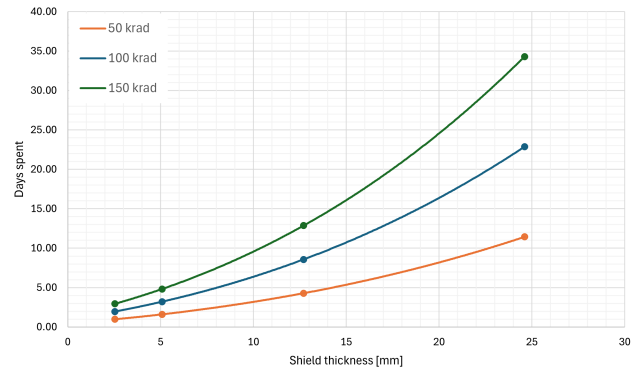**Figure 7.9:** Years spent in phase 1 to receive a given TID vs. Aluminium shield thickness

Figure 7.10: Days spent in phase 2 to receive a given TID vs. Aluminium shield thickness

According to the figures above, the radiation dose that the spacecraft receives, given a certain aluminium shield thickness throughout its 1-year and 4-month journey from Jupiter to Europa, is approximately comparable to that in Europa's orbit in 7 days of reconnaissance. Thus, the design strategy for radiation is to design for half of the maximum allowable TID for phase 1, and the second half for phase 2. Following this strategy, the aluminium shield thickness for components able to withstand 100 krad will be designed for 50 krad in phase 1 and 50 krad in phase 2. The components with maximum TID of 200 krad and 300 krad will be treated similarly. On top of that, safety margins of 20% are applied to account for the uncertainty and errors and ensure that the doses are not exceeded in the case of schedule delays. This means that the components are designed to survive 1.6 years in phase 1 instead of 1.33 years to receive the design TID. Similarly, phase 2 with the margin included shall be able to last a minimum of 8.4 days. Using these values and the relations depicted in Figure 7.9 and Figure 7.10, the aluminium radiation shielding was sized as shown in Table 7.20.

It is acknowledged that the shielding around the bay for the competition rover will most likely not be sufficient for its survival during the entire mission. However, as the rover design will be chosen in a competition, this introduces an important design challenge for a mission to Europa where radiation is a largely limiting factor. It should also be noted that even though no designated radiation shielding was placed around the probe, multiple design strategies were applied to ensure it withstands the radiation environment during the journey to Europa. The torus propellant tanks described in Section 7.3 positioned around the probe will significantly limit the TID received. The skin of the probe shall also be made of titanium as will be explained in Section 8.9 later. Titanium offers great radiation protection capabilities similar to those of Aluminium and is also commonly used in space missions [53]. Once the probe is in the ice and subsequently water, these mediums will shield it from radiation as discussed earlier for the electronics box.

Table 7.20: Radiation shielding of components.

Component	Design TID [krad]	Al shield thickness [mm]	Mass of shielding [kg]
Electronics box	100	24.6	33.40
LIDAR	100	24.6	18.46
Star trackers	100	24.6	28.36
IMU	100	24.6	14.16
Cameras	100	24.6	13.51
Sun sensors	200	16.7	1.18
Reaction wheels	300	13.6	34.75
Competition rover	2000	4.91	13.97

7.7. Communication Subsystem

This section details the design of the communication subsystem for the AlienDive mission lander based on the requirements. First, the required energy per bit to noise spectral density ratio (Eb/No) for viable uplink and downlink communication with Earth must be determined. Once established, the necessary components for the communication system can be selected. Following this, the shape and size of the high-gain antenna (HGA) will be defined, after which link budget analyses will be conducted to define the maximum data rates

achievable by the antennas.

7.7.1. Communication Subsystem Requirements

AD-PERF-05-LD-01-COM-01: The lander communication subsystem shall establish communication with a BER of 1 × 10^{-5} or lower for uplink.

AD-PERF-05-LD-01-COM-02: The lander communication subsystem shall establish communication with a BER of 1 × 10^{-6} or lower for downlink.

AD-PERF-05-LD-01-COM-03: The lander communication subsystem shall employ binary phase-shift keying.

AD-PERF-05-LD-01-COM-04: The lander communication subsystem shall establish communication with an $\frac{Eb}{No}$ of 9.095 or higher for uplink.

AD-PERF-05-LD-01-COM-05: The lander communication subsystem shall establish communication with an $\frac{Eb}{No}$ of 11.298 or higher for downlink.

AD-PERF-05-LD-01-COM-06: The lander communication subsystem shall incorporate a redundant antenna.

AD-PERF-05-LD-01-COM-07: The lander communication subsystem shall establish communication with the NASA Deep Space Network.

AD-PERF-05-LD-01-COM-08: The lander communication subsystem shall incorporate a high gain antenna with a diameter of no more than 4.6 m.

AD-PERF-05-LD-02-COM-09: The lander communication system shall establish communication with the RF relay transceivers in the UHF band.

7.7.2. Energy per Bit to Noise Spectral Density Ratio

The energy per bit to noise spectral density ratio is dependent on the required bit error rate (BER) and signal modulation type employed by the communication system [54]. Due to several mission similarities to the AlienDive mission, BER requirements are derived from the Juno spacecraft requirements: a BER of 10^{-5} and 10^{-6} are required for uplink and downlink respectively [55]. The signal modulation type to be employed by the communication system is chosen to be binary phase-shift keying (BPSK) due to its power efficiency and simple implementation [31]. The relation between BER and Eb/No for BPSK modulation is given by Equation 7.15 [54]:

$$BER = \frac{1}{2} erfc \sqrt{\frac{Eb}{No}} \tag{7.15}$$

Utilizing Equation 7.15 yields the following requirement for Eb/No:

Table 7.21: Modulation, BER, and E_b/N_o required for lander-Earth communication

Link Type	Modulation	BER	$\frac{Eb}{No}$
Uplink	BPSK	10^{-5}	9.095
Downlink	BPSK	10^{-6}	11.298

7.7.3. Component Selection for the Communication System

Before selecting components, it's essential to determine which elements are required for a deep-space communication system. After careful evaluation of three deep-space missions, Juno, the Mars Exploration Rover and the Casini Orbiter it was determined the lander needs to be equipped with the following components [55, 56, 57]:

- **Transponder**: the transponder is responsible for demodulating received commands and transmitting the demodulated signals to the onboard computer. Furthermore, it modulates and transmits signals from the onboard computer to the ground station on Earth.[15]

---

[15]From `https://www.thalesgroup.com/sites/default/files/database/d7/asset/document/Deep_Space_Secure_Transponders.pdf`, accessed on 13/06/2024.

- **Power amplifier**: the power amplifier is responsible for amplifying the RF output power originating from the transponder [56]. Two types exist: travelling wave tube amplifiers (TWTA) and solid-state power amplifiers (SSPA) [56, 55].
- **Diplexer**: The diplexer enables simultaneous transmission and reception using the same antenna by separating signals based on different frequencies [55].
- **Switch**: the switch, either a coaxial or waveguide switch, is responsible for selecting the antenna to be used for transmitting and receiving signals [56].
- **Redundant low (LGA) or medium (MGA) gain antenna(s)**: the redundant low or medium gain antenna(s) are responsible for low data rate communication during cruise or in case of emergency [55].
- **High gain antenna**: the high gain antenna is responsible for high data rate communication with Earth. It can be used at every stage of the mission. [55]

Commercially available products exist for all components except the high-gain antenna, which must be custom-designed to meet specific mission requirements. Therefore, commercially available products are selected first. Subsequently, the shape and size of the high-gain antenna are defined to determine the maximum achievable data rates through link analyses. The selected components constrain the communication to be done using X-band frequencies, as the S-band will not be available for future space missions [31] and Ka-band components are not readily available.

Transponder
The selected transponder is the X/X/Ka DST from Thales Alenia. This transponder can handle signals at both X-band and Ka-band frequencies, supports BPSK modulation and is compatible with the NASA Deep Space Network. Furthermore, this transponder is used in the BepiColombo mission, having proved its capability and reliability in harsh space environments.[16]

Power amplifier
The power amplifier selected is the Spaceborne X-Band Solid State Power Amplifier by General Dynamics. This power amplifier has a nominal RF power output of 17 W and has been implemented in the communication systems of the Mar Exploration, Curiosity and Perseverance rovers, displaying its effectiveness and reliability in demanding space conditions.[17]

Diplexer
The diplexer selected is the WiRan X-Band Diplexer. This diplexer is lightweight and low in volume while maintaining high power-handling capabilities.[18]

Switch
The selected switch is the Coaxial SPDT Switch by Radiall. This switch is lightweight and possesses ample power-handling capabilities.[19]

Redundant antenna
The redundant antenna selected is the X-band medium gain waveguide pipe TTC antenna by Beyond Gravity. This antenna features a lightweight design while providing gains of 14 dB and 15 dB for uplink and downlink respectively.[20]

Table 7.22 shows the mass and power consumption of the selected components for the communication system for the lander of the AlienDive mission. This overview includes components chosen for communication through the ice crust of Europa, these components will be elaborated on in Section 8.7. Furthermore, this overview includes the high gain antenna, elaborated on in Subsection 7.7.5.

---

[16]From `https://www.thalesgroup.com/sites/default/files/database/d7/asset/document/Deep_Space_Secure_Transponders.pdf`, accessed on 13/06/2024.

[17]From `https://gdmissionsystems.com/-/media/general-dynamics/space-and-intelligence-systems/pdf/spaceborne-x-band-sspa-datasheet.ashx`, accessed on 13/06/2024.

[18]From `https://www.wiran.pl/en/x-band-diplexer`, accessed on 13/06/2024.

[19]From `https://satsearch.co/products/radiall-low-power-coaxial-spdt-switch`, accessed on 13/06/2024.

[20]From `https://www.beyondgravity.com/sites/default/files/media_document/2023-11/X-band-TTC-Antennas.pdf`, accessed on 13/06/2024.

Table 7.22: Mass and power overview of lander communication components

Component	Name (Company)	Mass [kg]	Power input [W]
Transponder	X/X/Ka DST (Thales Alenia)	3.7	32
Power amplifier	SSPA (General Dynamics)	1.37	65.5
Diplexer	X-Band Diplexer (WiRan)	0.115	-
Coaxial switch	Coaxial SPDT Switch (Radiall)	0.072	-
Redundant antenna	X-band MGA (Beyond Gravity)	0.41	-
High gain antenna	In-house design	100	-
Coax cables	-	0.122	-
Transceiver relays	PULSAR-UTRX (AAC Clyde Space)	0.1	5.1
Patch antenna	UHF Antenna III (EnduroSat)	0.085	-
Diplexer relays	In-house design	0.115	-
Total	-	**106.1**	**102.6**

7.7.4. The NASA Deep Space Network

Every deep space mission requires a ground system on Earth for communication. The NASA Deep Space Network (DSN), being one of the most sophisticated and extensive of its kind, has been selected to support the AlienDive mission. Table 7.23 displays some of the key features of the satellite dishes of the DSN (when communicating at X-band frequencies) [58].

Table 7.23: Characteristics of the DSN satellite dishes

Dish	Uplink Gain [dB]	Downlink Gain [dB]	RF Power Output [W]	System Noise Temperature [K]
34-m BWG	67.1	68.2	20000	29.2
70-m	73.2	74.6	20000	29.2

7.7.5. High-Gain Antenna Design

The cost of establishing contact with the DSN starts at 1057 \$/hour and only increases with mission specifics [59]. Therefore, to minimize the cost of utilizing the DSN, designing the high-gain antenna aims to maximise the data rates at which viable communication is possible. Equation 7.16 shows the expression for the energy per bit to noise spectral density ratio [31].

$$\frac{E_b}{N_o} = \frac{P_t G_t G_r}{(4\pi d/\lambda)^2 k T_s R_{data}} \sin^2(\beta) \tag{7.16}$$

Here, P_t is the transmit power, G_t is the transmitter gain, G_r is the receiver gain, d is the distance between transmitter and receiver, λ is the wavelength of the transmitted signal, k is the Boltzmann constant, T_s is the system noise temperature, R_{data} is the data rate and β is the phase modulation index. It is apparent that to maximise data rates, the high-gain antenna's transmitter or receiver gain needs to be maximised. To maximise the transmitter or receiver gain of the HGA, the diameter of the parabolic reflector of the HGA needs to be maximised. The antenna dish needs to fit in the fairing of the Falcon Heavy, which has an inner diameter of 4.6 m [60]. Therefore, the diameter of the HGA is constrained to be 4.6 m. The diameter is related to the physical aperture of the parabolic reflector according to Equation 7.17 [31]:

$$A_{ph} = \frac{1}{4}\pi D^2 \tag{7.17}$$

However, not all of the physical aperture is effectively used for capturing and transmitting energy. Therefore, the relationship between the physical aperture and the effective aperture is determined by the aperture efficiency factor, seen in Equation 7.18 [61]:

$$A_{eff} = \epsilon_{ap} A_{ph} \tag{7.18}$$

The aperture efficiency can be optimized for maximum gain using Equation 7.19 [61]:

$$\epsilon_{ap} = 24\{\sin\left(\frac{\theta_0}{2}\right)^2 + \ln\left[\cos\left(\frac{\theta_0}{2}\right)\right]\}^2 \cot\left(\frac{\theta_0}{2}\right)^2 \tag{7.19}$$

Here, θ_0 is the maximum angle between the focal point, F, and the edge of the dish as illustrated in Figure 7.11. Furthermore, this figure displays the dish depth, H_{depth}, and the diameter, D.
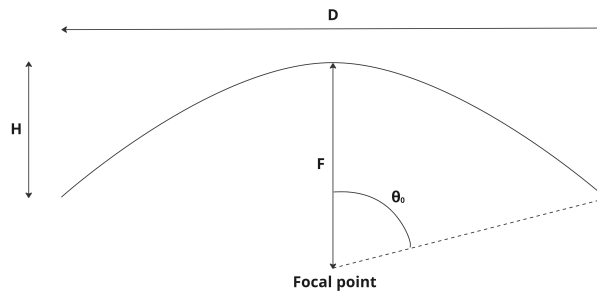
Figure 7.11: Antenna dimensions

The focal length is the optimal point of placement for the feedhorn of the antenna and is related to the dish depth, θ_0 and antenna diameter according to Equation 7.20 and Equation 7.21 [61]:

$$\frac{F_{focal}}{D} = \frac{1}{4\tan\left(\frac{\theta_0}{2}\right)} \tag{7.20}$$

$$F_{focal} = \frac{D^2}{16 H_{depth}} \tag{7.21}$$

The shape of the parabolic reflector can be described by a parabola according to Equation 7.22 and Equation 7.23 [61]:

$$y = a_{par} x^2 \tag{7.22}$$

$$a_{par} = \frac{1}{4F} \tag{7.23}$$

Finally, the gain of a parabolic reflector antenna is determined by its effective aperture and the signal wavelength (0.0414 m and 0.0357 m for uplink and downlink respectively, constrained by the communication components), as described by Equation 7.24 [31]:

$$G = \frac{4\pi A_{eff}}{\lambda^2} \tag{7.24}$$

Titanium is selected as the material for the parabolic reflector HGA, resulting in a mass of 100 kg, when the antenna has a thickness of 1 mm and taking into account a film layer of copper, according to CATIA. Table 7.24 shows the characteristics of the parabolic reflector HGA for the AlienDive mission:

Table 7.24: Characteristics of the parabolic reflector HGA for the AlienDive mission

Parameter	D	A_{ph}	θ_0	ϵ_{ap}	A_{eff}	F	H_{depth}	a_{par}	G_t	G_r	m
Value	4.6	16.6	66	0.83	13.8	1.78	0.75	0.14	136082	101372	100
Unit	m	m^2	deg	-	m^2	m	m	-	-	-	kg

7.7.6. Link Budget Analyses

Link budget analyses are conducted using Equation 7.16 to determine the maximum data rates for maintaining the required energy per bit to noise spectral density ratio for both the HGA and the MGA, as illustrated in Table 7.25:

Table 7.25: Link budget analyses for the HGA and MGA

	HGA		MGA	
Parameter	Uplink	Downlink	Uplink	Downlink
$\frac{Eb}{No}$ [-]	9.095	11.298	9.095	11.298
P_t [W]	20000	11.494	20000	11.494
G_t [-]	5128614	136082	5128614	31.623
G_r [-]	101372	6606934	25.119	6606934
d [m]	0.968×10^{12}	0.968×10^{12}	0.968×10^{12}	0.968×10^{12}
λ [m]	0.0414	0.0357	0.0414	0.0357
T_s [K]	389.54	29.2	389.54	29.2
β [°]	90	90	90	90
R [bps]	2456525	19530.5	608.701	4.539

The $\frac{Eb}{No}$ values come directly from the analysis performed in Subsection 7.7.2. The transmit power for uplink is the RF output power of the DSN dishes, as seen in Table 7.23. The transmit power for the downlink is calculated by taking the RF output power of the SSPA and subtracting the insertion losses of the diplexer and coaxial switch, which are 1.5 dB and 0.2 dB respectively. This results in a transmit power of 11.494 W. The transmitter and receiver gain for the ground station on Earth have conservatively taken to be those of the 34-m BWG dish of the DSN, as seen in Table 7.23. The transmitter and receiver gain of the HGA were the result of the HGA design, summarized in Table 7.24. The transmitter and receiver gain of the MGA can be found in Subsection 7.7.3. The distance between the transmitter and receiver is conservatively taken to be the largest distance Earth and Jupiter can be apart.[21] The (conservative) values for the wavelength of the signals are 0.0414 m and 0.0357 m for uplink and downlink respectively, constrained by the communication components. The system noise temperature is taken from the DSN for downlink, as seen in Table 7.23. For uplink, the system noise temperature of the lander was assumed to have the same value as the Juno spacecraft [55]. The phase modulation index is 90° for BPSK modulation [31].

7.7.7. Architecture Block Diagram of the Communication System of the Lander
Figure 7.12 shows the architecture block diagram of the communication system of the lander. Again, this block diagram contains components needed for communication with the probe through the ice, elaborated on in Section 8.7.
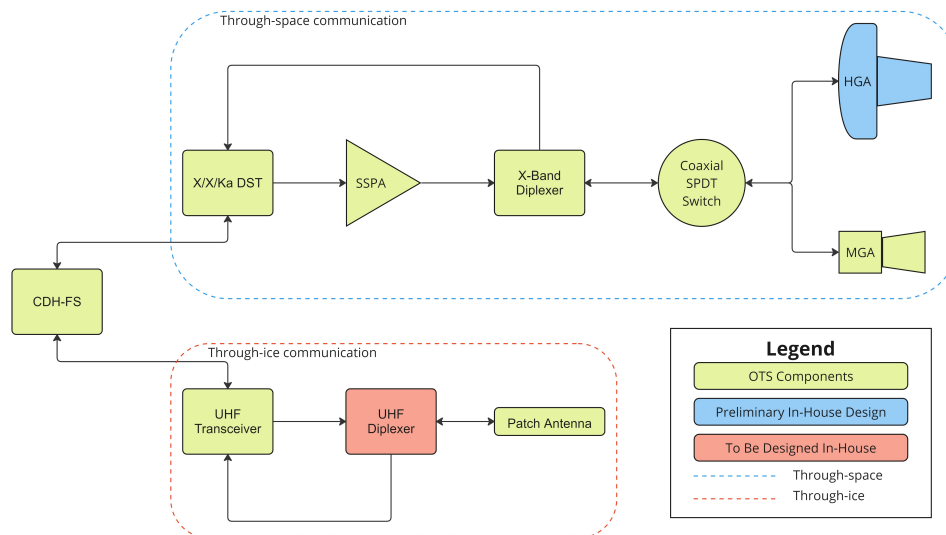
Figure 7.12: Architecture block diagram of the communication system of the lander

---

[21]From `https://www.space.com/18383-how-far-away-is-jupiter.html`, accessed on 13/05/2024.

7.8. Command and Data Handling Subsystem

This section details the design of the command and data handling system for the AlienDive mission lander based on the requirements. It starts with a presentation of the data handling block diagram, after which the necessary functions of the system are explained. Finally, the specifications of the selected onboard computer, which serves as the command and data handling system, are provided.

7.8.1. CDH Subsystem Requirements

AD-PERF-05-LD-01/02-CDH-01: The lander command and data handling system shall be able to acquire commands, housekeeping data and scientific data.

AD-PERF-05-LD-01/02-CDH-02: The lander command and data handling system shall be able to process data.

AD-PERF-05-LD-01/02-CDH-03: The lander command and data handling system shall be able to analyze data.

AD-PERF-05-LD-01/02-CDH-04: The lander command and data handling system shall be able to check data for errors.

AD-PERF-05-LD-01/02-CDH-05: The lander command and data handling system shall be able to compress data.

AD-PERF-05-LD-01/02-CDH-06: The lander command and data handling system shall be able to store data.

AD-PERF-05-LD-01/02-CDH-07: The lander command and data handling system shall be able to encode data.

AD-PERF-05-LD-01/02-CDH-08: The lander command and data handling system shall be able to encrypt data.

7.8.2. Command and Data Handling Functions

Figure 7.13 presents the data handling block diagram of the lander of the AlienDive mission, including through-put data rates. Through-put data rates include the maximum downlink data rate as calculated in 7.7.6, maximum command data rates assumed to be equal to those of the Juno spacecraft [55], assumed to be distributed evenly across the subsystems, the maximum payload data rate experienced during reconnaissance as calculated in Section 5.3, housekeeping data rates assumed to be 0.16 kbps for all subsystems (summing up to 10 % of the average probe scientific data rate), and maximum data rates transmitted to and received from the relay system, elaborated on in Section 8.7. The amount of data gathered, housekeeping and scientific, is discussed in Section 5.1. Furthermore, this section details the transmission time needed to relay the gathered information to the DSN.
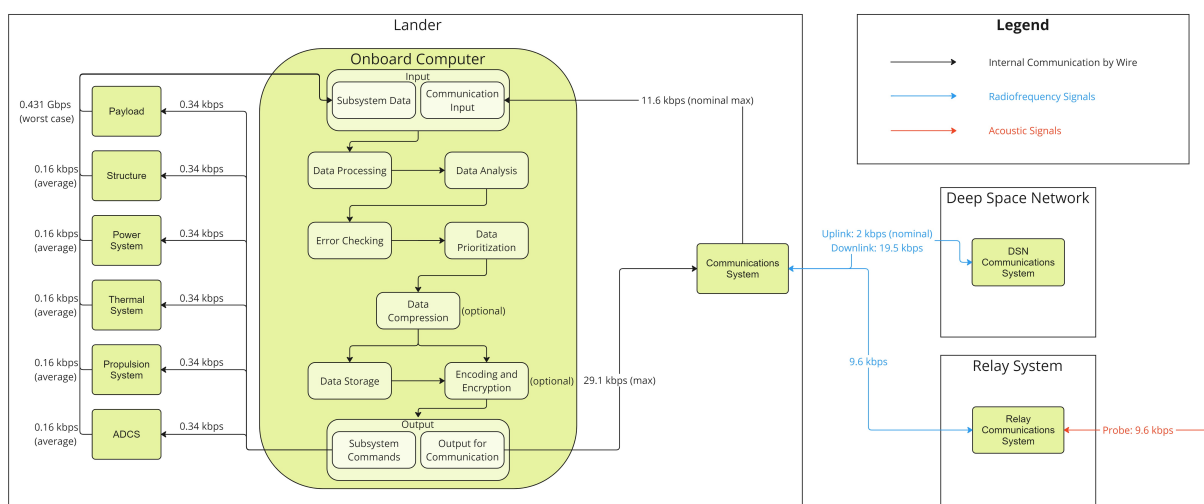
Figure 7.13: Data handling block diagram of the lander of the AlienDive mission

As can be seen, the onboard computer handles various tasks, elaborated on below[22]:

---

[22]From `https://science.nasa.gov/learn/basics-of-space-flight/chapter11-1/`, accessed on 16/06/2024.

- **Data acquisition**: commands, housekeeping data, and scientific data must be acquired by the onboard computer via the input ports.
- **Data processing**: data processing includes filtering sensor noise and organizing data from multiple sources.
- **Data analysis**: data analysis entails the preliminary onboard analysis of the scientific and system health data.
- **Error checking**: error checking involves utilizing error-detection and correction algorithms to ensure data integrity.
- **Data prioritization**: data prioritization means determining the transmission priority for different data types.
- **Data compression**: data compression primarily applies to scientific data, such as camera footage used in reconnaissance and supplying landing data, which often results in high data rates for the onboard computer. This footage must be transmitted to Earth at reduced data rates, necessitating compression.
- **Data storage**: to minimize the contact time with the DSN, data is stored onboard for transmission to Earth at certain distance intervals.
- **Encoding and encryption**: encoding and encryption primarily apply to downlink data and include formatting data for transmission, ensuring data integrity and securing data to protect the information from unauthorized access.

7.8.3. Onboard Computer

The selected onboard computer for the lander of the AlienDive mission is the CDH-FS by CAVU Aerospace UK. This computer features a fully redundant design by implementing a backup processor in case the main processor fails and provides ample data storage space. It is designed to withstand various space hazards, including radiation, cosmic rays and solar flares. The main features of the CDH-FS are listed in Table 7.26.[23]

Table 7.26: Main features of the CDH-FS onboard computer

Parameter	Value
Mass [kg]	4.25
Power [W]	5
Storage [Gb]	24

7.9. Structure

In this section, the design of the structure subsystem of the lander is discussed in detail. First, an analysis is done on the limiting load case of the structure, after which the design of the structure is described. Furthermore, the design of the landing legs is discussed.

7.9.1. Structures Requirements

The subsystem-level requirements to be fulfilled by the structure subsystem are listed below.

AD-ENG-02-LD-01-STRUC-01: The structure shall withstand lateral launch loads of $\pm 2\,$g.

AD-ENG-02-LD-01-STRUC-02: The structure shall withstand axial loads between $-2\,$g and $6\,$g.

AD-ENG-02-LD-02-STRUC-03: The structure shall have a natural frequency higher than $25\,$Hz in the axial direction.

AD-ENG-02-LD-02-STRUC-04: The structure shall have a natural frequency higher than $10\,$Hz in the lateral direction.

AD-PERF-01-LD-01-STRUC-05: The structure shall withstand a minimum temperature difference of $30\,$K from its production state.

7.9.2. Structure Design

The shape of the lander consists of two distinct elements: A cuboid lower part and a cylindrical upper part. The lower part has a square cross-section of 0.85 m x 0.85 m to allow for more space-efficient placement

---

[23] From `https://cavuaerospace.uk/wp-content/uploads/2024/01/CAVU-CDH-FS-Br-v2024.2.pdf`, accessed on 16/06/2024.

of internal components and has a height of 4.55 m. A truss structure was chosen for this lower part after calculation showed it was more mass efficient rather than using a shell structure, as the prevention of the plate buckling failure mode required a very large wall thickness. The upper part only has to support the communications dish and house the already cylindrical electronics compartment that will be lowered into the ice, and can thus be a thin cylindrical shell with a radius of 0.16 m and a height of 0.55 m.

The limiting load case to be carried by the main structure of the lander is again the launch of the spacecraft. The structure is thus designed for the loads and frequencies of the launch as described in Subsection 6.5.1, but now only has to carry the mass of the lander and the probe. The sizing of the lower truss structure uses the same method as described earlier in Section 6.5, designing for strength, stability and vibration. The lower truss structure consists of four vertical beams divided into three sections by horizontal beams. In addition, two crossbeams with the same shape and size as the horizontal beams are added to these sections for extra stability. Titanium will again be used for the design of these parts due to high its strength and stiffness.

Since the shape of the lower truss structure is very tall and slender, buckling turned out to be the most limiting failure mode. To account for this, the beams are again chosen to have a hollow cylindrical shape for its high buckling resistance. The sizes of all three different elements are found in Table 7.27

Table 7.27: Sizing of beam elements of the lower part of the lander structure.
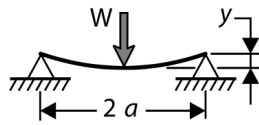
Element	Failure mode	Total length [m]	Radius [mm]	Thickness [mm]
Vertical beam	Buckling	4.55	34.1	4
Horizontal/crossbeam rod	Buckling	0.85/1.74	19.8	1

For the cylindrical upper part, the shell buckling failure mode has to be analysed in addition to the already mentioned modes. Shell buckling occurs under axial compression, but requires empirical, iterative equations that were standardised by NASA, which is found in Equation 7.25 and Equation 7.26 [62]. Here, R is the radius, t is the thickness of the shell, E is the elasticity modulus and ν is the Poisson ratio of the material.

$$\sigma = \gamma \frac{E}{\sqrt{3(1-\nu^2)}} \left(\frac{t}{R} \right) \qquad (7.25)$$

$$\gamma = 1 - 0.901(1 - e^{-\frac{1}{16}\sqrt{\frac{R}{t}}}) \qquad (7.26)$$

For the upper part, this shell buckling was found to be the limiting failure mode. The radius of the cylinder is 0.16 m and the design thickness is 1 mm.

After the primary structure has been sized, the secondary and tertiary structures need to be sized. The secondary structures include the plates between sections: one circular plate for the cylindrical upper part and four rectangular plates for the lower truss structure. For estimating the circular plate of the upper cylindrical section, it is assumed to carry the load of the probe mass (553.8 kg + 25% margin) as a point load and is simply supported. The most critical load case would be during launch (6g + 10% yield margin). To design for yielding, the plate's thickness can be determined by rewriting the equation given in Figure 7.14 to solve for t.

$$\sigma = \frac{3\,W\,(1+v)}{2\,\pi\,t^2} \left(\frac{1}{v+1} + \log\frac{a}{r_0} - \frac{1-v}{v}\frac{r_0^2}{4\,a^2} \right)$$

$$\delta_{\text{Max.}} = \frac{3\,W\,a^2\,(1-v)\,(3+v)}{4\,\pi\,E\,t^3}$$

Figure 7.14: Point loading of a simply supported circular plate [63]

Here σ is the stress, W the point load, v Poisson's ratio, a the radius of the plate, and r_0 the radius of the load. Assuming r_0 is equal to a, substituting the values results in a required plate thickness of 2.88 mm. With a radius of 0.16 m, this leads to a total mass of 1.57 kg.

A similar approach was used for the secondary structures of the lower truss. It was assumed that the plates could support the probe mass during launch and were simply supported on all sides. For simplicity, the hole in the middle was not considered in this analysis. Additionally, in reality, these plates would likely not support the probe mass during launch; however, this assumption provides a sufficient first-order estimate. To calculate

the thickness Equation 7.27 [64] can be used.

$$t = \sqrt{\frac{\beta q b^2}{\sigma_{max}}} \tag{7.27}$$

Here β is equal to 0.2874 for a square plate [64], q the uniform loading, b the width of the plate, and σ_{max} the yield stress. The uniform loading is equivalent to the point loading from the previous case divided by the width of the plate. Substituting the values gives a required thickness of 3.95 mm. With a width of 0.8 m, this results in a mass of 11.32 kg per plate. Since four plates are needed, the total mass for the secondary structures of the lower truss is 45.29 kg. Estimating the tertiary structures' mass, including components such as attachments, is challenging. Therefore, their mass is approximated as 5% of the primary structure mass.

Table 7.28: Mass breakdown of the transfer stage structure.

Element	Mass [kg]
Lower primary structure	99.53
Lower secondary structures	45.29
Upper primary structure	1.71
Upper secondary structures	1.57
Tertiary structures	5.06
Total mass	**153.18**
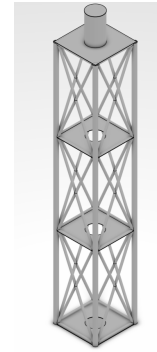
Figure 7.15: Visualisation of the layout of the lander structure

7.9.3. Landing leg design

To safely land on the surface of Europa, landing legs have to be sized that support the weight of the lander, keep the lander from tipping over on landing, and dampen the impact after the final burn. While designed to descend and land at a constant velocity of 0.5 m/s towards the surface from 50 m, the legs are to survive free fall from 10 m in case of propulsion loss during the final seconds of this descent phase above the surface.

To prevent tip-over, the landing legs must be wide enough for the centre of gravity to stay within the range of the legs when landing on an incline. Based on slope probability models of Europa, the cumulative probability of slopes steeper than 20 degrees take up less than 10% for the worst-case terrain, based on the plot found in Figure 7.16 [65].

The design requirements for the landing legs are specified below:

- **AD-LAND-01-LD-02-LL-01**: Shall damp a landing impact when free-falling from 10 meters above the surface
- **AD-LAND-01-LD-03-LL-02**: Shall support the landed dry mass of the lander
- **AD-LAND-01-LD-03-LL-03**: Shall be stable landed at slopes of 15 degrees in its deployed state
- **AD-LAND-01-LD-03-LL-04**: Shall not slip after landing
- **AD-ENG-02-LD-03-LL-05**: Shall not be wider than 1 meter in its stored state

The landing legs are placed on the corners of the main truss structure of the lander, to limit the required strut length, and prevent interference with the exhaust plume of the landing thrusters. In addition, the landing legs do not block any other useful areas of the rectangular lander body that are used up by other components.

The length of the legs is calculated assuming the centre of gravity is at the top of the spacecraft. This is a conservative assumption since the CG is always a bit lower, meaning the actual tip-over angle of the lander is larger. In addition, the required length is designed for the horizontal struts being at an angle of 60 degrees with the surface normal, in case of rocks or other obstacles requiring deployment at angles lower than 90 degrees.

Since the landing legs extend far from the central body, a deployment mechanism is chosen to reduce the size taken up within the fairing. The selected mechanism is a parallel linkage configuration similar to the first stage of the New Shepard launcher, using one vertical and two horizontal struts per landing leg, as can be seen in Figure 7.17.[24] In addition, a guiding rod is put between the lower connection at the spacecraft body

---

[24] From `https://www.blueorigin.com/new-shepard`, accessed on 14/06/2024.

and the upper connection on the vertical strut. An example of the mechanism is shown in Figure 7.18. In its stored state, the landing leg can fit flush against the wall of the lander. In its nominal deployed state, the vertical and horizontal struts are at an angle of 90 degrees to maximise the ground footprint. For the joints of the legs, simple pin joints are used that are locked after deployment to prevent further movement.
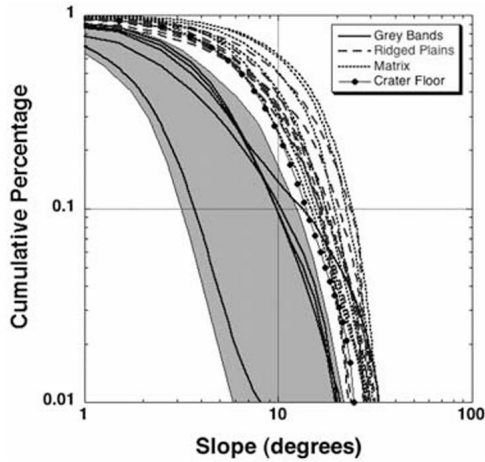

Figure 7.16: Histogram of the cumulative slope probability for four terrain types on Europa using 30-45 m resolution [65, p. 3]

Figure 7.17: Landing legs of the New Shepard launcher[24]

For sizing of the struts, it is designed for the load to be carried by only one of the horizontal struts, and the other strut is just used for the mechanism. In practice, this means the strength and stiffness of the horizontal part of the landing legs are higher. The guiding element in the mechanism is not load-bearing. Again, all struts are designed for strength, stability and their natural frequency, similar to the truss structures of the transfer stage and lander. The load to be carried by the landing legs is the weight of the total landed dry mass of the system on the surface of Europa, multiplied by a safety factor of 1.5.

For both struts, the limiting failure mode is the compressive strength under bending. The vertical strut is a cylindrical rod with an inner radius of 12.8 mm and an outer radius of 15.0 mm. Its total length is 1 m, of which 0.5 m is below the lander in its 90° deployment state. The horizontal struts have a similar shape, with an inner radius of 20.2 mm and an outer radius of 23.7 mm, and have a length of 1.6 m. The mass of the joints in the legs is based on a similar design case [66].

The final part of the landing legs to be designed in detail is the landing pad and the shock dampers. To prevent slipping, the bottom of the landing pad consists of a large surface with a diameter of 0.2 m with a coarse surface finish to maximise friction. This, in addition to the fact that the ice on Europa's surface should not be very slippery relative to the ice at a temperature around its melting temperature due to there not being a thin layer of liquid water [67], as a result of the cold temperatures and the near vacuum pressure on the surface. This should keep the lander from moving around after landing.

Since the lander only has to land on the surface one time, the shock dampeners can be designed to be single-use. These shock dampers prevent damage upon landing impact, and reduces the probability of bouncing off the surface. To not risk leaking fluids, the dampener uses a sacrificial aluminium foam cylinder which absorbs the impact energy, as has been used in previous space applications [68]. For a free-fall height of 10 meters on Europa, the impact velocity is 2.56 m/s. Based on this velocity, the kinetic energy to be absorbed is found. A coarse aluminium foam is chosen with a density of 107.6 kg/m^3, and a specific energy absorption of 366 940 J/m^3 [69]. The foam has a diameter of 15 cm and a height of 20.7 cm.

An overview of the mass of the landing legs is found in Table 7.29.
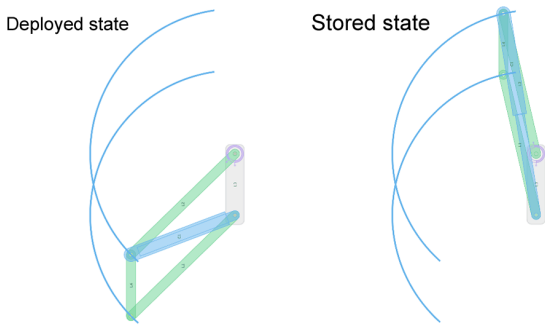
Figure 7.18: Visualisation of the landing leg deployment mechanism in its deployed (60 deg) and stored state.

Table 7.29: Mass breakdown of the landing legs subsystem.

Element	Mass [kg]
Vertical Strut	3.9
Horizontal Strut	27.5
Landing Pad & Dampener	11.7
Joints	20
Landing Leg Mass	63.1

7.10. End-of-Life Procedures

After gathering scientific data and communicating with Earth, the lander needs to be properly shut down. Luckily, the lander is on the surface. This will imply a low chance of leaking radioactive substances into the subsurface ocean. Due to the RTGs constantly producing power, it will be hard to fully turn off the lander. Nevertheless, the tough radiation on Europa will make sure the mission will not function for a long time past the mission end. The radioactive material will not come in contact with the subsurface ocean and the radiation due to Jupiter is higher than the radiation due to the RTGs [44]. No real procedures will need to be taken in the end-of-life of the lander, since it can just stay stationary and it will not endanger the moon.

7.11. Visualisation of Layout

The lander layout was determined by making an assembly in CATIA. The result of this assembly can be seen in the following figures, where Figure 7.19 shows the isometric view of the full lander, Figure 7.20 shows an isometric view with a transparent bus, excluding antenna, to show the inner components, Figure 7.21 shows a cross-sectional view with components and dimensions specified, and Figure 7.22 shows a cross-sectional view from another side.
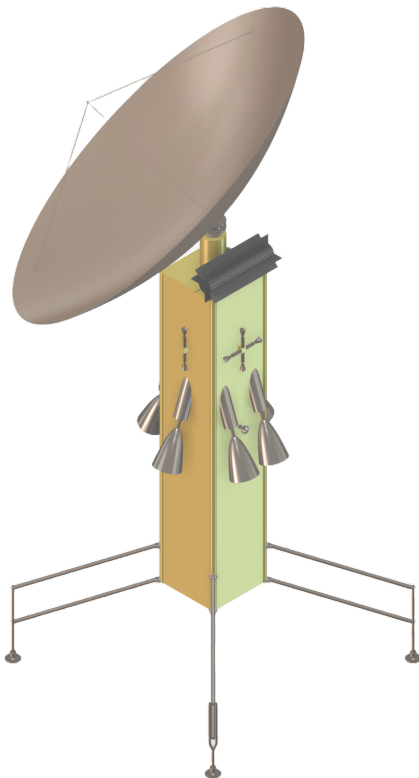

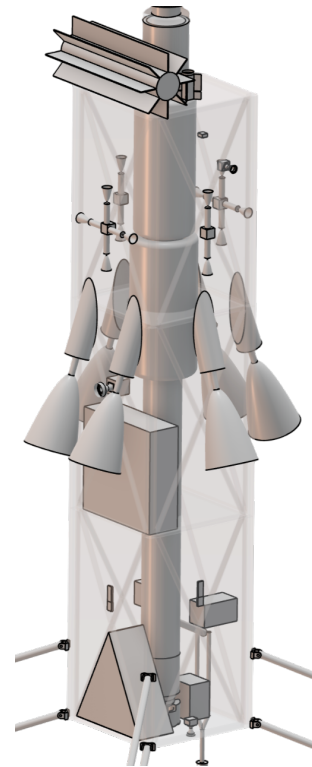
Figure 7.19: An isometric view of the Lander

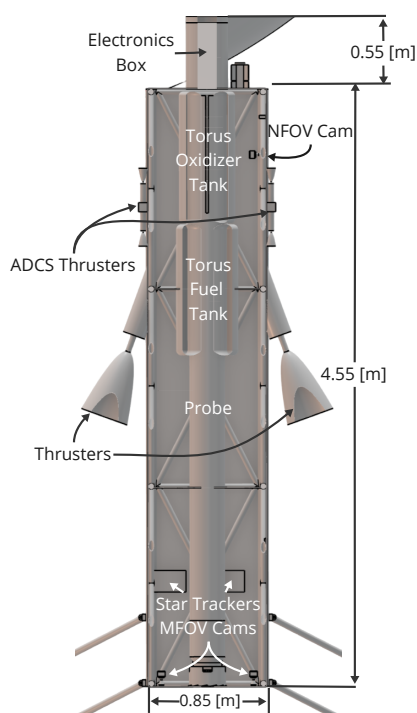Figure 7.20: A transparent isometric view of the lander, excluding the relay antenna.

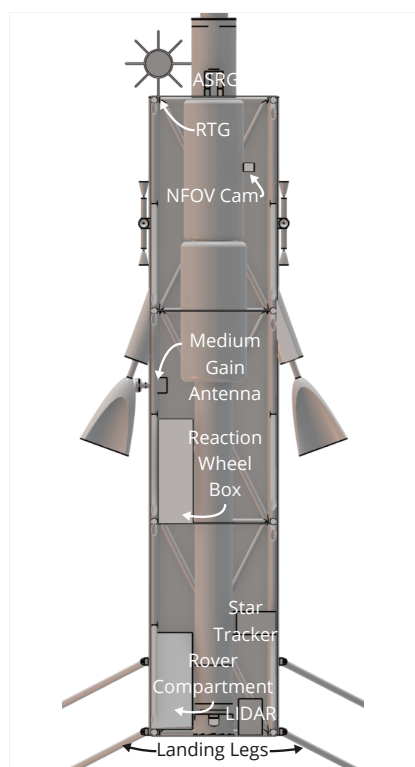**Figure 7.21:** A cross-sectional view of the lander

Figure 7.22: A cross-sectional side view of the other side of the lander

As explained in Section 7.4, the lander has 12 ADCS thrusters divided into 4 sets, located on the 4 sides of the lander towards the top of the bus. There are also 6 regular thrusters, located on all 4 sides of the spacecraft. There is a medium gain antenna that sticks out between two thrusters. The high-gain antenna is located on a gimbal at the very top of the spacecraft. The landing legs are located on the corners. The seismometers are located on the landing legs as they are closest to the ground. The RTG and ASRG are located on the top of the box part of the bus. This reduces the need for thermal control, as their heat can easily radiate out into space, rather than into the structure. The regular RTG had to be placed on its side due to its size, so a custom mounting system would have to be designed to keep it in place.

On the inside, there are 2 propellant tanks around the probe. These are placed around the critical electrical components of the probe so that they are shielded from radiation during orbit. Above the tanks, within the cylinder part of the bus, is the electronics box, with a separable radiation shield around it This contains all the critical electrical components of the spacecraft. Above that, there is some empty space, which would contain the probe-lowering mechanism and some cables. The magnetometer is not visible in the cross-sections but is located near the top to allow for it to be shot out, away from the electronics. The probe itself spans nearly the entire length of the bus. Two Medium Field-Of-View (MFOV) cameras and one Narrow Field-Of-View (NFOV) camera are placed on the bottom and higher side of the lander respectively. Two star trackers are placed on two adjacent sides, with 2 sets of one coarse and one fine sun sensor located on the other two sides. The latter are too small to see in the figures, however. A LIDAR is mounted on the bottom of the spacecraft to ensure line of sight with the surface during landing. Lastly, the triangular rover compartment is fitted on the very bottom as well. A hatch will open to ensure the rover can drive down onto the surface.

The dimensions are shown in Figure 7.21. The lander has a total height of 5.1 m, excluding the antenna, and a width and length of 0.85 m. The box has a slightly greater height than the probe to allow for the structure and cables. The landing legs extend about 0.5 m below the bottom of the lander bus when deployed.

8 Probe Design

In this chapter, the design of the probe responsible for penetrating the ice and reaching the subsurface ocean will be discussed. An overview is given in Section 8.1. The subsystems will be discussed in Section 8.2, Section 8.3,Section 8.4,Section 8.5,Section 8.6,Section 8.7, Section 8.8 and finally, Section 8.9.

8.1. Probe Overview

The probe is the main system used to reach the scientific goals of the mission, as this is the part of the spacecraft that reaches the subsurface ocean of the moon. Within its body, it carries a large selection of payload instruments as listed in Section 4.2:

In short, as was shown in Section 5.1, the operations of the probe after deployment consists of first moving down and through the icy crust of Europa, during which initial measurements of the crust are taken and relays are deployed at a constant interval. Once the probe nearly reaches the mushy ice-ocean interface, it deploys its anchor into the solid ice and starts its final descent into the ocean along a tether. Using controlled vertical movement along the tether, measurements are taken of the ice-ocean interface and the subsurface ocean, which are then transmitted to the lander via a chain of acoustic and RF relays.

The probe is built as a cylindrical pressure vessel to withstand the large hydrostatic pressures in the ocean. Next to its structural purpose, this shell functions as radiation shielding and thermal isolation. Powered by two finless radioisotope thermoelectric generators, the probe uses a heated drill to remove ice quickly and melt the ice chips to prevent getting stuck. The heat is provided by the RTGs, using a pumped fluid loop to move the thermal energy to the locations where it is needed.

For communication through the water to the anchor, acoustic communication is used. From there, the communication through ice is done via UHF RF relays. The anchor and relays are deployed by driving rods with heated pins into the icy walls around the probe using springs. The relays are then locked into the ice and detach from the probe once it keeps moving down. The interaction of all the subsystems in the probe and also how they are linked to the relays is illustrated in Figure 8.1.

An overview of the main design parameters of the probe is found in Figure 8.13.

8.1.1. Probe System Requirements

The system requirements for the probe are listed below:

> **AD-SCI-02-PR-01**: The probe shall be able to enter the subsurface ocean.
>
> **AD-PERF-02-PR-01**: The probe shall be able to traverse the ice.
>
> **AD-PERF-03-PR-01**: The probe shall be able to determine its attitude while traversing the ice.
>
> **AD-PERF-03-PR-02**: The probe shall be able to detect obstacles along its path.
>
> **AD-REL-01-PR-01**: The probe shall be able to arrive at the subsurface ocean with a probability of 0.5.
>
> **AD-REL-01-PR-02**: The probe shall be able to withstand the corrosive subsurface environment.
>
> **AD-ENG-01-PR-02**: The probe shall not be longer than 6m.
>
> **AD-ENG-02-PR-01**: The probe shall withstand the static loads of the Falcon Heavy.
>
> **AD-ENG-02-PR-02**: The probe shall withstand the dynamic loads of the Falcon Heavy.
>
> **AD-PERF-05-PR-01**: The probe shall be able to communicate with the lander.
>
> **AD-PERF-01-PR-01**: The probe shall be powered appropriately during its lifetime.
>
> **AD-PERF-01-PR-02**: The probe shall have a lifetime of at least 14 years.
>
> **AD-PERF-01-PR-03**: The probe shall withstand the radiation environments encountered throughout the mission.
>
> **AD-SCH-01-PR-01**: The probe shall be produced and tested before 2035.

Figure 8.1: Hardware and software diagram for the probe system
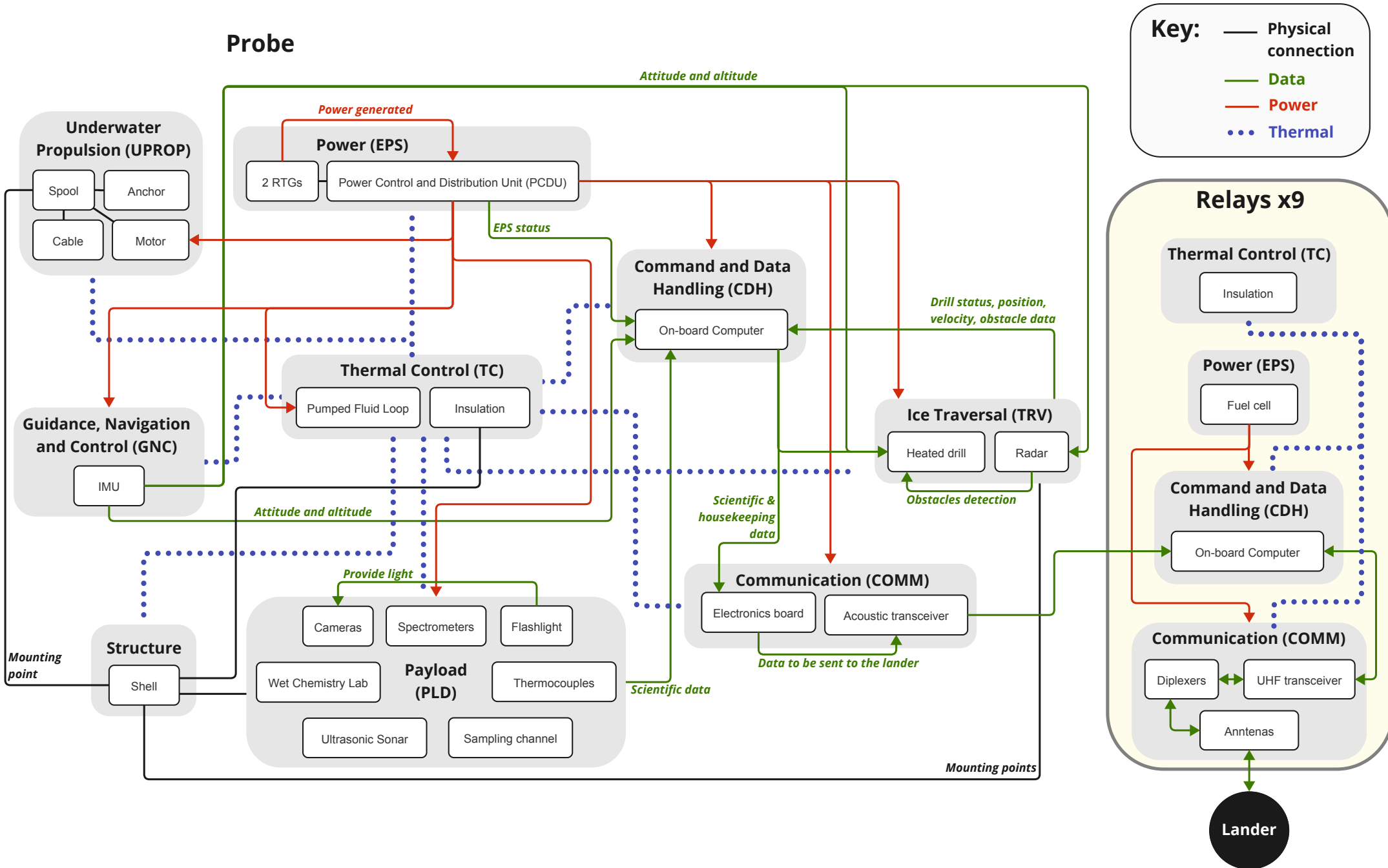
8.2. Power Subsystem

The power system on the probe is needed for drill, gathering data and transmitting data to the lander. It also needs to make sure the other subsystems which are important for the mission get enough energy, such as the thermal control. The EPS is thus of vital importance and if it stops functioning, it will likely have disastrous consequences. It should also be designed according to COSPAR regulations since it should not contaminate the environment.

Even though it is among the most critical subsystems, the EPS subsystem for the probe is one of the most difficult puzzles to solve. Due to the long mission lifetime, high power requirements, and underground deployment the EPS is hard to design. To start, a power budget is needed. Here the EPS subsystem is assumed to use 10% of the maximum begin-of-life power. The power usage of each subsystem can be seen in Table 8.1.

Table 8.1: Power budget for the AlienDive Lander

ID	Subsystem	Power Input [W]
1	Scientific payload	145.5
2	Traversal (Drilling)	500
3	Thermal control	3.85
4	Guidance, Navigation and Control	35
5	Electronic Power Supply	60.43
6	Communication during drilling	20
7	Communication during scientific phase	20
8	Command and Data Handling	5
9	Reel	200
10	Propulsion	500

This can be divided into different power modes which fit the mission phases: Ice penetration mode, Reel mode, Science mode, Communication mode, Safe mode, and Propulsion support mode. The power required for these modes and the active subsystems can be seen in Table 8.2

Table 8.2: Power modes of the AlienDive Lander

Mode	Power Required [W]	Active Subsystems
Ice penetration mode	604.28	2,3,4,5,8
Reel mode	304.28	3,4,5,8,9
Science mode	249.78	1,3,4,5,8
Communication	269.78	1,3,4,5,7,8
Safe Mode	69.28	3,5,8
Propulsion support mode	589,28	3,5,8,10

Due to the large power surplus during travel, power can be used to optimise the propulsion. Further, an additional payload, a cosmic dust collector, which would operate during the journey to Europa was considered because of this surplus, but it was discarded due to the high gain antenna blocking the flow of cosmic dust. A solution would be to rotate the spacecraft during the journey, however, this was deemed too risky.

8.2.1. EPS selection

Using an ESA recommended margin of 20% [27], the end-of-life power required is 725.13 W. Using Figure 7.2, the two feasible power options seem to be a radioisotope thermal generator (RTG) and a nuclear microreactor. Fuel cells and batteries do not have a high enough energy density. Solar panels will not function under ice layers and experimental ways of generating power are too risky and drive the reliability of the mission too far down.

Important parameters for the EPS are power generated, mass, and diameter. New nuclear microreactors can be found from one kW to several kWs [70]. They are often heavy and large in diameter [70]. RTGs are less heavy and occupy less volume, but produce less power [44]. Due to the heavy radiation on Europa, it is generally recommended to keep the mission as short as possible [29] and thus make sure the diameter is as small as possible. RTG was thus a more favourable choice.

With the selection of RTGs, Equation 7.1 can be used. This will result in an additional margin of 17%. The design power at begin-of-life should thus be 849.3 W.

8.2.2. EPS Subsystem Requirements
Now that all the needs for the EPS subsystem have been formulated, the requirements can be created. They can be seen below:

AD-PERF-01-PR-01-EPS-01: The EPS subsystem shall provide the probe with an average peak power of 850 W at begin-of-life.

AD-PERF-01-PR-01-EPS-02: The EPS subsystem shall distribute and condition all the EPS power.

AD-PERF-01-PR-01-EPS-03: The EPS subsystem shall provide health and safety information containing the produced power and power usage.

AD-PERF-01-PR-01-EPS-04: The EPS subsystem shall protect itself and others from electromagnetic interference, transients, bus faults, and load faults, such as filtering, overvoltage, and short circuit protection.

AD-PERF-01-PR-01-EPS-05: The EPS subsystem shall provide appropriate voltage levels for all the subsystems.

AD-PERF-01-PR-02-EPS-01: The EPS subsystems shall have a lifetime of at least 14 years.

AD-PERF-01-PR-02-EPS-02: The EPS subsystems shall have a diameter of less than 0,25m.

AD-PERF-01-PR-03-EPS-01: The critical EPS subsystem components shall withstand 100 krad of radiation during its lifetime.

AD-ENG-01-PR-02-EPS-01: The EPS subsystem shall have a length of less than 3m.

AD-ENG-02-PR-01-EPS-01 The EPS subsystem shall withstand the launch loads.

AD-ENG-02-PR-02-EPS-01 The EPS subsystem shall not resonate with the launcher.

AD-SCH-01-PR-01-EPS-01: The EPS subsystem shall be developed before 2035.

8.2.3. RTG selection
The RTG(s) would have to fulfil the above requirements. RTGs generally generate low power, thus it would be probable to have multiple RTGs. The current RTGs were unfeasible and would drive the design to unachievable numbers. Concepts were examined to see if these would fit the requirements. The 16-GPHS-STEM-RTG seemed like the most viable. One produces 425 W, has a diameter of 0.47 m, and length of 1.07 m [44]. It should be mentioned that the TRL of this design was only 2 in 2015. It should be ready for planetary exploration in 2029 [44]. Due to the diameter requirement, this RTG should be made smaller. This can be done by removing the heat sink fins on the outside of the RTGs for the probe. This would reduce the diameter to 0.2 m, which complies with the requirements. This will pose an additional probe for thermal control, but this will be solved with fluid cooling.

The main problem is that this will still be a concept and should be verified thoroughly. Experts have claimed that it should be possible to alter the design of an RTG to handle this and it has been on the agenda of NASA to develop this [71]. It has also been incorporated in NASA conceptual missions such as Tunnelbot [72]. Nevertheless, this will be a large liability for the design of AlienDive. According to an expert in the field of ice-penetrating probes[1], the EPS subsystem can often be a showstopper in these kinds of missions.

Two of the 16-GPHS-STEM-RTG will meet all of the requirements. The RTGs will together be a 2.14 m long cylinder with a diameter of 0.2 m. Together it will have a mass of 105.6 kg and it will produce 850 W at the beginning of life [44].

8.2.4. PCDU selection
The Power Conditioning and Distribution Unit (PCDU) is important for providing appropriate voltages to all the subsystems. It should be able to handle 850 W and minimise mass and volume. Using the same estimation

---

[1]Private communication with an expert on this topic

techniques used in Subsection 7.2.5 would result in a mass of 12.4 kg and 5.9 kg. As a conservative assumption the highest mass, 12.4 kg, is used. The volume will be estimated below <1000 cm^3 as can be found in COTS components [45].

8.2.5. Harness Selection

To connect to all the subsystems an electrical harness needs to be designed. The wiring of a spacecraft is complicated and is out of the scope of this project. Basic estimates can be given about the harness. The mass will be around 38% of the RTG mass which is 40.4 kg. The volume of the wiring is hard to estimate and should be done when the design is more detailed.

Inside the probe will be four types of wires: 5V, 24V, 28V, and HV cables. The High Voltage (HV) cables will be used between the RTG and the PCDU to minimise the power loss in this part.

8.2.6. Ocean Thermal Energy Conversion

A new type of payload can be added to investigate novel energy generation on Europa. This will likely be a small probe, which will be ejected into the ocean. The power supply will be a module which can generate power from thermal differences in the ocean. Furthermore, it will also include a communication system to transfer the data back to the probe, this will be acoustic due to low attenuation in water. Lastly, it will likely include an accelerometer, which will help to detect possible tidal movements in Europa. The design is still under development and should be worked out in more detail in later design phases. It will not occupy much space and will have a minimal mass.

Depending on the weight and volume of these OTEC probes, big swarms could be made to analyse tidal movement in a larger area and collect more diverse data as well.

8.2.7. Total EPS cost

One disadvantage of an RTG is the steep cost associated with them. RTGs often cost around 109 $M to produce and 83 $M to develop [73]. Not to mention the cost of the wiring and PCDU. For this, a margin of 10% of the RTG cost is used (10.9 $M per RTG). Lastly, the cost of modifying an RTG to be finless has to be considered. This should not cost as much as redesigning an entire RTG. For this, a margin of 10% of the development cost is used. An overview of the total EPS cost can be found in Table 8.3.

Table 8.3: Cost overview of the EPS subsystems

Probe	Cost [$M]	Lander	Cost [$M]
Producing RTGs	218	Producing RTG	109
Developing finless RTG	8.3	Developing RTG	83
Harness and PCDU	21.8	Harness and PCDU	10.9
Cost of EPS for Probe	248.1	Cost of EPS for Lander	202.9

8.2.8. Probe EPS overview

After sizing all of the components, the final estimations can be given. This can be seen in Table 8.4. The harness design, including the voltages, can be seen in the electrical block diagram in Figure 8.2.

Table 8.4: Mass overview of the EPS subsystem on the probe

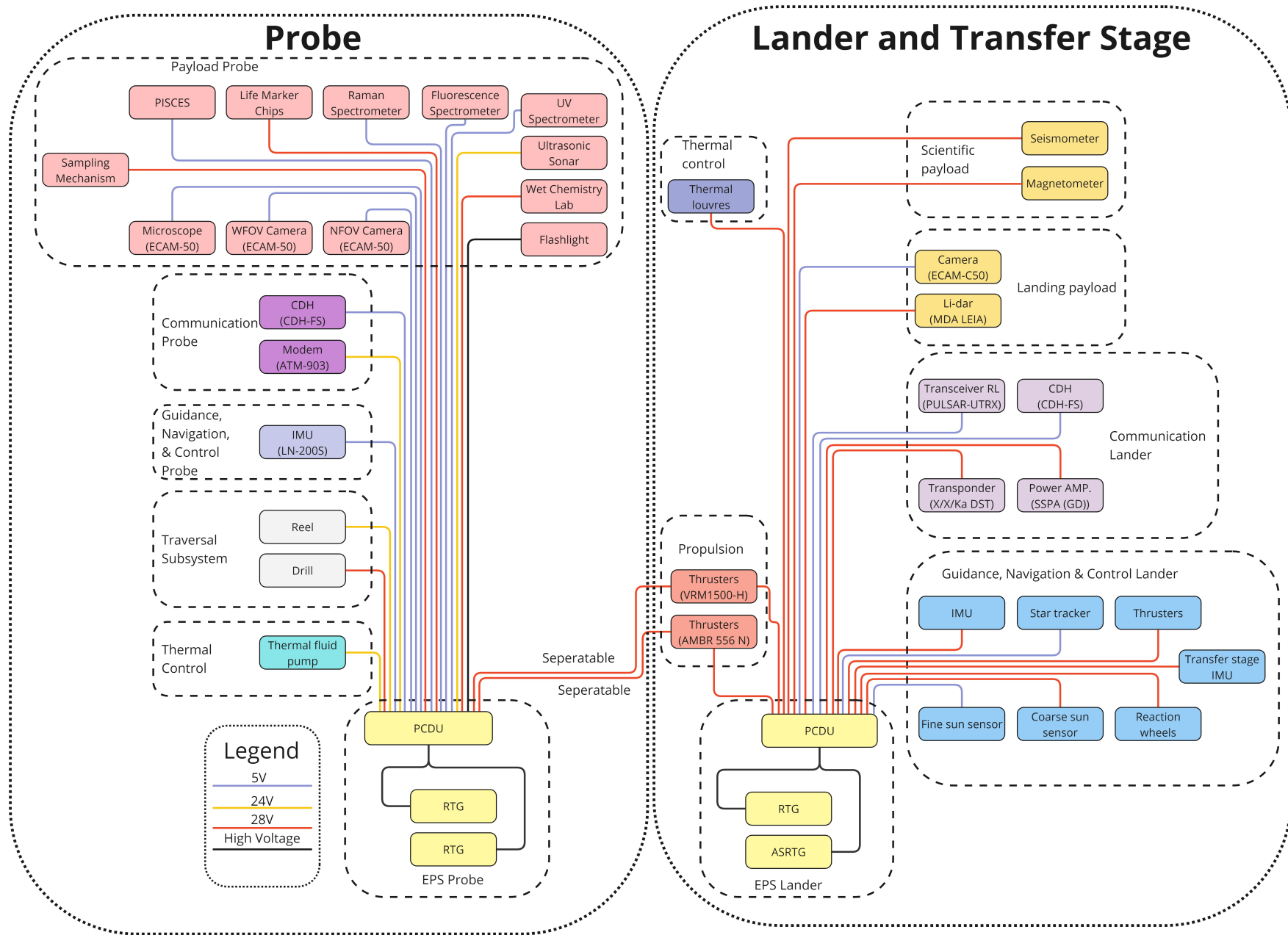| Component	Mass [kg]
16-GPHS-STEM-RTGs	105.6
PCDU	12.4
Harness	40.4
Total	**158.4**

Figure 8.2: Electrical block diagram of the probe and lander systems

8.3. Ice Traversal System

The ice traversal requirements are listed below:

AD-PERF-02-PR-01-ICE-01: The drill bit shall have a diameter that is at least 1cm bigger than the probe.

AD-PERF-02-PR-01-ICE-02: The drill shall include a percussion mechanism.

AD-PERF-02-PR-01-ICE-03: The drill shall be able to withstand the corrosion of the ice.

AD-PERF-02-PR-01-ICE-04: The drill shall be able to withstand fatigue caused by drilling through the ice up to 30km.

A heated percussion drill will be used to traverse the ice crust of Europa. First, the ice will be crushed and hammered into chips, these chips will then be pushed inwards by the slanted teeth on the drill bit. The drill bit teeth will be coated with a thick layer of tungsten carbide to harden them and minimise wear [74]. Transporting the chips into the drill before heating was chosen to minimise losses to surrounding ice. Inside the drill bit, a large-surface-area heating rod will partially melt the chips so an ice-water substance is created. This 'slush' is then carried up through the holes in the drill bit and transported around the probe. One important part of this design is that the drill bit is bigger than the probe so there is room for the slush to move past the probe. The four main components of the ice traversal system are the motor, the percussion hammer, the drill bit and the ice-penetrating radar (IPR). The drill bit and heating rod can be seen in detail in Figure 8.3 and the full heated drill assembly is shown in Figure 8.4.
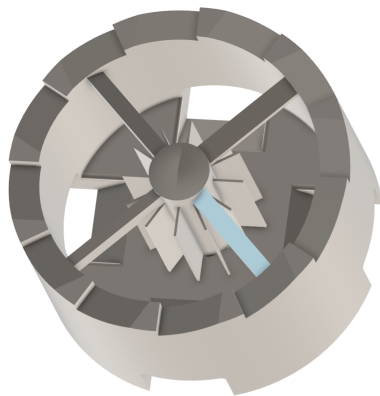

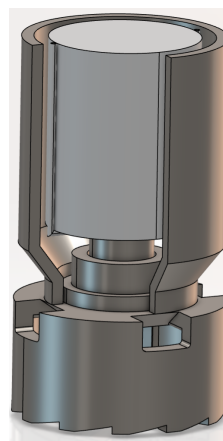**Figure 8.3:** Drill bit and heating rod architecture

Figure 8.4: Heated drill assembly

In space mission mass estimations are often a first step in mission sizing, this was done for all main components of the ice traversal system and is shown in Table 8.5.

Table 8.5: Traversal system mass estimation

Characteristic	Mass [kg]
Motor	10
Hammer	3.15
Bit	19.85
IPR	0.5
Total	**33.5**

The mass for the hammer and drill bit were calculated with volume and TiAl6V4's material density. The IPR was estimated using commercial products, one design even claims a total transmitter mass of 3.5 g.[2] However, 0.5 kg was chosen as IPR mass, given the many unknowns surrounding this sensor, it is discussed more in

---

[2]From `https://marshallradio.com/ww/product/micro-transmitter/`, accessed on 19/06/2024.

Section 8.5. The motor was also based on commercially available products[3] and was assumed to be custom designed as electric motors are widely used. A safety factor of roughly 2 was used to include the unknowns of motor control hubs and attachment masses, full specifications are listed in Table 8.6. As a way to counter the torque of the drill to ensure the probe stays fixed in place, leaf springs are added on top of the probe as these are deemed one of the most effective anti-torque mechanisms for suspended drills [75]. Finally, the most important ice traversal system characteristics are listed in Table 8.7. The traversal speed was calculated with experimental data from [15], using a penetration energy of 0.095×10^6 Wh/m^3. As can be seen in Section 11.4, the heated drill mechanism and its workings currently don't have a high technology readiness, therefore values listed here are prone to changes as the design is developed further. It should also be noted that currently, materials are chosen to minimize corrosion, wear, and the associated fatigue effects. The exact fatigue effects these cause will be investigated and addressed during mechanism development.

Table 8.7: Ice traversal system characteristics

Characteristics	Value	Unit
Drill bit diameter	0.28	[m]
Drill power allocation	500	[W]
Thermal power allocation	3000	[W]
Conduction efficiency	0.95	[-]
Traversal system length	0.5	[m]
Traversal system mass	33.5	[kg]
Traversal speed	0.495	[m/s]

Table 8.6: Drill motor Specifications

Specifications	Value	Unit
Diameter	0.2	[m]
Length	0.25	[m]
Mass	10	[kg]
Optimal performance power	500	[W]
Voltage	28	[V]

8.4. Hydrodynamics Subsystem

Once the probe has penetrated the icy crust of Europa, it will need to be able to stay in the subsurface ocean for some time to take scientific measurements. To do this, the probe shall be kept from sinking into the depths, to stay within communications range and prevent failure due to the large hydrostatic pressures of the subsurface ocean. In addition, the interface between the ocean and the ice shell is expected to be a so-called mushy layer rather than a sudden transition from ice to water and could take up to 5% of the ice shell thickness [76]. As a result, the probe cannot simply stick out of the solid ice into the liquid water and has to find a way to navigate this layer.

8.4.1. Hydrodynamics Subsystem Requirements

The subsystem requirements for the hydrodynamics subsystem are listed below:

- **AD-SCI-02-PR-01-HYD-01**: The hydrodynamics subsystem shall allow diving to a 1-kilometre depth in the subsurface ocean below the ice layer
- **AD-SCI-02-PR-01-HYD-02**: The hydrodynamics subsystem shall allow movement in at least one direction.
- **AD-SCI-02-PR-01-HYD-03**: The hydrodynamics subsystem shall prevent sinking upon entering the ocean.
- **AD-PERF-01-PR-02-HYD-04**: The hydrodynamics subsystem shall prevent sinking for at least one year.
- **AD-PERF-05-PR-01-HYD-05**: The hydrodynamics subsystem shall ensure the probe stays within communications range.

8.4.2. Concept analysis and Trade-off

To comply with these requirements, four different options are considered which are listed below. This subsystem especially deals with the navigation of an ocean, which is not as an unfamiliar environment as is usual for space missions. As a result, the concepts can be mostly inspired by technologies on Earth.

The first concept is inspired by submarines, having close to neutral buoyancy and allowing control over the vertical position by regulating the amount of water in ballast tanks. Furthermore, the probe is propelled by a single thruster utilising the same motor as the drill and uses rudder fins for steering. However, due to the thin

---

[3]From https://www.amazon.com.au/s?k=electric+motor+500+watt&crid=1XF66KL03HDQ7&sprefix=electric+motor+500+watt%2Caps%2C225&ref=nb_sb_noss_2, accessed on 19/06/2024.

diameter required for the traversal subsystem and the limited length due to launcher constraints, the displaced volume of water due to the probe created only a quarter of the required buoyancy force. A lightweight inflatable sphere with a diameter of around 1 meter would be required for neutral buoyancy, but the pressures of the ocean are too large for this inflatable to be feasible. In addition, since there is no air on Europa, changing the ballast can be performed by boiling water and venting most of the water vapour to reduce the density. The power required for boiling this water is very high and would take hours even when using kilowatts of power.

The second concept is to anchor the probe in the solid ice just before reaching the mushy layer and lowering the probe down into the ocean via a relatively short cable. Designing for 1 km of diving depth and a mushy layer of 1.8 km (5% of 30 km with a 20% margin on top), a total cable length of 2.8 km is required. To prevent shock loads and allow vertical control, a magnetic brake and a winch system is used, only requiring a few 100 watts based on Earth examples. This system would have a mass between 50 and 100 kg.

The third concept is inspired by quadcopter aircraft, using four underwater thrusters to keep the probe from sinking and for control in six degrees of freedom. This would work well in terms of mass, only adding around 50 kg, and having nearly no effect on the volume. This concept would however require a large amount of power to provide the required thrust. Due to the low efficiency of underwater electric thrusters, the required power would be in the order of a few kilowatts.

Lastly, instead of using four thrusters to provide a force equal to the weight of the probe, inspiration is taken from aircraft to use lifting surfaces and a single propelling thruster by again reusing the motor of the drill. Since the density of water is large, a minimum constant velocity of only 2 m/s is required to generate enough lift using hydrofoils to keep the probe "afloat". Although the drag force is quite large even at these speeds, the slender shape of the probe is already quite efficient, reducing the power required to only a few 100 watts. By using titanium foldable wings, only a slight increase in structural mass and diameter is needed for this concept. The main drawback is however the amount of moving parts that could fail, causing the probe to sink.

A trade-off is then performed on these options based on six different criteria with weights that sum to 100%: The mass is given a weight of 20% since the mass of the probe should be minimized; The performance risk is given a weight of 30% since failure of the subsystem results in no data being gathered; The required power is given a weight of 15% since the probe has a limited power budget; The science potential of the mission is dependent on the ability to move underwater, and is given a weight of 15%; The volume is given a weight of 10% since an increase in diameter causes an increase in the drilling time and thus radiation dose, and an increase in length results in an increase in structural mass; The end-of-life options are given a weight of 10% since the amount of radioactive material leaked to the ocean should be minimized.

The concepts are scored on the criteria on a scale of 0 to 3, ranging from unacceptable (0) to excellent (3), based on predetermined scoring ranges which can be found in Table 8.8. The trade-off summary table is found in Table 8.9, ordered based on the total scores. The conclusion of the trade-off is that while the aircraft design allows more movement and has a lower mass, the tether & anchor design has a lower risk, volume and better end-of-life prospects. The other two options were infeasible due to power and structural constraints.

Table 8.8: Scoring ranges for each of the criteria

Scoring criteria	Performance risk	Mass	Power	Science potential	Volume	End-of-life
Excellent (3)	No moving elements, one failure point	0-25 kg	0-200W	Can move and stay stationary in both depth and lateral directions	No diameter increase, 0-1m length increase	Will never sink
Nominal (2)	Moving elements, Multiple failure points	25-100 kg	200-500 W	Can move in both depth and lateral directions	No diameter increase, 0-2m length increase	Sinks after failure, not after power loss
Acceptable (1)	Moving elements, Multiple failure points	100-200 kg	0.5-1 kW	Can move and stay stationary in only one direction	Diameter increase, or 2+ m length increase	Sinks after failure or power loss
Unacceptable (0)	Unfeasible with current materials	200+ kg	1-10 kW	Cannot move	Diameter increase, and 2+ m length increase	Will always sink

Table 8.9: Scoring ranges for each of the criteria

Concepts	Performance risk	Mass	Power	Science potential	Volume	End-of-life	Total
Weights	*30*	*20*	*15*	*15*	*10*	*10*	*100*
Tether & Anchor	Risk cable unable to withstand forces (3)	Around 50-100 kg (2)	O(200-500W) (2)	Multiple depths, can stay stationary at locations (1)	1-1.5 m length, little to no diameter (2)	Hang onto cable until anchor fails (2)	215
Aircraft	Deployment failure, not enough lift/thrust, (drill) engine fatigue (1)	Wings 20 kg, but structure becomes a bit heavier as well (3)	O(200-500W) (2)	Multiple lateral locations and depths, needs to move constantly (2)	Little to no length, 0-5 cm diameter (1)	Sink after power loss (1)	170
Quadcopter	Engine failure (2)	Around 50 kg (2)	O(1-10 kW) (0)	Multiple lateral locations and depths, can stay stationary at locations (3)	0-1 m length, little to no diameter (3)	Sink after power loss (1)	155
Submarine	Pressures too high for feasible balloon (0)	200+ kg due to high pressures (0)	O(1-10 kW) (0)	Multiple lateral locations and depths, can stay stationary at locations (3)	2+ m length, little to no diameter (1)	Float until balloon fails (2)	75

8.4.3. Tether & Anchor detail design

Three main elements are to be designed: The tether, the anchor and the winch-controlled spool. The system is designed for the mushy layer of 1.5 km, and a diving depth of 1 km, for a total descent of 2.5 km.

In designing the cable, an additional margin was taken on top of this descent distance of 20%, giving a total cable length of 2.8 km. Although the buoyancy of the probe will lighten the load to be carried by the cable, the cable is designed for the entire weight of the probe with a load factor of 1.5. While shear forces could be induced in the cable by differential movement of ice layers due to faults in the ice, these events are expected to occur mostly around the surface [77], not posing a significant threat to the cable around the ice-ocean interface. To account for some shear due to currents, it is assumed the maximum shear force does not exceed the weight of the probe.

Titanium is chosen for the cable for its high corrosion resistance and high relative strength, reducing the required diameter and thus spool size on the probe. Next to the cable diameter, the spool sizing depends on the method used to wind the cable onto the spool. Using orthocyclic winding, a fill factor of 90% is obtainable [78], but to have some margin for error the fill factor is set to 85%. Using this factor, the required spool area can be determined, and by setting the inner and outer diameter of the barrel based on the probe dimensions, the required spool length is determined using Equation 8.1. Since the spool does not need to carry any loads, a lightweight material can be used. The polymer PEEK is chosen for its low density with high chemical and thermal resistance.[4]

$$L_{spool} = \frac{L_{cable}(D_{cable})^2}{FF_{ortho}(D_{o_{spool}}^2 - D_{i_{spool}}^2)} \tag{8.1}$$

The winch assembly consists of three main elements, the geared motor providing the torque, the pulley inducing the motor torque on the cable and ensuring no slipping by locking its movement, and a magnetic brake to prevent shock loads and limit the velocity at which the cable can move downwards. Based on commercially available 24V DC winch motors, a 200 W motor can provide enough pulling force to lift and lower the probe at a velocity of around 0.2 m/s. The mass estimate for the entire assembly is around 10 kg.

---

[4]From `https://www.curbellplastics.com/materials/plastics/peek/`, accessed on 10/06/2024.

The anchor should be able to carry the weight of the probe and the anchor itself. It is crucial to design the anchor with adequate margins to ensure that end-of-life procedures can be executed properly.

The anchor will be set in place by four beams, which will be pressed into the ice using spring force, these springs will provide 3.64 N.[5] The beams come equipped with heat tips to melt into the ice. This should not take long and the surface area of the beams will be very small (1.5 cmx3 cm). The main stress is produced by the bending stress put upon the beams. The beams were designed to hold the probe up with two of the four beams properly deployed. It was also made sure that the hole for the wire that will heat the tip was accounted for by taking a stress concentration of 3 [79]. An additional safety factor of 1.5 was taken to make sure it would function if properly deployed.

The titanium anchor has a skin thickness of 5 mm to shield the inside from potential harmful factors. It has a diameter of 0.25 m and a height of 0.28 m to fit an acoustic relay, RF relay, CDH, and a 11.25 kg fuel cell [80]. To make sure it will not fail under pressure, the anchor will be filled with resin. The total weight of the anchor will be 23.16 kg.

An overview of the mass breakdown of the hydrodynamics assembly is found in Table 8.10

Table 8.10: Mass overview of the hydrodynamics subsystem on the probe

Component	Mass(kg)
Cable Mass	21.92
Winch Mass	10
Spool ass	0.92
Anchor mass	23.16
Total mass (w/o Margin)	55.99
Total mass (inc. Margin)	67.19

8.5. Guidance, Navigation & Control Subsystem

While traversing through the ice, the probe must determine its direction and speed. Additionally, it is crucial for the probe to be able to detect obstacles in its path to avoid navigating blindly. If any obstruction is detected, the probe must be able to identify it and manoeuvre around it.

8.5.1. GNC Subsystem Requirements

The subsystem requirements of the probe GNC subsystem are listed below:

- **AD-PERF-03-PR-01-GNC-01**: The GNC subsystem shall be able to perform inertial measurements.
- **AD-PERF-03-PR-01-GNC-02**: The GNC subsystem shall be able to detect obstacles that are 20cm or bigger in diameter.
- **AD-PERF-03-PR-01-GNC-03**: The GNC subsystem shall be able to change the attitude of the probe.

8.5.2. Probe Navigation

To perform inertial measurements the LN-200HPS[6] IMU will be used on the probe. Its specifications are shown in Table 8.11. This model was selected for its low mass and proven flight heritage, having been used on the Spirit, Opportunity, Curiosity, and Perseverance rovers.

The probe has a high chance of encountering cavities, especially in the upper ice layer [81], these and other obstacles pose a significant risk to mission success. In order to detect these the probe will need an Ice Penetrating Radar (IPR). An IPR functions by sending radio waves through a medium and then waiting for reflected waves, with this obstacles can be detected. Placing one of these behind the drill head or even behind the RTGs would probably pose problems with receiving signals as these would interact with or bounce off the metal parts. This causes a need for a custom radar design that is integrated into the drill bit. It is suggested that the spokes are used as receivers, while the transmitter is integrated into the tip, see Figure 8.5.

---

[5]From `https://docs.rs-online.com/b860/0900766b8150d614.pdf`, accessed at 12/06/2024.
[6]From `https://cdn.northropgrumman.com/-/media/wp-content/uploads/LN-200S-Inertial-Measurement-Unit-IMU-datasheet.pdf?v=1.0.0`, accessed on 15/06/2024.

Table 8.11: Product specifications of the LN-200HPS[6]

Parameter	Value	Unit
Mass	0.748	kg
Dimensions	⌀88.9 x 85.1	mm
Power	12	W
Radiation Resistance	>25	krad
Rotational Measurement Range (max)	1000	deg/s
Linear Measurement Range (max)	40	g
Operating Temperature	-54 to +71	°C
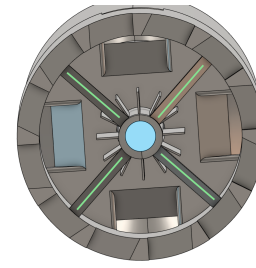
Figure 8.5: Proposed radar infrastructure, receiver antennas are shown in green, transmitter in blue

The spokes would be used as 'whip' antennas, of which the quarter-wave whip antennas are the most popular and efficient versions.[7] Measuring the spokes gives a maximum length of 8 cm or 0.08 m each, leading to a wavelength of 0.32 m. Alternatively, the spokes could be connected through the middle and form two 0.21 m long antennas. From these values and the ice wave velocity [82], the receiver frequencies can be calculated, both options are listed in Table 8.12.

Table 8.12: IPR configuration calculations

Characteristic	Separate spoke antennas	Connected spokes antennas	Unit
Quantity	4	2	[-]
Antenna length	0.08	0.21	[m]
Maximum wavelength	0.32	0.84	[m]
Ice wave speed	2.29×10^8	2.29×10^8	[m/s]
Minimum frequency	716	273	[MHz]

These frequencies are part of the Very High Frequency (VHF) and Ultra High Frequency (UHF) spectra, which are often used in radioglaciology [83]. These findings suggest that the proposed antenna system would be feasible. Additionally, small UHF and VHF transmitters are already available on the market today.[8] Using more individual antennas might aid in locating obstacles while using wider antennas might increase penetration depths (longer waves).[9] IPR is known to reach penetration depths of more than a kilometre [83], though those ranges are probably not attainable for small systems. Considering the low speed of traversal of the probe, a maximum penetration depth of 100 m would probably be sufficient for this mission. Exact penetration depths and locating capabilities will have to be investigated in further design phases. Finally, the drill would need to stop for some time during measurements, leaving plenty of power supply for the IPR.

8.5.3. Probe Control
Should the probe want to steer around an obstacle it will do this by heating specific areas of the probe and attaining the desired angle before continuing the traversal process. The orientation time is calculated by finding the volume of ice that needs to be melted and finding the area needed for this. Preliminary calculations show that attaining an angle of 20 degrees would take 28.5 h.

8.6. Thermal Control Subsystem
In this section, The probe's TCS will be sized. As the probe needs to survive the cold temperatures of the ice, two TCS solutions were sized to address this. The first solution was using insulation around the probe to isolate it from the cold environment. The second solution was to use a pumped fluid loop to deliver heat to the drill and to distribute the heat throughout the probe and to the sides of the probe. For each solution, the theory will be introduced and then the solution will be sized accordingly

8.6.1. TCS Requirements
The subsystem requirements of the Thermal Control Subsystem.

---

[7]From `https://www.enocean.com/wp-content/uploads/application-notes/AN102_ANTENNA_DESIGN_2019.pdf`, accessed on 18/06/2024.

[8]From `https://marshallradio.com/eu/product/rt-uhf-transmitter-worldwide/`, accessed on 18/06/2024.

[9]From `http://everything.explained.today/Radar_for_Europa_Assessment_and_Sounding%3A_Ocean_to_Near-surface/`, accessed on 18/06/2024.

- **AD-PERF-01-PR-02-TCS-01:** The TCS shall be able to maintain the temperature within the allowable range of all onboard components.

- **AD-PERF-02-PR-01-TCS-01:** The TCS shall be able to deliver 3000 W to the heated drill.

8.6.2. Insulation

In this subsection, a background on the theory of thermal conduction from Yunus Cengel's book [84] will be given and this will afterwards allow the shielding to be sized according to what is needed.

Background

Unlike the vacuum of space, where radiation is the dominating heat transfer method, conduction will be the dominating heat transfer method for the probe drilling through Europa's subsurface ocean. Therefore, Fourier's law of heat conduction has to be used given in Equation 8.2. Where $\dot{Q}_{cond}$ is the heat conduction flow rate with a temperature gradient of $\frac{\partial T}{\partial x}$ through the surface of area A with thermal conductivity k. This is the one-dimensional case of heat conduction. In the case of the probe, it can be idealised as a cylinder with multiple layers. The heat conduction through a cylinder is given in Equation 8.3, where Figure 8.6 describes each parameter.
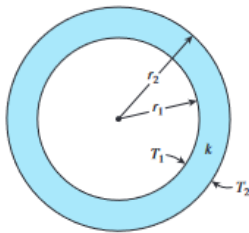
$$\dot{Q}_{cond} = -kA\frac{\partial T}{\partial x} \quad (8.2) \qquad \dot{Q}_{cond,cyl} = -2\pi Lk\frac{T_1 - T_2}{ln\left(\frac{r_2}{r_1}\right)} \quad (8.3)$$

Figure 8.6: Heat Conduction through a cylinder

Another useful thing that can be done with heat transfer is converting the model into a thermal resistance network which is analogous to how the flow of electricity is modelled. The equation for heat conduction turns into Equation 8.4. Where R is the resistance of the material to thermal change. For the case of the heat conduction through the cylinder, the thermal resistance of that is given in Equation 8.5. This is useful because multiple layers could be stacked on top of each other and their resistance will be in series with each other thus making it simple to calculate the total thermal resistance of the model given different layers of thickness.

$$\dot{Q}_{cond} = \frac{T_1 - T_2}{R_{total}} \qquad (8.4) \qquad\qquad R_{cyl} = \frac{ln\left(\frac{r_2}{r_1}\right)}{2\pi Lk} \qquad (8.5)$$

Assumptions

The heat conduction is assumed to be the only method of heat transfer. It is also assumed that the heat conduction only happens radially through the probe. The ice close to the probe is taken to be close to the melting temperature of the ice. This assumption was made because modelling the conduction through the ice gave extreme values of thickness which reflects the fact that the model has a low fidelity and it would be required to increase the fidelity of the model to be able to take into account accurately. Moreover, it is assumed the ice around the probe will have time to heat up to that temperature while the probe is still attached to the lander and being lowered to the ice. Nevertheless, this model comes closer to reality because when the probe goes deeper the temperature of the ice increases up until it matches this assumption. The temperature of the insulator could be taken as equal to the temperature of the ice as it can be assumed those two surfaces are in equilibrium.

Insulation Sizing

If the insulation is modelled as two layers of a hollow cylinder over each other the resulting thermal resistance network of the probe is shown in Figure 8.7.
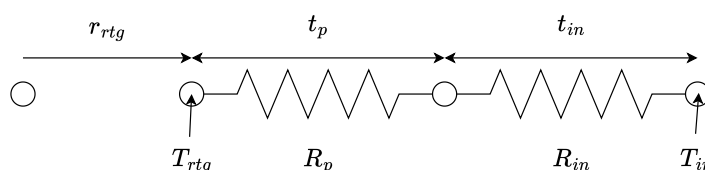

Figure 8.7: Thermal Resistance Network of the Probe

Where r_rtg is the radius of the RTG, t_p and t_in is the structural thickness of the probe and insulator respectively, R_p and R_{in} is the thermal resistance of the probe structure and insulator respectively and finally T_{in} and T_{rtg} are the temperatures of the insulator and cold end of the RTG respectively. The total resistance of this model is given in Equation 8.6.

Here, k_p and k_{in} are the conductivity of the Ti-6Al-4V and insulator respectively. Plugging Equation 8.6 into Equation 8.4 results in Equation 8.7.

$$R_{Total} = \frac{ln\left(\frac{r_{rtg}+t_p}{r_{rtg}}\right)}{2\pi L k_p} + \frac{ln\left(\frac{r_{rtg}+t_p+t_{in}}{r_{rtg}+t_p}\right)}{2\pi L k_{in}} \quad (8.6) \qquad \dot{Q}_{rtg} = \frac{T_{rtg} - T_{in}}{\frac{ln\left(\frac{r_{rtg}+t_p}{r_{rtg}}\right)}{2\pi L k_p} + \frac{ln\left(\frac{r_{rtg}+t_p+t_{in}}{r_{rtg}+t_p}\right)}{2\pi L k_{in}}} \quad (8.7)$$

The heat flow is assumed to equal the heat generated by the RTG. The insulator used is silica aerogel, an insulation that has a heritage in space and was used on JPL's Rover Sojourner to ensure that the electronics survived the cold Martian night [38].

All the variables of Equation 8.5 are known except t_{in}. Plugging in the known variables in Table 8.13 and solving Equation 8.7 results in the output in Table 8.13. If the insulation is wrapped around the probe, it will result in a total mass shown in Table 8.14.

Table 8.13: Input and Output of the Probe Thermal Model

Parameter	Value	Unit	Reference
Input Variables			
Radius of RTG	0.2	m	[44]
Thickness of the probe	16	mm	-
Length of the probe	4.5	m	-
Ti-6Al-4V Conductivity	6.7[10]	W/m^{1}K^1	-
Aerogel Conductivity	0.05	W/m^{1}K^1	[85]
RTG Cold End Temperature	473	K	[44]
Insulator Temperature	273.2	K	[86]
Q$_{rtg}$	7150	W	[44]
Output Variable			
t_{in}	4.4	mm	-

Table 8.14: Density and Mass of the Insulation around the Probe

Parameter	Value	Unit
Density	225	kg/m^3
mass	3.40	kg

8.6.3. Pump Fluid Loop

In this subsection, a background on the theory of thermal convection and pumps will be given and this will afterwards allow the pump fluid looped to be sized according to what is needed.

Background

In pumped fluid loops, the main components are heat exchangers, a pump and the pipes carrying the fluid. As the water is a fluid the main mechanism that is used for heat transfer is convection. This can be represented by Newton's law of cooling shown in Equation 8.8, where h is the heat transfer coefficient, A is the surface area of convection, and T_s and T_∞ are the surface and fluid temperatures, respectively. Equation 8.8 will be used to calculate the area required to exchange the heat to the drill and to the sides of the probe.

The next important relation to size the pump from Gilmore's Thermal Control Handbook [38] is Equation 8.9, where P_p is the power of the pump, Δp is the pressure drop through the pipes, $\dot{m}$ is the mass flow rate of the water through the pipe, ρ is the density of water, and finally η_p is the efficiency of the pump. The pressure drop can then be calculated using Equation 8.10.

$$\dot{Q}_{conv} = hA(T_s - T_\infty) \quad (8.8) \qquad P_p = \Delta p \frac{\dot{m}}{\rho} \frac{1}{\eta_p} \quad (8.9) \qquad \Delta p = \frac{\rho V^2}{2} \frac{0.079}{Re^{0.25}} \frac{L_p}{D_p} \quad (8.10)$$

where V is the speed of the water, f relates to the Reynolds number of the probe, L_p is the length of the pipe and D_p is the diameter of the pipe. $\dot{m}$ and V can be calculated using Equation 8.11 and Equation 8.12, where $\dot{Q}_{required}$ is the required heat flow rate at a heat exchanger. In this case, there will be different $\dot{m}$ depending

---

[10]From `https://www.matweb.com/search/DataSheet.aspx?MatGUID=b350a789eda946c6b86a3e4d3c577b39&ckck=1`, accessed on 19/06/2024

on which heat flow is limiting the design. A_{cross} is the cross-section of the pipe. The pipe length is restricted by the probe length and the length needed around the contact area of the heat exchangers.

Pump Fluid Loop Sizing
For the pump fluid loop sizing, the equations in the previous section are used to size the heat exchangers and the pump of the fluid loop. Given the requirement **AD-PERF-02-PR-01-TCS-01** the heat exchangers could be sized. It is also assumed that while the water is flowing through the loop it will lose 3000 W to the surrounding. Taking into account the power used for the drill, the overall heat left for the sides would be 4754 W. This makes it possible for the heat exchangers to be sized as shown in Table 8.15.

Table 8.15: Pipe length needed for the Pump Fluid Loop System

Parameter	Value	Unit
Pipe Length Around RTG	3.45	m
Pipe Length Around drill	3.18	m
Pipe Length Around the Sides	5.04	m
Pipe Length for Transport	6	m
Total Pipe Length Needed	**17.68**	**m**

$$\dot{m} = \frac{\dot{Q}_{required}}{c_p(T_s - T_\infty)} \quad (8.11) \qquad V = \frac{\dot{m}}{\rho A_{cross}} \quad (8.12)$$

Using the total pipe length it is possible to characterise the needed pump that is needed which is shown in Table 8.16. The pump suitable for this is the NLR pump f412 [11] which has been used in space, therefore, it has heritage making it a reliable option.

The total mass of the Thermal Control System is found in Table 8.17.

Table 8.16: Pump specification

Parameter	Value	Unit
Δp	84127	Pa
Required Power	3.82	W
Mass Flow Rate	0.023	kg/s
Volumetric Flow Rate	**0.38**	**ml/min**

Table 8.17: Total TCS Mass of the Probe

Parameter	Value	Unit
Mass of Insulator	3.40	kg
Mass of Pump Fluid Loop System	1.17	kg
Total Mass	**4.57**	**kg**

8.7. Communication Subsystem

This section details the design of the communication system for the AlienDive mission probe. The probe needs to communicate with the lander traversing two media types: ice and water. First, the through-ice communication system is discussed, including a link budget analysis. Next, the through-water communication system is elaborated on.

8.7.1. Communication Subsystem Requirements

AD-PERF-05-PR-01-COM-10: The probe communication system shall incorporate RF relay transceivers throughout the ice crust.

AD-PERF-05-PR-01-COM-11: The probe communication system shall incorporate RF relay transceivers communicating with the lander in the UHF band.

AD-PERF-05-PR-01-COM-12: The probe communication system shall incorporate an acoustic modem communicating with the RF relay transceivers.

AD-PERF-05-PR-01-COM-13: The probe communication system shall incorporate an acoustic modem able to withstand pressures up to 38.3 MPa.

8.7.2. Through-Ice Communication Component Selection

Communication through the ice between the probe and the lander is a significant challenge as information needs to travel across multiple kilometres of ice. Direct RF contact between the lander and the probe is deemed infeasible without excessive power requirements due to ice attenuation [72]. Therefore, RF relay transceiver modules need to be placed at certain distance intervals throughout the ice as the probe descends to ensure a sufficient energy per bit to noise spectral density ratio. Before a link budget analysis can be performed

---

[11]From `https://www.nlr.nl/downloads/f412-advanced-satellite-thermal-control---pump.pdf`, accessed on 19/06/2024

to determine the distance interval and the number of RF relay modules necessary for viable communication, commercially available communication components for the RF relay modules are selected first. Recent studies on using RF relays to communicate through the ice crust of Europa have focussed on communicating in the UHF band. The UHF band provides an optimal balance between the desired performance of the antenna's radiation pattern (which benefits from higher frequencies) and the need to minimize attenuation through ice (which benefits from lower frequencies) [87]. Therefore, components designed for communication in the UHF band are selected for the RF relay modules.

Transceiver

The selected transceiver is the PULSAR-UTRX by AAC Clyde Space. This transceiver operates in the UHF band, is capable of AFSK and GMSK modulation, has a maximum data rate of 9600 bps and features a lightweight and compact design, making it ideal when taking into account dimensional constraints for the RF relay modules.[12]

Diplexer

A commercially available UHF band diplexer for space applications is not available. Still, simultaneous transmission and reception using the same antenna is desired. Therefore, the UHF diplexer present in the RF relay modules needs to be designed in-house. For now, it is assumed the UHF diplexer will have the same characteristics as the WiRan X-Band Diplexer selected in Subsection 7.7.3. Two UHF diplexers are required in the RF relay modules to facilitate both the transmission and reception of signals between the lander and the probe.

Antenna

The selected antenna is the UHF Antenna III by EnduroSat. This antenna features a compact and lightweight design, making it ideal for the dimensional constraints of the RF relay modules. The patch antenna provides a gain of 0 dB. Two patch antennas are required in the RF relay modules to facilitate both the transmission and reception of signals between the lander and the probe.[13]

Processor

The processor selected is the CP400.85 Payload Processor Module by AAC Clyde Space. This processor features high computing power and low overall power consumption in a compact design.[14] The processor module is mainly included for redundancy, as data storage and processing is done in the onboard computer of both the lander and the probe.

As the lander needs to communicate with the RF relay modules in the UHF band, the lander is incorporated with a PULSAR-UTRX, a UHF diplexer and a UHF Antenna III, as displayed in Table 7.22 and Figure 7.12.

Table 8.18 shows the mass and power consumption of the selected components for the communication system of the RF relay modules of the AlienDive mission.

Table 8.18: Mass and power overview of relay communication components

Component	Name (Company)	Units	Mass (Total) [kg]	Power input [W]
Transceiver	PULSAR-UTRX (AAC Clyde Space)	1	0.1	5.1
Diplexer	To be designed in-house	2	0.115 (0.23)	-
Antenna	UHF Antenna III (EnduroSat)	2	0.085 (0.17)	-
Processor	CP400.85 (AAC Clyde Space)	1	0.007	1
Coax cables	-	-	0.0103	-
Total	-	-	**0.5173**	**6.1**

The relay module closest to the subsurface ocean will be in direct contact with the probe. Therefore, this relay includes communication components necessary for through-water communication, elaborated on in Subsection 8.7.6. Table 8.19 shows the mass and power consumption of the selected components for the communication system of the so-called hybrid RF/acoustic relay.

---

[12]From `https://satsearch.co/products/aac-clyde-pulsar-utrx-uhf-uhf-transceiver`, accessed on 17/06/2024.

[13]From `https://satsearch.co/products/endurosat-uhf-antenna-iii`, accessed on 17/06/2024.

[14]From `https://satsearch.co/products/aac-clyde-cp400-85-payload-processor-module`, accessed on 17/06/2024.

Table 8.19: Mass and power overview of the hybrid RF/acoustic relay communication components

Component	Name (Company)	Units	Mass (Total) [kg]	Power input [W]
Transceiver	PULSAR-UTRX (AAC Clyde Space)	1	0.1	5.1
Diplexer	To be designed in-house	1	0.115	-
Antenna	UHF Antenna III (EnduroSat)	1	0.085	-
Processor	CP400.85 (AAC Clyde Space)	1	0.007	1
Coax cables	-	-	0.0639	-
Acoustic modem	ATM-903 (Teledyne Benthos)	1	2.83	20
Total	-	-	**3.2009**	**26.1**

8.7.3. Through-Ice Communication Link Budget Analysis

To determine the distance interval and number of relays needed for viable communication between the lander and probe, a link budget analysis is conducted using Equation 8.13. This equation is the same as Equation 7.16, except for the inclusion of an ice attenuation of 16 dB/km or an ice loss, L_{ice}, of 1.0037 per meter [72].

$$\frac{E_b}{N_o} = \frac{P_t G_t G_r}{(4\pi d/\lambda)^2 k T_s R L_{ice}{}^d} \sin^2(\beta) \tag{8.13}$$

Table 8.20 shows the outcome of the link budget analysis. 9 relay transceiver modules are necessary for viable communication over a 30 km ice crust, placed at a distance interval of 3614.3 m. Furthermore, in case one relay fails, the maximum data rate of the remaining relays drops to 4.8 kbps, which is half of the original maximum. While this reduces the data transmission capacity, communication is maintained despite the relay failure. Therefore, adding redundant relays is not considered worthwhile due to the additional mass and length they would add to the probe. Lastly, in case data provided by Europa Clipper indicates a different ice crust thickness, the number of relays can be reconsidered.

Table 8.20: Link budget analysis for the RF relay transceiver modules

Parameter	$\frac{Eb}{No}$	P_t	G_t	G_r	λ	T_s	R	L_{ice}	β	d	Number of Relays
Value	11.298	2	1	1	0.7495	600	9600	1.0037	90	3614.3	9
Unit	-	W	-	-	m	K	bps	m^{-1}	deg	m	-

The required $\frac{Eb}{No}$ value has been assumed to be the same as the downlink $\frac{Eb}{No}$ requirement for the lander, explained in Subsection 7.7.2. The transmit power, transmitter gain, receiver gain and maximum data rate for the relay transceivers can be found in Subsection 8.7.2. The (conservative) value for the wavelength is 0.7495 m, constrained by the components. The system noise temperature was taken from a preliminary RF relay transceiver module design by the Jet Propulsion Laboratory (JPL) [88]. The phase modulation index is assumed to be 90 °.

8.7.4. Relay design

The relays are critical for the mission to succeed, thus they should be designed with caution. The relays were designed with the same method as the anchor. Four spring-loaded beams with heated tips can carry the weight of the relay itself. Two of the beams should be able to hold the relay in case of beam deployment failure. The beams will have a dimension of 20 mmx5 mmx1.5 mm (LxHxW). The relay itself will have a skin thickness of 2 mm, a height of 80 mm, and a diameter of 250 mm. The relay shells will be made out of titanium due to its high stress-bearing capabilities and corrosion resistance. Next to the communication parts, the relay will include a 3.06 kg fuel cell [80], this fuel cell is designed with a 1.4 factor due to how crucial the relays are for the AlienDive mission. Just like the anchor they will be filled with resin, which will result in a total relay mass of 5.26kg per piece.

8.7.5. Architecture Block Diagram of the Communication System of the RF Relays

Figure 8.8a and Figure 8.8b show the architecture block diagrams of the communication system of the nominal RF relay modules and the hybrid RF/acoustic relay module. Again, the hybrid RF/acoustic relay module contains components needed for communication with the probe through the subsurface ocean, elaborated on in Subsection 8.7.6.
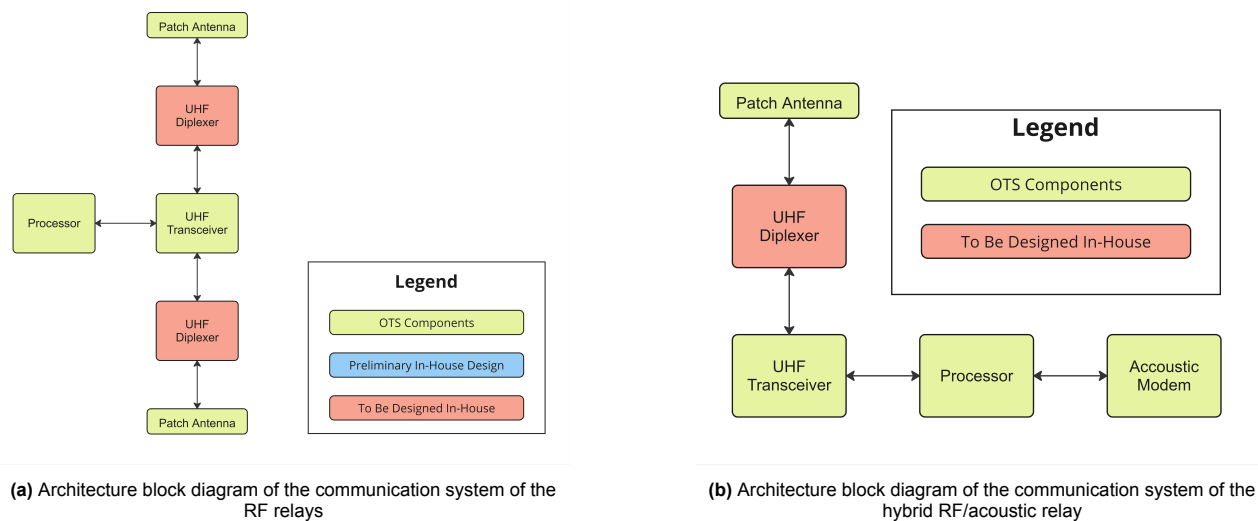

(a) Architecture block diagram of the communication system of the RF relays

(b) Architecture block diagram of the communication system of the hybrid RF/acoustic relay

Figure 8.8: Comparison of architecture block diagrams

8.7.6. Through-Water Communication

While RF signals get highly attenuated in water, only making viable communication possible over a distance of up to 100 m, acoustic signals can travel distances of over 1000 km through water [89]. Therefore, the probe and the relay module closest to the subsurface ocean must be incorporated with an acoustic communication system. Commercially available acoustic communication systems exist; the selected acoustic modem is the ATM-903 by Teledyne Benthos. This modem features a compact design, has proven its reliability and capability in existing Autonomous Underwater Vehicles and has ample range for communication across 2.8 km of water as elaborated on in Subsection 8.4.2. It is important to note that if a mushy layer exists between the subsurface ocean and the ice crust, it is assumed that acoustic signals can propagate through this layer effectively. The main features of this acoustic modem are summarized in Table 8.21.[15]

Table 8.21: Main features of the ATM-903 acoustic modem

Parameter	Value	Unit
Mass	2.83	kg
Power input	20	W
Range	6000	m
Max. data rate	15.36	kbps
Operating depth	6000	m

The operating depth of 6000 m is particularly important. As calculated in Subsection 8.9.3, the probe and its components need to withstand pressures up to 38.3 MPa. The sea pressure on Earth at 6000 m is 60.23 MPa.[16] The ATM-903 acoustic modem must reliably withstand the high pressures found in Europa's subsurface ocean.

8.8. Commmand and Data Handling Subsystem

This section details the design of the command and data handling system for the AlienDive mission probe. It starts with a presentation of the data handling block diagram, whereafter the main features of the selected onboard computer are provided.

---

[15]From `https://www.teledynemarine.com/en-us/products/SiteAssets/Benthos_Modem_PSG.pdf`, accessed on 17/06/2024.

[16]From `https://bluerobotics.com/learn/pressure-depth-calculator/`, accessed on 18/06/2024.

8.8.1. CDH Subsystem Requirements

The subsystem requirements of the CDH subsystem are listed below:

AD-PERF-05-PR-01-CDH-09: The probe CDH subsystem shall be able to acquire commands, housekeeping data and scientific data.

AD-PERF-05-PR-01-CDH-10: The probe CDH subsystem shall be able to process data.

AD-PERF-05-PR-01-CDH-10: The probe CDH subsystem shall be able to analyze data.

AD-PERF-05-PR-01-CDH-11: The probe CDH subsystem shall be able to check data for errors.

AD-PERF-05-PR-01-CDH-12: The probe CDH subsystem shall be able to compress data.

AD-PERF-05-PR-01-CDH-13: The probe CDH subsystem shall be able to store data.

AD-PERF-05-PR-01-CDH-14: The probe CDH subsystem shall be able to encode data.

AD-PERF-05-PR-01-CDH-15: The probe CDH subsystem shall be able to encrypt data.

8.8.2. Command and Data Handling Functions

Figure 8.9 presents the data handling block diagram of the probe of the AlienDive mission, including through-put data rates. Through-put data rates include the maximum uplink and downlink data rates as constrained by the RF relays, discussed in Subsection 8.7.2, the average payload data rate of 7.9 kbps, determined by the scientific instruments of the probe Section 4.2, maximum command data rates assumed to be equal to those of the Juno spacecraft [55], assumed to be distributed evenly across the subsystems and housekeeping data rates assumed to be 0.16 kbps for all subsystems (summing up to 10 % of the average payload data rate). The amount of data gathered, housekeeping and scientific, is discussed in Section 5.1. Furthermore, this section details the transmission time needed to relay the gathered information to the lander.
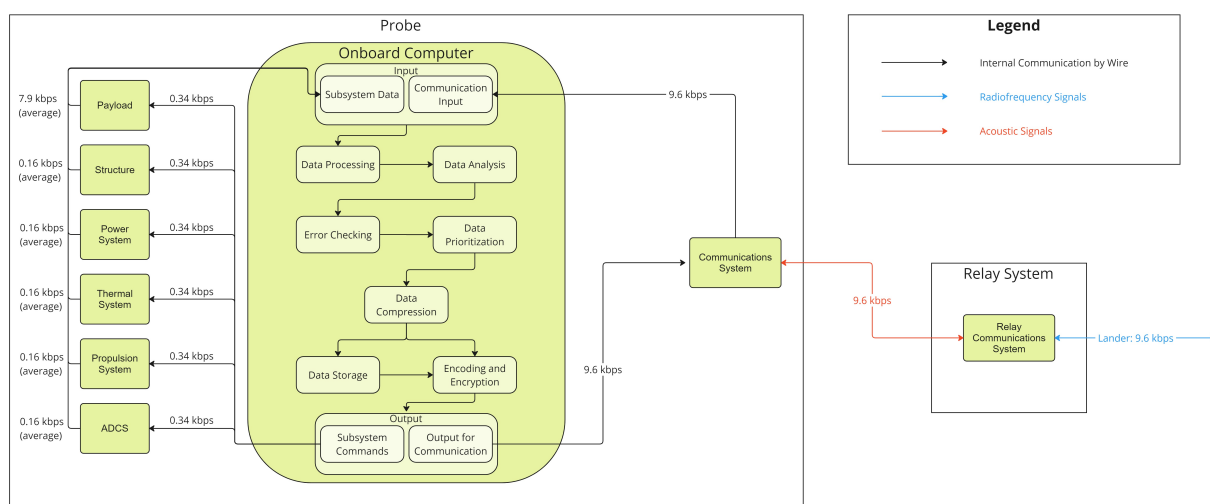
Figure 8.9: Data handling block diagram of the probe of the AlienDive mission

As can be seen, the onboard computer of the probe needs to handle similar tasks to the onboard computer of the lander, as elaborated on in Subsection 7.8.2.

8.8.3. Onboard Computer

The selected onboard computer for the AlienDive mission probe is the CDH-FS from CAVU Aerospace UK, the same model chosen for the lander, as elaborated on in Subsection 7.8.3. Its main features are iterated in Table 8.22.

Table 8.22: Main features of the CDH-FS onboard computer

Parameter	Value
Mass (kg)	4.25
Power (W)	5
Storage (Gb)	24

8.9. Structures

Since the probe is limited by diameter, it was opted to make the skin of the probe load-carrying and to not use stringers as they would add more width than necessary.

Two loading conditions were taken into consideration: the launch loads and the pressure loads of Europa's subsurface ocean. These two loading conditions were considered to be the most likely to drive the design. During the next phase of the design, other conditions such as the landing should be looked at.

8.9.1. Requirements

The subsystem requirements for the probe structure are listed below:

AD-ENG-02-PR-01-STRUC-01: The structure shall withstand lateral launch loads of 2 g.

AD-ENG-02-PR-01-STRUC-02: The structure shall withstand axial loads between −2 g and 6 g.

AD-ENG-02-PR-02-STRUC-03: The structure shall have a natural frequency higher than 25 [Hz] in the axial direction.

AD-ENG-02-PR-02-STRUC-04: The structure shall have a natural frequency higher than 10 Hz in the lateral direction.

AD-REL-01-PR-01-STRUC-05: The structure shall withstand a maximum temperature difference of 30 K.

AD-REL-01-PR-02-STRUC-06: The structure shall withstand the corrosive environment of Europa.

8.9.2. Launch Loads

Since the probe is a cylinder, and thus isotropic in the lateral plane, only one lateral direction has to be taken into account as all other directions behave identically. Again the two critical expected loads are 6 g axially and 2 g laterally. Three failure conditions were taken into account: material yield away from the neutral axis, material yield at the neutral axis and column buckling.

Material Yielding

Conservative preliminary estimates were made about the material yield failure mode. Since it turned out it was not the driving failure mode, there were no in-depth calculations done. It was assumed the lander was fixed to the bottom of the probe and there were no supports higher up. This is a conservative estimate. For yielding the important stresses are the axial stress, which is constant over the cross-section; bending stress, which scales linearly with distance from the neutral axis; and shear stress which is maximal at the neutral axis. For yielding away from the neutral axis, the stresses are thus the axial and bending stresses. The bending stress is tensile on one side of the neutral axis, and compressive on the other. Since the axial stress is compressive and stresses can be added in the same direction, the compressive bending stress is the critical stress.

The maximum axial stress occurs at the connection between the probe and the lander at the bottom of the probe. This coincides with the location of maximum bending stress. The equation is given by Equation 8.14.

$$\sigma = \frac{ma}{2\pi rt} \tag{8.14}$$

The governing equation for bending stress is Equation 8.15, where y is the distance from the neutral axis, I is the area moment of inertia and M is the moment. Equation 8.16 is the maximum bending stress for the probe. This occurs at the connection of the lander and probe. It is assumed that the probe has a thin-walled structure and that the lateral launch load is an equally distributed load.

$$\sigma_b = \frac{My}{I} \tag{8.15}$$ $$\sigma_{b,max} = \frac{maL}{2\pi r^2 t} \tag{8.16}$$

Combining Equation 8.14 and Equation 8.16 and solving for t results in Equation 8.17. Here σ_y is the yield stress of the material, which is the stress at which the material enters the plastic regime and undergoes permanent deformation.

$$t_{min} = \frac{ma_{ax}r + ma_{lat}L}{2\pi r^2 \sigma_y} \tag{8.17}$$

The failure mode at the neutral axis is the combined load of shear and axial stress. These cannot be added together and instead can be combined using the von Mises stress criterion as seen in Equation 8.18. In the final simplification, only the axial stress and transverse shear are non-zero.

$$\sigma_v = \sqrt{\frac{(\sigma_{xx} - \sigma_{yy})^2 + (\sigma_{yy} - \sigma_{zz})^2 + (\sigma_{zz} - \sigma_{xx})^2 + 6(\sigma_{xy}^2 + \sigma_{yz}^2 + \sigma_{zx}^2)}{2}} = \sqrt{\sigma^2 + 3\tau^2} \tag{8.18}$$

The axial load is the same as in the bending condition described above and the shear is described by Equation 8.19, I is the moment of inertia of a thin-walled circle, Q is the first moment of area of the shape above the neutral axis.

$$\tau = \frac{V_{shear}Q}{It} \tag{8.19}$$

Combing equations 8.18, 8.14, 8.19 and combining it with a thin-walled cylinder geometry results in Equation 8.20

$$t = \frac{m}{\pi r \sigma_y} \sqrt{\frac{a_{ax}^2}{4} + \frac{16a_{lat}^2}{3}} \tag{8.20}$$

The bending stress scales with distance from the NA and shear stress is inversely proportional to the distance to the NA. There might be a maximum total stress between the two, but it is unlikely to be large enough to affect the analysis.

Buckling
Another failure mode is the buckling of the probe shell under launch loads. Preliminary estimates were made about the buckling. Since it turned out it was not the driving failure mode, there were no in-depth calculations done. It was assumed that the load was a point load in the top of the cylinder, instead of distributed over the length. It is likely that this is not a conservative estimate as shell buckling and Euler buckling will interact [62]. However as the pressure buckling was estimated to require 20 times more thickness, and the project was time-constrained, no non-linear analysis was done to find the required thickness.

The equation used to estimate the buckling behaviour was the Euler buckling formula (also known as column buckling) seen in Equation 8.21. In this equation, K is a factor depending on the end condition. When the column is fixed on one end and free on the other K is 2.

$$P_{cr} = \frac{\pi^2 EI}{(KL)^2} \tag{8.21}$$

8.9.3. Pressure
The external pressure of Europa's subsurface ocean on the probe can lead to two failure modes, namely: material yield and buckling.

The pressure one kilometre below the surface was estimated by 8.22. Where h is the thickness of the relevant layer (The probe is designed for 30 km ice thickness and a 1 km depth in the ocean below the ice), g_{europa} the gravitational acceleration of Europa (1.315 m/s^2), and ρ the density of the ice (971 kg/m^3) or water (1008 kg/m^3). This leads to a total pressure of 38.3 MPa. This equation makes a few assumptions: constant density, no cavities, constant gravity, small curvature, constant thickness, earth-ice density, earth-water density, no tidal forces, no microporosity in ice, pure ice and pure water.

$$p_{dive} = g_{Europa} \cdot (h_{ice} \cdot \rho_{ice} + h_{dive} \cdot \rho_{water}) \tag{8.22}$$

Material Yield

For a cylinder loaded by pressure the (compressive) stress is given by Equation 8.23 and Equation 8.24, where p is the pressure difference ($p_{out} >> p_{in}, p_{diff} \approx p_{out}$), r is the radius, and t is the thickness. Since $r >> t$ implies $r/t >> 1$, the radial stress is much smaller than the others and can be neglected.

$$\sigma_h = \frac{pr}{t} \qquad (8.23) \qquad\qquad \sigma_l = \frac{pr}{2t} \qquad (8.24) \qquad\qquad \sigma_r = p \approx 0 \qquad (8.25)$$

As can be seen from the equations, the hoop stress is limiting. Rewriting as a function for thickness we obtain Equation 8.26. In this particular case, the Tresca criterion was chosen as it is more conservative than von Mises (˜15%) which justifies the assumption that the radial stress is small.

$$t = \frac{pr}{\sigma_y} \qquad\qquad (8.26)$$

Buckling

The probe can also fail through buckling. The cylinder might rapidly decrease in volume because of the external pressure.

For a long cylinder under hydrostatic pressure, the critical pressure is given by Equation 8.27 [90, 62]. Here γ is the correlation factor between theory and practice. According to NASA for long cylinders, a factor of $\gamma = 0.9$ should be used [62]. E is the elastic modulus and ν the Poisson ratio.

$$p = \frac{\gamma E}{4(1 - v^2)} \left(\frac{t}{r}\right)^3 \qquad\qquad (8.27)$$

Equation 8.27 is only valid for a "long" cylinder. Two different definitions were found, Equation 8.28 and Equation 8.29 by [90] and [62] respectively. Both conditions are met.

$$\left(\frac{L}{r}\right)^2 > 5\left(\frac{r}{t}\right) \qquad\qquad (8.28)$$

$$\gamma Z = \gamma \frac{L^2 \sqrt{1 - v^2}}{rt} > 4000 \qquad\qquad (8.29)$$

8.9.4. Results

An overview of the required thickness for the probe structure is given in 8.23. Here the Length is 3.6 m and the inner radius 0.135 m

Table 8.23: Summary of probe structure design

Load Case	Failure Mode	Expected Forces	Required Thickness [mm]
Launch	Yielding away from neutral axis	39 kN axial, 12 kNm at the bottom	0.34
Launch	Yielding at neutral axis	39 kN axial, 6.5 kN shear.	0.07
Launch	Buckling	39 kN axial.	0.82
Subsurface	Material Failure	48 MPa of hydrostatic pressure.	6.85
Subsurface	Pressure shell buckling	48 MPa of hydrostatic pressure.	15.92

8.9.5. Vibrations

Vibration analysis was done after the first design. In order to avoid resonance during launch there are minimum natural frequencies provided by the launch vehicle operator. According to the Falcon Heavy manual[39], the probe should be designed with a natural frequency of at least 10 Hz in the lateral direction and at least 35 Hz in the axial direction. Assuming the probe is a rod with uniformly distributed mass fixed at one end the formulas for the natural frequencies are 8.30 and 8.31 [40]. The formulas used are conservative as the probe is held at the top, to guide the probe down after landing. The natural frequencies are 219 Hz axially and 13 Hz laterally. Thus both requirements are met.

$$f_{ax} = 0.25\sqrt{\frac{AE}{mL}} \qquad (8.30) \qquad\qquad f_{lat} = 0.56\sqrt{\frac{EI}{mL^3}} \qquad (8.31)$$

8.10. End-of-Life Procedures

The probe will go into the subsurface ocean, this will bring dangerous radioactive pellets into the ocean. The risk of this leaking should be minimised at end-of-life. Due to the probe design, it will be hanging in the water connected to the ice with an anchor. It will be difficult for the probe to return from the subsurface ocean. The anchor was designed with a big margin to buy as much time as possible for the radioactive substance to decay. The substance in the RTG is plutonium 238. It is highly radioactive and has a half-life of 87.7 years. The plutonium decay is a long path which leads to lead 206 in the end. The entire decay chain of plutonium 238 can be seen in Figure 8.10. For this chart, only the highest probability path was shown.
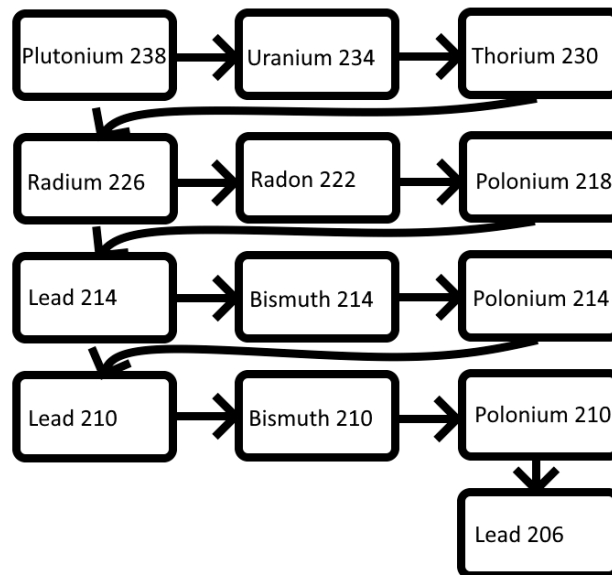

Figure 8.10: Decay chain of plutonium 238 (only the highest probability is taken into account)

When all the atoms decay to lead 206, the fuel will no longer be radioactive. This will take a massive amount of time due to the half-life of uranium 234 and thorium 230, which have a half-life of 245500 and 75438 years, respectively [91]. This is way more than the half-life of plutonium (87.7 years) [43] and will thus be likely what will be left in thousands or even millions of years.

If the cable snaps or the anchor breaks, the probe will sink to the bottom of the ocean. Due to the immense pressures on Europa, which was estimated to be between 130-260 MPa [92, 93] on the seafloor, the probe will likely implode. This will cause the fuel to leak and contaminate the ocean. What fuel gets spilt in the ocean depends on when the anchor system fails. The change in number of atoms of each material over time can be seen in Figure 8.11. In this plot, polonium 214 was neglected due to its very short half-life of 164 μs [94]. Only the highest probability path was explored.

The first rise of Uranium is due to the fast decay of plutonium, after this, it can be seen that the lead continues to rise until the very end. After one million years most of the material has been converted to lead 206. Thus if the cable or anchor fails after one million years, the highly radioactive plutonium will be gone for a while, nevertheless, there will still be leftover uranium. This uranium will still be harmful, but due to the dampening properties of water, this should be less of a problem, it is however not negligible. Another strategy when it comes to saving the subsurface ocean of radioactive materials is a retrieval mission. This will include a follow-up mission, which will 'rescue' the probe. This would likely not be possible in the following years, yet, if technology advances quickly enough, this might be a possibility in the future.
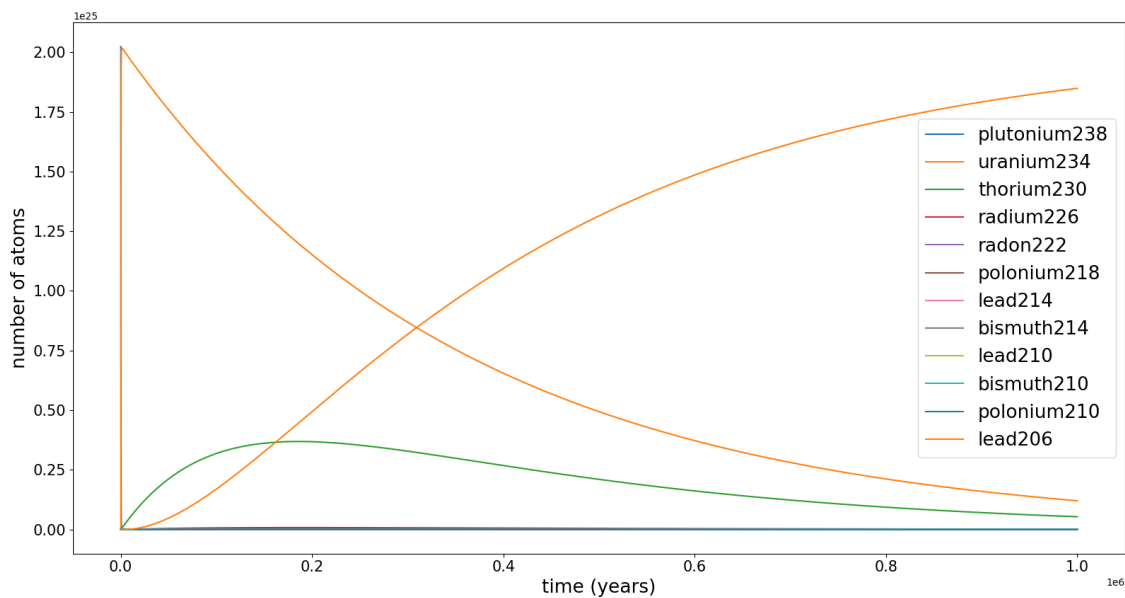
Figure 8.11: Decay of plutonium 238 (only the highest probability is taken into account)

8.11. Visualisation of Layout

As with the transfer stage and lander, the probe was also assembled in CATIA. Figure 8.12 and Figure 8.13 show the external and cross-sectional view of the probe respectively

Figure 8.12: An external view of the probe
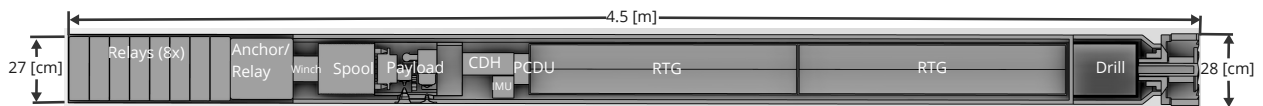
Figure 8.13: A cross-section of the probe

The probe is 4.5 m long with a drill diameter of 28 cm and a body diameter of 27 cm. Right behind the drill, the two RTGs are placed, to reduce heat loss when transporting their heat towards the drill. As explained, this heat transport will be done using water pipes. These pipes are not modelled but shall be located in the area between the components and the start of the wall. This area will also contain insulation to ensure minimal heat loss to the ice. Behind the RTGs are the PCDU, IMU, CDH and Payload. This area will be shielded from radiation by the torus tanks, inside the lander. Some of the payload components have to extend to the wall, as they have to sample or image the ocean. However, this does not pose any issue to the thermal pipes, as they would go around these extensions. Then there is the spool that contains the cable, with a winch on top of it. The cable connects to the anchor through a plate behind the winch. This plate will prevent flooding once the anchor is deployed. Finally, in the very back of the probe there are 8 regular relays, that will be deployed at specific locations as the probe moves through the ice. The anchor also contains a specialised relay that is able to receive signals from a small transmitter located near the winch.

9 Sensitivity Analysis

Now that the design has been completed, a sensitivity analysis can be performed to investigate the effect of a change in important system parameters on the final design. This analysis shows the flexibility of the solution and shows to what extent new information on the mission can impact the design. In this chapter, the strategy for the sensitivity analysis is first discussed. Afterwards, the sensitivity analysis is performed on all three elements of the system, and an overview is given of the results.

9.1. Analysis Strategy

It is very likely that during the further development of the AlienDive mission, new information becomes available or new problems are found that can influence the mission parameters. For this sensitivity analysis, two different types of parameter changes are considered, which will be explained below.

The first type of parameter changes is technical parameter changes. These changes can originate in a large variety of ways. Some components used in the design of the mission have a very low technology readiness level, such as the two types of RTG and the torus-shaped fuel tanks. While performance estimates are available for these components, it is very likely that once the technology gets closer to completion, different and more accurate data becomes available on these components that may or may not hurt the design. In addition to this, changes could happen due to problems with manufacturing or integration. For example, due to the tight fitting within the shell of the probe, it might be required for cutouts to be added to the design, thus requiring an increase in the structure around those cutouts to prevent failure, which would increase the mass of the probe and thus the system. Furthermore, some ideas that seem feasible during this preliminary design phase might turn out not to be during early testing, requiring changes to the design. A possible area where this could happen is the anchor and spool system, in case the spool size or orientation would need to change for the effective winding and unwinding of the tether. Another possible component that could be affected is the drill, in case the drill does not extend far enough from the main body and the probe gets speed limited by the removal of ice chips.

The second type of changes are changes to the scientific consensus or knowledge on Europa. Currently, a lot is still unknown about the moon; the thickness of the ice shell is based on predictions, and the size and composition of the ice-ocean interface are based on simple models. Furthermore, new information for example on surface composition could change the area of interest for the mission, thus changing the required trajectory around and towards Europa. With the JUICE mission already on its way to the Jovian system, and with Europa Clipper planning to launch towards Europa in October 2024[1], the probability of more accurate data becoming available about the moon and its environment in the near future is very high. It is thus important to study the effects of any of these changes on the design to see whether or not the design is easily adjusted to new conditions.

An overview of the parameters that are analysed in this sensitivity analysis, the range at which changes were performed, and the justification behind changing that specific parameter is found in Table 9.1.

---

[1] From `https://europa.nasa.gov/`, accessed on 18/06/2024.

Table 9.1: Parameters analysed during the sensitivity analysis

	Parameter	Current value	Tested Range	Reasoning
T	Probe diameter	0.27 m	-10% to +50%	The outer diameter of the probe can change due to multiple reasons: The layout of the internal components could be modified, the structure strengthened, or additional width is required for a specific component. Since the probe is already quite optimised around the widest component (RTG), it is again more likely that the diameter will increase rather than decrease.
T	Additional probe RTG	2 RTGs	3 RTGs	The drilling speed of the probe is limited by the amount of power delivered to the drill. In case more power is desired for the drill, additional power sources could be required, changing the layout and mass of the spacecraft. Furthermore, since the TRL of the main RTG is very low (TRL 3), the delivered power of this RTG could decrease to such an extent that an additional one is needed.
T	Probe mass	554 kg	-20 to 20%	To study the effect of larger magnitude changes to the design, the mass of the probe is modified by around 20%.
T	Lander mass	1.6 t	-20 to 20%	To study the effect of larger magnitude changes to the design, the mass of the lander is modified by around 20%. For example, if a lander is desired with many more scientific instruments on board, the payload mass could change.
S	Ice-crust thickness	30 km	15 - 50 km	The current estimated ice crust thickness ranges from best case scenario 15 km [77], to best estimate 24.3 km and a worst case scenario of 47.1 km [2]. In case new data becomes available that changes the required design thickness, how does the design change?
S	Ice-ocean interface shear	730 N	2 kN	Currently, it is predicted that shear forces are not a large issue around the ice-ocean interface. If new data shows this is the case, the tether must be strengthened. An increase of around 300% is tested to ensure the change is visible, decreasing does not affect the design as it stays tension-limited.
S	Orbit Inclination Change	10°	0° - 12°	In case the area of interest of the mission changes due to new data availability, the required inclination change at Europa could change. The range selected studies inclination changes of 0 to 12 degrees. Initially a larger range was selected, but any value larger than 12° would increase the system mass to unacceptable levels.

9.2. Technical Sensitivity Analysis

In this section, the results of the modification of the technical parameters of Table 9.1 are discussed both qualitatively and quantitatively. For all parameters, the effect on the main system is summarised in Table 9.2. Any other relevant effects due to changes in the parameter are discussed in each separate section.

Table 9.2: Overview of the technical sensitivity parameters on the system level parameters.

Parameter	Test Range	Probe Mass	Lander Wet Mass	Landed Dry Mass	TS Propellant Mass	Total system mass
Probe diameter	-10% to +50%	-8.2% to +51.5%	-1.3% to +7.6%	-3.7% to +22.9%	-3.2% to +20.1%	-3.2% to +20.2%
Additional probe RTG	3 RTGs	+27.8%	+12.7%	+18%	+15.8%	+15.9%
Probe mass	-20% to 20%	N/A	-3.3% to +3.1%	-9.4% to 9.3%	-8.3% to +8.1%	-8.3% to +8.2%
Lander mass	-20% to 20%	0%	N/A	-12.4% to +12.6%	-10.8% to +11.0%	-10.7% to +10.8%

Diameter of the probe : For an increase in the diameter of the probe, it is logical that the structural mass of the probe increases, which will then snowball into a larger system mass increase as the lander and transfer stage have to deal with larger. In addition, the total drilling time of the probe increases, since more ice now has to be removed using the same amount of power. In addition to the system parameters, lowering the probe diameter by 10% reduces the structural mass by 18.9%, while the maximum increase of 50% results in an increase in structural mass of 124.2%.

Additional Probe RTG : In case an additional RTG is required to be added, either due to a desire for faster drilling or due to disappointing results from RTG prototypes. The mass of all three elements of the system increases, both directly due to the extra RTG and due to the extra structural mass for the extra probe length added. For a 50% increase in EPS mass, a 61.7 % increase is seen in the structural mass. The budgeted power for the drill does however increase by 54%, allowing for faster drilling. It should be mentioned however that changes in radiation shielding due to changes in drilling length were not taken into account. While a higher drilling speed is desired, an additional RTG would put the landed dry mass of the spacecraft above the required value.

Probe & lander mass   : Increases in the overall mass of the probe or lander logically lead to increases in the elements above it due to structural considerations and required propellant levels. A change in lander mass does affect the design more than the probe, meaning that optimisation of the lander and its structure could improve system mass significantly.

9.3. Mission Sensitivity Analysis

In this section, the three parameters that are more related to the mission and the knowledge about Europa are discussed. An overview of the system level effects of these parameters is found in Table 9.3

Table 9.3: Overview of the mission sensitivity parameters on the system level parameters.

Parameter	Test Range	Probe Mass	Lander Wet Mass	Landed Dry Mass	TS Propellant Mass	Total System Mass
Ice crust thickness	15 km to 50 km	-13.6% to +14.9%	-5.0% to +6.3%	-7.9% to +9.4%	-7.0% to +8.2%	-7.0% to +8.2%
Ice-ocean interface shear	2 kN	+10.4%	+3.3%	+5.8%	+5.1%	+5.1%
Orbit Inclination change	0° to 12°	0%	0%	0%	-69.7% to +277%	-61.3% to 254.3%

Ice crust thickness   It is quite likely that more accurate estimates of the ice crust thickness become available. Our design is however quite easily modified for these new distances. The structural mass changes between -19.8% to +40.1% due to different hydrostatic pressures. Furthermore, the amount of required relays varies between 4 and 13 instead of the 8 required for the current design ice thickness, and thus also the required lander length due to more relays being stacked on top of the probe. Drilling time would change as well, The effects on the system level are, however, quite small, meaning that the risk of losing money on redundant development is low.

Ice-ocean interface shear   In case the shear at the ice-ocean interface turns out to be higher than currently assumed, the cable diameter likely has to be increased, thus also increasing the required length of the spool. For the tested value, the spool length increases by +156.0%, thus also increasing the probe and lander lengths. However, the effects on the system level again remain limited, reducing development risk.

Orbit inclination change   Opposite to the other two parameters, a change in orbit inclination change has a significant effect on the required propellant mass of the mission, both in the positive and negative sense. The parameter taken is the actual change, not the change relative to the current value. Taking any larger inclination change than the current value of 10° results in the design not being able to launch on the Falcon Heavy, while changing the inclination less results in significant mass savings on propellant. Initially, it was planned to test inclination changes up until 15°, but after only 12° the system mass increased to unacceptable levels.

9.4. Sensitivity discussion

Based on the parameters tested during the sensitivity analysis, a few conclusions can be made about the flexibility of the design.

Firstly, the spacecraft design concept is flexible for changes in the ice sheet thickness and is able to be easily modified to account for the new knowledge on the characteristics of Europa. This is a result mostly due to the lander and probe not being connected after deployment, and the maximum distance through ice thus only being limited by the amount of relays taken and the amount of radiation to be survived by the electronics-box below the ice.

Furthermore, based on new data about the moon, it should be reconsidered whether or not to go to the polar regions. While these regions reduce the required radiation shielding mass, the required inclination change increases the system mass significantly. Furthermore, since the design can deal with different ice thicknesses quite flexibly, a new analysis on the optimal landing location for the design concept should be performed once more data is available.

Finally, in the case that the performance of the low TRL components of the mission is worse than initially expected, the mass of the system would increase. It is thus important to monitor the development of these components closely, to reduce the risk of mission costs increasing significantly or the mission development being cancelled due to too large decreases in mission performance.

10 Risk Management

This chapter elaborates on the technical risk management related to the AlienDive mission. Risk management entails identifying uncertainties during operation and mitigating these uncertainties as much as possible. First, a discussion of the risk management methodology is included in Section 10.1. Next, all technical risks are identified and assessed in Section 10.2. Finally, for each risk, mitigation and contingency plans are presented in Section 10.3, whereafter risk heat maps are displayed before and after mitigation.

10.1. Risk Management Methodology

The risk analysis consists of four main components: risk identification, assessment, mitigation, and contingency planning. Firstly, risks are identified and assessed in a risk identification table, where each risk is given a unique identifier and qualifications for its probability of occurrence and the severity of the consequence. Table 10.1 and Table 10.2 show the qualification bases for the probability of occurrence (PO) and severity of the consequence used in the risk analysis, respectively. The percentages listed in Table 10.1 are provided as an indication of the likelihood of an event[1] and have not been calculated through statistical analysis. Next, mitigation and contingency plans are presented for each risk, which expectantly reduce the probability of occurrence and/or the severity of the consequence. Finally, the risks are displayed in a risk map, providing insight into the most critical risks before and after mitigation.

Table 10.1: Qualification basis of probability of occurrence

Estimated Probability of Occurrence	
Very High	$PO \geq 70\%$
High	$50\% \leq PO < 70\%$
Moderate	$30\% \leq PO < 50\%$
Low	$1\% \leq PO < 30\%$
Very Low	$PO < 1\%$

Table 10.2: Qualification basis of severity of consequences

Severity of consequences	
Catastrophic	Project failure
Critical	Questionable success of project
Marginal	Degradation of secondary tasks
Negligible	Minor inconvenience

It should be noted that the midterm report already addressed some technical risks. However, it focused only on a limited number of subsystems necessary for the concept trade-off. As a result, technical risks for the remaining subsystems, as well as risks related to planetary protection, were not identified. This report aims to provide a more comprehensive overview of all technical risks associated with the AlienDive mission.

10.2. Risk Assessment

Each technical risk is assigned an ID indicating the category it belongs to. The risks are divided into those related to the scientific payload (PAY), travelling to Europa (TRA), the reconnaissance orbit (REC), landing on Europa (LAN), the propulsion system (PRO), the thermal control system (THE), the structure of the system (STR), the power system (POW), the guidance, navigation and control system (GNC), radiation (RAD), the communication system (COM), the command and data handling system (CDH), the ice-traversal method (ICE), hydrodynamics (HYD) and planetary protection (PLA).

---

[1]Values taken from Lecture #3 - Risk Management & Concurrent Engineering from AE3211-1 Systems Engineering & Aerospace Design

Table 10.3: Risk identification table of technical risks

Risk	Cause	Probability	Consequence	Severity	Responsible Member
TR-PAY-01: Sampling mechanism failure	Mechanical jamming/clogging	Moderate	Inability to correctly conduct scientific research	Critical	Isabelle
TR-PAY-02: Unclear/ambiguous data	Unknown chemicals/saturation of spectrometer	High	Drawing false conclusions	Marginal	Isabelle
TR-PAY-03: Camera view obstruction	Grime or dust obscuring camera lens	Low	Images appearing blurry or obstructed	Critical	Isabelle
TR-PAY-04: Life marker chips depleted	Algorithm controlling life marker chips lacks sufficient specificity	Moderate	No further measurements taken for the remainder of the mission	Marginal	Isabelle
TR-TRA-01: Falcon Heavy unavailable	Falcon Heavy retracted from use	Very low	Inability to launch AlienDive mission using the Falcon Heavy	Marginal	Lievijn
TR-TRA-02: Inability to meet optimal launch date	Atmospheric conditions/delays	Moderate	Additional delta-V required	Critical	Marta
TR-TRA-03: Suboptimal flyby trajectory	Imperfect trajectory model	Moderate	Unable to achieve required inclination changes/suboptimal landing spot	Critical	Marta
TR-REC-01: Inability to take reconnaissance pictures	Reconnaissance camera failure	Low	No high resolution pictures of regions of interest	Catastrophic	Marta
TR-LAN-01: Transfer stage separation mechanism failure	Mechanical malfunction/structural failure	Low	Crash landing	Catastrophic	Laurens
TR-LAN-02: Deployment failure of the landing legs	Joints experiencing friction or seizing	Low	Unstable landing/touchdown	Critical	Pepijn
TR-LAN-03: Propulsion failure upon landing	Overheating/component failure due to high stresses	Low	Freefall to the surface	Critical	Hugo

Table 10.3: Risk identification table of technical risks (continued)

Risk	Cause	Probability	Consequence	Severity	Responsible Member
TR-LAN-04: Tipping over upon landing	High CG/unsuitable landing spot	Moderate	Inability to insert probe into ice	Catastrophic	Pepijn
TR-PRO-01: Engine failure transfer stage	Overheating/component failure due to high stresses	Low	Inability to reach Europa	Catastrophic	Hugo
TR-PRO-02: Fuel tank rupture	Overheating/component failure due to high stresses	Low	Failure of the propulsion system	Catastrophic	Hugo
TR-PRO-03: Failure of one of the lander engines	Overheating/component failure due to high stresses	Low	Hampered landing	Critical	Hugo
TR-PRO-04: Failure of the feed system	Bursting of pipes	Moderate	Fuel is not reaching the engine from the tanks	Catastrophic	Hugo
TR-THE-01: Degradation of the MLI	Micrometeorites hitting the MLI	High	Spacecraft experiences increased cooling	Marginal	Zayid
TR-THE-02: Louvres malfunctioning	Mechanical failure/structural damage	Low	Hindered thermal control in critical mission phases	Critical	Zayid
TR-THE-03: Failure of the pump fluid loop	Mechanical issues/loss of pressure	Low	Probe experiences localized heating at the RTG	Catastrophic	Zayid
TR-THE-04: Probe overheating	Approaching a plume too closely	Low	Exceeding maximum temperature for critical components	Catastrophic	Zayid
TR-STR-01: Failure of probe structure	Higher than anticipated loads	Low	Inability to continue mission	Catastrophic	Laurens
TR-STR-02: Material degradation	Radiation/thermal fluctuations/cyclic loads	Moderate	Material failure	Critical	Laurens
TR-STR-03: Probe lowering malfunctions	Hatch fails to open or cable malfunctions	Low	Inability to lower probe onto the ice	Catastrophic	Laurens
TR-STR-04: Gimball failure	Software failure/mechanical obstruction/freezing causing jamming	Low	Inability to point high gain antenna to Earth	Critical	Laurens

Table 10.3: Risk identification table of technical risks (continued)

Risk	Cause	Probability	Consequence	Severity	Responsible Member
TR-POW-01: PCDU malfunction	Short-circuit/manufacturing defect	Low	System is non-functional	Catastrophic	Lucas
TR-POW-02: Radioactive fuel leaking	Unforeseen forces/damage	Low	Radioactive contamination of Europa	Catastrophic	Lucas
TR-POW-03: Improperly connected electrical harness	Insufficient checking of connections	Low	Components not receiving adequate power supply	Marginal	Lucas
TR-POW-04: Intended RTG unavailable	RTG still in development or banned due to legislation	Low	Inability to power probe using the intended RTG	Critical	Lucas
TR-GNC-01: Sun sensor failure	Radiation	Low	Inability to determine attitude using the sun	Marginal	Sunny
TR-GNC-02: Star tracker failure	Radiation	Very low	Inability to determine attitude using the stars	Marginal	Sunny
TR-GNC-03: IMU failure	Launch loads/radiation/wear	Very low	Inability to measure rotational and translational accelerations	Critical	Sunny
TR-GNC-04: Reaction wheel failure	Launch loads/radiation/wear	Low	Inability to control spacecraft around one axis	Critical	Sunny
TR-GNC-05: Reaction control thruster failure	Overheating/component failure due to high stresses	Low	Inability to dump momentum/rotate/translate	Critical	Sunny
TR-GNC-06: Sensor inaccuracy	Noise from other components/background noise/calibration issues	High	Inaccurate attitude determination	Marginal	Sunny
TR-RAD-01: Surface radiation exceeding anticipated levels	Insufficient information available	Moderate	The system fails due to radiation earlier than anticipated	Catastrophic	Marta
TR-COM-01: RF relay failure	Damage/power outage	Moderate	Communication loss	Catastrophic	Cas

Table 10.3: Risk identification table of technical risks (continued)

Risk	Cause	Probability	Consequence	Severity	Responsible Member
TR-COM-02: RF relay deployment failure	Relay fails to disconnect from probe/relay does not freeze in place	Moderate	Suboptimal placement of relays	Critical	Cas
TR-COM-03: Space communication failure	Unexpected link losses	Very low	Communication loss	Critical	Cas
TR-COM-04: Acoustic modem failure	Damage/power outage	Low	Communication loss	Catastrophic	Cas
TR-CDH-01: CDH system failure	Damage/power outage	Low	Inability to store and process data	Catastrophic	Cas
TR-ICE-01: Probe obstruction	Non-melting layers	Moderate	Slower movement/getting stuck	Critical	Lievijn
TR-ICE-02: Drill failure	Damage/power outage	Low	Slower movement	Critical	Lievijn
TR-ICE-03: Crack encounter (<20cm)	Unknown structure of the ice crust	High	Movement slightly inhibited	Negligible	Lievijn
TR-ICE-04: Cavity encounter (<5m)	Unknown structure of the ice crust	Moderate	Movement moderately inhibited	Marginal	Lievijn
TR-ICE-05: Void encounter (>5m)	Unknown structure of the ice crust	Low	Movement significantly inhibited	Critical	Lievijn
TR-ICE-06: Ice penetration radar failure	Power loss/damage	Low	Inability to detect obstacles/goals	Critical	Lievijn
TR-ICE-07: Chip removal failure	The chips are excessively large/have inadequate melting rates	Low	Inhibited movement through ice crust	Critical	Lievijn
TR-ICE-08: Ice layer exceeds 30 km in thickness	Insufficient knowledge on ice crust of Europa	Very low	Extended mission time/lowered data rates through relays	Marginal	Lievijn

Table 10.3: Risk identification table of technical risks (continued)

Risk	Cause	Probability	Consequence	Severity	Responsible Member
TR-HYD-01: Cable failure	Unexpectedly high shear forces	Low	Sinking of the probe	Catastrophic	Pepijn
TR-HYD-02: Anchor failure	Anchor fails to adhere	Low	Sinking of the probe	Catastrophic	Pepijn
TR-HYD-03: Cable spool jammed	Mechanical jamming/freezing	Low	Inability to lower probe in the subsurface ocean	Critical	Pepijn
TR-HYD-04: Winch motor failure	Overloading/overheating/electrical issues	Low	Inability to control the descend of the probe	Marginal	Pepijn
TR-PLA-01: Biological contamination of Europa	Lander/probe contains organisms from Earth	Low	Harmful contamination/adverse changes to environment	Catastrophic	Lievijn

10.3. Risk Mitigation

Table 10.4: Mitigation methods and contingency plans for the identified technical risks

Risk	Mitigation Strategy	Mitigation Plan	Adjusted Probability	Adjusted Severity	Contingency Plan
TR-PAY-01	Reduce	Flush/clean sampling bay in between samples	Low	Critical	Attempt flushing/cleaning procedure
TR-PAY-02	Reduce	Incorporate redundant instrumentation	Moderate	Marginal	Attempt to recreate data on Earth for reference
TR-PAY-03	Accept	N/A	Low	Critical	Instruct probe to agitate to dislodge grime
TR-PAY-04	Reduce	Check incoming data and update the software to improve selectivity	Low	Marginal	Continue making observations with other instruments
TR-TRA-01	Accept	N/A	Very low	Marginal	Make use of a different launcher
TR-TRA-02	Reduce	Incorporate safety margins on delta-V budget	Moderate	Negligible	Reschedule for a new launch window prior to 2035
TR-TRA-03	Reduce	Conduct thorough V&V	Low	Critical	Assess implications and take corrective actions
TR-REC-01	Reduce	Incorporate shielding for external hazards	Very low	Critical	Analyze images of Europa Clipper and Juice
TR-LAN-01	Reduce	Conduct V&V/testing	Low	Marginal	Assess the situation for next steps
TR-LAN-02	Reduce	Conduct testing and optimization	Very low	Critical	Check CG for a three-point landing
TR-LAN-03	Reduce	Design landing legs to absorb impacts from at least 10 meters	Very low	Critical	Assess damage to lander/probe
TR-LAN-04	Reduce	Design landing legs for high CG	Low	Critical	Use landing legs/excess fuel for elevation adjustment
TR-PRO-01	Reduce	Conduct prototyping/V&V/testing	Very low	Catastrophic	Assess the situation for next steps
TR-PRO-02	Reduce	Non-destructive testing/add redundant volume to tank	Very low	Catastrophic	Assess the situation for next steps

Table 10.4: Mitigation methods and contingency plans for the identified technical risks (continued)

Risk	Mitigation Strategy	Mitigation Plan	Adjusted Probability	Adjusted Severity	Contingency Plan
TR-PRO-03	Reduce	Conduct prototyping/V&V/testing	Low	Critical	Shut down specific engines for balance and expedite landing
TR-PRO-04	Reduce	Use stronger/more reliable feed system components	Low	Catastrophic	Assess the situation for next steps
TR-THE-01	Accept	N/A	High	Marginal	Close the louvre to retain more heat
TR-THE-02	Reduce	Incorporate redundant points of failure	Very low	Critical	Transmit scientific data to Earth promptly
TR-THE-03	Reduce	Implement thermal insulation enhancements around the pump fluid loop	Very low	Critical	Transmit scientific data to Earth promptly
TR-THE-04	Reduce	Incorporate instruments to detect plumes	Very low	Catastrophic	Transmit scientific data to Earth promptly
TR-STR-01	Reduce	Test/Iterate design after data from Europa Clipper	Very low	Catastrophic	Assess the situation for next steps
TR-STR-02	Reduce	Incorporate safety factors/testing/radiation resistant materials	Low	Marginal	Assess damage
TR-STR-03	Reduce	Conduct prototyping/V&V/testing	Very low	Catastrophic	Update the hatch software if feasible
TR-STR-04	Reduce	Conduct prototyping/V&V/testing	Low	Critical	Transmit data less frequently
TR-POW-01	Reduce	Conduct prototyping/V&V/testing	Very low	Catastrophic	Assess the situation for next steps
TR-POW-02	Reduce	Incorporate safety margins	Very low	Catastrophic	Isolate damaged RTG and incorporate decontamination plan
TR-POW-03	Reduce	Conduct redundant checks	Very low	Marginal	Assess the situation for next steps
TR-POW-04	Accept	N/A	Low	Critical	Incorporate different type of power system

Table 10.4: Mitigation methods and contingency plans for the identified technical risks (continued)

Risk	Mitigation Strategy	Mitigation Plan	Adjusted Probability	Adjusted Severity	Contingency Plan
TR-GNC-01	Reduce	Incorporate redundancy/high reliability and radiation resistant components	Very low	Negligible	Use star tracker/redundant system
TR-GNC-02	Reduce	Incorporate redundancy/high reliability and radiation resistant components	Very low	Negligible	Use sun sensor/redundant system
TR-GNC-03	Reduce	Incorporate highly reliable and radiation resistant components	Very low	Critical	Use IMU of different system
TR-GNC-04	Reduce	Incorporate redundancy/high reliability and radiation resistant components	Very low	Marginal	Use redundant component/thrusters for control
TR-GNC-05	Reduce	Conduct prototyping/V&V/testing	Very low	Critical	Use reaction wheels/other thrusters
TR-GNC-06	Reduce	Testing/filtering noise/calibration	Moderate	Negligible	Update the sensor software if feasible
TR-RAD-01	Reduce	Incorporate safety margins of 50%	Low	Catastrophic	Assess damage
TR-COM-01	Reduce	Utilize protective housing able to withstand harsh conditions/implement redundant relays	Low	Marginal	Attempt to restart the RF relay
TR-COM-02	Reduce	Implement redundant relays	Low	Marginal	Adjust placement of subsequent relay
TR-COM-03	Reduce	Utilize conservative estimates and safety margins	Very low	Critical	Attempt to reestablish contact when closer to Earth
TR-COM-04	Reduce	Utilize protective housing able to withstand harsh conditions	Very low	Catastrophic	Attempt to restart the acoustic modem
TR-CDH-01	Reduce	Incorporate redundancy in CDH design	Very low	Marginal	Switch to redundant processors/use RF relays for data storage and processing

Continued on next page

Table 10.4: Mitigation methods and contingency plans for the identified technical risks (continued)

Risk	Mitigation Strategy	Mitigation Plan	Adjusted Probability	Adjusted Severity	Contingency Plan
TR-ICE-01	Reduce	Incorporate systems able to detect non-melting layers	Very low	Marginal	Increase temperature and RPM of heat drill
TR-ICE-02	Reduce	Utilize materials able to withstand harsh conditions	Low	Critical	Attempt to restart the drill
TR-ICE-03	Reduce	Incorporate systems able to detect cracks	Moderate	Negligible	Proceed as planned
TR-ICE-04	Reduce	Incorporate systems able to detect cavities	Low	Marginal	Incorporate shock absorbers and orientation control systems
TR-ICE-05	Reduce	Incorporate systems able to detect voids	Very low	Critical	Incorporate shock absorbers and orientation control systems
TR-ICE-06	Reduce	Conduct prototyping/V&V/testing	Very low	Critical	Use thermal couples for temperature monitoring to detect anomalies
TR-ICE-07	Reduce	Ensure proper heat supply	Very low	Critical	Increase heat allocation to the drill
TR-ICE-08	Accept	N/A	Very low	Marginal	Continue drilling until ocean is reached
TR-HYD-01	Reduce	Add extra cable margin to allow slack	Very low	Critical	Take numerous measurements during gradual descent
TR-HYD-02	Reduce	Incorporate redundant adhesion rods	Very low	Critical	Freeze probe top in slush/take numerous measurements during slow descent
TR-HYD-03	Reduce	Heat elements around rotating parts to seal spool area	Very low	Marginal	Continue measurements at stuck location
TR-HYD-04	Reduce	Ensure the motor is designed for high stress and environmental conditions	Very low	Marginal	Use the magnetic break to slow down descend
TR-PLA-01	Reduce	Use clean rooms/sterilization during manufacturing	Very low	Catastrophic	Assess contamination for next steps

Table 10.5: Risk map of technical risks associated with the AlienDive mission before mitigation

Severity ↑ / Probability →	Very Low	Low	Moderate	High	Very High
Catastrophic		TR-REC-01 TR-LAN-01 TR-PRO-01 TR-PRO-02 TR-THE-03 TR-THE-04 TR-STR-01 TR-STR-03 TR-POW-01 TR-POW-02 TR-COM-04 TR-CDH-01 TR-HYD-01 TR-HYD-02 TR-PLA-01	TR-LAN-04 TR-PRO-04 TR-RAD-01 TR-COM-01		
Critical	TR-GNC-03 TR-COM-03	TR-PAY-03 TR-LAN-02 TR-LAN-03 TR-PRO-03 TR-THE-02 TR-STR-04 TR-POW-04 TR-GNC-04 TR-GNC-05 TR-ICE-02 TR-ICE-05 TR-ICE-06 TR-ICE-07 TR-HYD-03	TR-PAY-01 TR-TRA-02 TR-TRA-03 TR-STR-02 TR-COM-02 TR-ICE-01		
Marginal	TR-TRA-01 TR-GNC-02 TR-ICE-08	TR-POW-03 TR-GNC-01 TR-HYD-04	TR-PAY-04 TR-ICE-04	TR-PAY-02 TR-THE-01 TR-GNC-06	
Negligible				TR-ICE-03	

A considerable number of technical risks have a low to moderate probability of occurrence with a critical or even catastrophic severity of consequence. As seen in Table 10.6, the mitigation strategies have led to a less daunting risk map.

Table 10.6: Risk map of technical risks associated with the AlienDive mission after mitigation

Severity ↑ / Probability →	Very Low	Low	Moderate	High	Very High
Catastrophic	TR-PRO-01 TR-PRO-02 TR-THE-04 TR-STR-01 TR-STR-03 TR-POW-01 TR-POW-02 TR-COM-04 TR-PLA-01	TR-PRO-04 TR-RAD-01			
Critical	TR-REC-01 TR-LAN-02 TR-LAN-03 TR-THE-02 TR-THE-03 TR-GNC-03 TR-GNC-05 TR-COM-03 TR-ICE-05 TR-ICE-06 TR-ICE-07 TR-HYD-01 TR-HYD-02	TR-PAY-01 TR-PAY-03 TR-TRA-03 TR-LAN-04 TR-PRO-03 TR-STR-04 TR-POW-04 TR-ICE-02			
Marginal	TR-TRA-01 TR-POW-03 TR-GNC-04 TR-CDH-01 TR-ICE-01 TR-ICE-08 TR-HYD-03 TR-HYD-04	TR-PAY-04 TR-LAN-01 TR-STR-02 TR-COM-01 TR-COM-02 TR-ICE-04	TR-PAY-02	TR-THE-01	
Negligible	TR-GNC-01 TR-GNC-02		TR-TRA-02 TR-GNC-06 TR-ICE-03		

11 Production Plan & Sustainable Development

Spacecraft components and assembly and mission sustainability are essential parts of every space mission, these will be explored in this chapter. Section 11.1 and Section 11.2 cover the material selection and production methods used, respectively. Section 11.3 covers Europa contamination calculations and Section 11.4 details the spacecraft assembly process. Lastly, Section 11.5 goes over the mission's sustainability efforts.

11.1. Material Selection

Titanium alloys were chosen for all primary structures that carry significant loads in this design as they have high specific strength at low temperatures and are very commonly used in the aerospace industry [95]. They are also known to be corrosion and radiation-resistant [96] and are often used in additive manufacturing, which will be elaborated on in the next section. The specific alloy selected for structural components was Ti-6Al-4V, which has a price of roughly 20 $/kg.[1]

11.2. Production Methods

The main production method chosen for the spacecraft components was powder bed fusion followed by hot isostatic pressing, which is a type of additive manufacturing. It wastes less material and is thus cheaper and more sustainable than other methods. It also aids in the integration of parts as various shapes can be manufactured. Reused titanium alloy powders can be used without decreasing material properties [97], which helps decrease costs. For the probe, all parts connected to the outer bus will be welded to ensure watertight seals.

11.3. Planetary protection

This project will comply with the COSPAR planetary protection policies. Within this five categories are defined ranging from no concern to highest concern, landers or orbiters to Europa are category IV and thus of quite high concern. Specifically, the probability of inadvertent contamination of the Europan subsurface ocean shall be less than 10^{-4} [41]. This probability was evaluated for all three of the spacecraft stages. According to Ref. [98], Any dose above 7 Mrad should cause any component to have a probability of contamination that is lower than 10^{-4}. It is also stated that outside components of spacecraft would phase a minimum of 10 Mrad/month, the lander and kick stage will thus receive more than enough radiation throughout their lifetime to comply with the COSPAR regulations. In Ref. [98], detailed calculation methods are also given and these are used to calculate the probability of the probe contaminating the subsurface ocean of Europa. They consider the following four types of organisms for calculations:

- Type A: Typical, common microorganisms
- Type B: Spores of microorganisms that are known to be resistant to environmental insults
- Type C: Spores that are especially radiation-resistant
- Type D: Rare but highly radiation-resistant non-spore microorganisms

The amount of organisms that survive to grow in the Europan ocean environment is calculated by multiplying the number of culturable organisms on the spacecraft with a list of factors. In this method, the products of these factors are summed for every organism type to obtain the probability of contamination, which is summarised in Table 11.1. As long as the products of factors is significantly smaller than one, they can be summed to get an accurate estimation of the probability of contamination [98]. For these calculations, only the components in contact with the Europan ocean are considered. As mentioned before implosion should be avoided for many years, see Section 8.10. Furthermore, samples taken from the ocean will never get back to the ocean as they are never removed from the probe, see Subsection 4.2.1. Consequently, organic compounds present in the payload are of low concern.

---

[1]From `http://www.metalspiping.com/titanium-alloy-ti-6al-4v.html` accessed 21/05/2024

Table 11.1: Probability of the probe contaminating the subsurface ocean of Europa [98]

		Type D	Type C	Type B	Type A
	Number of Culturable Organisms on Spacecraft	15000	300	300000	15000000
F1	Total cells/CFUs	1000	1000	1000	1000
F2	Survival of Sterilisation Fraction	0.0001	0.0001	0.0001	0.0001
F3	Cruise Survival Fraction	0.5	1	1	1
F4	Radiation Survival Fraction	0.8	0.0363	0.00003	1×10^{-10}
F5	Probability of Reaching the Ocean	0.505	0.505	0.505	0.505
F6	Probability of Survival and Proliferation	1×10^{-7}	1×10^{-7}	1×10^{-7}	1×10^{-7}
	Product of Factors	3.03×10^{-5}	5.5×10^{-8}	4.55×10^{-8}	7.58×10^{-12}
	Sum of Products	**3.04×10^{-5}**			

For these results, the radiation on the outside of the probe was assumed to be 1 Mrad for the radiation survival fraction. The probability of reaching the subsurface ocean was taken from Section 13.5. The probability of survival and proliferation was lowered by an order of magnitude because of the heat and environment changes the outside of the probe will experience during traversal. The survival of sterilisation fraction was taken from Ref. [98], for highly sterilised components and use of cleanrooms. The relevant other factors were copied from the example in Ref. [98], as they were reasonable and well-supported.

11.4. Manufacturing, Assembly & Integration Plan

A list of all primary components, their supplier, Technology Readiness (TRL) and origin was constructed, which can be seen in Table 11.2. This Table is split up into the transfer stage, lander and probe, and components are listed under their respective stage. Each component type gets a number which will be used in the assembly flow diagram later, see Figure 11.1. Components with A TRL of 7 or lower will be analysed in the technology development phase, this is discussed in more detail in Section 14.1. Whenever possible, off-the-shelf components were used to increase TRL, the scale was taken from NASA.[2] Custom parts were assigned to companies with expertise when needed. Undeveloped and simple isolated mechanisms were left to currently not determined EU aerospace companies to increase mission support and awareness, as discussed in Section 2.5. To give an insight on where components are produced, their origin is also listed.

Table 11.2: List of primary components and their characteristics

Nr.	Component Type	Product Name	TRL	Supplier	Origin
Transfer Stage					
1	Transfer Stage Bus	-	9	ESA	EU
2	Transfer Stage Oxidizer Tank	-	9	ESA	EU
3	Transfer Stage Fuel Tank	-	9	ESA	EU
4	Transfer Stage Thruster	VRM1500-H	6	Sierra Space	US
5	Transfer Stage Fuel Pipes	-	9	ESA	EU
6	Fairing Adapter	-	9	SpaceX and ESA	US
7	Transfer Stage-Lander Coupling	-	9	ESA	EU
8	Transfer Stage IMU	ASTRIX 1000	9	Northrop Grumman	US
9	Lander to Engine Power Cable	-	9	ESA	EU
Lander					
10	ADCS Thrusters	DST-11H	9	Moog	US
11	Reaction Wheels	HR12-50	9	Honeywell	US

---

[2]From https://www.sofeast.com/glossary/what-are-trl-technology-readiness-levels/ accessed 21/06/2024.

Table 11.2: List of primary components and their characteristics

Nr.	Component Type	Product Name	TRL	Supplier	Origin
12	Lander Oxidizer Tank	-	2	ESA	EU
13	Lander Fuel Tank	-	2	ESA	EU
14	Lander Thruster	AMBR 556 N	6	Aerojet Rocketdyne	US
15	MFOV Camera	ECAM-C50	9	MSSS	US
16	NFOV Camera	ECAM-C50	9	MSSS	US
17	LIDAR	LEIA	9	MDA Space	CA
18	Stirling RTG	-	2	NASA	US
19	Lander GPHS RTG	16-GPHS STEM	2	NASA	US
20	Medium Gain Antenna	Waveguide Pipe TTC	9	Beyond Gravity	CH
21	High Gain Antenna	-	9	ESA	EU
22	Lander Coaxial Splitter	Low Power SPDT Switch	8	Radiall	FR
23	Lander Diplexer	X-Band Diplexer	9	WiRan	PL
24	Power Amplifier	SSPA	9	General Dynamics	US
25	Transponder	S/S DST	9	Thales Alenia Space	FR
26	Radiator	-	9	ESA	EU
27	E-Box to Lander Comms Cable	-	9	ESA	EU
28	E-Box CDH	CDH-FS	9	CAVU-UK	UK
29	E-Box Lowering System	-	9	EU Company	EU
30	Seismometer	-	9	NASA	US
31	Fuel Tank Attachment	-	9	ESA	EU
32	Oxidizer Tank Attachment	-	9	ESA	EU
33	Probe Lowering Wheels	-	9	EU Company	EU
34	Probe to Radiator Architecture	-	7	ESA	EU
35	Fuel Pipes	-	9	ESA	EU
36	Probe Hatch	-	9	EU Company	EU
37	Landing Legs Structure	-	9	ESA	EU
38	Landing Legs Damping System	-	7	EU Company	EU
39	Fine Sun Sensor	Leonardo S3	9	Leonardo S.p.A.	IT
40	Coarse Sun Sensor	Solar MEMS ACSS	9	Solar MEMS	ES
41	Star Tracker	Leonardo SPACESTAR	9	Leonardo ASS	IT
42	Magnetometer	ECM	9	JPL	US
43	Lander IMU	ASTRIX 1090	9	Northrop Grumman	US
44	Probe to Lander Power Cable	-	6	ESA	EU
45	Lander PCU	-	9	ESA	EU
46	Lander Bus	-	9	ESA	EU
Probe					
47	Heated Drill Mechanism	-	5	ESA	EU
48	Ice Penetrating Radar	-	6	ESA	EU
49	Drill Motor	-	9	EU Company	EU
50	Drill Bit	-	9	EU Company	EU
51	Probe Finless GPHS RTG	16-GPHS STEM	2	NASA	US
52	Probe CDH	CDH-FS	9	CAVU-UK	UK

Table 11.2: List of primary components and their characteristics

Nr.	Component Type	Product Name	TRL	Supplier	Origin
53	Sonar Communication System	ATM-903 series	6	Teledyne Benthos	US
54	Relay CDH	CP400.85	8	AAC Clyde Space	SE
55	Relay Diplexer	-	5	ESA	EU
56	Relay Antenna	UHF Antenna III	8	EnduroSat	BG
57	Probe IMU	LN-200S	9	Northrop Grumman	US
58	Probe PCU	-	9	ESA	EU
59	Anchor and Cable Mechanism	-	9	EU Company	EU
60	WFOV Ext. Camera	ECAM-C50	9	MSSS	US
61	NFOV Ext. Camera	ECAM-C50	9	MSSS	US
62	Microscope	ECAM-C50 + Narrow FOV lens	8	MSSS	US
63	Thermocouple	-	9	ESA	EU
64	Capillary Electrophoresis System	PISCES	6	JPL	US
65	Life Marker Chips	-	6	ESA	EU
66	Raman Spectrometer	C14214MA	6	Hamamatsu	JP
67	Fluorescence Spectrometer	C10082CAH	6	Hamamatsu	JP
68	UV Spectrometer	C16767MA	6	Hamamatsu	JP
69	Ultrasonic Sonar	Ping360	6	BlueRobotics	US
70	Wet Chemistry Lab	-	9	JPL	US
71	Flashlight	-	9	EU Company	EU
72	Sampling Mechanism	-	9	ESA	EU
73	Thermal Loop Pipes	-	7	ESA	EU
74	Thermal Fluid Pump	-	9	ESA	EU
75	Probe Bus	-	9	ESA	EU

From this table, it is obvious that the assembly process for this mission is a logistic challenge. This is further enhanced by the challenges that come with incorporating RTGs into the assembly. The United States is part of the Treaty on the Non-Proliferation of Nuclear Weapons (NPT), causing the export of RTGs to be subject to many regulations. It is stated that: "Each State Party to the Treaty undertakes not to provide: (a) source or special fissionable material, or (b) equipment or material especially designed or prepared for the processing, use or production of special fissionable material, to any non-nuclear-weapon State for peaceful purposes, unless the source or special fissionable material shall be subject to the safeguards required by this Article."[3] To avoid this process and because the launch site is also located in the United States it was decided to complete full spacecraft assembly in the United States. One advantage of this is that the RTGs will only be integrated in the last stages of the design, which increases personnel safety.

Therefore, the assembly is split up into two phases. During the first phase, many processes will happen at the same time. The spacecraft is mostly assembled and tested at the European Space Research and Technology Centre (ESTEC), which is the European Space Agency's main technology development and test centre for spacecraft, it is situated in Noordwijk, South Holland. Components not assembled here include all thrusters, all RTGs, the fairing adaptor, the probe bus and probe heating pipes. These last two are left to phase two because both of these can only be fully assembled with the RTG present. At the end of phase one, an almost complete system test can be performed, using dummies for the missing components. This will be done at ESTEC and includes tests on mass, size, power consumption, vibrations, operational temperature, radiation doses, pointing accuracy, pointing stability, signal strength, resolution, spectral range and reliability. At the same time, the busses will be replicated and load tested at Airbus Defence and Space in the UK. Materials

---

[3]INFCIRC/140, NPT, Article III, 2.

corrosion resistance will be tested at the Kennedy Space Centre in the US. The ice breaking capabilities will be tested with a replicated probe at the Amundsen-Scott lab in Antarctica, dummy weights and power supply will be inserted. Thruster Delta-V's will be tested at the Marshall Space Centre in the US. Finally, a payload replica will be subjected to concentration detection, sample size, flow particle velocity detection, flow particle direction detection and waterproof tests at the Ocean Worlds Lab in the US.

After the spacecraft and dummy systems pass these tests, the stages will be transferred to the Goddard Space Flight Centre. Here they will be fully assembled and tested. The probe specifically will be tested on water and air tightness before being sterilised and inserted into the lander and connecting all stages. Next, a total system test will be performed on: mass, size, power consumption, vibrations, operational temperature, radiation doses, pointing accuracy, pointing Stability, signal strength, reliability and loads. Even though all assembling will be done in specialised clean rooms the system will be subject to a final sterilisation before launch. Lastly, an organism inventory will be taken from the production sites to avoid false positives when detecting organisms on Europa. The assembly process flow chart can be seen in Figure 11.1.
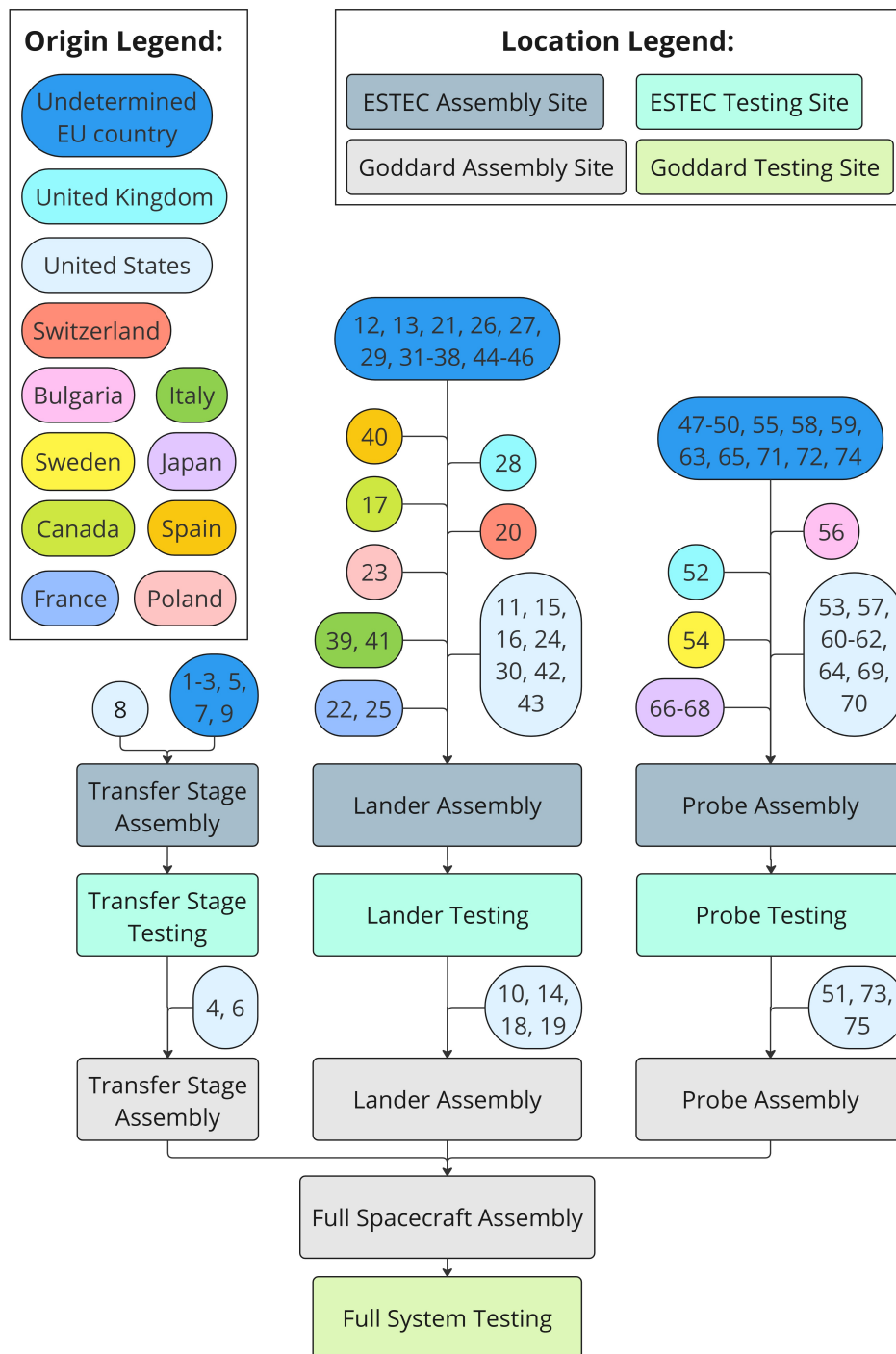

Figure 11.1: Assembly process flow chart for mission spacecraft

Due to the usage of radioactive materials, certain measures need to be taken to ensure the safety of the personnel and the population. Luckily, RTGs will not explode like nuclear reactors might. They do need to be assembled with care, however. Plutonium decays into uranium which releases alpha radiation (helium ion), it might also decay and release gamma radiation, however, this is negligible compared to alpha radiation. Alpha radiation is characterised by its high energy and low penetration, it can not penetrate the skin through protective clothing. Therefore it is no cause for concern. Personnel should be supplied with protective clothing and briefed about the danger of alpha radiation. The RTGs will not pose a problem for the general public unless the launch vehicle explodes. Even then the RTG will likely still be properly protected[4], which will render it safe to be close to it. Nevertheless, in such a scenario emergency broadcasts should be shown to the public about RTG safety.

11.5. Sustainability Efforts

A project's sustainability can be evaluated by looking at its economic, social and environmental impacts. By optimising the mission's consideration of these three pillars a high mission development sustainability can be reached. The efforts regarding sustainability during the AlienDive mission are summarised in Figure 11.2.
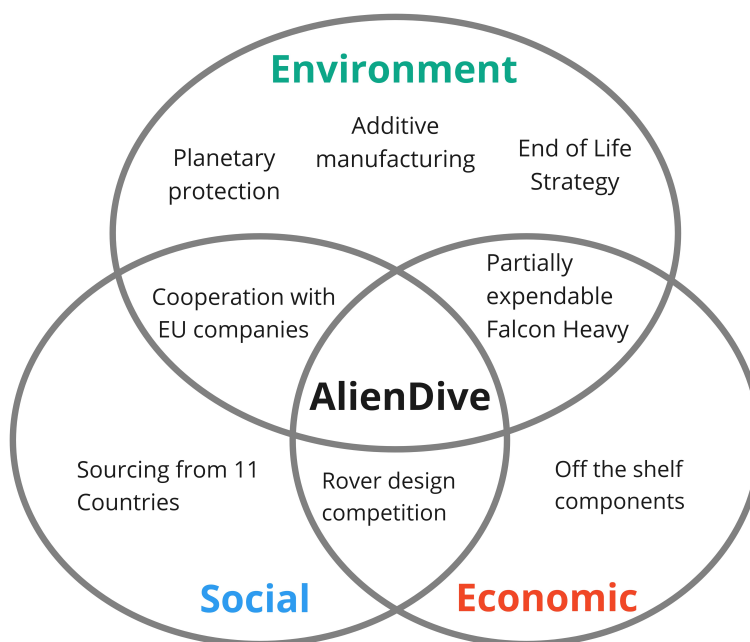

Figure 11.2: Sustainability efforts in AlienDive

From this figure it is clear how AlienDive's efforts impact the different sustainability pillars. These efforts are listed and elaborated on below.

- To minimise mission development costs, off-the-shelf components were used whenever available.
- The partially expendable Falcon Heavy was selected to minimise launch cost and materials wasted on fully expended rockets.
- Additive manufacturing is used for the main spacecraft structures to minimise material waste.
- Planetary protection measures are taken to avoid inadvertently contaminating Europa.
- An end-of-life strategy is formulated to minimise ecological impacts on Europa.
- Cooperation with EU companies for the development of simple systems was decided on to source products locally and increase international relations.
- In this phase of the design, companies located in 11 different countries are already selected to be part of this mission, increasing international cooperation.
- An open rover design competition will be organised to give opportunities to universities and small companies to be involved in this mission and to drive down internal design costs.

---

[4]From   https://cosmos.esa.int/web/ulysses/rtg:~:text=Safety%20Design,those%20expected%20from%20most%20accidents., accessed on 19/06/2024

12 Cost Analysis

12.1. Cost Breakdown

To determine the cost of a mission many aspects need to be taken into account. It does not solely include the cost of design and production of the subsystems but also many auxiliary costs, such as integration of the entire assembly, management and ground equipment costs. Since this mission is still early in its design stages and therefore not all specific components that are to be used for the mission are known, it is difficult to assess the cost of all the mission components in a bottom-up manner. Because of this, the best method to determine the cost is to use different cost estimation methods. The best cost estimation method is parametric cost estimation, which uses historical data of similar missions to develop a regression based on different inputs, such as weight and power. However, as this mission is highly unique, there is not a lot of data on past missions and it is thus hard to find parametric cost estimation relationships (CERs) for all aspects of the mission, which is why next to CERs, also analogous estimation and self-made substantiated estimations are used. Unlike the order in the rest of the report, the cost estimation for the lander is presented first, followed by the transfer stage and subsequently the the probe. This is because the transfer stage estimation depends partly on the lander cost estimation. After all three subsystems are analysed, the cost for other mission aspects is also examined.

12.1.1. Lander

For the lander, the cost of the individual subsystems and the cost of integrating them into one whole assembly is taken mainly from parametric CERs from an article that has very detailed cost estimation relationships for spacecraft subsystems [99]. This article stems from 1992, which means that inflation has to be taken into account to convert the value of the budget from 1992 to 2024. The total inflation is 123.56 %, which means that any cost obtained from these relationships shall be multiplied by 2.2356 to get its value for the current time period.[1] One issue with using the CERs in this article is that they are mainly targeted for satellites, which in many aspects are substantially different to landers. For example, the cost of a propulsion subsystem for a lander cannot be estimated using relations for a satellite, as they act completely differently.

For some subsystems, however, especially in this mission, the architectures are similar to satellites, meaning that the CERs can be used. The reasons why the CERs of these subsystems can be used for the lander cost estimation are explained in the following paragraph. Unlike many other CERs, these do not only take mass into account as an input but also other variables specific to each subsystem. These are also explained below.

Before explaining the CERs for each subsystem, there is one final note. For each subsystem, there are generally three CERs. The first one is called Hardware Engineering and it is a nonrecurring cost. It entails the costs related to design, development, planning studies etc. [99], also known as "Design, Development, Testing, and Evaluation" (DDT&E) [100]. The second one is called nonrecurring Hardware Manufacturing, which includes fabrication, assembly, tests, subsystem tooling etc. The last one is recurring hardware manufacturing and contains fabrication, assembly, integration, tests, etc. The difference between the latter two is that the first one is more related to the manufacturing of things during the design stage, which includes prototypes and other tools. For example, this could include manufacturing of dies that are needed to produce a specific metallic part. As soon as these are made, they can be used indefinitely and no more money has to be invested to make more. The recurring manufacturing costs address the costs related to actually manufacturing a subsystem. This means that if you need multiple copies of a certain subsystem, as for a Starlink mission, where many individual satellites are made, then this recurring cost has to be multiplied by the number of copies needed.

The first subsystem, whose CERs for satellites are transferable to the lander is the thermal control subsystem. The range of steady-state temperatures within the spacecraft of the missions used to develop the CER for this subsystem is $-10\,°$ C to $40\,°$ C. The temperature range of the lander is $7\,°$ C to $21\,°$ C, as explained in Section 7.5 which fits within this range. The inputs for the CERs are the maximum steady state temperature and the minimum steady state temperature in Fahrenheit, the mass of the subsystem in pounds and the design life in months and whether it is a NASA mission or not.

The recurring manufacturing cost CER for this subsystem is shown below:

$$C_{th_{HE}} = 1.86 \cdot M_{SC}^{0.60} \cdot M_{TC}^{0.33} \cdot 0.48^{NASA} \tag{12.1}$$

---

[1]From `https://smartasset.com/investing/inflation-calculator`, accessed on 15/06/2024.

M_{SC} is the mass of the spacecraft, M_{TC} is the mass of the thermal system and the last term is an indicator of whether it is a NASA mission or not. In case it is not a NASA mission, the exponent is zero and in case it is a NASA mission the exponent is one, meaning that the cost reduces by a factor of 0.48. The other CERs for this and other subsystems are not explained further but can be found in the aforementioned article from 1992 [99].

The second subsystem for which CERs are used is the GNC subsystem, as the chosen sensors and actuators for this mission are commonly used in satellite missions as well. For this subsystem, there are CERs specific to the sensors, as well as to the actuators.

The third and final subsystem for which the CERs are applicable is the communications subsystem. The communication of the lander to Earth is identical to that of a satellite around Europa to Earth. This is because there is no atmosphere on Europa, which means that there is no additional signal loss on the transfer to Earth, compared to a satellite orbiting Europa.

For three of the remaining subsystems, the cost is estimated by using the same portion that each subsystem costs in a lander mission to Mars [101]. According to NASA, structures account for 28 % of the total subsystem cost and CDH for around 7.8 %. Furthermore, the propulsion subsystem is around 1.5 times more expensive than the GNC actuators. Taking all of this into account, it is possible to estimate the cost of these three subsystems, such that in the end, the subsystems have the correct cost portions compared to the total cost. According to the same NASA study, the power subsystem only accounts for four per cent of the cost. This is not the case in this mission, as an expensive RTG is used. That is why the power subsystem cost is treated separately. According to early estimates the design and production of the lander RTG is around 119 M$. Adding all of the previous information together in a table leads to the following result for the lander subsystem production cost.

Other than the development and production of the individual subsystems, there are costs regarding the integration and assembly of the lander. These are also estimated with CERs [99]. The entire cost is shown in Table 12.1.

Table 12.1: Production and Assembly Cost of Lander

Subsystem	Dry Mass [lbs]	Cost FY1992 [M$]	Cost FY2024 [M$]
Structures	957.03	62.17	138.99
Thermal	37.36	1.99	4.44
ADCS (Sensors)	144.71	20.24	45.25
ADCS (Actuators)	117.42	28.89	64.58
Propulsion	122.45	43.33	96.88
Communications	233.93	10.12	22.62
Payload	35.94	38.86	86.87
CDH	9.37	16.4	36.67
Power	187.87	-	202.9
Production Cost	-	-	699.29
Integration and Assembly	-	3.37	7.54
Total Cost	-	-	**706.83**

12.1.2. Transfer Stage

For the transfer stage, the production costs are calculated using a CER, which is valid for propulsive stages using storable (non-cryogenic) propellant, which fits exactly within the characteristics of the transfer stage [100]. This CER is based on the dry mass of the entire stage and gives the entire cost for the entire transfer stage:

$$C = 1.8650 \cdot M_{s/c}^{0.4782} \tag{12.2}$$

With a transfer stage dry mass of 898.86 kg, the production cost comes at $48.210M\$$. The development costs are estimated based on the average ratio of development costs to production costs of the lander, which turns out to be 3.61. This means that the development cost of the lander is estimated to be $174.041M\$$. Taking into

account that this estimate is from 2012, and the total inflation since then is 36.63 %, the total cost comes out to be $303.66M\$$.

12.1.3. Probe
For the probe, an analogous estimation was done, since this is a unique mission, that has not been researched enough to develop CERs. The estimated cost is based on the tunnelbot concept, which uses a similar probe to penetrate Europa's ice shell [72]. Conveniently, the tunnelbot also uses finless RTGs, which means that comparing this mission to theirs can lead to quite accurate cost estimations. Since there are accurate cost estimates for the RTG of AlienDive's probe, only the cost of the other subsystems of tunnelbot are compared to the probe. In 2018, the tunnelbot subsystems, excluding the power subsystem, cost $241M\$$, which means that it costs $301M\$$ in 2024. The probe weighs a total of 553.8 kg, whereas the tunnelbot weighs 750 kg. Assuming that the cost varies linearly with mass, this means that the probe would cost $222.28M\$$. Adding to that the already estimated development and production cost of the RTG, which is $248.1M\$$, the probe turns out to cost $470.38M\$$. The cost breakdown of the subsystems of the probe is analysed in more detail in the cost breakdown tree, which is shown in Figure 12.1. For the subsystems, the same percentages of total cost are used as for the tunnelbot.

12.1.4. System Level Costs
Next to the development and production costs of the three vehicles, there are other costs that need to be taken into account that substantially influence the mission. These are related to ground operations and tests etc.. A cost overview for these activities is shown in Table 12.2. These are again calculated with CERs from 1992 [99]. The launch cost is based on the average cost for a Falcon Heavy launch.[2]

Table 12.2: Cost of Mission Level activities

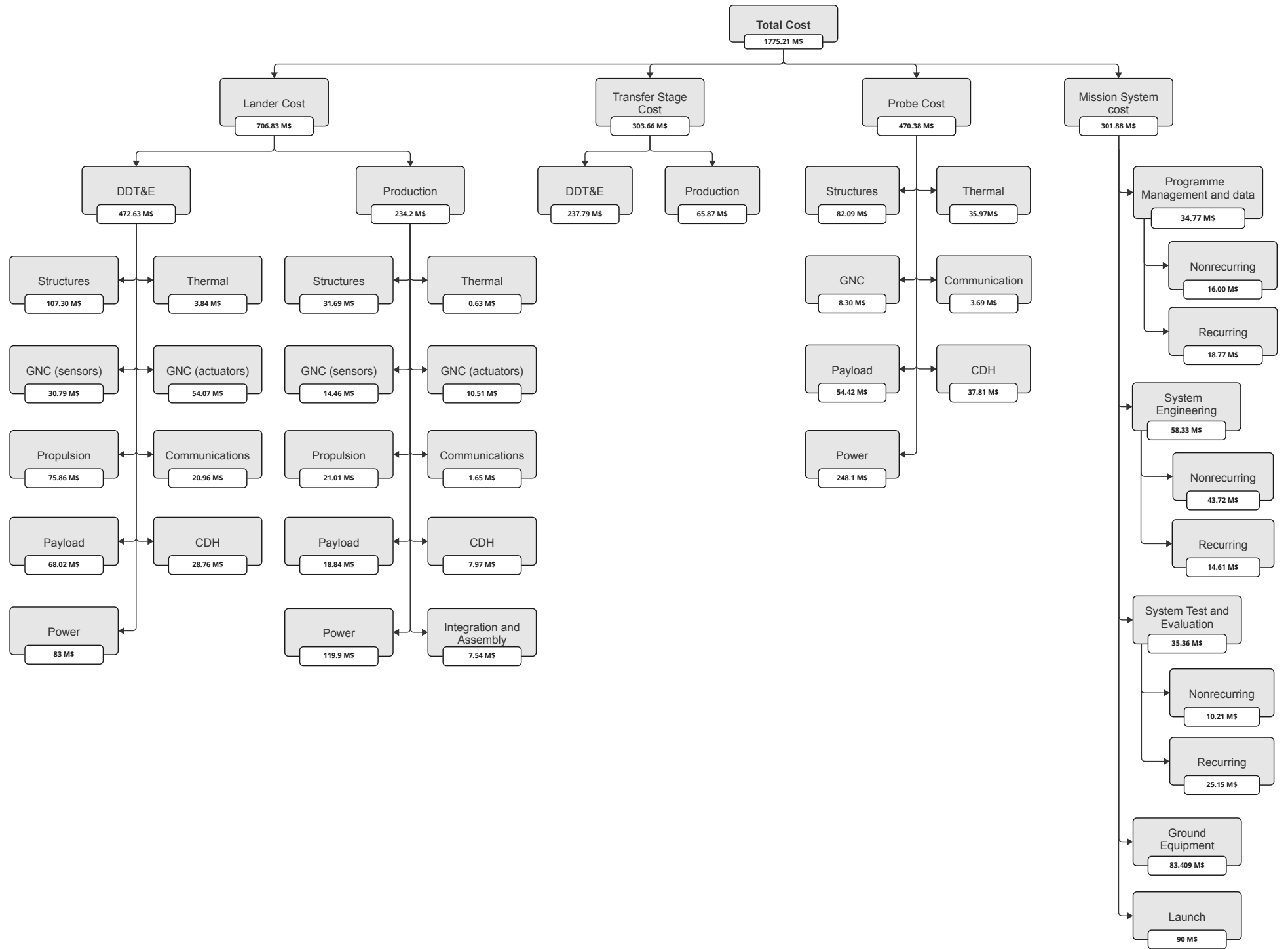| System Level Whole Mission Cost	Cost FY1992 [M$]	Cost FY2024 [M$]
Programme Management and data	15.55	34.77
System Engineering	26.09	58.33
System Test and Evaluation	15.82	35.36
Ground equipment	37.31	83.41
Launch	-	90
Total System Level cost	**94.77**	**301.88**

12.1.5. Cost Breakdown Tree
To visualise the entire cost structure, that was explained beforehand, a cost breakdown tree is developed. This is shown in Figure 12.1. As can be seen, the total cost of the mission is 1.75 billion dollars. This is higher than the cost of an ESA large class mission, an example of which is JUICE (1.2 billion dollars).[3]

---

[2]From `https://nstxl.org/reducing-the-cost-of-space-travel-with-reusable-launch-vehicles`, accessed on 19/06/2024.
[3]From `https://spaceanddefense.io/esas-director-general-bullish-on-juices-mission-to-jupiter/`, accessed on 15/06/2024.

Figure 12.1: Cost breakdown tree of the AlienDive mission

13 Verification & Validation

Verification and validation are a critical part of the design process, ensuring that the final product complies with the requirements and performs how it is supposed to. To do this, multiple elements of the design process must be investigated. First, the main assumptions of the design, their effects and justification are listed. Next, the tools used for the design are tested on their reliability. Afterwards, the product is in compliance with the requirements. Finally, while validation of a preliminary design is difficult, the validation plan is revised.

13.1. Assumptions

In this section, the main assumptions made during the design are listed, their effects are explained, and the validity of the assumptions is discussed.

Astrodynamics

- **ASM-AST-1**: *The burns of the transfer stage are impulsive shots.*
  With this assumption, the full burn occurs instantaneously, thus resulting in no gravitational losses. This assumption is valid due to the choice of the engine, as it has a high mass flow and low burn times.

- **ASM-AST-2**: *Burns of the transfer stage are performed parallel to the orbiting body.*
  Due to this assumption, no gravity losses have to be taken into account. This assumption is valid for the same reasons as ASM-ORB-01, being the low burn times.

- **ASM-AST-3**: *The Falcon Heavy launcher provides the required Delta-V for the VEEGA trajectory.*
  The transfer stage then only has to deal with operations around Jupiter. Since the launch mass of the spacecraft is below 15 tons[1], the Falcon Heavy is able to provide enough Delta-V for injection into the trajectory

- **ASM-AST-4**: *The same sequence of gravity assists around Ganymede and Callisto is flown as done in the Europa Lander 2012 report [25].*
  Due to these flybys, the amount of Delta-V required for Europa Orbit Insertion is reduced. The orbits of Europa and Ganymede are in orbital resonance, meaning the configuration repeats itself on a regular basis. While the orbit of Callisto is not in a constant ratio with the others, it is likely that a trajectory is available with similar reductions in required Delta-V.

- **ASM-AST-5**: *The same 10° orbit inclination change is done around Europa as was used in the Europa Lander 2012 report [25].*
  This is because similarly to the Europa Lander 2012 report this mission requires a near-polar reconnaissance orbit. As the same flybys between JOI and EOI are used, it can be assumed that with DSM during the trajectory, the orientation of the spacecraft can be altered in the same way to reduce the needed inclination change to only 10°.

- **ASM-AST-6**: *Earth's, Jupiter's, and Europa's orbits are in approximately the same plane.*
  Earth and Jupiter have an inclination with respect to the Sun's equator of 7.25° and 6.09°, respectively. Then, Europa's orbit is negligibly inclined 0.47° relative to Jupiter's equatorial plane. Thus, it can be assumed that these inclinations are negligible for the communication time between Earth and a spacecraft in orbit around Europa.

Propulsion

- **ASM-PROP-1**: *The propellant tank does not carry any loads except its own weight and pressure loads.*
  As a result, the structure of the propellant tanks can be significantly lighter. This assumption is justified, as the primary structure is designed to carry all loads, and the tanks are not part of this structure.

Thermal

- **ASM-TCU-1**: *The temperature calculated in Equation 6.11 is taken as the temperature of the entire spacecraft and not one particular part of it.*

---

[1]From `https://space.stackexchange.com/questions/25452/how-much-payload-can-falcon-heavy-reusable-lift`, accessed 19/06/2024

The RTGs are positioned in three different spots which will distribute the heat. Moreover, the heat could be spread across the whole spacecraft using heat sinks that are attached from the spacecraft to sufficiently enough components.

- **ASM-TCU-2**: *Any heat generated from electronics is assumed to be spread across the spacecraft uniformly and is not concentrated.*
  The RTGs are positioned in three different spots which will distribute the heat. Moreover, the pumped fluid loop could be activated to distribute the heat more if needed.

- **ASM-TCU-3**: *The view factor will not be taken into account in the calculation.*
  The temperatures calculated This is a conservative assumption as the limiting case is the upper range of the temperature and not the lower range. In the case where the lower temperature range is limiting it will be an under-conservative estimate however, the primary source of heat is the RTG and not the heat flux.

- **ASM-TCU-4**: *The temperature of the ice is taken to be close to the melting temperature of ice*
  This assumption is made as it is assumed the ice around the probe will have time to heat up to that temperature while the probe is still attached to the lander and being lowered to the ice. As the probe goes deeper, this assumption comes closer to reality because the temperature increases until the probe reaches the subsurface ocean.

Power

- **ASM-POW-1**: *The RTG degredation, is only due to the fuel decay.*
  RTGs degrade over time due to the decay of the fuel pellets. It is useful to take this as a first estimation for a conceptual RTG [40]. This can later be changed if necessary since the lifetime has quite a large margin compared to the estimated lifetime.

- **ASM-POW-2**: *The RTGs will decay following the highest probability path.*
  When plutonium decays there is a big chance to emit alpha radiation, however, this is not the only option. Gamma decay can also happen, which results in a different decay path[43]. Due to the high probability of alpha decay, this is assumed to only happen for the EOL calculations.

Ice traversal

- **ASM-TRV-1**: *The ice shell thickness does not exceed 30 km.*
  Critical to the success of the design, the probe is designed so that it can reach the subsurface ocean. The thickness of the icy crust is uncertain, one paper on the geodynamics of the shell suggests a thickness of around 15-18 km [77], while a NASA study predicts a best estimate of 24.3 km [2]. It is thus deemed a valid design choice to design for 25 km with a 20% margin, thus designing for 30 km of thickness. In addition, due to the probe being mostly autonomous and disconnected from the probe, the design can be easily adjusted for different thicknesses, once more detailed information becomes available based on data from the JUICE or Europa Clipper missions.

Hydrodynamics

- **ASM-HYD-1**: *The thickness of the mushy ice-ocean interface equals 5% of the ice shell thickness.*
  This parameter determines in part the required tether length and would limit mission results if underestimated. Based on models of the ice-ocean interface, the interface could take up to a maximum of 5% of the ice shell thickness [76]. It is thus deemed valid to design the cable for this worst-case layer thickness

- **ASM-HYD-2**: *The magnitude of the shear force in the tether does not exceed the weight of the probe.*
  In case the cable gets pinched by the differential movement of layers, a shear force could form in the tether. Since sudden shear in the ice layer, due to for example faults, occurs in the upper layer, the risk of these large events on the tether around the ice-ocean interface is minimal [76]. Furthermore, the margin on the cable length allows for slack in the cable to prevent these loads from occurring. If a current or object in this interface or the ocean could cause a shear larger than the weight of the probe, the probe itself should also move, causing tension in the cable rather than shear.

Guidance, Navigation & Control

- **ASM-GNC-1**: *The spacecraft's vertical axis is a principal axis*
  This assumption reduces the mass moment of inertia around the z-axis and the product moments of inertia to zero, providing a sufficiently accurate initial estimate for the disturbance torques.

- **ASM-GNC-1**: *The spacecraft's mass is uniformly distributed*
  This assumption simplifies the calculation of the mass moments of inertia and is sufficient for an initial estimate of the disturbance torques.

- **ASM-GNC-1**: *Cyclic disturbance accumulates in 1/4 of the orbit and is sinusoidal*
  The cyclic disturbances can be simplified by assuming it accumulates in 1/4 of the orbit and is sinusoidal [48]. This gives a good first estimate of the momentum storage required.

Communications

- **ASM-COM-1**: *The system noise temperature of the lander is equal to 389.54 K.*
  The system noise temperature is assumed to have the same value as the Juno spacecraft [55] as this parameter is challenging to estimate. The Juno spacecraft is considered to be similar to the AlienDive lander; therefore, the lander is expected to have a similar system noise temperature.

- **ASM-COM-2**: *The $\frac{Eb}{No}$ required for through-ice communication is the same as the downlink $\frac{Eb}{No}$ requirement for the lander.*
  For AFSK and GMSK modulation, estimating the $\frac{Eb}{No}$ required is challenging. The downlink requirement for the lander is considered a conservative value.

- **ASM-COM-3**: *The system noise temperature of the RF relay transceiver modules is equal to 600 K.*
  The system noise temperature is assumed to have the same value as the preliminary relay puck design by JPL [88]. This value for the system noise temperature is regarded as conservative.

- **ASM-COM-4**: *The phase modulation index of the RF relay transceiver modules is equal to 90 °.*
  The phase modulation index is assumed to have the same value as the preliminary relay puck design by JPL [88].

- **ASM-COM-5**: *Acoustic signals can propagate through the mushy layer between the subsurface ocean and ice crust, should one exist.*
  Acoustic signals can propagate for several kilometres through water, although they experience greater attenuation in ice. Research should be done on the propagation of acoustic signals in mushy liquid-ice water bodies.

- **ASM-COM-6**: *The UHF diplexer to be designed in-house has the same mass, power and size characteristics as the selected WiRan X-Band Diplexer present in the lander*
  Commercially available UHF diplexers for space applications do not exist. Therefore the UHF diplexer needs to be designed in-house. A more accurate estimation would require a more detailed design analysis.

Command and Data Handling

- **ASM-CDH-1**: *The total command data rate to the lander and the probe is equal to 2 kbps.*
  The total command data rate is assumed to have the same value as the maximum command data rate of the Juno spacecraft [55], as estimating this parameter accurately would require a more detailed design analysis. The Juno mission is considered to have multiple similar elements to the AlienDive mission, therefore, the lander and the probe are expected to receive similar command data rates.

- **ASM-CDH-2**: *The command data is evenly distributed over all subsystems.* Some subsystems might need to receive more command data than other subsystems. A more accurate estimation would require a more detailed design analysis.

- **ASM-CDH-3**: *The total housekeeping data rate is equal to 10 % of the average probe scientific data rate for both the lander and the probe.*
  For the Juno spacecraft, housekeeping data is 1.25 % of the scientific data gathered. Therefore, housekeeping data for the AlienDive mission being 10 % of the scientific data is considered a conservative estimate.

- **ASM-CDH-4**: *All subsystems (except payload) have an equal share in the generation of the total housekeeping data.*
  Some subsystems might generate more command data than other subsystems. A more accurate estimation would require a more detailed design analysis.

Structures

- **ASM-STRUC-1**: *For natural frequency estimations, the structure is modelled as a simple beam with a point mass on top.*

This assumption simplifies the calculation process while being the most conservative approach to estimating the natural frequency. This means the actual natural frequency is higher than the calculated value and thus safer.

- **ASM-STRUC-2**: *Torsional loads during the mission are negligible for the transfer stage and lander.* Since no torsional loads are specified by the launcher, and only small torques are applied by the attitude control system, these loads are assumed negligible meaning the shear load is slightly underestimated. Shear was however not found as the main failure mode for any of the structural elements, and the hollow cylindrical rods are efficient against torsion.

13.2. Tool Verification

The design of a space mission is very complex and requires dealing with many relations between subsystems. To effectively design tools are needed for calculation and modelling. It is important to verify that these tools do not contain errors, as these errors

13.2.1. Excel

The Excel design spreadsheet is the main tool used for system integration, being set up in a way that every subsystem can use and provide constantly up-to-date values for other subsystems to use. To ensure this happens smoothly, a branched structure is used where each subsystem works in different sheets, with one system overview sheet which is the central database. By running all values through this central database, errors are easily detected and isolated.

Unit tests are performed on individual cells of the sheet. Since the formulas are inserted by hand, visual inspection is already performed. For larger formulas that are not as easily read, these cells are verified using comparison to a manual calculation using the same inputs, with the outcomes of the calculations equalling each other with an error dominated by machine precision. However, with the amount of calculations done in a design project of this scale, it is extremely time-consuming to test every single cell. Since time is limited in this project, larger (sub)system tests are performed to make up for this. Two different types of system tests are performed. The first type of analysis is performing sensitivity analyses on the different subsystems. This was already done in Chapter 9 to investigate the effect of small design changes, but is also used to check that a modification of an input parameter results in a logical output. For example, increasing the height of the lander should increase the mass of the structure, and decreasing the transfer stage dry mass should result in a lower required propellant mass. Furthermore, simple edge-case scenarios are tested, for example, if the shear load in a beam element is zero, the required thickness to carry shear should also be zero.

The second method used is convergence analysis of iterative procedures. Again taking the example of the transfer stage, since an increase of the mass requires more propellant, larger propellant tanks are required, which then again increase the mass of the system. If the calculations are correct, this should converge to a near-constant value after a few iterations. A graph showing an iteration of the propellant mass can be seen in Figure 13.1.

The third method used for verification is to use the CAD model and the CAD software to compare the mass and volume values of individual components. For example, the estimated mass of the communications disk was found to be lower than it should be, allowing correction. A larger mistake found with this method is the volume of the fuel tanks. The designed tank volume turned out to be larger than required, resulting in a significant mass reduction after correcting the error. This method does rely on a third-party tool, the verification of which is discussed in Subsection 13.2.3.
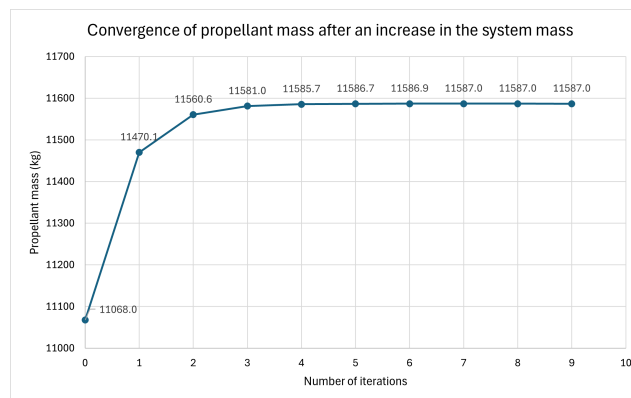

Figure 13.1: Propellant mass value for an increasing number of iterations.

Finally, another possible type of verification would be to compare the model's output with actual flown spacecraft. However, this approach is challenging because our mission is unconventional, and there are no previous missions sufficiently similar to provide a valid comparison.

13.2.2. Python

Next to Excel tools, python was used for more complex modelling. It is again important that these tools are verified and no errors are found within them. The first step in the verification of these tools is again to perform unit tests. Python functions were used in four different subsystems to estimate parameters that were used for the final design: Communications, Thermal, Ice traversal and Astrodynamics. An overview of the unit tests performed is found in Table 13.1

Table 13.1: Overview of the unit tests performed on the Python functions.

Subsystem	Function Description	Unit Test Description	Expected Outcome	Result
COM	C-1. Determines the required maximum relay distance and number of required relays.	Test the link budget equation for the relays by manual calculation.	Calculated energy per bit to noise power spectral density should match code output	Pass
	C-2. Sizes the antenna angle for optimal aperture efficiency	Test the equation for the antenna aperture efficiency by manual calculation.	Calculated aperture efficiency matches code output within machine precision.	Pass
TCU	T-1. Calculates the required insulation thickness	Test all four intermediate equations by manual calculation	Calculated values should match code output within machine precision.	Pass
TRV	I-1. Estimates the time it takes to penetrate ice crust.	Test the equation for the time with a heated drill by manual calculation.	Calculated value should match code output within machine precision.	Pass
	I-2. Estimates the time it takes to reorient in the ice.	Test the equation for the wall melting speed and the orientation time by manual calculation.	Calculated value should match code output within machine precision.	Pass
AST	A-1. Models the spacecraft trajectory in freefall	Test all calculation steps in the model.	Calculated value should match code output within machine precision.	Pass
	A-2. Models the spacecraft trajectory in powered descent	Same procedure as for freefall	Calculated value should match code output within machine precision.	Pass
	A-3. Models the spacecraft trajectory during landing	Same procedure as for freefall	Calculated value should match code output within machine precision.	Pass

The unit tests cover most of the code used in the project, but some elements of the code cannot be directly verified. For example, some functions from the Numpy package are used, which cannot be fully verified within the time limits of the project. However, these packages are widely used and receive regular updates, and it is thus deemed safe to assume there to not be any errors in these functions. In addition to the unit tests, system tests were performed on the thermal and astrodynamics subsystems as those functions included some form of iteration or simulation. An overview of these system tests is found in Table 13.2

Table 13.2: Overview of the system tests performed on the Python functions.

Sub-system	System Test Description	Expected Outcome	Result
TCU	Perform sensitivity analysis on the required insulation for different input temperatures	Lower temperatures lead to increased insulation thickness	Pass
AST	Perform initial value tests on the entire simulation	The time for descent and landing heavily depends on the velocity at the start of powered descent, which is determined by the initial altitude, velocity, and gravitational acceleration.	Pass
AST	Perform sensitivity analysis on the starting mass for powered descent and landing	For higher or lower starting masses, the expelled propellant is also correspondingly higher or lower.	Pass

13.2.3. Third Party Software

The verification of third-party software, while important, is less critical to be performed by the design team. For the design of the mission, the following third-party software was used:

- 3DExperience/CATIA
- General Mission Analysis Tool (GMAT)

Since these external programs are commercially or freely available, it is deemed safe to assume that these products have also been extensively tested for proper performance. Care was however taken during the entire design process to inspect whether the results of these programmes were logical. In addition, prior to the use of these tools, it was assessed if the program was designed to deal with parameters similar to the AlienDive mission, and if these parameters were within the boundaries of the system.

13.3. Product Verification

In this section, the verification of the product with respect to the requirements is described. First, a compliance matrix is presented. Afterwards, the strategy for verification after production is described.

13.3.1. Compliance Matrix

The requirements compliance matrix can be found in Table 13.3. This includes only top-level user requirements from Section 2.2. The method of verifying each requirement is denoted by letters A, I, D, and T. They stand for analysis, inspection, demonstration, and testing, respectively.

Table 13.3: Compliance matrix of the AlienDive mission

Identifier	Requirement	Check	Justification	Method
AD-SCI-01	**The mission shall be able to unambiguously detect life.**	✓	Science-traceability matrix (Table 4.1)	A
AD-SCI-02	**The mission shall provide imagery of Europa's subsurface ocean and the ice-ocean interface.**	✓	Camera are included (Section 4.2)	I
AD-PERF-01	**The mission shall deliver a probe to Europa's subsurface ocean.**	✓	Probe includes a drill (Section 8.3)	A
AD-PERF-02	**The probe shall enable sampling and analysis of both ice shell and ocean material.**	✓	The probe includes a sampling mechanism	D
AD-PERF-03	**The probe shall operate autonomously.**	✓	Autonomous operation with commands	D
AD-PERF-04	**The probe shall operate for a minimum of a year.**	✓	Lifetime is longer (Section 8.3)	A

Table 13.3: Compliance matrix of the AlienDive mission (Continued)

AD-PERF-05	**The system shall be able to communicate with Earth.**	✓	Link budget (Subsection 7.7.6)	A
AD-SCH-01	**The mission shall launch no later than 2035.**	✓	It launches 2034(Section 5.2)	D
AD-SCH-02	**The probe shall arrive at Europa within 7 years after launch.**	✓	6.1 years	A
AD-SAF-01	**The use of hazardous materials for personnel involved shall be minimized.**	✓	RTG are added to the assembly at the end (Chapter 11)	I
AD-SAF-02	**In case radioactive materials are used, a plan shall be put in place to minimise risk to personnel and the population.**	✓	A plan was created (Chapter 11)	I
AD-REL-01	**The probability that a probe is delivered to the subsurface ocean shall be higher than 50%**	✓	Reliability is above 0.5 (Section 13.5)	A
AD-SUST-01	**The mission shall comply with the COSPAR Policy on Planetary Protection.**	✓	COSPAR regulations have not been violated (Section 11.5)	A
AD-SUST-02	**A clear end-of-life strategy shall be included in the mission design.**	✓	Shown after every system	I
AD-SUST-03	**In case radioactive materials are used, a plan shall be put in place to minimise environmental impact.**	✓	This was made (Section 11.5)	A
AD-SUST-04	**The spacecraft shall contain at least <10> % of reused materials.**	✓	Titanium is reusable (Section 11.5)	I
AD-SUST-05	**A radioactive propulsion system shall not be used.**	✓	Chemical propulsion (Section 6.2)	I
AD-ENG-01	**The landed dry mass of the system shall not exceed 1,500 kg**	✓	1367.5 kg (Section 5.5)	I
AD-ENG-02	**The total system shall be launched in a single Falcon Heavy or SLS launch.**	✓	Launch in Falcon Heavy (Section 5.1)	A
AD-COST-01	**The total cost of the mission, excluding launch and operations, should be within that of an ESA Large class mission.**	Fail	1.7 billion USD, more investors must be found (Chapter 12)	A
AD-LAND-01	**The mission shall land a lander on Europa's surface.**	✓	Lander present, sufficient amount of Delta-V	A

13.3.2. Verification After Production

While compliance with the requirements has been mostly reached on paper, it is important to verify compliance with the requirements after and during the production process described in Section 11.4. Product verification, therefore, must be performed to ensure that the end product meets the user, system and subsystem requirements.

Four main methods for conducting product verification are listed below.[2]

- Analysis: Verify that the product meets the requirement using mathematical models and/or analytical techniques.

- Demonstration: Verify that the product meets the requirement by showing how the product performs.

- Inspection: Verify that the product meets the requirement by visual examination or taking product measurements.

- Test: Verify that the product meets the requirement by testing the product.

---

[2]From `https://www.nasa.gov/reference/5-3-product-verification/`, accessed 17/05/2024

Instead of assigning the verification methods, specific facilities, expected availability, and estimated cost to each requirement, these will be more generally assigned to the parameters that the requirements encompass. The final result is shown below in Table 13.4. The second column shows what unit the parameter is going to be measured in and verified.

Table 13.4: Verification method(s), test(s), and facilities for each parameter [7].

Parameter	Unit	Method(s)	Tests	Facilities
Mass	kg	Inspection	Weigh product	ESA Test Center, *Noordwijk, Netherlands*
Size	m^3	Inspection	Measure dimensions	ESA Test Center, *Noordwijk, Netherlands*
Power Consumption	W	Demonstration	Connect the instrument and measure power consumption	ESA Test Center, *Noordwijk, Netherlands*
Loads	g	Test	Static test	Marshall's Structural Strength Test Lab, *Huntsville, Alabama*; Airbus DS, *Stevenage, UK*
Vibrations	Hz	Test	Hydraulic shaker test	SEC Mechanical Vibration Facility, *Cleveland, Ohio*; ESA Test Center, *Noordwijk, Netherlands*
Operational Temperature	K	Test	Thermal balance test	Johnson Space Center Thermal-Vacuum Test Facilities, *Houston, Texas*; ESA Test Center, *Noordwijk, Netherlands*
Radiation dosis	Sv	Test/Analysis	Radiation test	NASA Space Radiation Lab, *Upton, New York*; ESA Test Center, *Noordwijk, Netherlands*
Corrosion-resistance	mm/yr	Test/Analysis	Chemical test	KSC Corrosion Engineering Lab, *Cape Canaveral, Florida*
Waterproofness	-	Demonstration/ Test	IP-rating test/submerge in water	MASER Engineering, *Enschede, Netherlands*; Ocean Worlds Lab, *Pasadena, California*
Pointing Accuracy	arcsec	Test/Analysis	Pointing test	ESA Test Center, *Noordwijk, Netherlands*
Pointing Stability	arcsec/s	Test/Analysis	Pointing test	ESA Test Center, *Noordwijk, Netherlands*
Signal Strength	dB	Test/Analysis	Send signal and measure strength	ESA Test Center, *Noordwijk, Netherlands*
Ice Breaking Capability	km	Demonstration/ Analysis	Demonstrate on block of ice and analyse for thicker ice	Amundsen-Scott Station, *Antarctica*, Station McMurdo, *Antarctica*
ΔV	km/s	Test/Analysis	Static fire test	NASA Marshall Space Flight Center, Huntsville, Alabama; ESA Propulsion Laboratory, *Noordwijk, Netherlands*

Table 13.4: Verification method(s), test(s), and facilities for each parameter [7].

Parameter	Unit	Method(s)	Tests	Facilities
Resolution	m/pixel	Demonstration	Modulation transfer function test (MTF)	Image Science, ESA Test Center, *Noordwijk, Netherlands*
Spectral range	μm	Test	Spectral response measurements	Bossard, *Zug, Switzerland*; ESA Test Center, *Noordwijk, Netherlands*
Concentrations	mol/L	Test	Measure with known concentration and compare results	Ocean Worlds Lab, *Pasadena, California*
Sample size	m^3	Test	Measure decreasing sample sizes	Ocean Worlds Lab, *Pasadena, California*
Flow Particle Velocity	m/s	Test	Simulate environment with known conditions and compare	Ocean Worlds Lab, *Pasadena, California*
Flow Particle Direction	-	Test	Simulate environment with known conditions and compare	Ocean Worlds Lab, *Pasadena, California*
Reliability	%	Test/Analysis	Probability Analysis and/or repeated measures test	ESA Test Center, *Noordwijk, Netherlands*

13.4. Validation

13.4.1. Design Tool Validation

For the validation of the design tools, the results have to be compared to real-world data. Ideally, the circumstances used are the same that are expected during the mission, however, it might be necessary to use simpler scenarios to obtain the required data. Of particular interest are the general parameter calculation functions. Excel was used to calculate many values, such as the thickness of structure elements or the diameter of the antenna. Testing whether the equations used for these calculations match with the real world is an important part of validation. This can be done, for example, by comparing the results to similar missions. Design methods can also be validated by comparing different methods to see if they agree.

Unfortunately, not every design tool could be validated due to time and cost constraints. However, some design tools were verified.

13.4.2. Product Validation

For product validation, there are four methods: analysis, demonstration, inspection and test[3]. With analysis, mathematical models can be used to predict the behaviour of the product. By using simulations the performance of the product can be validated. Analysis is not as accurate as real-life testing but early in the design phase, it can help find problems early and without using an expensive prototype. An example of analysis is Finite Element Analysis (FEA). Some FEA validation has already been used on more complex shapes to validate they can withstand the expected conditions. FEA has been used on the antenna dish, to validate it during the launch phase.

"[Demonstrations are] generally a basic confirmation of behavioral capability, differentiated from testing by the lack of detailed data gathering."[3] As of this report no demonstrations have been done, however, it could be useful in the next stages of development. One possible demonstration could be using the payload to find life in a low-life-density area on Earth and check whether it does not find life in a lifeless environment. This would demonstrate that the payload is capable of meeting the requirements.

With inspection, the final product can be visually examined. Since nothing physical has been made, no inspections have been performed. It can be useful to check whether all components have been installed correctly and whether no visible damage exists before launch.

Testing is used to obtain detailed data. It is the most expensive technique in validation but also provides

---

[3]From `https://www.nasa.gov/reference/5-4-product-validation/` Accessed: 19/06/2024

the most accurate results. Many tests could and should be performed to increase the likelihood of mission success. Some examples are testing the relays at low temperatures and testing their range through ice. Other tests could be testing the probe structure under high pressure or testing drill speed through hard ice.

13.5. Reliabilty

Having a reliable lander is critical for a mission to succeed. According to the stakeholder requirements, the probe should have a 50% chance to make it to the subsurface ocean. To analyse this, different stages of the journey to the subsurface ocean need to be explored.

13.5.1. Launch

The launch of the spacecraft is the first step on its journey towards Europa's ocean. A Falcon Heavy will be used for the launch. This launch vehicle has an exceptional track record of nine out of nine launches succeeding.[4] This would be very optimistic to assume since that would mean it would never fail. Instead, to take a margin, the Falcon 9 will be used to calculate the reliability. The Falcon 9 had two launches fail [102] out of the 345 launches[4]. This will result in a reliability of 99.42%.

13.5.2. Journey to Europa

For the journey to Europa, a VEEGA trajectory is used. This is commonly used to get to Jupiter of beyond [24, 26]. After launch, the reliability is also affected, the failure rate for orbiters after launch is around 5%.[5]

13.5.3. Landing

Soft landings, excluding crashing into a planet, have historically been very difficult. Due to the intricate procedures that need to be taken during landing, this will be the most unreliable part of the journey. Since the first successful Mars lander, 9 out of 12 landers have succeeded in landing on Mars. This will induce a reliability of 75%. This will impact the mission greatly.

13.5.4. Ice Penetration

The riskiest step in the mission will likely be getting to the subsurface ocean. The largest unknown variable is the ice thickness. The best estimate given on the ice thickness is 24.3 km [2], this is, however, uncertain. To increase the reliability of the mission, the ice thickness has been given a margin of 20%. The design is also easily scalable to compensate for a larger ice thickness. The relays will still be able to function, but the data rate will be a bit lower. Thus, a larger ice shell will not mean total mission failure. RTGs can provide a lot of power without running out for years, thus the probability of the probe reaching is pretty high. For this, a reliability of 75% has been utilised.

13.5.5. Subsystem failure

Due to the reliability requirement, a greater than 50% chance of delivering the probe to the subsurface ocean means that there will be a 5% margin for subsystem failure. The most critical subsystems are the thermal control, electrical power supply and communications as these are often showstoppers for these kinds of missions. Due to the measures taken during the design of the subsystems, this is believed to be possible to be reduced to 5%.

---

[4]From `https://www.spacex.com/`. Accessed on 19/06/2024
[5]From `https://www.bbc.com/future/article/20230518-what-are-the-odds-of-a-successful-space-launch`, Accessed on 19/06/2024

14 Future Development

This chapter outlines the project development that will occur in the next stages of mission design. The project design & development logic is presented in Section 14.1. At the end, the post-DSE Gannt Chart is presented in Section 14.2.

14.1. Project Design & Development Logic

This section will discuss what will happen after the Design Synthesis Exercise to accomplish the mission. In Figure 14.1, an overview is shown of the timeline. From the figure, it can be seen that five significant phases will occur. These are the design iteration, technology development, production phase, operation and logistics, and end-of-life procedures.

Figure 14.1: Flow chart of post DSE activities

Design Iteration

This phase focuses on going through another iteration of the design and covering the finer details of the design that were not able to be analysed because of time and resource constraints. These include looking at various mechanisms that will aid the probe in reaching the subsurface ocean and various simulations that will increase the fidelity of the design. Towards the end of this phase, the necessary existing components and technology required to be developed will be determined and the technical resource allocations will updated to reflect any changes. This will result in a cost budget that will have to be approved by the stakeholders who can either choose to continue with developing the project or stop the design process depending on the feasibility of the project.

Technology Development
This phase is dedicated to developing the technology needed to proceed with the mission. A lot of the components have turned out to have a low TRL. Therefore, the goal of this phase is to increase the TRL by doing research into these specific components and afterwards, verifying and validating them. This will then lead to another design iteration of the mission depending on how the technology development phase progresses and whether changes to the design are required as a result of this.

Production Phase
Once the design has been finalised with the final iteration in the technology development phase, the production phase will begin. This is the phase where all the components will be produced, furthermore, the qualification model and flight model will be assembled. After manufacturing every component and model, there will be verification and validation activities that will be performed to ensure that they comply with the requirements of the mission.

Operations and logistics
After the flight model is verified and validated, the operations and logistics phase will commence. This is the phase where the mission will be carried out. This includes Travelling to Europa, traversing through the ice, conducting scientific operations, Communicating the data back to Earth and then finally decommissioning the spacecraft at starting the End of Life Procedures.

14.2. Post-DSE Gantt Chart

The Gantt Chart in Figure 14.2 shows the timeline of the tasks to be done that was previously previewed in Section 14.1.

Figure 14.2: Post-DSE Gantt Chart

ID	Task Mode	Task Name	Duration	Start	Finish	Predecessors	Resource Names
1		DSE Design Iteration	50 days	Mon 4/22/24	Fri 6/28/24		
2		**Design Iteration**	**100 days**	**Mon 7/1/24**	**Fri 11/15/24**	**1**	
3		Develop the Design Further	4.75 mons	Mon 7/1/24	Fri 11/8/24		
4		Determine off-the-shelf components to be used	3 mons	Fri 7/19/24	Thu 10/10/24		
5		Determine Technology needed to be developed	3 mons	Fri 7/19/24	Thu 10/10/24		
6		Perform Detailed Simulation and Analysis	3 mons	Fri 8/23/24	Thu 11/14/24		
7		Update Technical Resource Allocation	0.75 mons	Fri 10/18/24	Thu 11/7/24		
8		Continue with Design Process decision	7 days	Thu 11/7/24	Fri 11/15/24	7	
9		**Technology Development**	**1593 days**	**Mon 11/18/24**	**Wed 12/25/30**	**2**	
10		Identify the Relevant Expertise Required	1 mon	Mon 11/11/24	Fri 12/6/24		
11		Design Technology	1460 days	Fri 12/6/24	Thu 7/11/30		
12		Perform Verification and Validation	365 days	Sat 12/6/25	Thu 4/29/27		
13		Iterate Mission Design if Required	1090 days	Thu 10/22/26	Wed 12/25/30		
14		**Production Phase**	**882 days**	**Thu 12/26/3**	**Fri 5/12/34**	**9**	
15		Produce All Required Components	757 days	Thu 1/2/31	Fri 11/25/33		
16		Perform Verification and Validation	6 mons	Mon 1/26/32	Fri 7/9/32		
17		Produce Qualification Model	6 mons	Mon 7/12/32	Fri 12/24/32		
18		Perform Verification and Validation	6 mons	Mon 12/27/32	Fri 6/10/33	17	
19		Produce Flight Model	6 mons	Mon 6/13/33	Fri 11/25/33		
20		Perform Verification and Validation	6 mons	Mon 11/28/33	Fri 5/12/34	19	
21		**Operations and Logistics**	**4032 days**	**Sun 5/14/34**	**Mon 10/25/49**	**14**	
22		Travel to Europa	1582 days	Sun 5/14/34	Sat 6/2/40		
23		Break Through the Ice	2190 days	Sat 6/2/40	Thu 10/22/48	22	
24		Conduct Scientific Operations	2451 days	Mon 6/4/40	Mon 10/25/49	22	
25		Communicate with Earth	4032 days	Sun 5/14/34	Mon 10/25/49		

Project: AlienDive_5
Date: Wed 6/19/24

Task | Milestone ◆ | Project Summary | Inactive Milestone ◇ | Manual Task | Manual Summary Rollup | Start-only ⊏ | External Tasks | Deadline ↓ | Manual Progress

Split | Summary | Inactive Task | Inactive Summary | Duration-only | Manual Summary | Finish-only ⊐ | External Milestone ◇ | Progress

Page 1

15 Conclusion

The objective of this report was to present the detailed design phase of the AlienDive mission. To do so, the design of the three main components of the AlienDive has been elaborated on: the transfer stage, the lander and the probe. This is followed by recommendations on how the design can be improved in the future.

The transfer stage is stadium-shaped and its dimensions are optimised to fit both propellant tanks for the liquid bi-propellant engine attached to the base of the stage. The thermal control subsystem of the transfer stage keeps the lander temperatures during transit within the acceptable range. The propulsion subsystem features a chemical bi-propellant engine providing the required Delta-V. The GNC subsystem allows for precise attitude determination. Finally, the structure of the transfer stage includes the separation mechanism and the radiation shielding.

The lander includes a limited number of scientific instruments for secondary science objectives as well as onboard systems for landing site selection. The lander is designed as a large truss structure fully covered in thermal protection measures such as MLI and radiators. It is powered by an RTG, as solar arrays or fuel cells are considered non-viable options for this mission. Precision in landing trajectory is ensured through variable thrust liquid bipropellant engines and a sophisticated GNC subsystem. The CDH subsystem handles the data processing of scientific, housekeeping and command data, while the communication subsystem manages data transmission and reception to and from the NASA Deep Space Network.

The probe includes numerous scientific instruments selected based on the science traceability matrix, ensuring life-detecting capabilities. The probe is designed as a cylindrical pressure vessel able to withstand large hydrostatic pressures experienced in the subsurface ocean of Europa. Beyond its structural role, this shell serves as both radiation shielding and thermal insulation. Powered by two finless radioisotope thermoelectric generators, the probe uses a heated drill to efficiently remove and melt ice chips, preventing jams. Heat is provided by the RTGs, using a liquid cooling loop to move the thermal energy to the locations where it is needed. The CDH subsystem handles the data processing of scientific, housekeeping and command data. Communication through the water to and from the anchor is acoustic-based, while through-ice communication to and from the lander is done via UHF relay transceiver modules. The anchor and relays are deployed by driving rods with heated pins into the ice walls around the probe using springs. Subsequently, the relays are locked into the ice and detached from the probe.

The spacecraft design is fairly flexible dealing with new knowledge on Europa, and minor design changes do not drive it to an unfeasible level. However, given the complexity of the mission and the limited time frame for the design, not every intricate detail could be thoroughly explored. Much of the information about Europa remains uncertain or unknown, and several technologies intended for use in the AlienDive mission still possess a low technology readiness level. Moreover, new issues may emerge during the continued development of the mission, potentially necessitating design changes. Therefore, a set of recommendations is provided in the next section.

Recommendations
First of all, it is recommended to thoroughly analyse data gathered by NASA's Europa Clipper and ESA's JUICE missions on the characteristics of Europa and use them to narrow down the landing site. As determined in the sensitivity analysis, the inclination change to achieve a polar orbit requires a large amount of Delta-V. The polar landing site should thus be reevaluated and possibly changed to a different location in a trade-off between radiation dose, ice thickness, and Delta-V required. Moreover, a more in-depth trajectory and landing analysis should be performed to see if other flybys can be done to minimise the Delta-V.

Secondly, carefully monitoring the technology readiness of certain technologies is advised for the AlienDive mission. Alternative solutions shall also be explored where necessary such as replacing the 16-GPHS-STEM-RTG with the GPHS-RTG[1] that is widely used in US space missions.

Thirdly, a more in-depth analysis of the payload should also be performed to ensure that all the instruments can be used and are effective in the harsh environment of Europa. besides, an investigation of the fatigue effects on the drill bit due to corrosion and erosion should also be performed. It is also recommended to do multiple experiments to determine the acoustic propagation through water-ice bodies.

---

[1]From `https://www.satcatalog.com/component/gphs-rtg/`. Accessed on 25/06/2024

Due to time constraints in this project, subsystems such as the structure have not been optimised at this conceptual stage. It is thus recommended to perform a more comprehensive design analysis. It would for instance be beneficial to perform a more detailed thermal analysis of every component by adding conductive links to the simulation. Another thing to be investigated is whether stringers could decrease the required mass for the probe structure.

Moreover, a more detailed look into the propulsion subsystem is required. One aspect that can be explored is whether the heat from onboard RTGs can be used to make the propulsion subsystem more efficient. Another challenge might be that the propellant tanks of the transfer stage are next to each other and the fuel and oxidiser are used up at different rates, shifting the centre of mass throughout the mission. A different config-uration, such as using a torus tank with a cylindrical tank inside, can be analysed to eliminate this issue. For the unconventional tanks of the lander, an appropriate feed system also needs to be designed. The configu-ration of the lander thrusters has to be analysed in further detail, as its exhaust can potentially damage other components on the lander. The possibility of using heat shields to minimise the impact should be explored.

If a mission to Europa's subsurface ocean is to be performed, it is recommended to first design a mission that delivers a lander to the surface. This would allow for additional knowledge to be gathered on the characteristics of Europa, and on the engineering challenges that appear with such missions. For example, the landing method can be adjusted more specifically to Europa's surface, and the probe can be designed with significantly less uncertainties. This would result in a higher probability of mission success for a follow-up mission similar to AlienDive. The measures discussed above are worth serious consideration, since the scientific potential of the AlienDive mission is immeasurable.

References

[1]   T. Bayer et al. "Europa Clipper mission: the habitability of an icy moon". In: *2015 IEEE Aerospace Conference*. 2015, pp. 1–12. DOI: 10.1109/AERO.2015.7118943.

[2]   S.M. Howell. "The likely thickness of Europa's icy shell". In: *Planetary Science Journal* 2 (4 2021). ISSN: 26323338. DOI: 10.3847/PSJ/abfe10.

[3]   K.P. Hand et al. "Astrobiology and the potential for life on Europa". In: *Europa* (2009), pp. 589–629.

[4]   S.E. Billings and Simon A. Kattenhorn. "The great thickness debate: Ice shell thickness models for Europa and comparisons with estimates based on flexure at ridges". In: *Icarus* 177.2 (2005). Europa Icy Shell, pp. 397–412. ISSN: 0019-1035. DOI: https://doi.org/10.1016/j.icarus.2005.03.013.

[5]   Engineering National Academies of Sciences and Medicine. *Origins, Worlds, and Life: A Decadal Strategy for Planetary Science and Astrobiology 2023-2032*. The National Academies Press, 2023. ISBN: 978-0-309-47578-5. DOI: 10.17226/26522.

[6]   C.B. Phillips and R.T. Pappalardo. "Europa Clipper Mission Concept: Exploring Jupiter's Ocean Moon". In: *Eos, Transactions American Geophysical Union* 95.20 (2014), pp. 165–167. DOI: https://doi.org/10.1002/2014EO200002.

[7]   DSE Group 24. *Midterm Report Final*. TU Delft, May 2024.

[8]   DSE Group 24. *Baseline Report Final*. TU Delft, Apr. 2024.

[9]   K. Enya et al. "Extraterrestrial Life Signature Detection Microscopy: Search and Analysis of Cells and Organics on Mars and Other Solar System Bodies". In: *Space Science Reviews* 218 (6 Sept. 2022). ISSN: 15729672. DOI: 10.1007/s11214-022-00920-4.

[10] Y. Lin. *Life detection in space: Current methods and future technologies*. Elsevier, Jan. 2022, pp. 221–253. ISBN: 9780128241622. DOI: 10.1016/B978-0-12-824162-2.00012-9.

[11] S.P. Kounaves et al. "The MECA wet chemistry laboratory on the 2007 Phoenix Mars Scout Lander". In: *Journal of Geophysical Research: Planets* 114 (3 Mar. 2009). ISSN: 01480227. DOI: 10.1029/2008JE003084.

[12] P. A. Willis et al. "Planetary In Situ Capillary Electrophoresis System (PISCES)". In: *International Workshop on Instrumentation for Planetary Missions* (2012).

[13] M.R. Sims et al. "Development status of the life marker chip instrument for ExoMars". In: vol. 72. Nov. 2012, pp. 129–137. DOI: 10.1016/j.pss.2012.04.007.

[14] M.A. Sephton et al. "Searching for biomolecules on Mars: Considerations for operation of a life marker chip instrument". In: *Planetary and Space Science* 86 (Sept. 2013), pp. 66–74. ISSN: 00320633. DOI: 10.1016/j.pss.2013.04.016.

[15] B. Dachwald et al. "Key Technologies and Instrumentation for Subsurface Exploration of Ocean Worlds". In: *Space Science Reviews* 216 (5 Aug. 2020). ISSN: 15729672. DOI: 10.1007/s11214-020-00707-5.

[16] B. Cavalazzi and F. Westall. *Advances in Astrobiology and Biogeophysics*. Springer Nature Switzerland AG, 2019. ISBN: 978-3-319-96174-3. DOI: https://doi.org/10.1007/978-3-319-96175-0.

[17] Y. Wei, Y. Duan, and D. An. "Monitoring fish using imaging sonar: Capacity, challenges and future perspective". In: *Fish and Fisheries* 23 (2022), pp. 1347–1370. DOI: 10.1111/faf.12693.

[18] R.L. Kovach and Christopher F. Chyba. "Seismic Detectability of a Subsurface Ocean on Europa". In: *Icarus* 150 (2 Apr. 2001), pp. 279–287. ISSN: 00191035. DOI: 10.1006/icar.2000.6577.

[19] C. Nunn et al. "Standing on Apollo's Shoulders: A Microseismometer for the Moon". In: *The Planetary Science Journal* 2 (2021). DOI: 10.3847/PSJ/abd63b. URL: https://doi.org/10.3847/PSJ/abd63b.

[20] K.K. Khurana et al. "Induced magnetic fields as evidence for subsurface oceans in Europa and Callisto". In: *Nature* 395 (Oct. 1998), pp. 777–780. DOI: 10.1038/27394.

[21] M.G. Kivelson et al. "The Europa Clipper Magnetometer". In: *Space Science Reviews* 219 (2023). DOI: 10.1007/s11214-023-00989-5. URL: https://doi.org/10.1007/s11214-023-00989-5.

[22] K.R. Fowler and Stephen A. Dyer. "Proposed landing on europa: Instruments, radiation shielding, planetary protection, and mission". In: *IEEE Aerospace and Electronic Systems Magazine* 33 (8 Aug. 2018), pp. 6–23. ISSN: 1557959X. DOI: `10.1109/MAES.2018.180009`.

[23] S.D. Vance et al. "Investigating Europa's Habitability with the Europa Clipper". In: *Space Science Reviews* 219 (8 Dec. 2023). ISSN: 15729672. DOI: `10.1007/s11214-023-01025-2`.

[24] C. Yang, B. He-xi, and L. Jun-feng. "Trajectory Analysis and Design for A Jupiter Exploration Mission". In: *Chinese Astronomy and Astrophysics* 37.1 (2013), pp. 77–89. ISSN: 0275-1062. DOI: `https://doi.org/10.1016/j.chinastron.2013.01.008`.

[25] Europa Study Team. *EUROPA STUDY 2012 REPORT*. May 2012.

[26] L.A. D'Amario, L.E. Bright, and A.A. Wolf. "Galileo trajectory design". In: *Space Science Reviews* 60 (1-4 1992). ISSN: 00386308. DOI: `10.1007/BF00216849`.

[27] European Space Agency. *Margin philosophy for science assessment studies*. June 2012.

[28] X. Huang, J.J. Masdemont, and S. Li. "Dynamic Analysis of Europa Probe Considering J2 Perturbation of Jupiter". In: *Journal of Guidance, Control, and Dynamics* 47.1 (2024), pp. 156–164. DOI: `10.2514/1.G007532`. eprint: `https://doi.org/10.2514/1.G007532`. URL: `https://doi.org/10.2514/1.G007532`.

[29] M.V. Podzolko et al. "Charged particles on the Earth–Jupiter–Europa spacecraft trajectory". In: *Advances in Space Research* 48.4 (2011). Europa Lander: Science Goals and Implementation, pp. 651–660. ISSN: 0273-1177. DOI: `https://doi.org/10.1016/j.asr.2010.11.011`.

[30] T. A. Nordheim, K. P. Hand, and C. Paranicas. "Preservation of potential biosignatures in the shallow subsurface of Europa". In: *Nature Astronomy* 2 (8 Aug. 2018), pp. 673–679. ISSN: 23973366. DOI: `10.1038/s41550-018-0499-8`.

[31] J.R. Wertz, D.F. Everett and J.J. Puschell. *Space Mission Engineering: The New SMAD*. Microcosm Press, 2011.

[32] M.C.V Salgado, M.C.N. Belderrain, and T.C Devezas. "Space Propulsion: a Survey Study About Current and Future Technologies". In: *Journal of Aerospace Technology and Management* 10 (2018). DOI: `10.5028/jatm.v10.829`.

[33] B.T.C. Zandbergen. *Thermal Rocket Propulsion*. 2022.

[34] C.B. Muratov, V.V. Osipov, and V.N. Smelyanskiy. *Issues of Long-Term Cryogenic Propellant Storage in Microgravity*. Oct. 2011.

[35] S.E. Kim and C.S. Kim. "Buckling strength of the cylindrical shell and tank subjected to axially compressive loads". In: *Thin-Walled Structures* 40 (2002). DOI: `10.1016/s0263-8231(01)00066-0`.

[36] H.P. Trinh, C. Brunside, and H. Williams. *Assessment of MON-25/MMH Propellant System for Deep-Space Engines*. 2019.

[37] H. Li et al. "Simulation Study of the Swirl Spray Atomization of a Bipropellant Thruster under Low Temperature Conditions". In: *Energies* 15.23 (2022). DOI: `10.3390/en15238852`.

[38] David G. Gilmore. *Spacecraft Thermal Control Handbook ed. by D.G. Gilmore. 1, Fundamental Technologies*. Knovel, 2007.

[39] *Falcon's user guide*. SpaceX. Sept. 2021.

[40] B. Zandbergen. *Spacecraft (bus/platform) design and sizing*. TU Delft, Oct. 2021.

[41] *COSPAR Policy on Planetary Protection*. June 2020.

[42] R. Pappalardo. "Seeking Europa's Ocean". In: *Proceedings of the International Astronomical Union* 6 (Jan. 2010), pp. 101–114. DOI: `10.1017/S1743921310007325`.

[43] G. Todd. *TOXICOLOGICAL PROFILE FOR PHOSPHATE ESTER FLAME RETARDANTS*. U.S. DEPARTMENT OF HEALTH and HUMAN SERVICES, Sept. 2012.

[44] Y. Lee and B. Bairstow. *Radioisotope Power Systems Reference Book for Mission Designers and Planners*. Jet Propulsion Laboratory, Sept. 2015.

[45] Ames Research Center. *State-of-the-Art Small Spacecraft Technology*. NASA, Feb. 2024.

[46] D.K. Bond et al. "Evaluating the effectiveness of common aerospace materials at lowering the whole body effective dose equivalent in deep space". In: *Acta Astronautica* 165 (10 2019). ISSN: 15581578. DOI: `10.1016/j.actaastro.2019.07.0224`.

[47] M. Paluszek. "Disturbances". In: *ADCS - Spacecraft Attitude Determination and Control*. Elsevier, 2023, pp. 117–145. ISBN: 9780323999151.

[48] S.R. Starin and J.S. Eterno. "Attitude Determination and Control Systems". In: *Engineering* (2010).

[49] J. E. P. Connerney et al. "A New Model of Jupiter's Magnetic Field at the Completion of Juno's Prime Mission". In: *Journal of Geophysical Research: Planets* 127.2 (2022). DOI: `https://doi.org/10.1029/2021JE007055`.

[50] K.V. Sathish. "Radiation shielding properties of aluminium alloys". In: *Radiation Effects and Defects in Solids* 178 (9-10 2023), pp. 1301–1320. ISSN: 10294953. DOI: `10.1080/10420150.2023.2249180`.

[51] T. A. Nordheim, K. P. Hand, and C. Paranicas. "Preservation of potential biosignatures in the shallow subsurface of Europa". In: *Nature Astronomy* 2 (8 2018). ISSN: 23973366. DOI: `10.1038/s41550-018-0499-8`.

[52] J.Z. Wang et al. "Optimization Design of Radiation Vault in Jupiter Orbiting Mission". In: *IEEE Transactions on Nuclear Science* 66 (10 2019). ISSN: 15581578. DOI: `10.1109/TNS.2019.2939184`.

[53] S.A. Walker et al. "Investigating material approximations in spacecraft radiation analysis". In: vol. 69. 2011. DOI: `10.1016/j.actaastro.2011.02.013`.

[54] J. Desai and S. Kulkarni. "Effect of noise on ber of bpsk qpsk dpsk and qam modulation techniques". In: *International Journal of Research and Scientific Innovation (IJRSI)* 3 (2016).

[55] R. Mukai et al. "Juno telecommunications". In: *NASA DESCANSO Design and Performance Summary Series* (2012).

[56] J. Taylor et al. "Mars exploration rover telecommunications". In: *Deep Space Communications* (2016), pp. 251–358.

[57] J. Taylor, L. Sakamoto, and C.J. Wong. "Cassini orbiter/huygens probe telecommunications". In: *DESCANSO Design and Performance Summary Series* (2002).

[58] J. Taylor and J. Kuiper. *Chapter 2: The Deep Space Network*. Descanso Design and Performance Summary Series. 2013.

[59] Jet Propulsion Laboratory. *NASA MOCS: Mission Operations Communications Services*. Pasadena, CA: NASA Jet Propulsion Laboratory, 2014.

[60] Space Exploration Technologies Corp. *Falcon User's Guide*. 2021.

[61] C.A. Balanis. *Antenna theory: analysis and design*. John wiley & sons, 2016. ISBN: 9786468600.

[62] NASA. *Buckling of Thin-Walled Circular Cylinders*. NASA/SP-8007-2020/REV 2, Nov. 2020.

[63] E. Alfredo Campo. "Engineering Product Design". In: *Complete Part Design Handbook*. Ed. by E.A. Campo. Hanser, 2006, pp. 115–209. ISBN: 978-3-446-40309-3. DOI: `https://doi.org/10.3139/9783446412927.002`.

[64] R.J. Roark, W.C. Young, and R.G. Budynas. "Flat Plates". In: *Roark's formulas for stress and strain*. McGraw-Hill, 2002, pp. 427–524. ISBN: 007072542X.

[65] P.M. Schenk. "Slope characteristics of Europa: Constraints for landers and radar Sounding". In: *Geophysical Research Letters* 36 (15 2009). ISSN: 00948276. DOI: `10.1029/2009GL039062`.

[66] P. Squillace. "Europa Lander Landing System, Study on Deployment, Landing and Preliminary Design". MA thesis. Delft University of Technology, 2022.

[67] K.A. Gross. "A Penetrating Look at Ice Friction". In: *Physics* 14 (2021). DOI: `10.1103/physics.14.20`.

[68] V.L. Pham et al. "Landing stability simulation of a 1/6 lunar module with aluminum honeycomb damper". In: *International Journal of Aeronautical and Space Sciences* 14 (4 2014). ISSN: 2093274X. DOI: `10.5139/IJASS.2013.14.4.356`.

[69] R. Liu et al. "Design and selection of aluminum foam for impact damper of legged lunar lander". In: 2008. DOI: `10.1109/ISSCAA.2008.4776270`.

[70] T. Godfroy D.I. Poston M.A. Gibson and P.R. McClure. "KRUSTY Reactor Design". In: *Nuclear Technology* 206.sup1 (2020), S13–S30. DOI: `10.1080/00295450.2020.1725382`.

[71] D.F. Woerner. *Next-Generation Radioisotope Thermoelectric Generator Study Final Report*. Jet Propulsion Laboratory, June 2017.

[72] S. Oleson et al. *Compass Final Report: Europa Tunnelbot*. June 2019.

[73] J. E. Werner et al. "Cost Comparison in 2015 Dollars for Radioisotope Power Systems – Cassini and Mars Science Laboratory". In: (July 2016). DOI: `10.2172/1364515`.

[74] K. Zacny et al. "SLUSH: Europa hybrid deep drill". In: vol. 2018-March. 2018. DOI: `10.1109/AERO.2018.8396596`.

[75] P. Talalay et al. "Anti-torque systems of electromechanical cable-suspended drills and test results". In: *Annals of Glaciology* 55 (68 2014). ISSN: 02603055. DOI: `10.3189/2014AoG68A025`.

[76] J. J. Buffo, C. R. Meyer, and J. R. G. Parkinson. "Dynamics of a Solidifying Icy Satellite Shell". In: *Journal of Geophysical Research: Planets* 126 (5 2021). ISSN: 21699100. DOI: `10.1029/2020JE006741`.

[77] F. Nimmo and M. Manga. "Geodynamics of Europa's Icy Shell". In: 2017. DOI: `10.2307/j.ctt1xp3wdw.22`.

[78] M. Masoumi et al. "Manufacturing Techniques for Electric Motor Coils with Round Copper Wires". In: *IEEE Access* 10 (2022). ISSN: 21693536. DOI: `10.1109/ACCESS.2022.3229024`.

[79] A.A. Shapoval, I. Savchenko, and O. Markov. "Determination coefficient of stress concentration using a conformed display on a circle of a single radius". In: *Solid State Phenomena* 316 (2021), pp. 928–935.

[80] D. Marsacq. *Micro-fuel cells*. CEA, 2005.

[81] J. Eluszkiewicz. "Dim prospects for radar detection of Europa's ocean". In: *Icarus* 170 (1 2004). ISSN: 00191035. DOI: `10.1016/j.icarus.2004.02.011`.

[82] A.J. Hirsch. *Nelson Physics 11. Solutions Manual*. Nelson Education Limited, 2001. ISBN: 9780176121075.

[83] D.M. Schroeder et al. "Five decades of radioglaciology". In: *Annals of Glaciology* 61 (81 2020). ISSN: 02603055. DOI: `10.1017/aog.2020.11`.

[84] Yunus A. Çengel and Afshin J. Ghajar. *Heat and Mass Transfer: Fundamentals and Applications*. 6th. New York, NY: McGraw-Hill Education, 2020. ISBN: 9781260269530.

[85] P.E. Okafor and G. Tang. "Study of effective thermal conductivity of a novel SiO2 aerogel composite for high-temperature thermal insulation". In: *International Journal of Heat and Mass Transfer* 212 (2023), p. 124242. ISSN: 0017-9310. DOI: `10.1016/j.ijheatmasstransfer.2023.124242`.

[86] J. Kimura, Y. Yamagishi, and K. Kurita. "Tectonic history of Europa: Coupling between internal evolution and surface stresses". In: *Earth, Planets and Space* 59 (2007), pp. 113–125. DOI: `10.1186/BF03352684`. URL: `https://doi.org/10.1186/BF03352684`.

[87] A. Lakey et al. "Free-Space Communication Through an Ocean World Ice Shell to Enable Ocean World Exploration". In: *2024 IEEE Aerospace Conference*. 2024, pp. 1–11. DOI: `10.1109/AERO58975.2024.10521002`.

[88] S. Bryant. "Ice-embedded transceivers for Europa cryobot communications". In: *Proceedings, IEEE Aerospace Conference*. Vol. 1. 2002, 1–356 vol.1. DOI: `10.1109/AERO.2002.1036854`.

[89] H. Kaushal and G. Kaddoum. "Underwater Optical Wireless Communication". In: *IEEE Access* 4 (2016), pp. 1518–1547. DOI: `10.1109/ACCESS.2016.2552538`.

[90] H. Becker G. Gerard. *HANDBOOK OF Structural STABILITY PART III - BUCKLING OF CURVED PLATES AND SHELLS*. NACA, Aug. 1957.

[91] H. Cheng et al. "The half-lives of uranium-234 and thorium-230". In: *Chemical Geology* 169 (Aug. 2000), pp. 17–33. DOI: `10.1016/S0009-2541(99)00157-6`.

[92] S. Vance et al. "Hydrothermal Systems in Small Ocean Planets". In: *Astrobiology* 7.6 (2007), pp. 987–1005. DOI: `10.1089/ast.2007.0075`.

[93] S. D. Vance, K. P. Hand, and R. T. Pappalardo. "Geophysical controls of chemical disequilibria in Europa". In: *Geophysical Research Letters* 43.10 (2016), pp. 4871–4879. DOI: `10.1002/2016GL068547`.

[94] Borexino Collaboration et al. "Lifetime measurements of 214 Po and 212 Po with the CTF liquid scintillator detector at LNGS". In: *The European Physical Journal A* 49 (2013), pp. 1–8.

[95] B.N. Bhat. *Aerospace Materials and Applications*. Progress in astronautics and aeronautics. American Institute of Aeronautics and Astronautics, Incorporated, 2018. ISBN: 9781624104886.

[96] K.R. Fowler and S.A. Dyer. "Proposed landing on europa: Instruments, radiation shielding, planetary protection, and mission". In: *IEEE Aerospace and Electronic Systems Magazine* 33 (8 2018). ISSN: 1557959X. DOI: `10.1109/MAES.2018.180009`.

[97] O.A. Quintana et al. "Effects of Reusing Ti-6Al-4V Powder in a Selective Laser Melting Additive System Operated in an Industrial Setting". In: *JOM* 70 (9 2018), pp. 1863–1869. DOI: `10.1007/s11837-018-3011-0`.

[98] National Research Council. *Preventing the Forward Contamination of Europa*. Washington, DC: The National Academies Press, 2000. DOI: `10.17226/9895`.

[99]   J. Bui et al. *FUNCTIONAL COST-ESTIMATING RELATIONSHIPS FOR SPACECRAFT*. 1996.

[100] D.C. Arney and A.W. Wilhite. "Rapid Cost Estimation for Space Exploration Systems". In: *AIAA SPACE 2012 Conference Exposition* (2012). DOI: `10.2514/6.2012-5183`.

[101] A.A Shapoval, I. Savchenko, and O. Markov. "Determination coefficient of stress concentration using a conformed display on a circle of a single radius". In: *Solid State Phenomena* 316 (2021), pp. 928–935.

[102] E. Seedhouse. "Falcon 9 and falcon heavy". In: *SpaceX: Starship to Mars–The First 20 Years*. Springer, 2022, pp. 71–93.